LEABHARLANN CHOLÁISTE NA TRÍONÓIDE, BAILE ÁTHA CLIATH | TRINITY COLLEGE LIBRARY DUBLIN
Ollscoil Átha Cliath | The University of Dublin

**Terms and Conditions of Use of Digitised Theses from Trinity College Library Dublin**

**Copyright statement**

All material supplied by Trinity College Library is protected by copyright (under the Copyright and Related Rights Act, 2000 as amended) and other relevant Intellectual Property Rights. By accessing and using a Digitised Thesis from Trinity College Library you acknowledge that all Intellectual Property Rights in any Works supplied are the sole and exclusive property of the copyright and/or other IPR holder. Specific copyright holders may not be explicitly identified. Use of materials from other sources within a thesis should not be construed as a claim over them.

A non-exclusive, non-transferable licence is hereby granted to those using or reproducing, in whole or in part, the material for valid purposes, providing the copyright owners are acknowledged using the normal conventions. Where specific permission to use material is required, this is identified and such permission must be sought from the copyright holder or agency cited.

**Liability statement**

By using a Digitised Thesis, I accept that Trinity College Dublin bears no legal responsibility for the accuracy, legality or comprehensiveness of materials contained within the thesis, and that Trinity College Dublin accepts no liability for indirect, consequential, or incidental, damages or losses arising from use of the thesis for whatever reason. Information located in a thesis may be subject to specific use constraints, details of which may not be explicitly described. It is the responsibility of potential and actual users to be aware of such constraints and to abide by them. By making use of material from a digitised thesis, you accept these copyright and disclaimer provisions. Where it is brought to the attention of Trinity College Library that there may be a breach of copyright or other restraint, it is the policy to withdraw or take down access to a thesis while the issue is being resolved.

**Access Agreement**

By using a Digitised Thesis from Trinity College Library you are bound by the following Terms & Conditions. Please read them carefully.

I have read and I understand the following statement: All material supplied via a Digitised Thesis from Trinity College Library is protected by copyright and other intellectual property rights, and duplication or sale of all or part of any of a thesis is not permitted, except that material may be duplicated by you for your research use or for educational purposes in electronic or print form providing the copyright owners are acknowledged using the normal conventions. You must obtain permission for any other use. Electronic or print copies may not be offered, whether for sale or otherwise to anyone. This copy has been supplied on the understanding that it is copyright material and that no quotation from the thesis may be published without proper acknowledgement.

# FORMULATION, PRODUCTION AND BIOINTERACTION OF MICRO AND NANO PARTICULATES WITH POTENTIAL FOR USE IN DRUG DELIVERY

Being a thesis submitted for the degree of

**Doctor of Philosophy**

**in**

**Pharmaceutics**

at

**University of Dublin**

**Trinity College**

**by**

**Xue Li**

Under the direction and supervision of

**Owen I. Corrigan, B.Sc. (Pharm) M.A. Ph.D. F.T.C.D.**

**Lidia Tajber, M.Sc. (Pharm), Ph.D.**

**March 2009**

TRINITY COLLEGE
10 AUG 2009
LIBRARY DUBLIN
THESIS
8712

# DECLARATION

This thesis is submitted by the undersigned to the University of Dublin, Trinity College for examination for the degree of Doctor of Philosophy. It has not been submitted as an exercise for a degree at this or any other university. It is entirely the candidate's own work except where duly acknowledged and the candidate agrees that the library may lend or copy the thesis upon request. This permission covers only single copies made for study purpose, subject to normal conditions of acknowledgement. This manuscript was completely written by me with the aid of editorial advice from Professor O.I. Corrigan and Dr. L. Tajber.

Li Xue

Xue Li

## Summary

The current study involved the preparation of a range of micro and nano particulates from known biocompatible pharmaceutical polymeric excipients: PLGA, chitosan and hyaluronic acid, using physical rather than chemical processes and evaluates the various aspects of their drug delivery potential, biointeraction and potential toxicity.

Emulsion techniques, including the double emulsion and single emulsion technique, are methods usually used in the manufacture of drug loaded PLGA (RG504) particles, as well as chitosan-PLGA particles. Cationically modified PLGA particles can efficiently bind the negatively charged DNA electrostatically, by using chitosan as adjuvant (Kumbar et al., 2002). Although release studies of proteins and drugs have been reported by numerous groups (Pean et al., 1998; Dunne et al., 2000; Gallagher and Corrigan 2000), there were large differences between the results. Therefore it is deemed necessary to explain the differences and conclude on the effects.

Chitosan microparticles (CL213 and CL213/GLU) were prepared by spray drying with and without crosslinking agent glutaraldehyde. Four different batches of chitosan nanoparticles (CS-F NP, CL113 NP, CL213 NP and G213 NP) were prepared by precipitation/coacervation. Although chitosan nanoparticles have been widely studied in both animal and cell models, their physical properties, such as morphologies of dry products and manufacture processes, did not receive much attention all these years. A model protein, OVA, was adsorbed onto chitosan nanoparticles to study its release from chitosan nanoparticles prepared by precipitation/coacervation.

Although polymeric particles have been widely studied for drug delivery systems, there is little work which has been reported on hyaluronic acid (HA) particulate systems, especially HA nanoparticles. As a biodegradable, biocompatible and

viscoelastic polymer (Zhong et al., 1994; Prestwitch et al., 1998; Balazs 1998; Brown and Jones 2004; Hahn et al., 2004), particulate HA has a potential as a nano-sized drug delivery carrier particularly when combined with chitosan. HA microparticles were manufactured by spray drying. HA/chitosan nanoparticles were manufactured by coacervation/precipitation. Two sodium hyaluronates and four chitosan salts (CL113, CL213, G113 and G213) were used to prepare HA-chitosan nanoparticles. The physical properties of the resultant nanoparticles were measured and compared. The two sodium hyaluronates were sodium hyaluronate (Fluka) and ultrapure sodium hyaluronate (NovaMatrix). Ultrapure sodium hyaluronate (NovaMatrix) presents a low endotoxin level smaller than 2.5 EU/g.

Since the potential of nanoparticles to induce platelet aggregation and precipitate thrombosis has been established (Glynn et al., 1965; Radomski et al., 2005; Bloom et al., 1955), it is important to screen the nanoparticles to establish their safety in this regard, especially when there are very limited published studies on these particles nowadays. Therefore, the effect of drug free PLGA, chitosan-PLGA and chitosan nanoparticles on human platelet aggregation and their effects on inhibition of the collagen induced aggregation *in vitro* were investigated. Indomethacin and ketoprofen were encapsulated into PLGA nanoparticles to formulate nanoparticulate drug delivery systems and the effects of the resultant nanoparticles on platelet aggregation were studied.

Chitosan nanoparticles were studied to see if they can activate bone marrow derived myeloid dendritic cells (DCs). The effectiveness of the different chitosan nanoparticles was also investigated. Endotoxin free chitosan nanoparticles were manufactured and the effect on inducing DCs maturation and cytokine production by DCs and spleen cells were measured and compared with chitosan solution. Finally, cytotoxicity of chitosan nanoparticles on DCs and spleen cells were investigated and compared to chitosan solution.

## Acknowledgements

I would like to thank my supervisor Professor Owen I. Corrigan for his advice, guidance and many useful pharmaceutics discussions through my postgraduate studies and in the preparation of this thesis. I would like to thank Dr. Lidia Tajber for her support, encouragement and proof reading of this thesis. I would like to also thank Professor Marek Radomski and Dr. Anna Radomska for their assistances of the platelet works, Dr. Ed Lavelle and Yuki Ozasa for their assistance of the cell works in this thesis.

I also express my gratitude to the Trinity Studentship for providing the award which made the research possible.

Many thanks to the academic and technical stuff of the School of Pharmacy for their assistance in technical matters, especially Patrick Quinlan, Brian O'Reilly, Conan Murphy and Brian Talbot. Thanks to Neal Leddy for the help with scanning electron microscopy (SEM).

Thanks to the postgrads Lorraine, Arun, Shadeed, Fiona for their advices, assistance and friendship. Especial thanks to Orla for her friendship and support during my postgraduate years. I wish her all the best in her career and her future.

Thanks to Dr. Majella Lane for her assistance to the early part of this thesis. Thanks to Professor Brian M. Adair and the student Alun for their supply of the peptide used in this thesis.

I am eternally grateful to my parents and husband for their support and all the patience throughout my education over the years.

## Presentations and publications associated with this thesis

### *Poster presentations*

Li, X., Radomski, A., Corrigan O.I. and Radomski, M.W

The effects of poly(lactide-co-glycolide) (PLGA) and chitosan based nanoparticles on human platelet aggregation 2

*3rd Pharmaceutical Sciences World Congress*, Amsterdam, April 2007

Li, X., Radomski, A., Corrigan O.I. and Radomski, M.W

The effects of poly(lactide-co-glycolide) (PLGA) and chitosan based nanoparticles on human platelet aggregation 1

*29th Joint Research Seminar*, Royal College of Surgeons Dublin, March 2007

Xue Li, Majella E. Lane and Owen I. Corrigan

Formulation and characterization of human serum albumin loaded microparticulate drug delivery systems

*28th Joint Research Seminar*, Queen's University Belfast, April 2006

Xue Li, Majella E. Lane and Owen I. Corrigan

Effect of organic solvent phase on characteristics of microcapsulated human serum albumin'

*27th Joint Research Seminar*, Trinity College Dublin March, 2005

# Abbreviations and symbols

| | |
|---|---|
| APC | antigen presenting cells |
| BALB/c | Bagg albino strain of laboratory mouse |
| BMDC | bone marrow-derived immature dendrite cell |
| BSA | bovine serum albumin |
| $C_s$ | solubility of the drug in the sink phase |
| $C_t$ | total amount of drug per unit volume of matrix |
| C3H/HeN | the C3H parent strain mouse |
| C3H/HeJ | the C3H parent strain mouse, endotoxin resistant |
| C60CS | C60 fullerenes |
| CB | carbon black |
| CD | coefficient of determination |
| CD80, 86, 40 | protein cluster of differentiation 80,86,40 |
| CD86-PE | phycoerythrin stain on protein cluster of differentitation 86 |
| CD80-FITC | fluorescein stain on protein cluster of defferentitation 80 |
| CD11c-APC | protein cluster of differentiation 11c |
| CD40-FITC | fluorescein stain on protein cluster of defferentitation 40 |
| CL113 | chitosan chloride salt low molecular weight |
| CL213 | chitosan chloride salt high molecular weight |
| CS | chitosan |
| D | diffusion coefficient |
| DCM | dichloromethane |
| DCs | dendritic cells |
| DPSS | Dulbecco's phosphate buffer saline |
| DSC | differential scanning calorimetry |

| | |
|---|---|
| EE% | encapsulation efficiency% |
| ELISA | enzyme-linked immuno sorbent assay |
| F | Fluka |
| FACs | fluorescence activated cell sorter buffer |
| $F_B$ | fraction of drug released in burst phase |
| FS | forward scatter |
| FTIR | Fourier transform infrared spectroscopy |
| G113 | chitosan glutamate salt 113 |
| G213 | chitosan glutamate salt 213 |
| GI | gastrointestinal |
| GPC | gel permeation chromatography |
| HA | hyaluronic acid |
| HAna | sodium hyaluonate |
| HMW | high molecular weight |
| $^1$H-NMR | $^1$H-Nuclear Magnetic Resonance Spectroscopy |
| H S A | human serum albumin |
| IFN-γ | interferon-gamma |
| IL-4, -5, -6, 12p40 | Interleukin-4, -5, -6, 12p40 |
| $K_B$ | release rate constant related to initial release |
| k | release rate constant |
| LMW | low molecular weight |
| LPS | lipopolysaccharide |
| $M_t/M_\infty$ | fraction of total drug content released |
| MCN | mixed carbon nanoparticles |
| MHC class II | major histocompatibility complex class II molecules |
| MHC II-PE | phycoerythrin stain on major histocompatibility complex class II molecules |
| MMW | medium molecular weight |

| | |
|---|---|
| MP | microparticles |
| MSC | model selection criterion |
| MWNT | multiplewall nanotubes |
| NP | nanoparticles |
| NSAIDs | nonsteroidal antiinflammatory drugs |
| OVA | ovalbumin |
| PAMAM | polyamidoamine |
| PAMPs | pathogen associated molecular patterns |
| PI | propidium iodide |
| PLGA | poly(lactide-co-glycolide) |
| PMA | phorbol myristate acetate |
| PRP | platelet-rich plasma |
| PRRs | pattern recognition receptors |
| PVA | poly(vinyl alcohol) |
| Q | amount of drug released |
| SDS-PAGE | sodium dodecyl sulphate page electrophoresis |
| SEM | scanning electron microscopy |
| SS | side scatter |
| SWNT | singlewall nanotubes |
| $T_{max}$ | time to maximum drug release rate |
| TCRs | T cell's receptors for antigen |
| $T_g$ | glass transition temperature |
| Th-1 or Th-2 | T helper cells |
| TLRs | toll-like receptors |
| TNF-β | tumour-necrosis factor-beta |
| XRD | X-ray diffraction |

## Origin and Scope

Microparticles are widely used in drug delivery systems to enhance oral bioavailability of poorly absorbed drugs or to induce mucosal immune response (Earley et al., 2001). There is now widespread research and considerable interest in the use of nano particulates for drug delivery and targeting. While there are many publications on the design of nano particulates for drug delivery and targeting, much less is known about their safety and/or toxicity and there is growing concern that there may be unforeseen risks associated with their uses.

The objective of this thesis was to prepare a range of micro and nano particulates from known biocompatible pharmaceutical polymeric excipients using physical processes and evaluate the various aspects of their drug delivery potential, biointeraction and potential toxicity. Polymers: PLGA, chitosan and hyaluronic acid are used in the current study because of their biodegradability and biocompatibility. The selection of antigenic compounds included human serum albumin, ovalbumin and ovalbumin coupled F/G peptide as they are commonly used as allergen models. Ketoprofen and indomethacin are low molecular weight NSAIDs (non-steroidal anti-inflammatory drugs) and they were also used as model drugs. Therefore, the NSAIDs together with the peptides were used to cover a wide range of molecular weights allowing for more thorough screening of properties of those compounds.

<u>The scope of this thesis was:</u>

- To examine the impact of the physical process (emulsion/evaporation, salt precipitation/coacervation and spray drying) employed for production on the physico-chemical properties of the PLGA, chitosan, chitosan-PLGA, hyaluronate-chitosan, chitosan-PVA and hyaluronic acid particles;
- To assess the delivery potential using particulates loaded with both high molecular weight actives such as human serum albumin, ovalbumin, ovalbumin

coupled F/G peptide and low molecular weight drugs such as indomethacin and ketoprofen.

- To assess the potential toxicity of nanoparticles on the basis of their interactions with human platelets and
- To assess the potential of nanoparticles as vaccine adjuvants on the basis of their biointeractions with dendritic cells and spleen cells.

# Table of contents

**Summary** i

**Acknowledgements** iii

**Presentation and publications associated with this thesis** iv

**Abbreviations and symbols** v

**Origin and Scope** viii

**INTRODUCTION**

**Chapter 1 Particulate drug delivery systems**

1.1 Introduction 1

1.2 Poly(lactide-co-glycolide) polymers and particles 2

1.2.1 Antigen delivery and adjuvants 4

1.2.2 Manufacture of PLGA particles 6

1.2.3 Particles stained with coumarin-6 8

1.3 Chitosan (CS) polymers and particles 9

1.3.1 The use of chitosan in antigen delivery 11

1.3.2 Manufacture of chitosan particles 13

1.4 Hyaluronic acid (HA) polymer 15

1.4.1 Antigen delivery using hyaluronic acid polymer 17

1.5 Release of therapeutic agent from particles 18

1.5.1 Mechanisms of drug release from PLGA particles 18

1.5.2 Release of drugs from PLGA particles 22

1.5.3 Release of drugs from chitosan particles 27

**Chapter 2 Nanotoxicity concerns in study of drug delivery system**

2.1 Toxicology in nanotechnology 29

2.1.1 Dendrimers 30

2.1.2 Carbon 30

2.1.3 Synthetic and natural polymers 31

2.2 Human health concerns under the development of nanotechnology 31
2.3 Routes of exposure 32
2.4 Toxicological properties of nanoparticles 34
2.4.1 Toxicological properties of environmental particulate matters 34
2.4.2 Toxicological properties of engineered nanoparticles 34

**Chapter 3 Vaccine adjuvant studies in mucosal vaccination delivery**

3.1 Vaccines and vaccine adjuvants 37
3.2 Immunity 39
3.3 Dendritic cell maturation 40
3.4 Cytokines 41
3.5 Toll-like receptors (TLRs) 42
3.6 T cell activation 43
3.7 Immunity of chitosan as adjuvant 44

**EXPERIMENTAL**

**Chapter 4 Experimental materials and methods**

4.1 Materials 45
4.1.1 Polymers, proteins and general materials 45
4.1.2 Solvents 46
4.1.3 Equipment 47
4.2 Characterisation of polymers 48
4.2.1 Measurement of molecular weight 48
4.2.2 Measurement of chitosan deacetylation 49
4.3 Preparation of micro and nanoparticles 50
4.3.1 Preparation of protein loaded PLGA micro and nano particles 50
4.3.2 Preparation of H S A loaded PLGA nanoparticles with coumarin-6 52
4.3.3 Preparation of OVA loaded chitosan-PLGA particles 53
4.3.4 Preparation of NSAID loaded PLGA nanoparticles 53

4.3.5 Preparation of chitosan microparticles by spray drying 54
4.3.6 Preparation of chitosan nanoparticles 54
4.3.7 Preparation of hyaluronic acid microparticles by spray drying 55
4.3.8 Preparation of hyaluronic acid/chitosan nanoparticles 55
4.4 Characterisation of micro and nanoparticles 56
4.4.1 Particle size analysis 56
4.4.2 Morphology 57
4.4.3 Thermal properties 57
4.4.4 Integrity study of encapsulated protein 58
4.4.5 Fourier Transform Infrared Spectroscopy 59
4.4.6 Crystallinity study 59
4.4.7 Protein loading assay 59
4.4.8 NSAID loading assay 60
4.4.9 Chitosan loading assay 60
4.4.10 Coumarin loading assay 61
4.4.11 Loading of OVA on chitosan nanoparticles 61
4.4.12 Measurement of PVA 62
4.4.13 Measurement of zeta potential 62
4.5 Release studies 62
4.5.1 Protein release studies from PLGA particles 62
4.5.2 NSAID release studies from PLGA particles 63
4.5.3 Coumarin release from PLGA particles 63
4.5.4 OVA release studies from chitosan particles 64
4.5.5 Mathematical modelling of drug release profiles 64
4.6 Measurements of platelet aggregation 65
4.7 Measurements of biointeractions with dendritic cells 66

**RESULTS AND DISCUSSION**

**Chapter 5 PLGA micro and nano particles**

5.1 Introduction 69

5.2 Measurement of polymer molecular weight 70

5.3 PLGA microparticles 71

5.3.1 Preparation of PLGA microparticles 71

5.3.2 Differential scanning calorimetry (DSC) of PLGA microparticles 82

5.3.3 Integrity of protein encapsulated 85

5.3.4 Release study of H S A 87

5.3.5 Release studies of proteins other than H S A 91

5.4 Preparation of PLGA nanoparticles 95

5.4.1 Properties of PLGA nanoparticles 95

5.4.2 Integrity of protein encapsulated 97

5.4.3 Drug free PLGA nanoparticles 98

5.4.4 H S A loaded PLGA nanoparticles stained with coumarin 99

5.4.5 Particle preparations with Digital Sonifier 104

5.5 PLGA nanoparticles loaded with OVA 104

5.5.1 Loading effects on the properties of nanoparticles 105

5.5.2 Loading effects on OVA release 107

5.5.3 Particle size effects on OVA release 111

5.6 PLGA nanoparticles loaded with indomethacin and ketoprofen 113

5.6.1 Properties of the PLGA nanoparticles 113

5.6.2 Differential scanning calorimetry (DSC) 117

5.6.3 Release studies of indomethacin and ketoprofen from PLGA nanoparticles 120

5.6.4 Comparison of ketoprofen and OVA release 125

5.7 Conclusion 127

**Chapter 6 Chitosan-PLGA micro and nano particles**

6.1 Introduction 131

6.2 Characterisation of chitosan 133

6.2.1 Molecular weight 133
6.2.2 Determination of degree of deacetylation of chitosan 134
6.3 Drug free chitosan-PLGA nano and micro particles 135
6.3.1 Drug free chitosan-PLGA nanoparticles 135
6.3.2 Chitosan effects on chitosan-PLGA particles 138
6.4 OVA release from chitosan-PLGA nanoparticles 143
6.4.1 OVA loaded chitosan-PLGA nanoparticles 143
6.4.2 OVA release from chitosan-PLGA nanoparticles 145
6.5 Conclusions 149

**Chapter 7 Chitosan micro and nano particles**

7.1 Introduction 151
7.2 Physicochemical properties of chitosan salts 152
7.2.1 Measurement of molecular weights 152
7.2.2 Measurement of degree of deacetylation 153
7.3 Manufacture of chitosan micro and nanoparticles 156
7.3.1 Preparation of chitosan microparticles by spray drying 156
7.3.2 Preparation of chitosan nanoparticles 159
7.4 In vitro release studies of OVA 165
7.4.1 Physical properties of OVA loaded chitosan nanoparticles 165
7.4.2 Release studies of OVA from chitosan nanoparticles 167
7.5 Conclusions 171

**Chapter 8 Hyaluronate micro particles and hyaluronate-chitosan nano particles**

8.1 Introduction 173
8.2 Hyaluronic acid particles 174
8.2.1 Hyaluronic acid microparticles prepared by spray drying 174
8.2.2 Hyaluronic acid (Fluka)/chitosan nanoparticles 175

8.2.3 Hyaluronic acid (NovaMatrix)/chitosan nanoparticles 180
8.3 Physicochemical properties of sodium hyaluronate 184
8.3.1 Measurement of molecular weights 184
8.3.2 Powder X-ray diffraction (XRD) 185
8.4 Conclusions 186

**Chapter 9 Effects of nanoparticles on platelet aggregation**

9.1 Introduction 187
9.2 Effects of nanoparticles on human platelet aggregation 188
9.2.1 PLGA and CS-PLGA nanoparticles 188
9.2.2 Chitosan nanoparticles 192
9.3 Effects of nanoparticles on collagen induced human platelet aggregation 194
9.3.1 PLGA and CS-PLGA nanoparticles 194
9.3.2 Chitosan nanoparticles 197
9.3.3 PLGA nanoparticles loaded with indomethacin and ketoprofen 198
9.4 Conclusions 201

**Chapter 10 Effects of chitosan nanoparticles on cells as adjuvant in vaccine study**

10.1 Introduction 202
10.1.1 Chitosan solutions induced DC maturation 202
10.1.2 Inducing of IL-6 production by chitosan 203
10.1.3 Application of toll like receptions 203
10.1.4 Toxicity to DCs and spleen cells 204
10.1.5 Chitosan nanoparticles 204
10.2 Effects of chitosan nanoparticles on DCs 205
10.2.1 Enhancement of IL-1ß production by DCs 205
10.2.2 Enhancement of IL-12p40 and IL-12p70 production by DCs 208
10.3 Endotoxin-free chitosan nanoparticles 209

10.4 Effects of endotoxin free chitosan nanoparticle on DCs and spleen cells 211
10.4.1 DC maturation induced by chitosan 211
10.4.2 Enhancement of IL-1β production by DCs with TLR agonists 214
10.4.3 Enhancement of IL-1βproduction by DCs at different concentrations 216
10.4.4 Enhancement of IL-6 and IL-10 production by DCs 217
10.4.5 Enhancement of IL-4 and IFN-γ production by spleen cells 218
10.4.6 Toxicity of chitosan particles to DCs and spleen cells 220
10.5 Conclusions 223

**Chapter 11 General discussion**

11.1 Introduction 224
11.2 Physical properties of micro and nano particles 224
11.2.1 Particle sizes produced under different techniques 224
11.2.2 Drug releases from different particulate formulations 227
11.3 Effects of nanoparticles on platelet aggregation 230
11.4 Immune effects of nanoparticles on dendritic cells (DCs) 232
References 233
Appendices 256

# INTRODUCTION

## Chapter 1 Particulate Drug Delivery Systems

## 1.1 Introduction

The use of polymers in drug formulation is a very large and diverse area of pharmaceutical research and development. Traditionally, polymers have been used as coating agents, capsule materials, binders and thickening agents in various types of therapeutic dosage forms. There are several reasons for encapsulating drugs and other active compounds. Certain drugs are encapsulated to protect the active ingredient against degradation from the environment while others have been encapsulated to reduce the unpleasant taste of certain materials (Schwarz et al., 1995). Encapsulation of drugs also has the potential for reducing both the amount of total drug dosed and the associated side effects as well as the elimination of the discomfort associated with multiple dosing/injection (Schwarz et al., 1995). There are various biodegradable polymers some of which could potentially be used in controlled drug delivery systems, such as poly (L-lactic acid), poly (glycolic acid), chitosan etc.

The desirable properties of a biodegradable polymer are as follows: it must be biocompatible, produce non-toxic degradation products and be degraded either hydrolytically, enzymatically or microbially with a rate that can be modulated according to polymer properties and environmental conditions, have suitable mechanical and physicochemical properties, be economically viable, sterilisable, suitable for processing and free from elutable impurities that may be toxic (Mills and Davis, 1987). Biocompatibility can be achieved by the use of natural polymers such as cellulose, chitin, and chitosan or by the employment of polymers made from naturally occurring monomers such as lactic and glycolic acids (Freiberg and Zhu, 2004).

In the current work, the polymers used were hydrophobic polymers like

poly(lactide-co-glycolide) (PLGA) and hydrophilic chitosan and hyaluronic acid polymers. The processes employed for production of particles were double (single) emulsion technique, precipitation/coacervation and spray drying.

## 1.2 Poly(lactide-co-glycolide) polymers and particles

A vast proportion of the current interest in biodegradable systems focuses on the use of the polyester series based on lactic and glycolic acid. These polymers have an additional advantage over other biodegradable polymers in that they are widely investigated in terms of toxicological and clinical data. Biocompatibility and regulatory approval have attracted investigators to these systems (Lewis, 1990). In 1966, Kulkarni et al. reported that PLA (polylactic acid) was a suitable material for surgical implantation because it was found to biodegrade to normal physiological components. The biocompatibility of polylactide and polylactide-co-glycolide was demonstrated using sutures by Cutrigh et al. (1971) and Craig et al. (1975) in rat tissue. These materials are well tolerated in living tissue and do not cause irritation (Bos et al., 1991), and are progressively degraded then resorbed followed by complete tissue recovery (Robert et al., 1993). Visscher and co-workers (1987) confirmed the biocompatibility of polylactide and poly (lactide-co-glycolide) injectable microspheres by examining tissue from the injected site over time.

Due to the excellent biocompatiblility and bioresorbability of lactide/glycolide based polymers, some of these bioresorbable materials have successfully been used in products for the medical industry. Examples include Dexon® Maxon® and Vicryl® as sutures as well as Biofix® and Phusiline® bone fracture internal fixation devices (Dunne, 2000). These materials have also been investigated for many medical applications including dental applications (Robert et al., 1993) and internal fracture fixation devices (Leenslag et al., 1987).

Poly (d,l-lactide-co-glycolide) (PLGA) is the polymerisation product of lactide and glycolide. The mechanism of co-polymerisation is shown in Figure 1.1 (Gilding and Reed 1979).

Glycolide

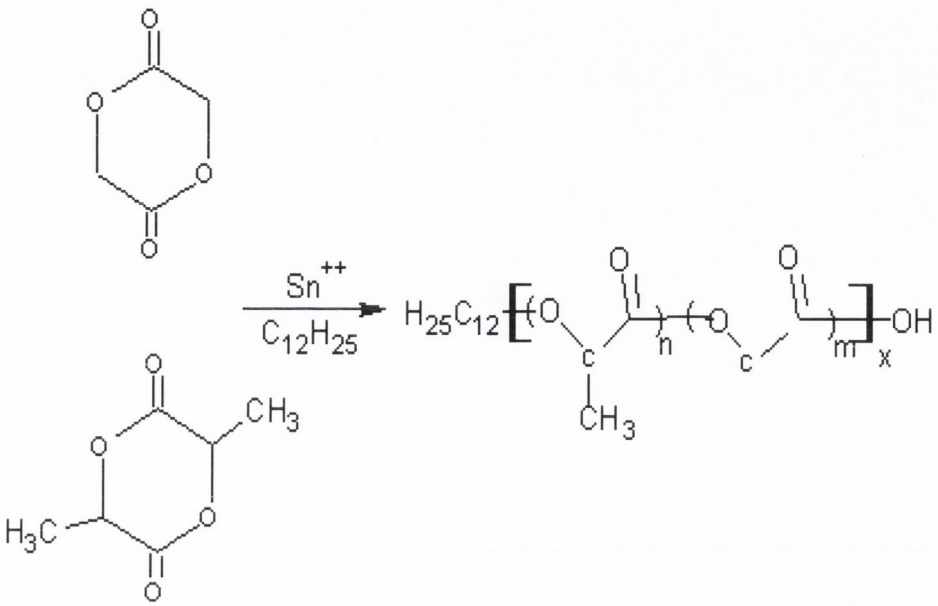


Lactide

n: number of units of lactic acid

m: number of units of glycolic acid

x: number of lactic acid/glycolic acid group

Figure 1.1 Polymerisation of lactide and glycolide to produce poly-lactide-co-glycolide polymers.

Lactic acid is more hydrophobic than glycolic acid and PLGAs with a higher lactic to glycolic ratio are more hydrophobic (Walter et al., 2001). Hence, PLGA polymers with higher lactic to glycolic ratios degrade more slowly, than those with higher glycolic acid ratios.

Poly (d,l-lactide-co-glycolide) undergoes biodegradation to form lactic and glycolic acid monomers, which are eliminated from the body via Krebs cycle. The l- (+) form of lactic acid is naturally produced and metabolised in the body; lactate is an intermediate or end product found in carbohydrate metabolism in all life forms. Lactate is oxidised to pyruvate, which is either converted to glucose or decomposed to carbon dioxide and water (Visscher et al., 1987). Glycolic acid is a physiological intermediate product in the degradation of the amino acid glycine and is converted to carbon dioxide by oxidative carboxylation (Visscher et al., 1987). The only condition required for degradation to occur seems to be the presence of an aqueous environment (Visscher et al., 1987).

### 1.2.1 Antigen delivery and adjuvants

Antigen, a foreign substance, is usually a protein that stimulates the body's immune system to produce antibodies. Adjuvants are added to antigens to improve the immune response and a combination of adjuvant with antigen formulates vaccine. Lactide/glycolide polymers have been extensively used in vaccine delivery studies as adjuvant because of their biocompatibility and biodegradability. By encapsulation, antigen could be protected and sustained antigen release could be obtained following the diffusion or a polymer degradation process. Microparticles made by such polymers offer a flexible choice of administration routes. They can be injected intravenously (i.v.), subcutaneously (s.c.), intramuscularly (i.m.) or intraperitoneally (i.p.) (Linhardt, 1990) for either sustained release depots or target drug carriers. Sustained release products have been formulated for injectable, topical, implantation and pulmonary application (Dunne, 2000).

In the early work reported by Eldridge and co-workers (1991), the utility of poly(lactide-co-glycolide) (PLGA) microparticles as a vaccine delivery system for the mucosal antibody responses was investigated. Intraperitoneal (i.p.) injection of

1–10 μm microspheres into mice with loading of approximately 1% by weight a formalinised toxoid vaccine of staphylococcal enterotoxin B (SEB), dramatically potentiated the circulating IgG anti-toxin antibody response as compared to the free toxoid (Eldridge et al., 1991). This was due to the fact that particles of less than 10 μm were phagocytosed by macrophages followed by migration of these cells to draining lymph nodes at the injection site (Eldridge et al., 1991). Microencapsulation stabilises the active material and also allows the drug to pass through the stomach unaffected by digestive enzymes which would normally degrade the drug (Eldridge et al., 1991).

Earley et al. (2001) investigated the suitability of a micro particulate vaccine delivery system to elicit mucosal antigen-specific immune responses in the upper respiratory tract of young calves. Microparticles containing ovalbumin (OVA) were prepared using PLGA polymer with molecular weight of 40-75 kDa and a lactide/glycolide ratio of 50:50. The microparticles were prepared by the double emulsion technique (Section 1.2.2) and the resultant particles presented particle diameter sizes smaller than 10 μm. The theoretical OVA loading of particles was 20% w/w. Microparticulate samples were administered into calve nasal cavities using an intranasal applicator attached to a 5 ml syringe. The presence of OVA-specific IgA antibody was detected from nasal washings. Significant levels of ovalbumin specific secretory IgA was detected as early as one week post-administration. The levels persisted throughout the duration of the study (4 month), demonstrating that intranasal administration of ovalbumin in biodegradable PLGA particles less than 10 μm in diameter generated an antigen-specific systemic and mucosal antibody response in calves. The persistence of antigen-specific IgA antibody in the nasal washings of immunised animals was a very encouraging feature of this vaccine delivery system and may generate long lasting levels of local anti-viral protection (Earley et al. 2001).

With concerns regarding PLGA specific potential for nasal vaccination, the results published over the last 10 years have led to the conclusion that the efficacy of PLGA microparticles as antigen carriers was correlated with their uptake into the specialised mucosal-associated lymphoid tissue (Singh and O'Hagan, 2002). An additional observation made by some authors was that the size of the particles influences the immune responses generated by the encapsulated antigens following nasal administration (Köping-Höggård et al., 2005). For example, Somavarapu et al., (1998) demonstrated that the immune response to encapsulated ovalbumin administered intranasally was significantly greater for PLA nanoparticles than for PLA microparticles. This result was thought to be due to the more efficient transport of nanoparticles compared with that of microparticles across the nasal mucosa (Köping-Höggård et al., 2005). In fact, several studies have demonstrated that the transport of model polystyrene particles across well-organised epithelia is clearly dependent on the size. This factor is thought to be more significant for nanoparticles than for microspheres (Florence, 1997).

### 1.2.2 Manufacture of PLGA particles

For biodegradable polymers like PLGA, the general methods of manufacture of drug-loaded microparticles are single or double emulsions (Fitzgerald, 1994). The single emulsion process involves oil-in-water emulsification. The polymer is first dissolved in an organic phase and the drug is then added to the polymer solution. This polymer-solvent-drug solution is then emulsified in a larger volume of water in the presence of emulsifier like PVA to yield an o/w emulsion. Finally, solvent is removed by rotary evaporation or extraction. Once formed, the particles are generally centrifuged down and washed to remove residual solvent. The particles are then freeze dried. One of the disadvantages of the o/w emulsification method is poor encapsulation efficiencies of moderately water-soluble and water soluble drugs (Jalil et al., 1990; Wu, 1995; Arshady, 1991). The drug may diffuse out or partition

from the dispersed oil phase into the aqueous continuous phase. This would result in poor trapping of the hydrophilic drug and high initial rapid release of the drug (Jalil et al., 1990). The o/w emulsification process is therefore widely used to encapsulate lipid-soluble drugs (Jalil et al., 1990).

The double emulsion process is a water-in-oil-in-water (w/o/w) method and is best suited to encapsulate water soluble drugs like peptides and proteins (Jalil et al., 1990; Wu 1995; Lewis, 1990). First, an aqueous solution of drug is added to an organic phase, consisting of PLGA solution in a solvent such as dichloromethane or ethyl acetate, to form the first w/o emulsion. This emulsion is further emulsified into an aqueous phase such as polyvinyl alcohol (PVA) solution to produce the final w/o/w emulsion. Finally, solvent is removed by rotary evaporation or extraction. Once formed, the particles are generally centrifuged down and washed to remove residual solvent. The particles are then freeze dried.

Processing parameters can be used to control particle morphology. Particle size is determined by the mixing speed, equipment and technique used (Watt et al., 1990). Increasing the rate and length of time of the emulsification process decreases the mean diameter of the microspheres and also reduces the particle size distribution (Benita et al., 1984; Jeffery et al., 1991 and Sansdrap et al., 1993). The particle size can be adjusted through the process parameters to produce particles in nano and micrometer (100 nm-2 mm) range (Arshay, 1991).

The most common disperse phase solvent employed for double emulsion procedures is dichloromethane (Suzuki and Price 1985; Spenlehauer et al., 1986, Benita et al., 1984). However the draw back in the use of dichloromethane is its toxicity (Martindale 1999) as quantities of solvent can remain in the microspheres after drying. Attempts have been made to substitute chlorinated solvents such as dichloromethane with alternative solvents such as ethyl acetate (McGee et al., 1995)

and halothane (Armstrong et al., 1994 and 1995). Spray drying can also be used to produce PLGA particles. More details about spray drying are discussed in Section 1.3.2.

### 1.2.3 Particles stained with coumarin-6

As an antigen carrier, it is important to study the kinetics of cellular and tissue uptake, intracellular distribution and retention, and *in vivo* biodistribution (Panyam et al., 2003). For example, it might be interesting to study the efficiency of nanoparticle localisation in a particular cell population, organ or specific tissue following their local or systemic administration to optimise drug therapy (Panyam et al., 2003).

The most common experimental approach found to study particle uptake *in vivo* or *in vitro* is the use of fluorescently or radioactively labelled particles because particle uptake by cells becomes detectable by fluorescence microscopy and the extent of particle uptake may be detected by flow cytometry (Pietzonka et al., 2002).

In the study reported by Pietzonka and the co-workers (2002), PLGA nanoparticles with size of 300-600 nm were prepared by the emulsion technique. Methylene chloride was used as solvent to which a lipophilic marker, coumarin-6, was added. The fluorescent marker loading of coumarin-6 to PLGA nanoparticles was over 95%. *In vitro* release study was carried out in Tris-borate (TB) buffer which contained potassium chloride, calcium chloride and magnesium chloride. The duration of the study was 180 minutes and demonstrated within this timeframe that only marginal marker release rates were detected and this was expected from the low water solubility of the lipophilic marker (Pietzonka et al., 2002). According to their fluorescent microscopy observations, particles were attached to the apical surface of the cells (Pietzonka et al., 2002).

In this study, coumarin-6 was loaded onto PLGA nanoparticles to evaluate visualisation of the particles under fluorescence microscope. It is preferred to use coumarin as fluorescent labelling because of easier handling, to avoid the problems associated with the use of radioactive material.

## 1.3 Chitosan (CS) polymers and particles

Chitin, derived from the exoskeletons of crustaceans, is an abundant natural polymer. Upon deacetylation, it yields the novel biomaterial chitosan. Chitins which have been deacetylated to a degree of between 40% and 98% are regarded as chitosan (Illum, 1998). Depending on the degree of deacetylation chitosans contain different numbers of acetyl groups. Chitosan (CS) is a polysaccharide with a structure comparable to cellulose (Domard et al., 1998); CS and cellulose are both made by a linearly β-(1→4)-linked monosaccharide. The essential difference between CS and cellulose is that CS is composed of 2-amino-2-deoxy-β-D-glucan combined by glycosidic linkages. The structure of chitosan is shown in Figure 1.2. Chitosan is insoluble at neutral and alkaline pH values but forms salts with inorganic and organic acids such as glutamic, hydrochloric, lactic and acetic acids (Illum, 1998).

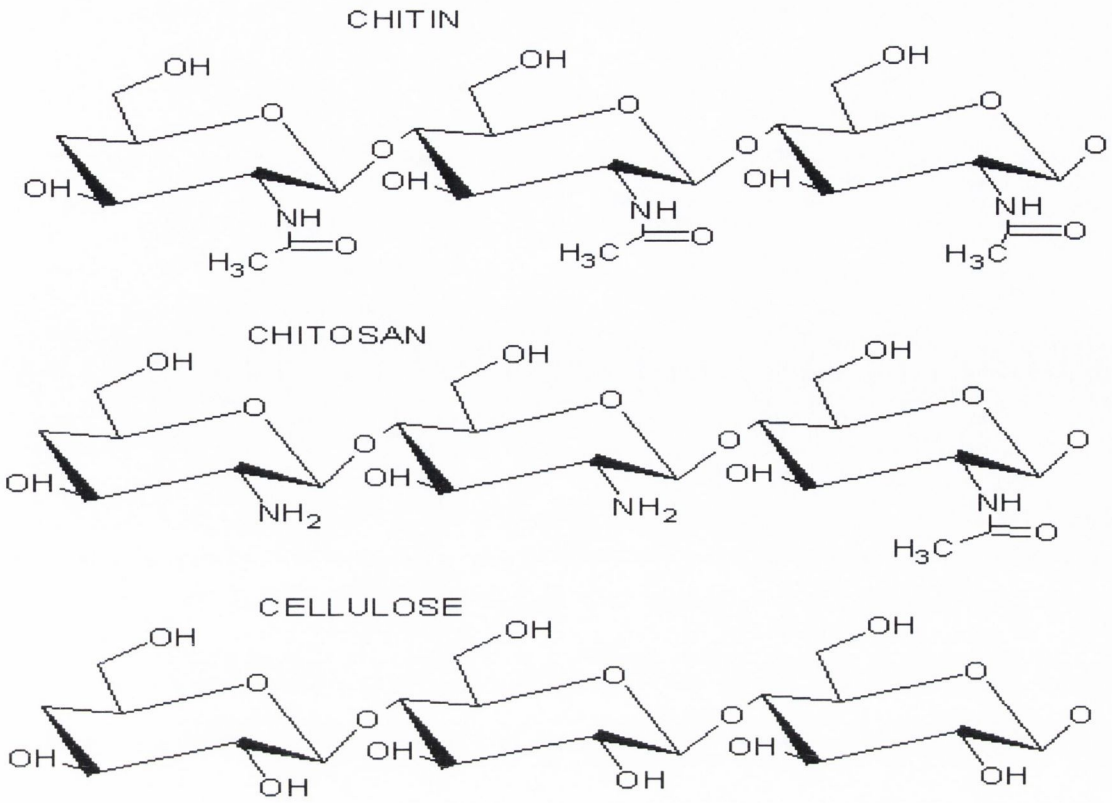


Figure 1.2 Chemical structures of chitin, chitosan and cellulose.

Paul and Sharma (2000) described medical and pharmaceutical applications of chitosan which include drug delivery, wound healing ointments and dressings, artificial skin, haemostatic agents, enzyme immobilization, dialysis membranes, contact lenses or eye bandages, orthopaedics, surgical sutures and dentistry. Chitosan has a lipid-lowering effect, is biocompatible, non-toxic and biodegradable (Paul and Sharma 2000; Pangburn et al., 1982; Dornish et al., 1996; Yang et al., 2003). Chitosan molecules are strongly positively charged at pH of 6.5 and also form gels with polycations at low pH. They are described as having antacid properties and anti-ulcer activity which may reduce drug irritation in the stomach. The U.S. F.D.A have approved chitosan as a food additive in animal feed and it is a generally recognised as safe (GRAS) substance (www.fda.gov). A study by Miura et al., (1995) showed that chitosan as a food additive in normal and neonatal streptozotocin-induced diabetic mice significantly reduced blood glucose, cholesterol and triglyceride level. Intramuscular injection of chitosan as

microspheres in rats showed tissue compatibility.

It has been reported that chitosan can aid the dissolution of poorly soluble drugs. Griseofulvin and prednisolone when ground with chitosan showed enhanced dissolution properties (Sawayanagi et al., 1982; Sawayanagi et al., 1983). They also described chitosan as an excipient for direct compression of tablets with 50% chitosan resulting in rapid disintegration. Ritthidej et al. (1994) showed that when chitosan was included in tablets in a concentration higher than 5% it was superior as a disintegrant to corn starch and microcrystalline cellulose. Chitosan was found to be a better tablet binder than methylcellulose and sodium carboxymethylcellulose by Upadrashta et al. (1992).

### 1.3.1 The use of chitosan in antigen delivery

From a biopharmaceutical point of view, chitosan displays several interesting properties that make it suitable as an adjuvant for mucosal vaccine delivery as adjuvant. In the work reported by Lehr et al., (1992), chitosan was examined for mucoadhesive properties by measuring the force of detachment of swollen polymer films from pig intestinal mucosa in a saline medium. Cationic polymer chitosan was shown to be fairly mucoadhesive in comparison to polycarbophil as a reference substance (Lehr et al., 1992). This may be an explanation of the work reported by Miyazaki et al., (1988), in which, after oral administration of granules prepared from a 1:2 mixture of drug and chitosan, the absorption of indomethacin in rabbits was prolonged.

In another work reported by Illum et al. (1994), a nasal solution formulation of the cationic material chitosan was shown to greatly enhance the absorption of insulin across the nasal mucosa of rat and sheep. The molecular weight of chitosan used was higher than 130 kDa. The absorption promoting effect was concentration

dependent with the optimal efficacy obtained for concentrations higher than 0.2% in rats and 0.5% in sheep (Illum et al., 1994). The absorption promoting effect was reversible with time (Illum et al., 1994).

Since high molecular weight chitosan solutions have been proposed as vehicles for nasal immunization (Illum et al., 1994), Vila et al. (2004) focused their work on the investigation of the potential utility of low molecular weight chitosan in the form of nanoparticles as nasal vaccine delivery vehicles. Chitosan nanoparticles (size range 350 nm) made of low molecular weight chitosan materials of 23 and 38 kDa were formulated by an ionic cross-linking technique. Tetanus toxoid was used as a model antigen. Following intranasal administration, tetanus toxoid loaded nanoparticles elicited an increased and long-lasting humoral immune response (IgG concentrations) as compared to the liquid vaccine (Vila et al. 2004). The confocal laser scanning micrographs indicated that chitosan nanoparticles can cross the nasal epihthelia and, transport the associated antigen (Vila et al. 2004).

Tozaki et al. (1997) investigated colon-specific bovine insulin delivery with chitosan capsules. They evaluated intestinal absorption of insulin by measuring plasma insulin levels and insulin's hypoglycemic affect. A hypoglycemic effect was observed which started 8 hours after the administration of chitosan capsules, which corresponded to the time the capsules entered the colon, evaluated by transit time experiments with chitosan capsules. Tozaki et al. (1997) described how, by targeting the drug to the colon, where there is a relatively low activity of proteolytic enzymes, sufficient drug was absorbed to produce a hypoglycemic effect.

In the work reported by Seferian and Martinez (2001), a synthetic peptide, recombinant beta-human chorionic gonadotropin (βhCG) was used as an antigen. Two new adjuvant formulations, a zinc-chitosan particle and an emulsion formulation containing chitosan were formed to investigate their potentials in

developing vaccines based on synthetic peptides and subunit antigens. Antibody analysis revealed an IgG1 response in mice immunised with zinc-chitosan particles and a mixed IgG1, IgG2a and IgG2b response with the emulsion (Seferian and Martinez, 2001). These chitosan based adjuvant formulations were effective in sensitising mice and guinea pigs for antigen specific, delayed type hypersensitivity responses, indicating that these adjuvants stimulate both B and T lymphocytes (Seferian and Martinez, 2001). The molecular weight of the chitosan was not reported.

Chitosan particles with different particle sizes (diameter range from 0.4 μm to 3 μm) were prepared in the work reported by Nagamoto et al. (2004). Three chitosans were used with molecular weight of 10kDa, 100kDa and 500kDa, respectively, and the technique used was coacervation and precipitation. IgG induced by intranasal administration (i.n.) of nanoparticles was comparable with that by intraperitoneal administration (i.p.) and IgA induced by i.n. of 0.4-μm and 1-μm size nanoparticles was significantly higher than control (OVA and CT) (Nagamoto et al. 2004). Most of the works based on chitosan were studied *in vivo*, rather than *in vitro* and it therefore becomes interesting to study their release behaviours *in vitro*.

## 1.3.2 Manufacture of chitosan particles

One of the methods which have been used to produce chitosan microparticles is spray drying. Spray drying is a method of powder production whereby a feed material is transformed from a liquid state into a dried particulate form in a one step process. Being in use since the early 1940s, it has been used for excipient production, microencapsulation, granulation and complex formation, modification of biopharmaceutical properties, solid dispersion production, dry powder aerosol formulation and processing of heat sensitive materials (Broadhead et al., 1992). The spray drying process involves four stages (Masters, 1985): (a) atomisation of feed

into a spray (b) spray-gas contact (c) evaporation (drying of spray) and (d) product recovery and air cleaning.

Atomisation involves the exertion of a force onto a liquid resulting in droplet formation. The Büchi Mini Spray dryer, used in this study, is a laboratory scale spray drier and contains a two fluid (pneumatic) atomiser. It operates co-current drying, by which the spray feed materials and drying air pass through the dryer in the same direction. Co-current is less economical in terms of heat utilisation but it is preferable for heat sensitive materials since the dry product is in contact with only the coolest air (Masters, 1985). While air is the most common drying gas, the drying air can be replaced by an inert gas, such as nitrogen, when using closed cycle spray dryers (Broadhead et al., 1992). Following atomisation of the feed, evaporation from the droplet begins.

A schematic diagram of a co-current spray dryer is shown in Figure 1.3 (Masters 1985).

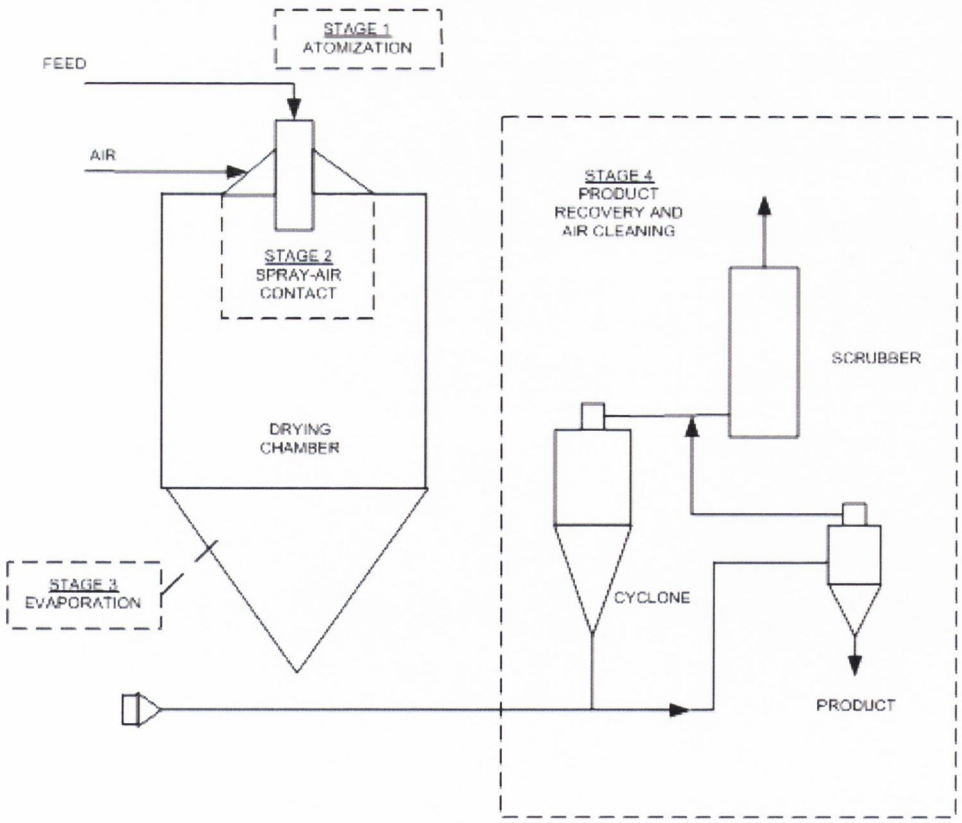


Figure 1.3 Schematic diagram of a co-current spray dryer.

Processing conditions can affect the properties of resultant powders in relation to appearance, particle size and size distribution, bulk density, particle density, porosity, moisture content, flowability, stability, dispersability, friability and compressibility (Masters, 1985).

Because chitosan particles swell quickly in water and there is evidence that cross-linking agent can hinder the swelling capacity of the uncross-linked chitosan microparticles (Desai and Park, 2005), the frequently used cross-linking agent glutaraldehyde was used in this study to cross-link chitosan during manufacture of microparticles.

Other methods can be used to formulate chitosan microparticles. Berthold et al. (1996) produced chitosan microparticles based on a precipitation process using sodium sulphate as a precipitant. Chitosan is poorly soluble in water. Addition of an acid improves the solubility of the protonation of the amino groups. The solubility is also dependent on other anions present in the solution. In the presence of acetate, lactate or glutamate chitosan shows good solubility, whereas phosphate, polyphosphates and sulphate decrease the solubility. For this reason, sulphate was used for microsphere formulation in the work of Berthold et al. (1996).

In the current work nanoparticles containing chitosan were successfully prepared, as single or complex formulations with PLGA, hyaluronic acid and PVA, using various methods and techniques. Microparticles of chitosan were prepared by spray drying.

## 1.4 Hyaluronic acid (HA) polymer

Hyaluronic acid (HA) comprises of linear, unbranching, polyanionic disaccharide units consisting of glucuronic acid (GlcUA) and N-acetyl glucosamine (GlcNAc)

(Figure 1.4) (Weigel et al., 1997; Weissmann and Meyer 1954). HA is biodegradable, biocompatible and viscoelastic (Zhong et al., 1994; Prestwitch et al., 1998; Brown and Jones 2004; Hahn et al., 2004) with a wide molecular weight range from 1000 to 10,000,000 Da. Carboxylic groups in the glucuronic acid unit are the activation centre of the enzyme hyaluronidase (Zhong et al., 1994). In the work reported by Zhong et al. (1994), water soluble HA degraded by the enzyme testicular hyaluronidase presented a sharp reduction of viscosity within 4.5 hours.

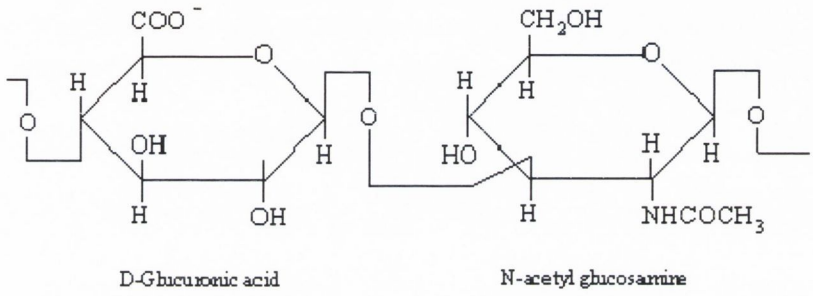


Figure 1.4 Disaccharide repeating unit of HA comprising GlcUA and GlcNAc.

HA is found in synovial fluid and extracellular matrix (ECM), with the highest concentration in soft connective tissues, such as skin and cartilage. It is present in hydrated networks with collagen fibres in the ECM (Fraser et al., 1997) and is a major component of joint tissue and influences the hydration of cartilage (Fukuda et al., 1996). HA plays an important role in maintaining and regulating the water balance to tissues and facilitating the transport of nutrients and waste and also it plays pivotal roles in wound healing, and in promoting cell motility and differentiation during development (Goa and Benfield, 1994).

Because of its various functions and physicochemical properties, HA and modified HA have been extensively investigated and used for arthritis treatment (Balazs and Denlinger, 1993), ophthalmic surgery (Balazs, 1983), drug delivery (Joshi et al.,

1992) and tissue engineering (Feinberg and Beebe 1983). In the study by Joshi and the co-workers (1992) drugs (hydrocortisone, hydrocortisone hemisuccinate sodium, fluorescein sodium, benzyl alcohol, mafenide acetate) were loaded into sodium hyaluronate membranes by means of either: 1) physical incorporation, 2) physical incorporation in the membrane, then lamination with a second polymer (ethyl or benzyl ester membranes) or 3) covalently bonding to the polymer. The release of the model compounds was found to be rapid when the compounds were physically incorporated; the release could be slowed by laminating the core membranes. When the drug was covalently bound to the polymer, the release was slow and near zero-order.

### 1.4.1 Antigen delivery using hyaluronic acid polymer

Rafi et al., (1997) investigated whether HA solution would induce a proliferate response in mouse lymphocytes. In their study, spleen cells exhibited strong proliferative responsiveness to stimulation with soluble HA. Purified B cells, but not T cells, were found to respond to HA. HA was unable to stimulate T cells, while in contrast, HA stimulated B cells *in vitro*, and led to B-cell differentiation as measured by production of IgM antibodies in addition to increased expression of CD44 (Rafi et al., 1997). CD44 is a widely distributed cell surface glycoprotein whose principal ligand has been identified as hyaluronic acid (Rafi et al., 1997). Also, HA-induced proliferation of B cells from lipopolysaccharide (LPS)-unresponsive C3H/HeJ mice strain responded strongly to stimulation with HA, indicating that the stimulation effects were not induced by LPS (Rafi et al., 1997). Such stimulations may play a critical role during normal or autoimmune responsiveness of B cells. The molecular weight of HA used was not reported. These results indicated the potential uses of hyaluronic acid as drug delivery adjuvant.

To date one work has been reported focusing on the delivering of hyaluronic acid as a particulate drug delivery system. In the work by Hahn et al. (2004), hyaluronic acid microparticles containing recombinant human growth hormone (SR-hGH) were prepared by spray drying and a sustained-release of hormone in beagle dog tests *in vivo* was detected. Bioavailability of SR-hGH was comparable to that of a conventional aqueous daily injection formulation with an equivalent dose. The administration of SR-hGH induced elevation of serum IGF-I level for 6 days with a maximum value higher than the predose level of 350 ng/ml between 48 and 72 h. After 6 days, IGF-I level returned to the initial baseline level. No adverse effects were observed during and after the beagle dog tests (Hahn et al. 2004).

## 1.5 Release of therapeutic agent from particles

### 1.5.1 Mechanisms of drug release from PLGA particles

Release of the entrapped therapeutic agent from the PLGA matrix has been found to occur through diffusion-cum-degradation-mediated process (Fitzgerald and Corrigan 1993). It has been demonstrated that during the early phases, the release of the entrapped therapeutic agent occurs mainly through its diffusion in the polymer matrix while during the later phases the release is mediated through both diffusion of the therapeutic drug and the degradation of the polymer matrix itself. Thus, the degradation of the polymer with concomitant release of the entrapped drug plays an important role in the release mechanism from biodegradable polymeric microparticles (Ramtoola et al., 1992; Anderson and Shive, 1997).

Diffusion can be defined as a 'process of mass transfer of individual molecules of a substance brought about by random molecular motion and associated with a concentration gradient'. Higuchi (1961) developed an equation for release of solid drug from an ointment base and later applied it to the diffusion of solid drug in a

granular matrix dosage system (Equation 1.1).

$$Q = \left(DC_m\left(2C_t - C_s\right)t\right)^{1/2} \qquad \text{Equation 1.1}$$

where Q is the amount of drug released per unit area of matrix, D is the diffusivity of the drug in the matrix, $C_t$ is the total amount of drug per unit volume of matrix, $C_m$ is the solubility of drug in the polymer matrix, $C_s$ is the solubility of the drug in the sink phase and t is the time.

This model assumes that 1) there was excess drug presented compared to the solubility of the drug in the polymer matrix, 2) a constant diffusion coefficient, 3) the drug particle size was small compared to the size of the matrix, 4) there was no interaction between the drug and the polymer, and 5) release study was under sink conditions.

In the work reported by Jalil and Nixon, the rate of phenobarbitone release from irregularly shaped poly-lactic acid microparticles can be adequately described using the Higuchi equation (Higuchi, 1961), describing drug release from a single surface granular matrix (Jalil and Nixon, 1990).

Assuming that the total quantity of drug initially present in the polymer matrix $C_0$ is in excess of the solubility of the drug in the matrix $C_m$, Equation 1.1 may be simplified to give Equation 1.2 (Fitzgerald, 1994).

$$\frac{M_t}{M_\infty} = Ht^{1/2} \qquad \text{Equation 1.2}$$

$M_t/M_\infty$ is the fraction of total drug content released at time t, H is a constant.
This relationship is similar to the general power law expression proposed by Peppas

and Sinclair in 1984 and further described by Ritger and Peppas (1987) (Equation 1.3).

$$\frac{M_t}{M_\infty} = Kt^n \qquad \text{Equation 1.3}$$

Where K is the diffusion constant, and n is the diffusion exponent.

If it is a diffusion controlled release, the diffusion exponent in Equation 1.3 is n=0.5, by assuming that the total quantity of drug initially present in the polymer matrix is in excess of the solubility of the drug in the matrix (Peppas and Sinclair, 1984; Fitzgerald, 1994). At n = 0.432 the equation describes the diffusion release from a sphere (Peppas and Sinclair, 1984).

The hydrolytic degradation of aliphatic polyesters of the PLGA type was characterised by a decreasing molecular weight and an increased uptake of water as degradation proceeds, generation of microporosity and weight loss or erosion (Hutchinson and Furr, 1990). The degradation is known to primarily depend on the kinetics of the cleavage of main chain ester bonds. The polyesters of α-hydroxy carboxylic acid are hydrolytically degraded into their corresponding monomeric hydroxyacids under environmental as well as under physiological conditions (Hutchinson and Furr, 1990). The principal parameters controlling degradation are polyester composition, polymer structure with regard to the distribution and segmental length of co-monomer units in polymer molecular weight and its distribution (Hutchinson and Furr, 1990).

Usually, drug release from PLGA particles is combined with a burst release, followed by a sustained drug release. If the initial fast release is considered to result from rapid dissolution of the drug domains at the solid-liquid surface, then its

magnitude will be dependent on the proportion of drug at the surface (Wagner, 1969) Assuming that there is no drug dissolved at time zero, the following equation (Equation 1.4) may be used to describe the initial surface drug dissolution process from PLGA discs (Gallagher and Corrigan, 2000):

$$W = W_L F_B (1 - e^{-K_B t}) \qquad \text{Equation 1.4}$$

W is the amount in solution at time t, $F_B$ is the fraction of the drug load released in the burst phase, $W_L$ is the total quantity of drug in the compact and the release rate constant $K_B$ can be described by Equation 1.5 (Gallagher and Corrigan, 2000):

$$K_B = DAC_s / W_L F_B h_l \qquad \text{Equation 1.5}$$

D and $C_s$ are the diffusion coefficient and solubility of the drug, respectively. A is the surface from which the drug is available for dissolution and $h_l$ is the apparent aqueous diffusion boundary layer thickness.

The second phase of drug release, controlled by a polymer degradation mechanism, may be described by an equation in the form of Equation 1.6 (Prout and Tompkins, 1944; Ramtoola et al., 1992). In the work reported by Ramtoola and co-workers, this equation was applied to the release of fluphenazine from PLGA microspheres.

$$ln\left(\frac{\chi}{1-\chi}\right) = kt + kT_{max} \qquad \text{Equation 1.6}$$

where $\chi$ is the fraction of drug released over time t, k and $T_{max}$ are the rate constant and time to maximum drug release rate, respectively. The values of k and $T_{max}$ are related to drug loadings and polymer composition (Ramtoola et al., 1992).

By combining Equation 1.4 and Equation 1.6, the total fraction of drug released at time t ($F_{TOT}$) is given by the sum of drug released by surface diffusion and that released by degradation control (Equation 1.7). This equation was applied to the release of levamisole from PLGA microspheres and co-evaporated discs (Gallagher and Corrigan, 2000).

$$F_{TOT} = F_B\ (1 - e^{-K_B t}) + (1 - F_B)\ (\frac{e^{kt-kT_{max}}}{1+e^{kt-kT_{max}}}) \qquad \text{Equation 1.7}$$

Equation 1.7 assumes two additive release processes: an exponential fast release phase with parameter $F_B$ which can be defined as the fraction of drug available for direct surface release. $K_B$ is the release rate constant related to the initial quantity of drug in the particles, drug solubility and surface area of drug available for dissolution. The second release process is a degradation controlled release phase with parameters k which is the rate constant and $T_{max}$, the time to maximum drug release rate. k is related to drug content (Fitzgerald and Corrigan, 1993).

## 1.5.2 Release of drugs from PLGA particles

In the work reported by Hutchinson and Furr (1990), the mechanism of zoladex (synthetic analogue of luteinizing hormone-releasing hormone LHRH) release from PLGA slabs was studied. It has been shown that release of zoladex occurs by diffusion through aqueous pores generated in the dosage form. These aqueous channels which facilitate drug release are generated by two distinct and separate mechanisms. The first involves leaching of drug from polypeptide domains at or near the surface and essentially is diffusion/dissolution controlled event through aqueous pores (Hutchinson and Furr, 1990). However, drug within the body of the

depot, existing in isolated domains not continuous or contiguous with the surface, cannot be released until the second mechanism becomes operative. This second mechanism involves degradation of the polymer and is associated with the generation of microporosity in, and enhanced water uptake by, the degradation polymer and, ultimately, erosion of the polymer carrier (Hutchinson and Furr, 1990). Typical parameters controlling the initial phase of release are drug loading and morphology, whereas the second phase is intrinsically related to the degradation properties of the polymer. The degradation of PLGA is dependent on molecular weight, polydispersity, polymer composition and polymer structure (Hutchinson and Furr, 1990). When these two phases of release do not overlap, discontinuous release is observed. However, by controlling the properties of the polymer, the initial phase of release can be made to overlap with the second phase, and depots can be defined which give continuous release over not less than 28 days (Hutchinson and Furr, 1990).

Yeh et al., (1995) reported that the release of ovalbumin (OVA) from PLGA (50:50 RG503, molecular weight 9000Da) microparticles showed a significant degradation controlled release over 35 days. A progressive formation of pores resulted in a continuous release of the active agent from these systems (Yeh et al., 1995). The PLGA microparticles were formulated by double emulsion technique and the mean particle size were 8.74 μm and 1.77 μm, with OVA loading of 3.73% and 7.55%, respectively. Around 50-60% of the encapsulated OVA was released from PLGA particles over 35 days in PBS (phosphate buffered saline) buffer (pH 7.4) at 37 °C, with a small burst protein release at the first day.

Using a phase separation technique, McGee et al., (1995) reported their OVA release profile from PLGA (50:50 RG503, molecular weight 9,000 Da) microparticles. These particles initially presented a burst OVA release of 8-15% and then followed by a release at a constant rate. Zero order release was achievable for 20 days in

PLGA systems at different particle sizes and loading levels. The loadings were 1.2 %, 2.7 % and 5.1 % with particle sizes of 6.2 μm, 9.8 μm, and 8.7 μm, respectively. In this work, OVA solution was dispersed in silicone oil and homogenised. During homogenisation, the silicone oil mixture was immersed in liquid nitrogen to keep to temperature at between 5 and 15 °C during the entire mixing process. Then, a solution of RG 503 in dichloromethane was added into the mixture via a syringe under homogenization. Finally, particles were transferred and stirred to and evaporate the solvent and collected by centrifugation. Most of the OVA were released out within 20 days in PBS buffer (pH 7.4) at 37 °C. Compared to the release work reported by Yeh et al., (1995), the protein release behaviours could be different under different particulate manufacture techniques, although using similar PLGA polymers.

Bovine serum albumin (BSA) was encapsulated in PLGA nanospheres by the double emulsion technique to evaluate how the solvent elimination procedure, the copolymer type (different molecular weight and number of carboxyl groups) and the surfactant Poloxamer 188 affected the properties of the nanoparticles (Blanco et al., 1997). The release studies were carried out over 30 days in PBS buffer (pH=7.4) at 37 °C. The three PLGA polymers used were RG 502 (50:50, molecular weigh 12 000Da), RG 503 (50:50, molecular weight 34 000Da) and RG 503H (50:50, molecular weight 34 000Da) with higher number of carboxyl groups than RG 503. The mean sizes of the nanoparticles ranged from 300 to 600 nm and by increasing PLGA molecular weight and by the incorporation of surfactant Poloxamer 188, particle sizes increased. The protein loading efficiency varied from 40 to 90% (loading from 0.4% to 0.9% of particles) (Blanco et al., 1997). PLGA nanoparticles made of lowest molecular weight presented relatively the highest BSA release rate constants and PLGA nanoparticles prepared by RG 503 presented higher release rate constants compared to nanoparticles prepared by RG 503H, indicating that both of polymer molecular weight and carboxyl groups number have effects on BSA release

from PLGA particles. Poloxamer 188 is a protein stabiliser with a theoretic loading of 1% w/v. The loading of poloxamer 188 increased the BSA release rate from PLGA nanoparticles. Both extraction and evaporation are ways to eliminate the solvent ethylacetate during particle preparations. In the study of Blanco et al. (1997), the releases were not significantly affected by using these different methods of solvent elimination.

Human serum albumin (H S A) was encapsulated as a model protein in microparticles of biodegradable and biocompatible polymers, such as poly(lactide-co-ethylene glycol) (PELA) and poly(lactide-co-glycolide) (PLGA) by a double emulsion technique (Gang et al., 2002). The particle sizes of PLGA microparticles were 24.8 μm and 6.7 μm, with protein loading of 1.93% and 1.65% of microparticles, respectively. The molecular weight of PLGA (50:50) was 40 000-75 000 Da. The particle sizes of PELA microparticles were 20.5 μm and 5.5 μm, with protein loading of 1.58% and 1.32% of microparticles, respectively. *In vitro* release studies were performed over 27 days. Compared with PELA, the polymer PLGA had slower H S A release at two particle sizes tested. Around 50-60% of the encapsulated H S A was released from PLGA particles within 27 days in PBS buffer (pH 7.4) at 37 ˚C, with a burst release of 30% of protein on the first day.

Other researchers used poly (ethylene glycol) (PEG) and sodium chloride (NaCl) as excipients in the PLGA (50:50, molecular weight 13, 000Da) microsphere preparation to stabilise protein OVA (Dorati et al., 2005). All microparticles were prepared using a double emulsion solvent evaporation method with particle size ranged from 15-50 μm. *In vitro* release studies were performed over 160 h. The protein releases from microparticles with PEG 4000 (with and without NaCl) presented high burst releases (around 70%) within the first day, and sustained and complete releases over 160 h. The PEG loadings were 30.726% and 14.372%, respectively. The presence of PEG in the microparticles modified both their

structure and the hydrophilicity of polymeric matrix and changed the protein release profile (Dorati et al., 2005). The release medium was PBS (pH 7.4) at 37 °C.

Most of the reported protein releases were under short-term examination around 30 days. It is necessary to study the release behaviours over a longer duration of time to have a complete investigation on the polymer involved drug release studies. Panyam et al., (2003) reported a longer duration of protein BSA release profiles from PLGA (50:50 molecular weight 120 000 Da). The release studies were conducted over 100 day period in PBS buffer (pH=7.4) at 37 °C. All the particles were made by a double emulsion technique, with particle size of 0.1 μm, 1 μm and 10 μm. The BSA loadings were 22.8%, 22.6% and 21.9% of particles, respectively. The use of higher molecular weights of PLGA led to a slow protein release profile over 100 days (<35%), with a smaller burst release (<5%) of protein at the first day, compared to the work reported by Blanco et al. (1997). Respectively, particles with sizes of 0.1 μm, 1 μm and 10 μm released 20%, 35% and 5% of total percentage of protein BSA from PLGA nano and micro particles within 100 days. Kavanagh et al., (2003) also reported a sustained OVA release profile from PLGA (50:50, molecular weight 40-75 kDa) microparticles over 70 days. Protein release presented a burst of 30% of protein released within the first day and a sustained and complete release over 70 days in PBS buffer (pH7.4) at 37 °C. The particle sizes were < 2.5 μm with a theoretical loading of 20% of microparticles.

Because of the large varieties of release profiles of the proteins from PLGA nano and microparticles reported so far, it is necessary to systematically evaluate these factors and conclude on their effects on antigen releases.

In the current study, active pharmaceutical ingredients release from PLGA micro- and nano- particles were evaluated under long time durations. The active pharmaceutical ingredients used included micromolecules: human serum albumin

(H S A), ovalbumin (OVA), OVA coupled F/G peptide (F peptide, from HIV-1 envelope protein gp120; G peptide, residues 41-56 from the protein G B1 domain) and low molecular weight molecules such as indomethacin and ketoprofen.

### 1.5.3 Release of drugs from chitosan particles

In the work reported by Hejazi and Amiji (2002), chitosan microspheres with an average diameter of 20-30 μm were formed by ionic cross-linking and precipitation with sodium sulphate. In method I, tetracycline was mixed with chitosan solution before the crosslinking and precipitation. In method II, the drug was incubated with pre-formed microspheres for 48 hour. When the drug was added to the polymer solution before cross-linking and precipitation, only 8% (w/w) was optimally incorporated in the final microspheres, while when the drug was incubated with the pre-formed microspheres, a maximum of 69% (w/w) could be loaded (Hejazi and Amiji, 2002). The release studies were carried out in a shaking water-batch at 37 °C. The release medium was hydrochloric acid solutions with pH 1.2, 2.0, 3.5 and 5.0. At pH 1.2 and 2.0, almost all the entrapped drug was released in one hour. The release profile of the drug at pH 3.5 and 5.0 was almost the same. This may be due to the fact that the degree of ionisation of the glucosamine groups of chitosan was almost the same at these pH values (medium ionic strength, 0.16) (Hejazi and Amiji, 2002). The molecular weight of chitosan was 750,000 Da.

In the work reported by Bozkir et al. (2004), chitosan nanoparticles were used for plasmid pDNA delivery. The chitosan-pDNA nanoparticles were formulated using complex coacervation with a size range of 450-820 nm. In the preparation, pDNA solution in sodium sulphate solution was added to chitosan solution under stirring. The high encapsulation efficiency (>90%) protected the encapsulated pDNA from nuclease degradation as shown by electrophoretic mobility analysis (Bozkir et al., 2004). The release of pDNA from the formulation prepared by complex

coacervation was completed in 24 hour. Three types of chitosan were used to prepare the nanoparticles with high molecular weight of 620,000 Da, medium molecular weight of 415,000 Da and low molecular weight of 137,000 Da. The release profiles were not statistically significant compared with formulations with different molecular weights ($p>0.05$) (Bozkir et al., 2004).

In the current study, OVA, as a model protein was adsorbed to pre-formed chitosan nanoparticles to study its release from chitosan nanoparticles prepared by the precipitation/coacervation technique.

# INTRODUCTION

## Chapter 2 Nanotoxicity concerns in study of drug delivery system

## 2.1 Development of nanotechnology in drug delivery

Industry and university researchers have published many hundreds of reports on nanotechnology in the past few years. The definition of nanotechnology was defined in the report written by the UK government from the Royal Society and the Royal Academy of Engineering in 2004 as: "Nanotechnologies are the design, characterization, production and application of structures, devices and systems by controlling shape and size at nanometer scale. It has wide applications in energy, medicine and computing."

Among the applications, drug delivery has been recognised as an important area which can be applied in nanotechnology. Drug delivery nanotechnologies are concentrating on reducing particle size or formulating therapeutic agents in biocompatible nancomposites including nanoparticles, nanocapsules, micellar systems and conjugates. The main applications of nanotechnology in drug delivery include (Furness, 2003):

- Reduction of particle size and increase of surface area, therefore enhancing solubility for injection or increasing oral bioavailability
- Targeting to tissues and cells
- Crossing biological membranes
- Artificial nanoporous membranes for controlled-release devices
- Surface engineering of implants to increase biocompatibility
- Gene and vaccine delivery
- Smart devices, which incorporate a nanosensor feeding back to a responsive delivery system

The advantages of the small sized nanoparticles are the following (Furness, 2003): they can penetrate into tissues through fine capillaries; they are taken up by cells,

allowing efficient delivery; attaching them to specific ligands allows delivery to specific target sites in the body. Also, control over the release of active substance from nanoparticles can be gained by modulating the polymer characteristics.

Under the developments in imaging techniques and the understanding of the biological systems at the nanometer scale, drug delivery nanotechnology has become one of the most interesting areas of sciences. Many of the early applications are studied by academic groups, and include the studies on dendrimers, carbon, synthetic polymer etc.

### 2.1.1 Dendrimers

Dendrimers range in size from 2-20 nm in size. They normally have three architectural components: core, branches and end groups. Polyamidoamine-based (PAMAM) dendrimers were the first type of dendrimers to be synthesised. They are very useful in drug delivery because of their large numbers of terminal groups for attachment of functional groups. Drug molecules can be associated with dendrimers in three places: within the core, in the cavities between the branches, or attached to the surface. These efficient drug delivery vehicles offer advantages like high loading capacity, high resistance to shear forces and low toxicity and immunogenicity (Furness, 2003).

### 2.1.2 Carbon

Carbon is one of the most useful chemical elements and forms the backbone of organic molecules. $C_{60}$, mostly used in drug delivery research, consists of 60 carbon atoms arranged in a spherical structure of adjacent hexagonal and pentagonal rings, similar to that of a soccer ball (Furness, 2003). Therapeutic molecules could be added to the core of $C_{60}$, and by adding functional groups, targeted delivery could

be achieved. Other applications of carbon are carbon nanotubes or nanocones.

### 2.1.3 Synthetic and natural polymers

Both synthetic and natural polymers have been used to formulate nanoparticles for drug delivery. Synthetic polymers are generally better at sustaining release of encapsulated active substance over longer periods than nature polymers (Furness, 2003). Mostly used synthetic polymers in particulate drug delivery study include poly(D,L-lactide-co-glycolide) (PLGA), polylactides (PLA) and poly(ethylene glycol) (PEG) etc.. In this thesis, application details of PLGA in drug delivery studies are discussed in Chapter 1.2. Chitosan and hyaluronic acid are naturally-occurring biopolymers used in drug delivery study. Their application details are discussed in Chapter 1.3 and 1.4.

## 2.2 Human health concerns under the development of nanotechnology

Asbestos is a small and incombustible fibre. It is used in hundreds of products including vehicle brakes, roof shingles, building panels, water and sewer pipes, roof coatings, floor tiles, electrical insulating materials, specialized thermal insulation, elevator brakes, and protective aprons and gloves. Yet by 1918, US insurance companies were refusing to insure asbestos (Shelley, 2006). Tens of thousands of shipyard workers are estimated to have died as a result of exposure to asbestos and up to half a million US citizens exposed to asbestos before 1980 may have died from resultant illness with 10,000 still dying each year, according to the Baltimore-based White Lung Association (Shelley, 2006). The danger posed by asbestos comes from the tiny size of its fibres. The fibres enter the body and cannot be expelled, leading to a range of cancers affecting many different parts of the body

(Shelley, 2006). Inhalation into the lung can lead to asbestosis, a scarring of lung tissue that progressively inhibits breathing (Shelley, 2006).

The toxicity of asbestos generates an amount of concern on the safety issue relating to nanoparticles. The particles may inhibit the operation of the lung after inhalation and the small nanoparticles may find their way through conventional protection such as face masks due to their size. Research was carried out on the adverse effects of engineered nanoparticles on human health. Hodgson and Jones (1985) studied the mortality in male carbon black (CB) workers in five factories in Great Britain. Their main results, based on 1147 male manual workers employed for 12 months or more, showed a statistically significant excess of lung cancer compared to different clear factories (Hodgson and Jones, 1985). However, since there was no evidence of cumulative exposure, risk factors, time to be employed etc., the effects of nanoparticles on human health cannot be concluded (Hodgson and Jones, 1985).

In the work reviewed by Morawsk et al. (2004), environmental exposure to outdoor air containing nanoparticles was associated with a very wide range of adverse health effects, such as cardio-respiratory mortality, increased hospital admission from respiratory and cardiac causes, exacerbations of asthma, changes in lung function and heart rate variability (Morawsk et al., 2004). The toxicological properties of environmental particles and engineered nanoparticles are discussed in Chapter 2.4.

## 2.3 Routes of exposure

Workers can be exposed to nanoparticles by three routes: inhalation, ingestion and dermal penetration. A few studies have been carried out on the uptake and disposition of nanoparticles to the gastrointestinal (GI) tract and most of the results show that they pass through the GI tract and are eliminated quickly (Oberdörster et al., 005). It is still unclear whether nanoparticles will penetrate the skin and cause

any toxicological problems (Tinkle, 2004). With respect to the respirable particle exposure, the biological effects of particle types, such as asbestos and particulate air pollution have been studied in animals and humans. Most of these particles enter the body via the lungs.

Once inhaled, nanoparticles will deposit in all regions of the respiratory tract with high efficiency dependent upon their particle size. In the study reported by International Commission on Radiological Protection (1994), 90% of the 1 nm particles are deposited in the nasopharyngeal region, with 10% in the tracheobronchial region and none in the alveolar region (ICRP publication, 1994). For 20 nm particles, 50% deposit in the alveolar region and 25% in the nasopharyngeal and tracheobronchial regions (ICRP publication, 1994). Once deposited, nanoparticles, in contrast to larger particles, appear to translocate to different organs in the body after penetrating the cell epithelium and entering the blood or lymph systems (ICRP publication, 1994).

The principal hypothetical routes of toxico-kinetics are shown in Figure 2.1 (Tran et al., 2007).

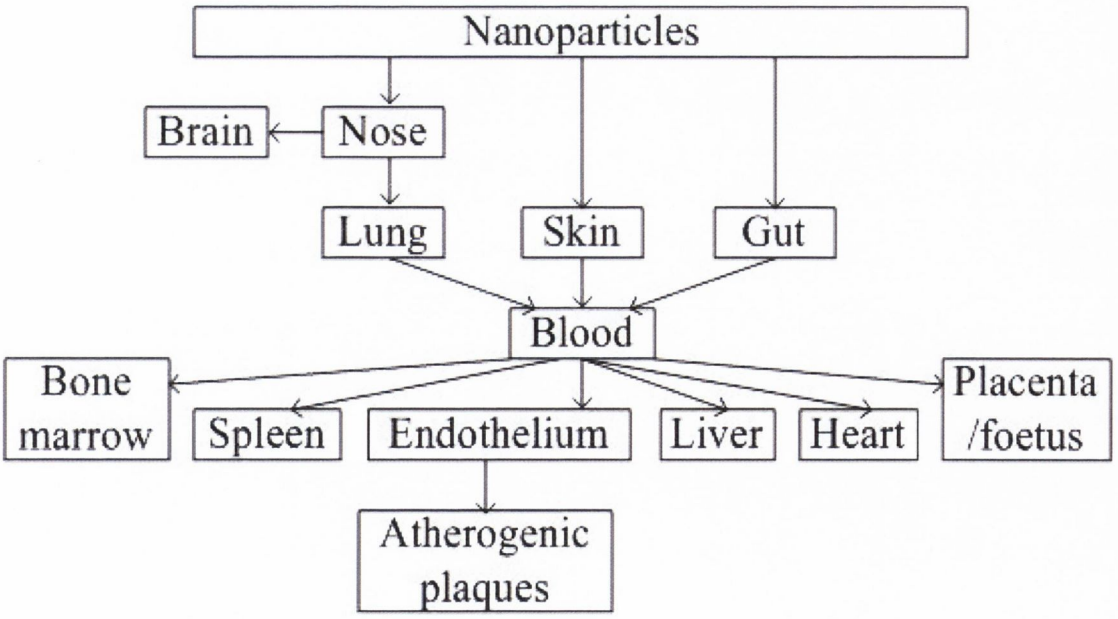


Figure 2.1 Hypothetical toxico-kinetic routes for nanoparticles (Tran et al., 2007).

The small size of nanoparticles makes it possible that some nanoparticles have the ability to cross the epithelial barrier at the lung surface and enter the interstitium (Tran et al., 2007). Also studies suggest that nanoparticles could gain access to the brain via the olfactory epithelium (Oberdörster et al., 2004) and through the blood/brain barrier (Kreuter, 2004).

## 2.4 Toxicological properties of nanoparticles

### 2.4.1 Toxicological properties of environmental particulate matters

Most of the studies of the toxicological mechanisms are concentrated around the ability of particles to cause inflammation, effects on the cardiovascular system and translocation from the site of deposition (Donaldson et al., 2005). In the work reviewed by Donaldson et al. (2005), nanoparticles cause inflammation and could adversely affect the cardiovascular system. The systemic inflammation is shown by elevated C-protein, blood leukocytes, platelets, fibrinogen and increased plasma viscosity (Donaldson et al., 2005). Atherosclerosis is the main cause of cardiovascular morbidity and mortality (Viles-Gonzalez et al., 2004). It is an inflammatory process, and the repeated exposure to particulate matter exacerbates the vascular inflammation of atherosclerosis and promotes plaque development or rupture (Suwa et al., 2002 and Sun et al., 2005).

Particles may also enter the blood and directly impact on the clotting system or on the atherothrombotic process in the plaques (Nemmar et al., 2004). Particles can also translocate from the lungs to the blood as studied in animal models (Nemmar et al., 2001) and affect platelets and thrombus formation (Nemmar et al., 2003).

## 2.4.2 Toxicological properties of engineered nanoparticles

Similar toxicology concerns of engineered nanoparticles to environmental particulate matters were studied, such as the cause of inflammation in the lungs, effects on the cardiovascular system and vascular clotting system.

$TiO_2$ and carbon black (CB) are nanoparticles produced in industry for decades. Rat lung overload studies indicated that CB nanoparticles with large surface area cause inflammation and failed clearance in rat lungs, culminating in fibrosis and cancer (Oberdörster, 1995 and Morrow et al., 1996). Instillation studies also show that the nanoparticles of CB and $TiO_2$ produce more inflammation than an equal mass of large particles (Hohr et al., 2002) of the same material. The surface area is found to be the driver of the inflammation (Duffin et al., 2002).

Radomski and the co-workers (2005) studied the effects of multi-wall and single-wall nanotubes, $C_{60}$ and mixed carbon black nanoparticles on human platelet aggregation *in vitro* and rat vascular thrombosis *in vivo*. Nanotubes and carbon black particles, but not $C_{60}$, stimulated the platelet aggregation and affected the rate of vascular thrombosis in rat (Radomski et al., 2005). There were differences between the different carbon nanoparticles as how to activate platelets and enhance vascular thrombosis. Other particulate materials shown to cause platelet aggregation were latex nanoparticles with sizes of 200-400 nm (Glynnet al., 1965) and titanium dioxide submicroscopic particles with sizes of 5 μm (Bloom et al., 1955).

When the blood vessels are injured, there is a response of accumulation of formed elements at the point of injury and stabilisation of the mass of material by the formation of a coagulum of protein (Zucker, 1947; Jorgensen and Borchgrevink, 1963). In mammals, the formed element that is involved in this basic biological reaction is the blood platelet (Zucker, 1947; Jorgensen and Borchgrevink, 1963).

Platelet metabolism includes a capability for protein synthesis (Warshaw et al., 1966) and synthesis of fatty acids (Majerus et al., 1969). The aggregation of platelets may have benefits on haemostasis, when the blood vessels are injured, but on the other hand, platelet aggregation may be harmful since the formation of platelet aggregation obstructs flow in blood vessel (thrombosis) leading to infarction of tissues supplied by the obstructed vessel.

In the current study, PLGA nanoparticles, including drug free and drug loaded (ketoprofen and indomethacin) chitosan nanoparticles and PLGA-chitosan nanoparticles were used to study their effects on human platelet aggregation. These tests are carried out to answer the toxicological concerns of engineered nanoparticles.

Several publications, some at government level across the world (e.g. the UK, Denmark, France, Canada, and Netherlands) have highlighted the issues associated with nanoparticles and highlight both opportunities and human health concerns associated with nanotechnology (Tran et al., 2007). The human health concerns were so far not been well investigated and safety issues have to be studied and developed.

# INTRODUCTION

## Chapter 3 Vaccine adjuvant studies in mucosal vaccination delivery

## 3.1 Vaccines and vaccine adjuvants

Vaccination has saved a vast number of human lives from pathogenic infections. Active immunization by vaccine administration provides immunological memory and allows efficient immune responses on subsequent interaction with specific antigen (Janeway, 1999). Vaccines can be living organisms, killed organisms or components of pathogens.

The choice of vaccine depends on the nature of the infection. Effective and appropriate protection against different pathogens requires distinct types of immune response. The efficacy of a vaccine can be increased by the induction of a specific immune response at the site of infection. Despite the fact that the majority of infections gain access via mucosal routes, the most commonly used way for vaccination is injection (Janeway, 1999). Oral polio vaccine is the classical oral-mucosal vaccine that reduced polio virus spread and saved lives (Holmgren and Czerkinsky, 2005). The advantages of orally or nasally delivered vaccines are that they can induce immune responses at the mucosal surfaces where the majority of infections gain access (Lavelle and O'Hagan, 2006), and avoiding the use of syringes and needles reduces the risk of infection and needle-stick injury.

However, many of the vaccines available, including protein antigens and DNA vaccines, are very unstable and need to be protected from degradation in the biologic environment (Schmidt and Hankeln, 1996). In addition, their efficacy is limited by their poor capacity to cross biologic barriers and reach the target sites (Schmidt and Hankeln, 1996). As a consequence, the design of effective vaccine adjuvants that could help overcome these problems, has become a significant challenge.

A vaccine adjuvant is a component of vaccine serving as an immunostimulatory agent that enhances immunogenicity of antigens (Janeway, 1999). Proteins by themselves are often poorly immunogenic and thus, require the help of adjuvants (Janeway, 1999). Adjuvants can be used to selectively promote distinct types of immune response (Janeway, 1999). The T cell is a type of white blood cell that attacks virus-infected cells, foreign cells, and cancer cells. Adjuvants like aluminium and calcium compounds have been shown to modulate Th-1 or Th-2 (T helper cells) immune response (Gupta and Siber, 1995). Application of appropriate adjuvants is important for vaccination to elicit antigen specific immune response. Th-1 and Th-2 cells are produced when matured dendritic cells present antigen to the T cell's receptor (TCR). The cytokines secreted by Th-1 cells are interleukin-2 (IL-2), interferon-gamma (IFN-γ) and tumour-necrosis factor-beta (TNF-β). The cytokines secreted by Th-2 are interleukin-4 (IL-4), interleukin-5 (IL-5), interleukin-6 (IL-6), and interleukin-10 (IL-10) (Janeway, 1999). The relationships between T cell, Th-1, Th-2 cells and their cytokines are shown in Figure 3.1. Th-17 is another T helper cell with IL-17 as a cytokine. The functions of the cytokines are discussed in Section 3.4.

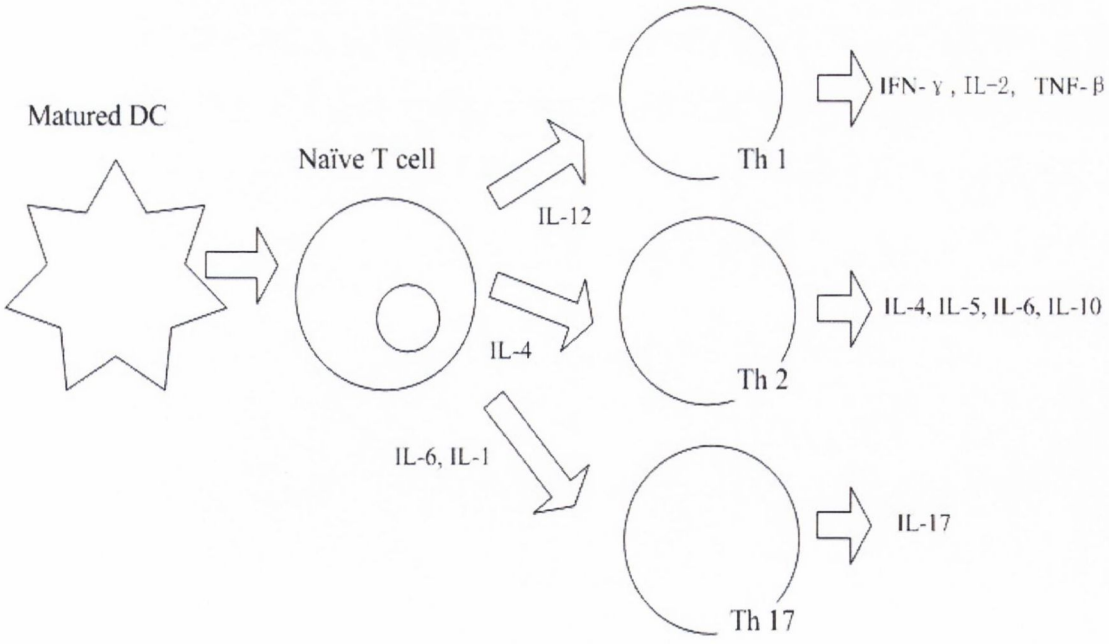


Figure 3.1 T helper (Th) cell subsets, Th-1, Th-2 and their secretin cytokines (Janeway, 1999)

Aluminium compounds such as aluminium hydroxide and aluminium phosphate are the only adjuvants used frequently in human vaccines (Johnson et al., 1999; Mason et al., 2004) such as tetanus, hepatitis B and hepatitis A. They enhance antibody response and act as a Th-2 cell stimulator (Lavelle, 2005; Audibert and Lise, 1993). The problem that aluminium adjuvants face is their limited abilities to induce a range of immune responses. Early studies demonstrated that an aluminium adjuvant failed to stimulate cell mediated immune responses, such as delayed type hypersensitivity (Bomford, 1980). While it can stimulate Th-2 type responses and the production of cytokines, such as IL-4 and IL-5, as well as B cell production of IgG1 and IgE (Lavelle, 2005; Audibert and Lise, 1993), the aluminium adjuvant fails to stimulate Th-1 responses, such as IFN-γ production and B cell IgG2a production (Grun and Maurer, 1989; Brewer and Alexander, 1997). This becomes a problem because the effectiveness of the vaccine against the three diseases: HIV, tuberculosis and malaria, are entirely or partially dependent on the generation of Th-1 type immunity. The developments of novel adjuvants are required in continued vaccine studies.

## 3.2 Immunity

The immune system has two functions, innate immunity and adaptive immunity. The innate immune system provides a first line of defence while adaptive immunity can confer memory (Janeway, 1999).

When foreign cells or virus invade, they are sensed by the innate immune cells in the body. Pathogens such as bacteria and viruses can be eliminated by various mechanisms promoted by the innate immune system including activation of complement, secretion of lysozyme, phagocyte oxidize, myeloperoxidase and

inflammatory mediators (Paul, 1992). The cells involved in innate immunity include macrophages, granulocytes, dendritic cells (DCs), neutrophils, basophils, mast cells, natural killer cells and epithelial cells lining mucosal surfaces (Paul, 1992). Neutrophils are the first cells to appear at the site of pathogen invasion and macrophages and lymphocytes (T cell, B cell) follow. Two major roles of innate system are the ability of innate immune cells to act as sentinels in the detection of infection and the other is induction of adaptive immunity appropriate for eradication of the infection. Among innate immune cells, DCs are the most potent antigen presenting cells (APC) and provide a bridge between innate and adaptive immunity (Paul, 1992). The properties of adaptive immunity are specificity and memory, allowing enhanced response on repeated encounter with antigens (Paul, 1992).

## 3.3 Dendritic cell maturation

DCs are derived from bone marrow precursors and they are distinguishable from macrophages on the basis of their movement, structure and endocytic capacity (Paul, 1992). They can be divided into subtypes: pre-dendritic cells, conventional dendritic cells and inflammatory dendritic cells which vary in their locations, function, activating stimuli and phenotypic markers. Conventional DCs (cDCs) can be further grouped as migratory and lymphoid-tissue-resident cDCs (Paul, 1992).

Maturation of DCs can be defined as a shift of DC function from antigen capture mode to T cell activation mode serving as an efficient antigen presenting cells (APC) (Janeway, 1999). DC maturation can be mediated in two ways: one is a direct recognition of pathogens through DCs and the other is by recognition of inflammatory cytokines such as IL-1ß and TNF- ß and chemokine (Janeway, 1999). A central feature of DC maturation is the upregulation of chemokine receptors such

as MHC class II, CD40, CD80 and CD86 (Janeway, 1999). Chemokines are a family of small cytokines or proteins secreted by cells.

## 3.4 Cytokines

Cytokines are proteins secreted by immune cells such as DCs and T cells. They are responsible for induction of further immune response including immune cell development, differentiation and cytolytic activity (Janeway, 1999). Interleukins (ILs) are a major family of cytokines. As shown in Figure 3.1, many types of ILs have been identified and their roles can be classified as pro-inflammatory, Th1 and Th2 cytokines (Paul, 1992; Janeway, 1999).

IL-1β, one family member of IL-1, regulates gene expression of other cytokines and promotes the induction of gene expression which is associated with inflammation and in turn temperature regulation, the first line of host defense (Dinarello 1997).

IL-6 serves as a pro-inflammatory cytokines or as an anti-inflammatory cytokine by modulating gene expression (Benveniste and Benos 1995). IL-6 production is facilitated by IL-1β and plays a key function in B cell activation (Paul 1992). Both of B cells and T cells belong to lymphocytes, one of the five kinds of white blood cells, circulating in the blood. Similar to IL-1β, IL-6 plays a crucial role in the elevation of body temperature (Benveniste and Benos 1995).

IL-10 is one of the major anti-inflammatory cytokines and functions to suppress multiple activities of the immune response. It has been shown that mice lacking immunosuppressive cytokines are prone to developing autoimmune diseases (Janeway 1999). IL-10 secreted by DCs facilitates T regulatory cell development (Paul 1992).

IL-12 is a heterodimer, consisting of p40 and p70 subunits which are bridged by disulfide bonds (Paul 1992). IL-12 family functions in IFN-γ induction and T cell proliferation (Paul 1992).

IFN-γ is Th-1 cytokine and plays a central role in macrophage activation (Paul 1992).

IL-4 is Th-2 cytokine and plays a central role in Th-2 development. It is synergistically enhanced by the presence of IL-6, and play roles in B cell proliferation (Paul 1992).

IL-5 is produced by Th-2 cells and its function is regulated by IL-10. IL-5 enhances eosinophil production and is associated with allergic reactions (Paul 1992).

IL-17 is a pro-inflammatory cytokine produced by Th-17 T cells (Table 3.1) and plays a crucial role in the pathogenesis of autoimmune disease and tissue damages (Stockinger 2007; Steinman 2007). IL-17 also has a role in protection of mucosal barrier function by stimulating tight junction formation and mucin secretion (Stockinger 2007).

## 3.5 Toll-like receptors (TLRs)

Pattern Recognition Receptors (PRRs) are expressed on immune cells such as DCs. Toll-like receptors (TLRs) are one of the major families of PRRs consisting of ten mammalian members to date (Paul, 1992). Pathogen Associated Molecular Patterns (PAMPs) including structures like lipid, carbohydrate and nucleic-acid which are expressed by bacteria and viruses (Paul, 1992). Each TLR is specialised to sense

particular PAMPs. For example, TLR4 is responsible for recognition of lipopolysaccharide (LPS) which is also known as endotoxin (Takeda et al., 2003; Poltorak et al., 1998). Engagement of TLRs with their specific ligands facilitates induction of distinct DC responses and adaptive immunity (Pulendran, 2004; Pulendran and Ahmed, 2006).

## 3.6 T cell activation

Three signals are required to fully activate and differentiate T cells. One is antigen presentation to T cell receptors (TCRs). The second signal is an antigen independent co-stimulatory signal (Lafferty et al., 1983; Mueller et al., 1989) leading to IL-2 production which promotes T cell proliferation. Activated T cells exhibit increased IL-2 receptor expression. In addition to these two signals, a third signal is required to promote T cells and T cell differentiation. Signal three can be cytokines produced by activated DCs (Sun et al., 2003).

T cells originate in the bone marrow and develop in the thymus where positive or negative selection takes place. Only 2% of naïve T cells survive from the selection and develop into T helper (Th) cells. Th-cells can differentiate into Th-1, Th-2, Th-17 (Janeway, 1999) (Figure 3.1). DCs are considered to play a fundamental role in Th subset polarization via the secretion of polarizing cytokines (Janeway, 1999). A variety of ligands for Pattern Recognition Receptors can stimulate different Th cell subsets via their effects on DCs. For example, DNA, LPS and Poly I:C (polyinosinic:polycytidylic acid) that binds to corresponding TLRs induces Th-1 response while ligands for C-type lectins elicit Th-2 responses such as IL-10 (Pulendran, 2004).

These Th subsets differ in the cytokines they produce and those cytokines play central roles in modulation of immune response. Th-1 cells promote cell mediated immune response by producing IL-2, IFN-γ and TNF-β and drive IgG2a and IgG3 production B cells which functions in opsonising intracellular parasites (Paul, 1992). In contrast, Th2 cells mainly promote humoral immune response by producing cytokines including IL-4, IL-5, IL-6 and IL-10 (Paul, 1992).

## 3.7 Immunity of chitosan as adjuvant

As mentioned in Section 1.3.1, chitosan has been used in mucosal delivery system since it has mucoadhesive properties. Immunologists have focused on chitosan as adjuvant or immune modulator.

Porporatto et al. (2004) studied the effect of the co-administration of antigen type II collagen (CII) and chitosan (50 kDa, 85% deacetylated) in rat. As a result, CII:chitosan-fed animals exhibited a reduced secretion of IL-2 with an increase of IL-10 in Peyer's patches (PP) and spleen respectively. Peyer's patches are aggregations of lymphoid tissue that are usually found in the lowest portion of the small intestine (ileum). In addition, in PP, CII:chitosan-fed rats showed increased levels of mRNA for transforming growth factor-ß, IL-4 and IL-10. The studies suggested that the co-administration with chitosan promotes an anti-inflammatory environment after feeding (Porporatto et al., 2004).

In the current study, the effects of chitosan nanoparticles (CS-F NP, CL113 NP, CL213 NP and G213 NP) on dendritic cells and spleen cells were examined to see their efficiency as vaccine adjuvants. This work was generously assisted by Dr. Ed Lavelle and his student Yuki Ozasa in the School of Biochemistry and Immunology at Trinity College Dublin.

# EXPERIMENTAL

## Chapter 4 Experimental materials and methods

# 4.1 Materials

## 4.1.1 Polymers, proteins and general materials

| Material | Supplier/Manufacturer |
|---|---|
| Ammonium persulphate (APS) | Sigma, USA |
| Boric acid | Sigma, USA |
| Brilliant blue R | Sigma, USA |
| Chitosan (low molecular weight) Batch No. 407568/1 50100 | Fluka, Germany |
| Chitosan chloride salt (CL213, high molecular weight 150,000-400,000 Da) | NovaMatrix, Norway |
| Chitosan chloride salt (CL113, low molecular weight 50,000-150,000 Da) | NovaMatrix, Norway |
| Chitosan glutamate salt (G213, high molecular weight 200,000-600,000 Da) | NovaMatrix, Norway |
| Chitosan glutamate salt (G113, low molecular weight 50,000-200,000 Da) | NovaMatrix, Norway |
| Coumarin-6 | Polysciences, Inc., USA |
| D-glucosamine | Sigma, USA |
| Dulbecco's Phosphate Buffered Saline (DPSS) | Biosera, UK |
| Glutaraldehyde solution ~ 50% in water | Fluka, Germany |
| Human serum albumin (H S A) | Sigma, USA |
| Hydrindantin | Sigma, USA |
| Hydrochloric acid 37% (HCl) | Riedel-de-Haën, Germany |
| Indomethacin | Sigma, USA |
| Ketoprofen | Sigma, USA |
| Lecithin | Sigma, USA |
| Lithium acetate dihydrate | Sigma, USA |
| Lugol solution ($I_2$/KI) | Fluka, Germany |
| Micro BCA$^{TM}$ Protein Assay Kit | PIERCE USA |
| Ninhydrin | Sigma, USA |
| N,N,N,N-Tetramethylethyl-enediamine (TEMED) | Sigma, USA |

| | |
|---|---|
| OVA coupled F/G peptide | Department of Veterinary Science, the Queen's University of Belfast |
| Ovalbumin (OVA) | Sigma, USA |
| PLGA Resomer 504 (50:50) Batch No. 640662 | Boehringer Ingelheim, Germany |
| Polystyrene GPC standards | Polymer Laboratories, Ireland |
| Potassium nitrate | Fluka, Germany |
| Polysorbate 80 | Fluka, Germany |
| Polyvinyl alcohol (PVA) | Sigma, USA |
| Potassium bromide | Sigma, USA |
| Protein marker, broad range (2-212 kDa) | New England Biolabs Inc., UK |
| ProtoGel | National diagnostics, USA |
| Pullulan GPC polysaccharides standards | Polymer Laboratories, Ireland |
| Sodium dodecyl sulphate (SDS) | Sigma, USA |
| Sodium hyaluronate | Fluka, Germany |
| Sodium hyaluronate | NovaMatrix, Norway |
| Sodium hydroxide (NaOH) | Riedel-de-Haën, Germany |
| Sodium sulphate | Fluka, Germany |
| Tris(hydroxymethyl) aminomethane | Sigma, USA |

### 4.1.2 Solvents

| Solvent | Supplier/Manufacturer |
|---|---|
| 2-butanol | Solvent stores, TCD |
| Acetic acid glacial | Riedel-de-Haën, Germany |
| Dichloromethane (DCM) | Solvent stores, TCD |
| Dimethylsulphoxide (DMSO) | Aldrich, UK |
| Ethanol | Solvent stores, TCD |
| Ethyl acetate | Solvent stores, TCD |
| Methanol | Riedel-de-Haën, Germany |
| Tetrahydrofuran (THF) | Solvent stores, TCD |

### 4.1.3 Equipment

| Equipment | Supplier/Manufacturer |
|---|---|
| ATTO electrophoresis unit | Medical Supply Co. Ltd., Japan |
| BECKMAN Model J2-21 centrifuge | Beckman |
| Bruker advance 400 NMR | Bruker, USA |
| Büchi Mini Spray Dryer B-191 | Büchi Laboratoriums-Technik AG, Switzerland |
| Büchi Rotavapor R-114, Vacuum controller V-800 | Büchi Laboratoriums-Technik AG, Switzerland |
| Differential Scanning Calorimeter 821$^e$ | Mettler-Toledo, Switzerland |
| Freeze drier BenchTop K series | VirTis, USA |
| Magnetic stirrer hotplate | STUART Scientific, UK |
| Malvern Mastersizer 2000 | Malvern, UK |
| Malvern Zetasizer nano ZS | Malvern, UK |
| Mettler Toledo STARe software version 6.1 | Mettler-Toledo, Switzerland |
| Plaquagel-OH mixed 8 μm GPC column | Polymer Laboratories Ltd., UK |
| Scanning Electron Microscope S4300 | Hitachi, Japan |
| Shimadzu class VP software (version 1.02) | Polymer Laboratories Ltd., UK |
| Siemens D500 Diffractometer | Siemens, Germany |
| Spectrofluorophotometer RF-1501 | Shimadzu, USA |
| Digital Sonifier 250 | Branson, USA |
| Ultrasonic Processor VC130 PB | SONICS, USA |
| Ultracentrifuge 113 | Sigma, USA |
| UV Microplate autoreader EL311 | BIO-TEK Instruments |
| UV-1700 spectrophotometer | Shimadzu, USA |
| Rotary evaporator R200 | Büchi, Switzerland |
| Styragel HPLC column | Waters, USA |
| Waters Millennium chromatography software version 2.0 | Waters, USA |
| Waters refractive index detector 410 and pump 510 | Waters, USA |
| XRD silicon mounts | Bruker AXS, UK |

# Experimental methods

## 4.2 Characterisation of polymers

### 4.2.1 Measurement of molecular weight

Gel Permeation Chromatography (GPC) was used to determine the molecular weight of polymers.

(a) PLGA systems

The gel permeation chromatography system consisted of a Waters Styragel HPLC column, a Waters 510 HPLC pump and a Waters Refractive index detector 410. 0.5 mg of each sample was weighed out into 10 ml of tetrahydrafuran (THF) and allowed to stand overnight. The mobile phase was THF and the flow rate was set at 1 ml/min. The internal and external temperatures of the detector were set to 30°C and 25°C, respectively. Millennium Chromatography software version 2.0 was employed to integrate the peaks and calculate the result. Samples were evaluated against a series of polystyrene standards with molecular weights of 13,100, 20,650, 39,000, 50,400, and 66,000. 200 µl volumes of samples or standards were injected in triplicate.

(b) Chitosan and hyaluronic acid systems

Gel Permeation Chromatography (GPC) was performed using a Plaquagel –OH mixed 8 µm 300 × 7.5 mm column (Polymer Laboratories Ltd., UK). For analysis of chitosan systems the method supplied by Polymer Laboratories (Technical Bulletin TB581) was followed substituting potassium nitrate for sodium nitrate. The mobile phase consisted of potassium nitrate 0.5 M and sodium phosphate monosodium 0.01 M brought to pH 2 with concentrated HCl. The detector and the HPLC system was Shimadzu with a LC-10AT VP pump, autosampler SIL-10AD

VP and SCL-10AVP system controller. Samples were prepared as 0.1% w/v solutions in concentrated HCl and brought to volume with mobile phase. Polysaccharides standards were used as standards with molecular weights of 5,900, 112,000, 212,000, 404,000, and 788,000 and prepared as 0.05 to 0.1% solutions in mobile phase. 200 µl volumes of samples or standards were injected in triplicate. Analysis was performed using Shimadzu Class VP software (version 6.10) with GPC for Class VP (version 1.02). The temperature of the detector was 40°C.

## 4.2.2 Measurement of chitosan deacetylation

(a) $^1$H-Nuclear Magnetic Resonance Spectroscopy ($^1$H-NMR)

Samples for $^1$H-NMR were prepared using the method of Hirai et al (1991). 20 mg samples were dissolved in 2 ml of 2% w/w deuterated acetic acid in deuterated water solution. The solutions were heated to 70°C to aid dissolution. Samples were analysed using a Bruker advance 400 NMR. The degree of deacetylation was determined by Equation 4.1 (Hirai et al., 1991) using the integral intensity, $ICH_3$, of the $CH_3$ residue and the sum of integral intensities $IH_2$-$H_6$ of the $H_2$, $H_3$, $H_4$, $H_5$, $H_6$ and $H_6$ protons.

$$\text{Degree of deacetylation (\%)} = \{1-(\frac{1}{3}ICH_3 / \frac{1}{6}ICH_2 - H_6)\} \times 100 \qquad \text{Equation 4.1}$$

(b) Ninhydrin assay

Ninhydrin assay is a ninhydrin colorimetric test that was used to determine the degree of deacetylation of chitosans (Curotto and Aros 1993; Corrigan 2002; Leane et al., 2004). The method involved preparation of calibration curves using solutions of chitosan and of D-glucosamine, respectively. A value of 100% of free amino groups was assigned to the slope of the D-glucosamine calibration curve and correspondingly the values for the slopes obtained with solutions of chitosan gave

the percentages of free amino groups. Samples were analysed in triplicate. The preparation of calibration curve is presented below:

Preparation of calibration curve:

Lithium acetate buffer (10 ml) was prepared by dissolving 4.08 g of lithium acetate dihydrate in approximately 6 ml of deionised water. The pH of the resulting solution was adjusted to 5.2 using acetic acid and the volume adjusted to 10 ml with deionised water. The ninhydrin reagent was freshly prepared on the day of the assay by adding 4 M lithium acetate buffer (10 ml) to 0.8 g ninhydrin and 0.12 g hydrindantin in 30 ml DMSO. For the assay, 0.5 ml of ninhydrin reagent was added to 0.5 ml sample and mixed under vortex. Then the sample and reagent were heated in boiling water for 30 min. After cooling, 15 ml of a 50:50 ethanol:water mixture was added. The absorbance of each solution was measured on UV spectrophotometer (UV-1700 spectrophotometer, Shimadzu) at 570 nm.

## 4.3 Preparation of micro and nanoparticles

### 4.3.1 Preparation of protein loaded PLGA micro and nano particles

Protein (H S A, OVA, OVA coupled F/G peptide) loaded PLGA microparticles were prepared by a double emulsion technique. OVA coupled F/G peptide is a conjugate antigen which is created by covalently attaching F peptide (from HIV-1 envelope protein gp120) and G peptide (residues 41-56 from the protein G B1 domain) (50:50) to a carrier protein OVA, thereby conferring the immunological attributes of carrier on the attached peptides. F/G peptide is attached to OVA to see its effect on OVA release study.

2 mg of protein was dissolved in 50 µl of deionised water, and then emulsified in a 2 ml solution of PLGA (50:50, RG 504, Ingelheim Boehringer) in ethyl acetate (EA) or dichloromethane (DCM) (100 mg/ml) by sonication (SONICS VC130PB) on ice. Then, 4 ml of an aqueous PVA solution (1% w/v) was added to this first emulsion and the resulting (w/o)/w emulsion was sonicated on ice again. The double emulsion was diluted with 90 ml PVA solution (0.3% w/v) and the solvent was rapidly eliminated by rotary evaporation (Büchi Rotavapor R200). Finally, the particles were isolated by centrifugation at 10,000 g (Beckman, Model J2-21 centrifuge) for half an hour and washed three times with water under the same centrifugation speed and processing time. Dry particles were collected by freeze drying. A range of experiments was carried out with different sonication times, powers and two different organic solvents during the preparations to compare their effects on the product properties. The details of rotary evaporation and freeze drying are presented below:

Rotary evaporation:

A rotary evaporator consists of a vacuum system, a rotating evaporation flask and a condenser with a condensate collecting flask. The system works because lowering the pressure lowers the boiling point of solvent, which allows the solvent to be removed without excessive heating. Particles after washing were resuspended in evaporation flask with deionised water. After putting the flask onto the evaporator, the solvent was evaporated at 40˚C using the vacuum pump (75 mm Hg).

Freeze drying process:

Freeze drying is a technique by which a liquid is frozen and then dehydrated by sublimation. This process presents a complete retention of sample form and produces no chemical damage. Sample solutions or suspensions in freeze drying flasks (VirTis, USA) were frozen in liquid nitrogen. The frozen sample was then attached to the vacuum chamber (VirTis, USA) where the freeze drying process

takes place and after 48 hours, the dry powders were collected. The vacuum set was smaller than 100 mTone.

Protein (H S A, OVA) loaded PLGA nanoparticles were prepared by increasing sonication time to 10 minutes and power to 4 watt keeping the other parameters the same.

### 4.3.2 Preparation of H S A loaded PLGA nanoparticles stained with coumarin-6

Protein (H S A) loaded PLGA nanoparticles were prepared by a double emulsion technique. 200 mg of the PLGA (RG 504) was dissolved in 2 ml of ethyl acetate. 50 µl of the coumarin-6 from stock (1 mg/ml in ethyl acetate) was added into PLGA solution. 2 mg H S A was dissolved in 50 µl of distilled water, and then emulsified in the PLGA (RG 504) solution by sonication (SONICS VC130PB) on ice. Then, 4 ml of an aqueous PVA solution (1% w/v) was added to this first emulsion and the resulting w/o/w emulsion was sonicated again on ice. The double emulsion was diluted with 90 ml of PVA solution (0.3% w/v) and the solvent was rapidly eliminated by evaporation (Section 4.3.1). Finally, the particles were isolated by centrifugation at 10,000 g (Beckman, Model J2-21 centrifuge) for half an hour and washed three times with water under the same centrifugation speed and processing time. The supernatant was collected and the content of coumarin-6 was measured by fluorimetry. Dry particles were collected by freeze drying (Section 4.3.1).

### 4.3.3 Preparation of OVA loaded chitosan-PLGA micro and nanoparticles

Protein (OVA) loaded PLGA nanoparticles were prepared by a double emulsion technique. 40 mg OVA was dissolved in 150 µl of deionised water, and then emulsified in a 2 ml solution of PLGA (RG 504) in ethyl acetate (100 mg/ml) by sonication (SONICS VC130PB) on ice. Then, 4 ml of an aqueous CS-PVA solution (1% w/v PVA, 0.2% w/v chitosan (Fluka) and 1% acetic acid) was added to this first emulsion and the resulting w/o/w emulsion was sonicated on ice again. The double emulsion was diluted with 90 ml PVA solution (0.3% w/v) and the solvent was rapidly eliminated by evaporation (Section 4.3.1). Finally, the particles were isolated by centrifugation at 10,000 g (Beckman, Model J2-21 centrifuge) for half an hour and washed three times with water under the same centrifugation speed and processing time. The supernatant was collected and the content of chitosan was measured by UV spectroscopy. The measurement method is described in Section 4.4.9. The resultant nanoparticles were lyophilised. Chitosan concentration in CS-PLGA solution was increased while keeping the concentration of PVA the same to investigate the effects of chitosan on product properties. Dry particles were collected by freeze drying (Section 4.3.1).

### 4.3.4 Preparation of NSAID loaded PLGA nanoparticles

NSAID (indomethacin and ketoprofen) loaded PLGA nanoparticles were prepared by a single emulsion technique. 40 mg NSAID was dissolved in 2 ml solution of PLGA (RG 504) in ethyl acetate (100 mg/ml). Then 4 ml of an aqueous PVA solution (1% w/v) was added and the resulting o/w emulsion was sonicated on ice. The emulsion was diluted with 90 ml PVA solution (0.3% w/v) and the solvent was rapidly eliminated by evaporation (Section 4.3.1). Finally, the particles were

isolated by centrifugation at 10,000 g (Beckman, Model J2-21 centrifuge) for half an hour and washed three times with water under the same centrifugation speed and processing time. Dry particles were collected by freeze drying (Section 4.3.1).

### 4.3.5 Preparation of chitosan microparticles by spray drying

Chitosan microparticles with or without a crosslinking agent glutaraldehyde (0.125% v/v) were prepared by spray drying using a Büchi Mini Spray Dryer B-191. The chitosan used was chitosan salt CL213 with high molecular weight (150,000-400,000 Da). The concentration of the chitosan solution was 0.2% w/v. The inlet and outlet temperatures were 140°C and 89-91°C, respectively, with air flow 600 nl/hr, pump rate 15% and aspirator rate 100%.

### 4.3.6 Preparation of chitosan nanoparticles

Chitosan (chitosan-Fluka, CL113, CL213 and G213) nanoparticles were prepared by precipitation/coacervation. Chitosan (CL113, CL213 and G213) (0.2 % w/v) was dissolved in deionised water containing 1% v/v polysorbate 80; Chitosan (chitosan-Fluka) was dissolved in 1% v/v acetic acid containing 1% v/v polysorbate 80. A solution of sodium sulphate (20 % w/v) was added dropwise (6 ml/min), under stirring (80 rpm) and sonication (SONICS VC130PB, power 80) conditions. The formation of nanoparticles was indicated by turbidity, examined by transmission measurements using spectrophotometer (UV-1700 spectrophotometer, SHIMADZU, USA) at 500 nm. After the addition of sodium sulphate, stirring and sonication were continued for another 1 h. The nanoparticles were purified by centrifugation at 13,000 rpm (Ultracentrifuge 113, Sigma) for 15 min and washed with water under the same centrifugation speed and processing time. The nanoparticles were collected after freeze drying (Section 4.3.1).

### 4.3.7 Preparation of hyaluronic acid microparticles by spray drying

Lecithin (0.2% w/v) was predispersed in deionised water under sonication, and the dispersion was filtered through a 0.2 μm filter. Lecithin was used as a surfactant in this preparation. The resultant dispersion was slowly mixed with sodium hyaluronate (0.1% w/v). The resultant mixture was spray dried using a Büchi Mini Spray Dryer B-191 to prepare HA microparticles. The inlet and outlet temperatures were 140°C and 89-91°C, respectively, with air flow 600 nl/hr, pump rate 15% and aspirator rate 100%.

### 4.3.8 Preparation of hyaluronic acid/chitosan nanoparticles

Hyaluronic acid/chitosan nanoparticles were prepared by precipitation/coacervation. Sodium hyaluronate (Fluka, NovaMatrix) and chitosan (CL113, CL 213, G113, and G213) were dissolved in deionised water to prepare 0.2% w/v solutions. Under stirring (80 rpm), the chitosan solution was added to the HA solution slowly to make a mixture with a ratio of 1:1 by weight. After 10 minutes of stirring, the mixture was filtered through a 5 μm filter and the resultant filtrate was collected. Sodium sulphate (20% w/v) was added dropwise (6ml/min), under stirring (80 rpm) and sonication (SONICS VC130PB, power 80) conditions. The formation of nanoparticles was indicated by turbidity, examined by transmission measurements using spectrophotometer (UV-1700 spectrophotometer, Shimadzu, USA) at 500 nm. After the addition of sodium sulphate, stirring and sonication were continued for another 1 hour. The nanoparticles were purified by centrifugation at 13,000 rpm (Ultracentrifuge 113, Sigma) for 15 min and washed with water under the same

centrifugation speed and processing time. The nanoparticles were collected after freeze drying (Section 4.3.1).

# 4.4 Characterisation of micro and nanoparticles

## 4.4.1 Particle size analysis

### 4.4.1.1 Laser diffraction analysis

The particle size was determined using Malvern Mastersizer 2000, with a Hydro μp sample dispersion unit attached. 5-10 mg of microparticles were dispersed in 1ml of deionised water and sonicated for 5 minutes before the sample addition. The sample was added into the Mastersizer measuring cell and the measurement process was controlled by the Malvern Mastersizer 2000 Software. The particle sizes were plotted as particle size distributions (by volume) and the span values were calculated. The span is a measure of the width of the volume distribution relative to the median diameter and is calculated as (D90%-D10%)/D50%. D90%, D50% and D10% is the particle diameter determined at the 90%, 50% and 10% volume distribution of cumulative particle, respectively. The samples were measured in triplicate.

### 4.4.1.2 Light scattering analysis

Particle sizes were also determined by Malvern Zetasizer Nano ZS. The nanoparticle were dispersed in deionised water (1mg/ml) and sonicated for 5 minutes prior to the measurement. Then the sample was transferred to a disposable polystyrene cuvette and the cuvette was inserted into the Zetasizer cell. The measurement process was controlled by the Malvern Zetasizer Nano ZS software. The particle size is presented as a Z-average diameter which is the mean diameter based upon the intensity of scattered light and polydispersity, which is the width of the size distribution.

### 4.4.2 Morphology

Particle morphology was determined by scanning electron microscopy (SEM). Samples were attached to a metal stub and gold coated by plasma coating and viewed under a Hitachi S43000 scanning electron microscope.

### 4.4.3 Thermal properties

Each amorphous substance or composite may be characterised by a glass transition temperature ($T_g$), which is a critical physical property that can affect the physical stability. When the polymer is cooled below this temperature, it becomes hard and brittle, like glass; when it is used above $T_g$, it becomes soft and flexible. An important application of DSC is the determination of possible interactions between a drug substance and the polymers used in formulation. By monitoring the changes of heat capacity under increasing temperatures, it is possible to detect if the drugs were physically dispersed in polymers or kept crystalline in the sample.

Thermal properties of polymers and particles were measured by differential scanning calorimetry (DSC). The measurements were conducted using a Mettler Toledo DSC 821$^e$ with a refrigerated cooling system (LabPlant RP-100). Nitrogen was used as the purge gas. Top pierced aluminium pans were used throughout the study with sample weights varied between 5-10 mg. The DSC system was controlled by Mettler Toledo STAR$^e$ software (version 6.10). Samples were characterised by DSC in the range of 25°C to 200°C at a heating rate of 10°C per minute. The glass transition temperature was defined as the midpoint of the transition and the melting points were reported as the onsets of the endothermic processes.

### 4.4.4 Integrity study of encapsulated protein

The integrity of encapsulated protein that was extracted from particles was studied by sodium dodecyl sulphate PAGE electrophoresis (SDS-PAGE). 100 mg of particles were suspended in 1 ml NaOH (0.1M) containing SDS solution (5 % w/v) and placed in a water bath at 60°C for 1 hour. After centrifugation, the supernatant was taken out for analysis.

SDS-PAGE was carried out using an ATTO electrophoresis unit with 10 % stacking gels and 12 % resolving gels for the detection of the H S A. protein. The following table details the contents of the various gel solutions. The volumes quoted are those required for the pouring of one gel (Table 4.1).

Table 4.1 Contents of gel solutions for SDS-PAGE

| Solution components | 10 % stacking gel (ml) | 12 % resolving gels (ml) |
|---|---|---|
| ProtoGel | 3.3 | 4.0 |
| Deionised water | 4.1 | 3.4 |
| 1.5 M Tris-HCl (pH 8.8) | ---- | 2.5 |
| 0.5 M Tris-HCl (pH 6.8) | 2.5 | ---- |
| 10 % SDS (w/v) | 0.1 | 0.1 |
| 10 % APS (w/v) | 0.05 | 0.05 |
| TEMED | 0.01 | 0.005 |

Polyacrylamide gels were run for approximately 2 hours at 25 mA and protein bands were detected using Brilliant blue.

### 4.4.5 Fourier Transform Infrared Spectroscopy

Infrared spectra were recorded on a Nicolet Magna IR 560 E.S.P. spectrophotometer equipped with MCT/A detector, working under Omnic software version 4.1. A spectral range of 650-4000 $cm^{-1}$, resolution 2 $cm^{-1}$ and accumulation of 64 scans were used in order to obtain good quality spectra. A KBr disk method was used with 1% sample loading.

### 4.4.6 Crystallinity study

Powder X-ray diffraction measurements (XRD) were carried out in low background silicon mounts, which consisted of cavities 0.5 mm deep and 9 mm in diameter (Bruker AXS, UK). A Siemens D500 Diffractometer was used. This consists of a DACO MP wide-range goniometer with a 1.0° dispersion slit, a 1.0° anti-scatter slit and a 0.15° receiving slit. The Cu anode X-ray tube was operated at 40 kV and 30 mA in combination with a Ni filter to give monochromatic Cu Ka X-rays. Measurements were generally taken from 5° to 35° on the 2 theta scale at a step size of 0.05° per second for qualitative analysis.

### 4.4.7 Protein loading assay

15 mg particles (PLGA, chitosan-PLGA) was dispersed in 3 ml of 0.1 M NaOH containing 5% (w/v) SDS. The suspension was incubated in a water bath at 60°C for 1 hour. Following centrifugation, 1 ml of the supernatant was removed and stained with Micro BCA™ Protein Assay Kit. Protein concentration was determined by using a UV spectrophotometer at 562 nm. The samples were measured in triplicate.

### 4.4.8 NSAID loading assay

The supernatant collected during the preparation of NSAID (indomethacin or ketoprofen) encapsulated PLGA nanoparticles were used to assay the loading of NSAID (indomethacin or ketoprofen) on PLGA particles. Indomethacin concentration was determined by using a UV spectrophotometer (UV-1700 spectrophotometer, Shimadzu, USA) at 318 nm (Puebla et al., 2005) and ketoprofen at 260 nm (Gabor et al., 1999).

### 4.4.9 Chitosan loading assay

The supernatant liquid was collected during the preparation process of chitosan-PLGA particles and used to assay the chitosan loading on resultant particles.

The quantity of chitosan was determined by ninhydrin assay which was described by Leane et al., (2004). Lithium acetate buffer (10 ml) was prepared by dissolving 4.08 g of lithium acetate dihydrate in approximately 6 ml of deionised water. The pH of the resulting solution was adjusted to 5.2 using acetic acid and the volume adjusted to 10 ml with deionised water. The ninhydrin reagent was freshly prepared on the day of the assay by adding 4 M lithium acetate buffer (10 ml) to 0.8 g ninhydrin and 0.12 g hydrindantin in 30 ml DMSO. For the assay, 0.5 ml of reagent was added to 0.5 ml of the sample. The sample and reagent were briefly shaken by hand and heated in boiling water for 30 min. After cooling, 15 ml of a 50:50 ethanol:water mixture was added to each sample and the mixture was vortexed for 15 s. The absorbance of each solution was measured with a UV (UV-1700 spectrophotometer, Shimadzu, USA) at 570 nm and the concentration of chitosan in

the sample was calculated from a standard calibration curve. The samples were measured in triplicate.

### 4.4.10 Coumarin loading assay

The supernatant liquid was collected during the preparation process of PLGA particles stained with courmain-6 and used to assay the coumarin loading on resultant particles.

6-coumarin was extracted by methylene chloride from the supernatant and the solvent was evaporated carefully. The materials were reconstituted in ethanol and measured by a spectrofluorophotometer (spectrofluorophotometer RF-1501, excitation wavelength: 458 nm and emission wavelength: 520 nm).

### 4.4.11 Loading of OVA on chitosan nanoparticles

60 mg chitosan particle was added to an aqueous suspension containing 30 mg of OVA in a total volume of 3 ml. The mixture was vortexed rapidly for 3-5 s and left for 24 hours for the formation of complexes. The resultant complexes were centrifuged at 13,000 rpm for 15 minute. The resultant pellet was freeze dried and the supernatant was collected and measured by UV spectroscopy (UV-1700 spectrophotometer, Shimadzu, USA) using Micro BCA$^{TM}$ Protein Assay Kit (Baki et al., 2002).

### 4.4.12 Measurement of PVA

Content of PVA associated with chitosan-PLGA particles was determined by a colorimetric method (Sahoo et al., 2002). To each sample, 3 ml of a 0.65 M solution of boric acid, 0.5 ml of $I_2$/KI (0.05/0.15 M) solution, and 1.5 ml of deionised water were added. Absorbance values of the samples were measured by using UV-1700 spectrophotometer (Shimadzu, USA) at 690 nm after 15 min incubation. A standard plot of PVA was prepared under identical conditions.

### 4.4.13 Measurement of zeta potential

Approximately 1 mg of sample was dispersed in 1 ml deionised water. The sample was measured by Malvern Zetasizer Nano ZS. Zeta potential readings were carried out five times for one sample and the average value of three samples was presented.

## 4.5 Release studies

### 4.5.1 Protein release studies from PLGA particles

20 mg of protein (H S A, OVA, OVA coupled F/G peptide) loaded PLGA particles was suspended in 20 ml PBS buffer (pH=7.4) in a conical flask. Flasks were shaken at 37°C in a water bath at 65 rpm. At different time intervals, a sample volume of 1.5 ml was transferred and centrifuged at 13,000 rpm for 15 min (Sah et al., 1994; Coombes et al., 1998)

A quantity of 1 ml of the supernatant was taken for measurement by UV spectroscopy (UV-1700 spectrophotometer, Shimadzu, USA) at 562 nm with Micro BCA™ Protein Assay Kit. 1 ml of fresh PBS buffer was added to the remaining 0.5

ml sample. 1.5 ml of the suspension was agitated vigorously by vortexing and replaced in the flasks. The samples were measured in triplicate.

### 4.5.2 NSAID release studies from PLGA particles

5 mg of indomethacin or ketoprofen loaded PLGA particles were suspended in 20 ml PBS buffer (pH=7.4) in conical flasks. Flasks were shaken at 37°C in a water bath at 65 rpm. At different time intervals, a sample volume of 1.5 ml was transferred and centrifuged at 13,000 rpm for 15 min. In order to guarantee sink conditions, the amount of drug-loaded particles was chosen such that indomethacin or ketoprofen content of particles was lower than 10% of the solubility of indomethacin (3.46 mg/ml, Horiike and Matsuzawa, 1995) or ketoprofen (9.68 mg/ml, Mollo 1999) in PBS buffer (pH=7.4).

A quantity of 1 ml of the supernatant was taken and measured by UV spectroscopy (indomethacin at 318 nm; ketoprofen at 260 nm; UV-1700 spectrophotometer, Shimadzu, USA). 1 ml of fresh PBS buffer was added to the remaining 0.5 ml sample. 1.5 ml of the suspension was agitated vigorously by vortexing and replaced in the flasks. The samples were measured in triplicate.

### 4.5.3 Coumarin release from PLGA particles

5 mg of PLGA particles stained with coumarin was suspended in 20 ml PBS buffer (pH=7.4) in conical flasks. Flasks were shaken at 37 °C in a water bath at 65 rpm. At different time intervals, a volume of 1.5 ml was transferred and centrifuged at 13, 000 rpm for 15 min. In order to guarantee sink condition, the amount of particles was chosen such that coumarin content of particles was lower than 10% of the solubility of coumarin (0.73 mg/ml, Naoko et al., 2006) in PBS buffer (pH=7.4). A

quantity of 1 ml of the supernatant was taken and 6-coumarin was extracted by methylene chloride and the solvent was then carefully evaporated under fume hood. The materials were reconstituted in ethanol and measured by a spectrofluorophotometer (spectrofluorophotometer RF-1501, excitation wavelength: 458 nm and emission wavelength: 520 nm). 1 ml of fresh PBS buffer was added to the remaining 0.5 ml sample. 1.5 ml of the suspension was agitated vigorously by vortexing and replaced in the flasks. The samples were measured in triplicate.

### 4.5.4 OVA release studies from chitosan particles

5 mg of OVA loaded chitosan particles were suspended in 40 ml PBS buffer (pH=7.4) in conical flasks. Flasks were shaken at 37°C in a water bath at 65 rpm. At different time intervals, a quantity of 100 µl of the supernatant was taken for measurement by UV spectroscopy (UV Microplate autoreader EL311) at 562 nm with Micro BCA™ Protein Assay Kit. The samples were measured in triplicate.

### 4.5.5 Mathematical modelling of drug release profiles

Micromath® Scientist® for Windows™, version 2.01, was used for the non-linear curve fitting of the drug release data. The coefficient of determination (CD) and model selection criterion (MSC) were used as measures of goodness of fit when evaluating the suitability of a model. The CD is defined by the following equation:

$$CD = \frac{\sum_{i=1}^{n} W_i (Y_i - \bar{Y})^2 - \sum_{i=1}^{n} W_i (Y_i - \hat{Y}_i)^2}{\sum_{i=1}^{n} W_i (Y_i - \bar{Y})^2}$$

Where n is the number of data points, $W_i$ are the weights applied to each point, and

$Y_i$, $\hat{Y}$, $\overline{Y}$ are the observed data points, the model-predicted data points and the weighted mean of the observed data respectively. The CD is a measure of the fraction of the total variance accounted for by the model (Scientist User Handbook, 1995).

The MSC is a normalised modification of the Akaike Information Criterion (AIC) (Wagner, 1993) and gives the same rankings between models but is independent of the scaling of the data points. The MSC is defined by the following equation:

$$\text{MSC} = \ln \frac{\sum_{i=1}^{n} W_i (Y_i - \overline{Y})^2}{\sum_{i=1}^{n} W_i (Y_i - \hat{Y}_i)^2} - \frac{2P_p}{n}$$

Where $P_p$ is the number of parameters estimated. When comparing two models with different numbers of parameters, the MSC places a burden on the model with the larger number of parameters to have a better coefficient of determination. When judging the fit of a particular model to experimentally determined data, the most appropriate model is that with the largest MSC. Equal weighting was used in the fitting of drug release profiles as it gave the best MSC and CD values.

## 4.6 Measurements of platelet aggregations

Platelet-rich plasma (PRP) was obtained from blood of healthy volunteers (six females and one male) who were not taking anti-inflammatory agents prior to the donating. 40 ml of blood was obtained by venous puncture and mixed with trisodium citrate (9:1, v/v). Platelets were enumerated using an automated platelet counting device. Platelet rich plasma (supernatant of whole blood after centrifugation at 250 g for 20 minutes at 18 °C) was prepared. PRP was

resuspended at a physiological concentration (2.5 $\times 10^{11}$/l) of platelets. Platelet aggregation was initiated by the addition of collagen (0.3–5 g/ml). Aggregation was studied in the presence or absence of nanoparticles (1-500 μg/ml) using a Chronolog whole blood optical lumi aggregometer linked to Aggro-Link data reduction system at 37 °C (Radomski et al., 2005). Nanoparticles were suspended in Dulbecco's Phosphate Buffer Saline (DPSS) and sonicated for 5 minutes before examination. The particles were examined with the assistance of Professor Marek Radomski and dr. Anna Radomska, School of Pharmacy and Pharmaceutical Sciences, Trinity College Dublin.

## 4.7 Measurements of biointeractions with dendritic cells

Nanoparticles (1 mg/ml) were suspended in Dulbecco's Phosphate Buffer Saline (DPSS) and sonicated for 5 minutes before examination. The particles were examined by Yuki Ozasa and Dr. Edward Lavelle, School of Biochemistry and Immunology, Trinity College.

Female BALB/c mice, C3H/HeN mice and C3H/HeJ mice, which were 6-8 weeks of age, were used. BALB/c mice, bagg albino strain of laboratory mice, are useful for research in both cancer and immunology. C3H/HeN and C3H/HeJ mice do not carry mouse mammary tumour virus. C3H/HeJ mice are endotoxin resistant. The C3H parent strain was developed by LC Strong in 1920 from a bagg albino female mouse. BALB/c mice were purchased from Bioresearch unit, TCD and C3H/HeN and C3H/HeJ were purchased from Harlan Olac (Bicester, U.K.) and maintained under regulations of the European Union and the Irish Department of Health. Bone marrow-derived immature dendrite cell (BMDC) was isolated from the femurs and tibia of mice with sterile dissection tools (Ozasa, 2007).

Sandwich ELISA (Enzyme-Linked Immuno Sorbent Assay) was used as a method to quantify cytokine production by cells. The level of production of IL-4, IL-5, IL-6, IL-12p40 and IFN-γ was measured by using matching antibody pairs for each cytokine purchased from BD PharMingen (Abingdon, U.K.), whereas the level of IL-1ß, IL-10, IL-12p70 and IL-17 was measured using Duoset ELISA kit purchased from R&D Systems. Data obtained were presented as the mean cytokine concentration from triplicate wells of an ELISA plate (Ozasa, 2007).

Flow cytometry were used to investigate the expression of various surface makers on cells such as MHC class II and the co-stimulatory molecules CD80, CD86 and CD40. DCs ($1\times10^6$ cells/ml) from Balb/c, C3H/HeJ and C3H/HeN mice previously treated with chitosan samples were stained with CD86-PE, CD80-FITC and CD11c-APC or CD40-FITC, MHC II-PE and CD11c-APC for 30 minutes at 4°C. Cells were washed twice with fluorescence activated cell sorter (FACs) buffer (2% w/v Foetal Calf Serum (FCS, Sigma-Aldrich) and 0.1% w/w sodium azide (Sigma-Aldrich)) and immunofluorescence analysis was performed on a FACScan (DakoCytomation CyAn) and data was analysed using Summit software (Ozasa, 2007).

The levels of endotoxin (LPS) in the samples were measured using a PyroGene® recombinant factor C assay kit (Cambrex). After incubating samples with recombinant factor C enzyme solution for one hour at 37°C, fluorescence was measured in a microplate reader using excitation/emission of 380/440nm (Ozasa, 2007).

Cytotoxic analysis was carried out by Propidium Iodide staining. Propidium Iodide (PI, Sigma-Aldrich) staining can be used to detect necrosis of cells as it is excluded by viable cells but can penetrate cell membranes of dying or dead cells. Chitosan

samples were incubated with cells over night at 37°C, and then were centrifuged at 1200rpm for five minutes. After the wash with FACs buffer, 150 µl of PI was added to the cells and cells were immediately read on a flow cytometry (Ozasa, 2007). Flow cytometry is the characterisation and measurement of cells as they travel in a stream. In order to take measurement, a laser beam is focused on the stream as cells travel. A detector is placed in line with laser path. The scattered light is collected and named Forward Scatter (FS). FS is proportional to cell size. The bigger the cell, the more light is scattered and the higher the signal detected. A second detector is placed perpendicular to the laser path to collect the scattered light and in this manner the light collected is named Side Scatter (SS). SS is proportional to cell complexity. The more organelles inside the cytoplasm the higher the signal. FS is plotted on the x-axis with SS plotted on the y-axis and each dot presents one cellular event. In this way the changes inside cells are presented between different cell treatments.

# RESULTS AND DISCUSSION

## Chapter 5 PLGA micro and nano particles

## 5.1 Introduction

Emulsion techniques, including the double emulsion and single emulsion technique, are methods usually used in the manufacture of drug loaded PLGA particles. Since process variables can affect the properties of the particles produced, different solvents, sonication times and powers were investigated to evaluate their effects on the physical properties of PLGA micro and nano particles. Investigated properties included size, morphology and drug loading.

Different compounds such as proteins (H S A, OVA, OVA-coupled peptide), NSAIDs (indomethacin, ketoprofen) were encapsulated in PLGA micro and nano particles. Since these substances have different physicochemical properties, their release profiles were compared and evaluated.

Release profiles from PLGA microparticles prepared using different solvents were compared to determine if the solvent used during manufacture had any impact on the drug release. Release profiles, with different drug loadings from PLGA nanoparticles, were estimated and compared, to evaluate the drug loading and particle size effects.

Coumarin-6 was loaded onto PLGA nanoparticles as a fluorescence marker. Its effect on the physical properties of PLGA nanoparticles were studied and coumarin-6 release experiments from PLGA nanoparticles were carried out to investigate the usability of these fluorescent particles in animal or cell uptake studies in the future.

Although release studies of macromolecular compounds have been reported by numerous groups (Blanco and Alonso, 1997, Pean et al., 1998; Hernadez et al.,

1998; Sandor et al., 2001), there were large differences between the results. It deemed necessary to evaluate the affecting factors and conclude on their effects on antigen releases.

## 5.2 Measurement of polymer molecular weight

The molecular weight of polymer PLGA RG504 was characterised by gel permeation chromatography (GPC). Table 5.1 shows the $M_w$, $M_n$, polydispersity (p) and the manufacturer data (Boehringer Ingelheim Pharma). $M_w$ is the weight average molecular weight of a polymer; $M_n$ is the number average molecular weight; the ratio of the weight average to the number average is called the polydispersity index.

The polymer was reported by the manufacturer to have intrinsic viscosity values of 0.16-0.24 dL/g, (0.1% w/v in chloroform 25 °C).

Table 5.1 Molecular weight characteristics of the PLGA polymer studied.

| PLGA Polymer (Batch34012) | $M_w$ (kDa) | $M_n$ (kDa) | Polydispersity | Manufacturer data $M_w$ (kDa) |
|---|---|---|---|---|
| RG 504 | 55.4 ±6.32 | 53.8 ±6.14 | 1.03 ±0.01 | 48 |

(Samples represent the mean of three determinations ±standard deviation)

The $M_w$ value obtained in the present work (Table 5.1) agreed with the values reported by the manufacturer and Mollo and Corrigan (2002) for the same batch of the product. In the study reported by Mollo and Corrigan, the molecular weight of RG 504 was measured by GPC under the same conditions and the $M_w$ was 54.123 kDa.

# 5.3 PLGA microparticles

## 5.3.1 Preparation of PLGA microparticles

A group of protein loaded PLGA microparticles (No. 1-5) was prepared to examine the sonication effects on the particle size, size span and protein loadings. The results are shown in Table 5.2. The protein encapsulated was human serum albumin (H S A). Dichloromethane (DCM) was chosen as the solvent in the initial studies as it is one of the solvents commonly used to prepare PLGA particles.

Table 5.2 Effect of sonication time and power on the preparation of PLGA micro particles with dichloromethane (DCM) as solvent.

| Sol-vent | No. | 1st[1] | 2nd[2] | D 50% (μm) | D 90% (μm) | Span | Yield% | Protein EE% | Protein Loading (% w/w) |
|---|---|---|---|---|---|---|---|---|---|
| DCM | 1 | 2 w, 30s | 2 w, 30s | 3.79 ±1.81 | 30.10 ±6.60 | 7.63 ±3.52 | 20.4 ±2.9 | 49.6 ±5.8 | 0.496 ±0.059 |
| | 2 | 2 w, 1min | 2 w, 30s | 2.98 ±1.04 | 9.40 ±1.65 | 2.97 ±1.15 | 21.4 ±5.4 | 54.3 ±9.7 | 0.543 ±0.098 |
| | 3 | 2 w, 1min | 2 w, 2min | 2.80 ±1.13 | 8.25 ±2.54 | 2.69 ±0.45 | 50.8 ±3.6 | 61.4 ±11.2 | 0.614 ±0.012 |
| | 4 | 4 w, 1min | 2 w, 2min | 1.90 ±1.06 | 6.16 ±5.32 | 2.46 ±1.29 | 53.1 ±4.6 | 67.8 ±1.9 | 0.678 ±0.019 |
| | 5 | 4 w, 1min | 4 w, 1min | 1.72 ±0.25 | 5.19 ±0.65 | 3.00 ±0.09 | 67.6 ±7.4 | 71.1 ±9.1 | 0.711 ±0.091 |

(Samples represent the mean of three determinations ±standard deviation)
1st: sonication time and power for 1st emulsion
2nd: sonication time and power for 2nd emulsion
w: Watt
EE%: encapsulation efficiency%

From Table 5.2, we can see that the particle size decreased with an increase in both sonication time and power. D 90% values ranged from 30.10 ± 6.60 μm to 5.19 ± 0.65 μm when the power increased from 2 watts to 4 watts and the sonication time from 30s to 1 minute. The median size, D 50% decreased from 3.79 ± 1.81 μm to 1.72 ± 0.25 μm under the same increase in the sonication time and power. The decreases in D 90% size were significant ($p<0.05$) between batches No.1 to No.5.

Size span describes the particle distribution. The smaller the span the more even the size of the microparticles, and the closer D 90% is to D 50%. In Table 5.2, the span decreased from 7.63 ± 3.52 to 3.00 ± 0.09 when the power increased from 2 w to 4 w and sonication time from 30s to 1 minute in emulsion No.1 and No.5, which means the particles were more even in size for the sample No.5 than No.1. The difference is significant ($p<0.05$). Furthermore, the H S A loading of PLGA particles and the encapsulation efficiency (EE %) were increased from sample No.1 to No.5. The relatively low EE % and yield % values for the batch No.1 may be due to the poor emulsification process produced by short sonication time and low power.

The particles D 50% and D 90% sizes are compared in Figure 5.1. The D 90% tends to decrease from No.1 to No.5. The D 90% value for the batch No.5 is similar to the D 50% value for batch No.1.

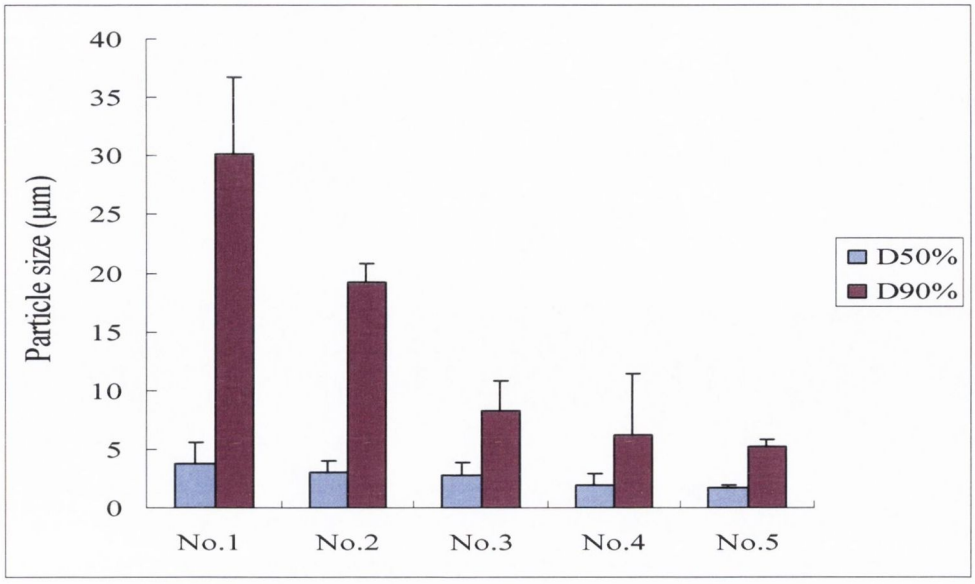


Figure 5.1 Particle sizes of PLGA microparticles (No.1-No.5) prepared with DCM as solvent.

The morphologies of the different PLGA microparticles (No.1-No.5) are shown in SEM (scanning electron microscopy) pictures (Figures 5.2, 5.3, 5.4, 5.5 and 5.6), together with the size distributions.

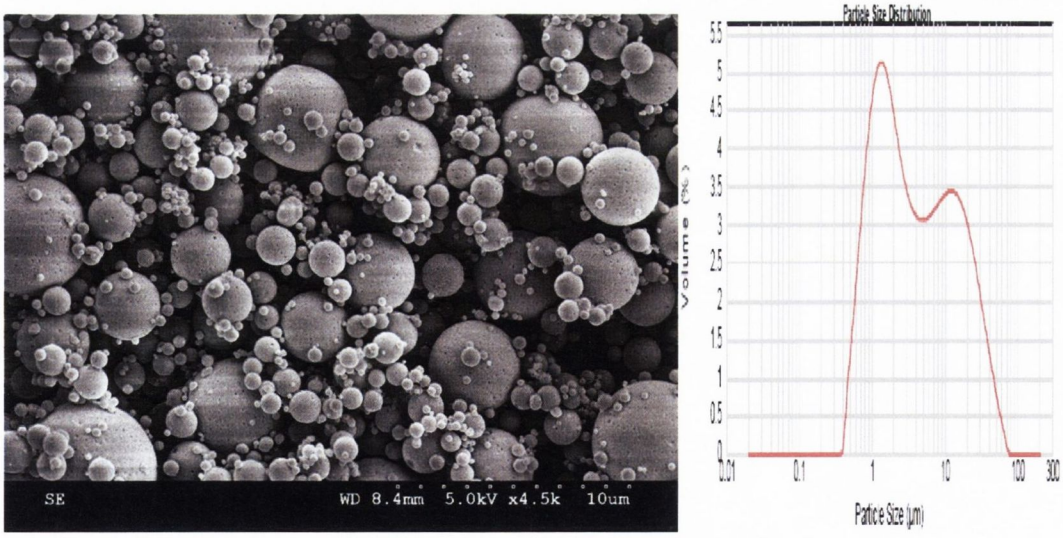


(a) (b)

Figure 5.2 (a) SEM picture, (b) size distribution of PLGA microparticles, batch No.1.

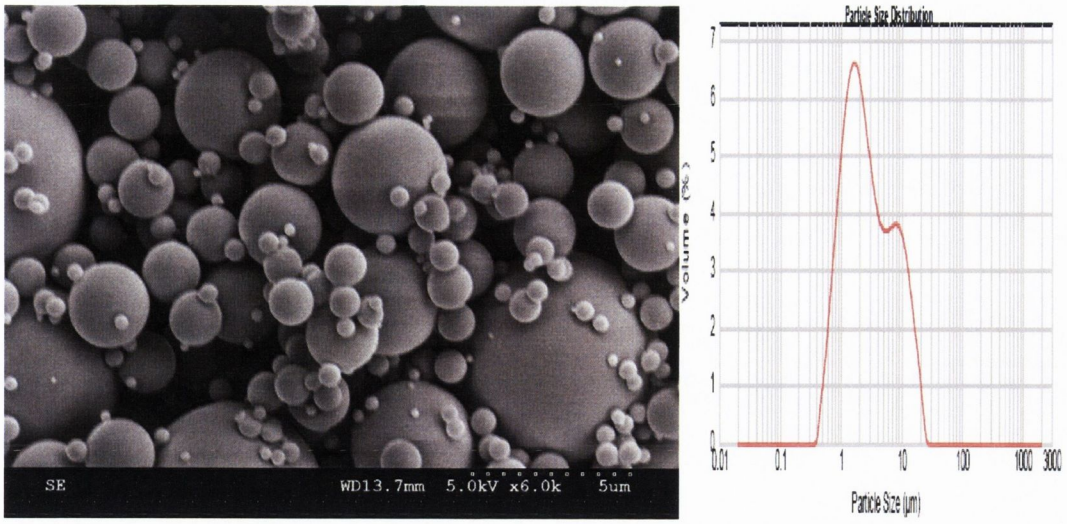


(a) (b)

Figure 5.3 (a) SEM picture, (b) size distribution of PLGA microparticles batch No.2.

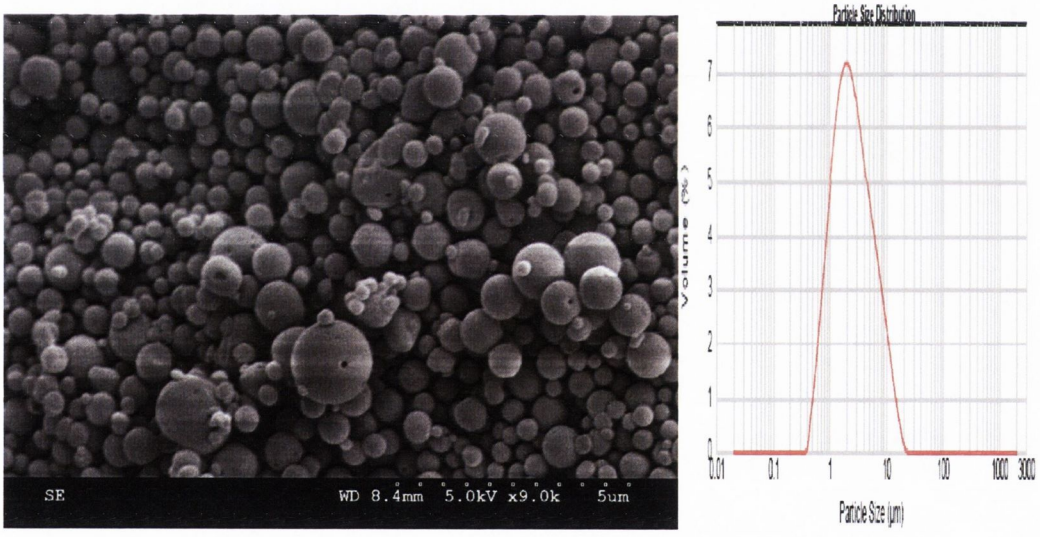


(a) (b)

Figure 5.4 (a) SEM picture, (b) size distribution of PLGA microparticles, batch No.3.

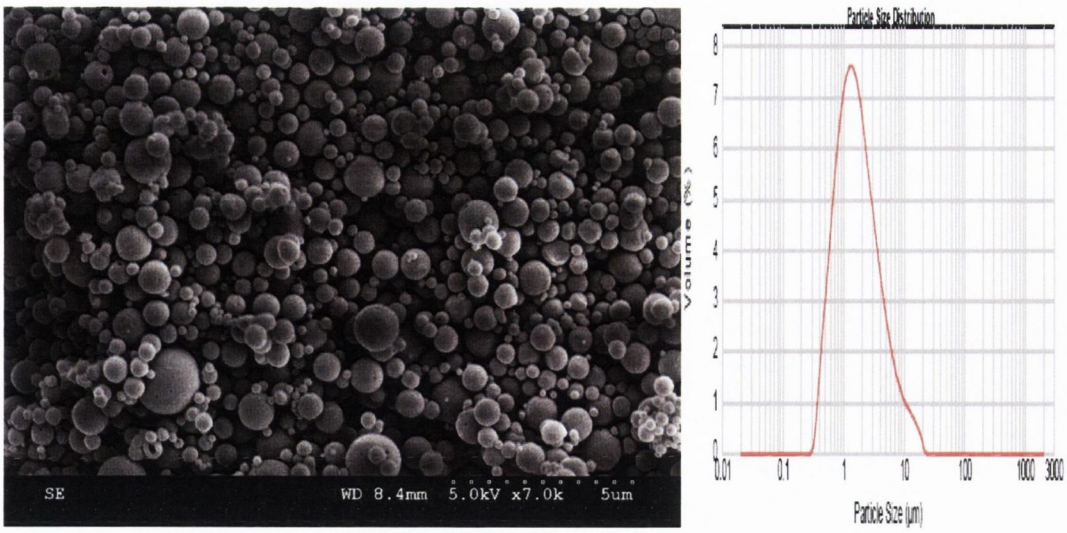


(a) (b)

Figure 5.5 (a) SEM picture, (b) size distribution of PLGA microparticles, batch No.4.

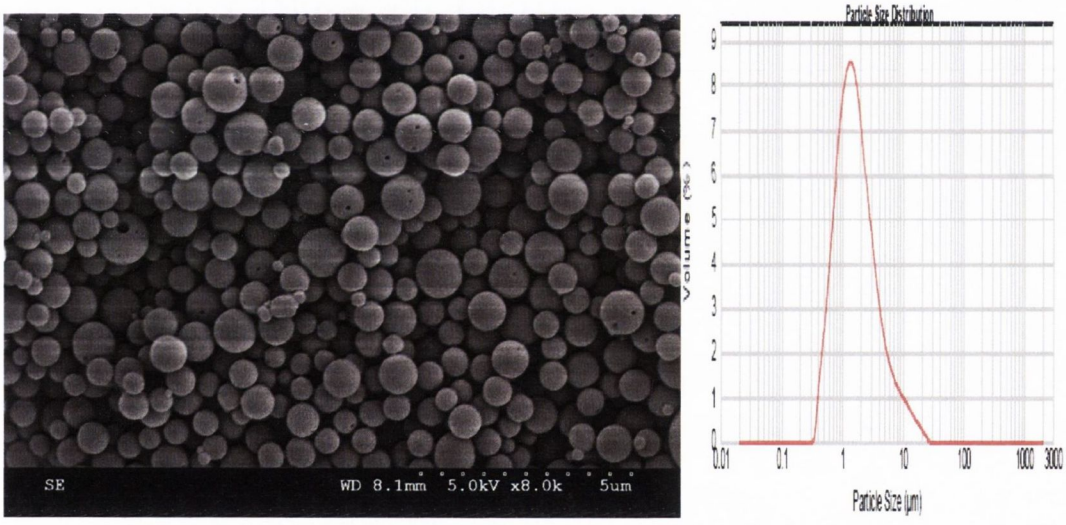


(a) (b)

Figure 5.6 (a) SEM picture, (b) size distribution of PLGA microparticles, batch No.5.

The SEM result indicated that as the sonication time and power increased, the spherical particles became more uniform in size. All the microparticles were shown to have relatively smooth surfaces.

Although DCM is one of the solvents commonly used to prepare PLGA particles, there are concerns over its environmental and human safety. DCM has been reported to be not biocompatible and a suspected carcinogen and mutagen (Sah et al., 1997). Ethyl acetate is another solvent which may be used to prepare PLGA particles, and ethyl acetate is considered to be less toxic than DCM (Sah et al., 1997). A series of PLGA microparticles (No.6-No.10) was prepared with ethyl acetate as a solvent to compare the solvent effects on the physical properties of PLGA microparticles prepared under the same sonication conditions as those used with DCM. The resultant particle sizes, spans, H S A loadings and EE % are shown in Table 5.3.

Table 5.3 Effect of sonication time and power on the preparation of PLGA micro particles with ethyl acetate as solvent.

| Sol-vent | No. | 1st[1] | 2nd[2] | D50% (μm) | D90% (μm) | Span | Yield% | Protein EE% | Protein Loading (% w/w) |
|---|---|---|---|---|---|---|---|---|---|
| Ethyl acetate | 6 | 2 w, 30 s | 2 w, 30 s | 3.71 ±1.03 | 14.10 ±2.90 | 3.56 ±1.50 | 49.3 ±0.9 | 67.6 ±3.6 | 0.676 ±0.036 |
| | 7 | 2 w, 1min | 2 w, 30 s | 3.43 ±0.89 | 12.50 ±3.70 | 3.34 ±1.70 | 51.8 ±1.0 | 45.2 ±11.1 | 0.452 ±0.111 |
| | 8 | 2 w, 1 min | 2 w, 2 min | 1.77 ±0.15 | 6.52 ±2.41 | 3.12 ±1.26 | 62.6 ±8.2 | 80.5 ±5.3 | 0.805 ±0.053 |
| | 9 | 4 w, 1 min | 2 w, 2 min | 1.82 ±0.07 | 5.87 ±1.79 | 2.67 ±1.14 | 65.6 ±1.0 | 67.2 ±5.4 | 0.672 ±0.054 |
| | 10 | 4 w, 1 min | 4 w, 1 min | 1.74 ±0.21 | 3.38 ±1.60 | 1.45 ±0.73 | 80.7 ±0.6 | 84.2 ±1.8 | 0.842 ±0.018 |

(Samples represent the mean of three determinations ±standard deviation)

1st: sonication time and power for 1st emulsion
2nd: sonication time and power for 2nd emulsion
w: watt
EE%: encapsulation efficiency%

From Table 5.3 we can see that the particle size decreased when both the sonication time and power increased. D 90% values ranged from 14.10 ± 2.90 μm to 3.38 ± 1.60 μm when the power increased from 2 watts to 4 watts and sonication time from 30s to 1 minute in both emulsions. The median size, D 50% also decreased from 3.71 ± 1.03 μm to 1.74 ± 0.21 μm for the batch No. 6 and 10, respectively. The span decreased from 3.56 ± 1.50 to 1.45 ± 0.73, which means the particles were more even in size for No.10 than No.6. The difference is significant ($p<0.05$). The yield% and H S A loading and EE % were increased with the increased sonication time and power.

The particle sizes D 50% and D 90% are shown in Figure 5.7. The D 90% tends to decrease when comparing the series of batches from No.6 to No.10. The decrease in D 90% was significant ($p< 0.05$). The particle size distribution for the batch No.10 is narrower than that of batch No.6.

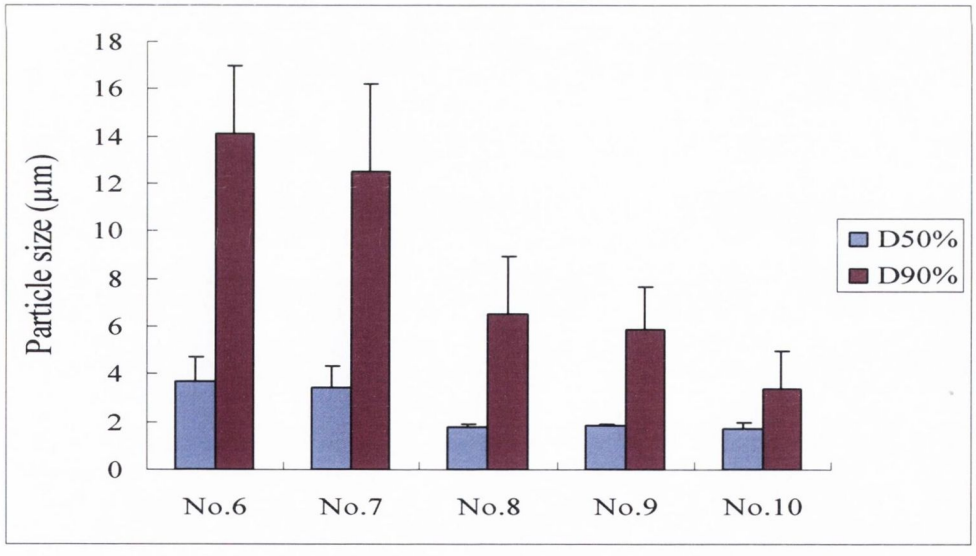


Figure 5.7 Particle sizes of PLGA microparticles (No.6-No.10) prepared with ethyl acetate as solvent.

The morphology of different PLGA microparticles (No.6-No.10) are shown in SEM (scanning electron microscopy) pictures (Figure 5.8, 5.9, 5.10, 5.11 and 5.12), together with the size distributions.

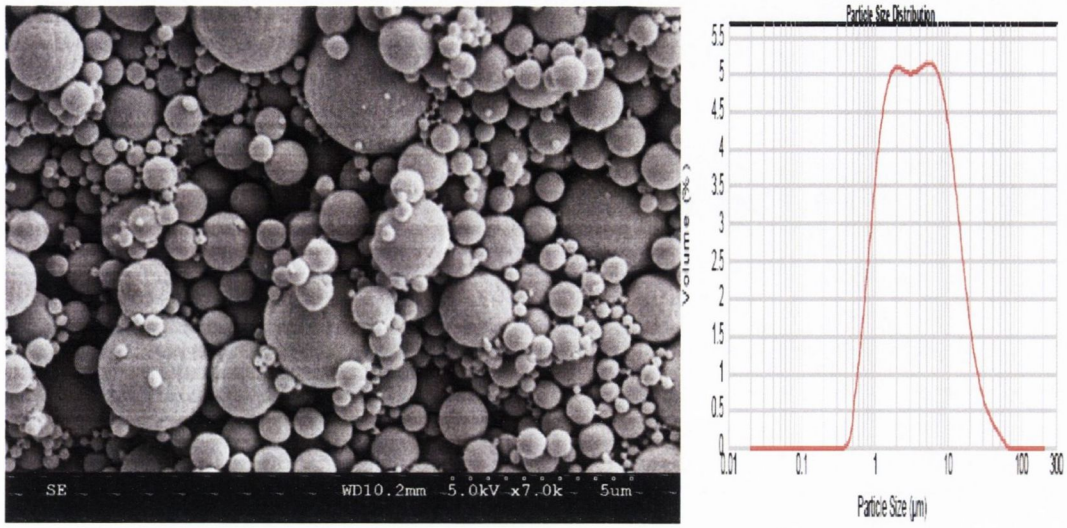


(a) (b)

Figure 5.8 (a) SEM picture, (b) size distribution of PLGA microparticles, batch No.6.

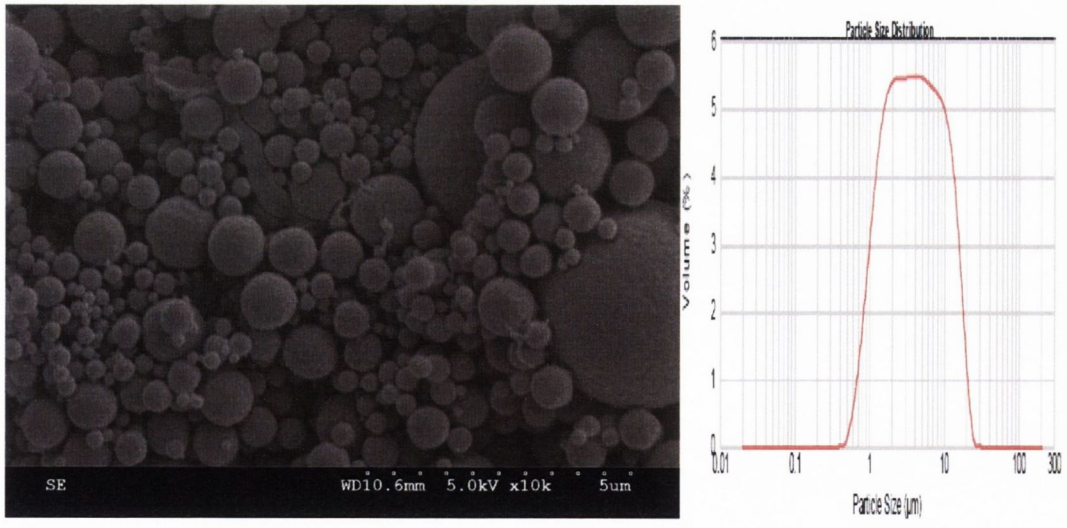


(a) (b)

Figure 5.9 (a) SEM picture, (b) size distribution of PLGA microparticles, batch No.7.

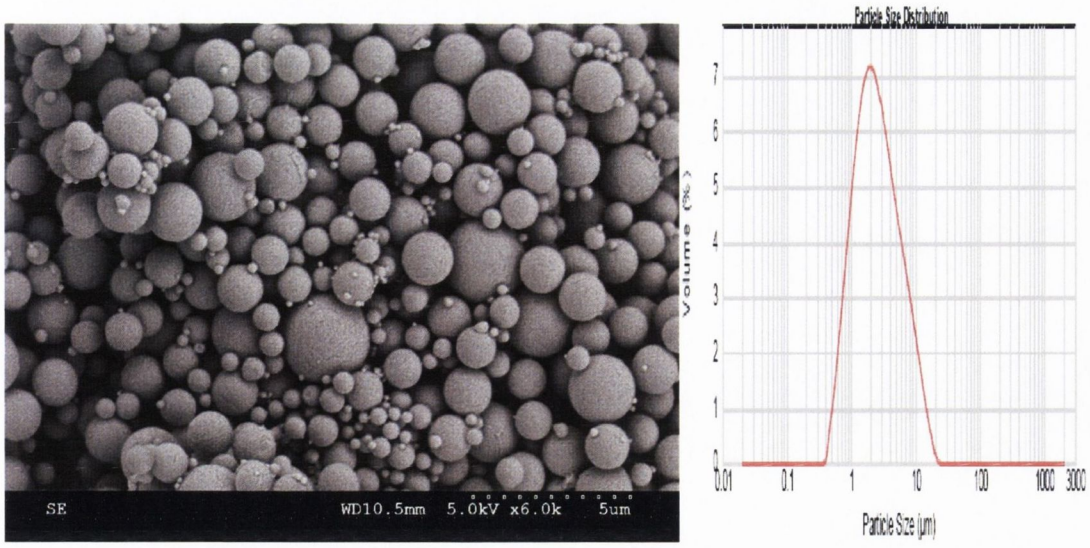


(a) (b)

Figure 5.10 (a) SEM picture, (b) size distribution of PLGA microparticle, batch No.8.

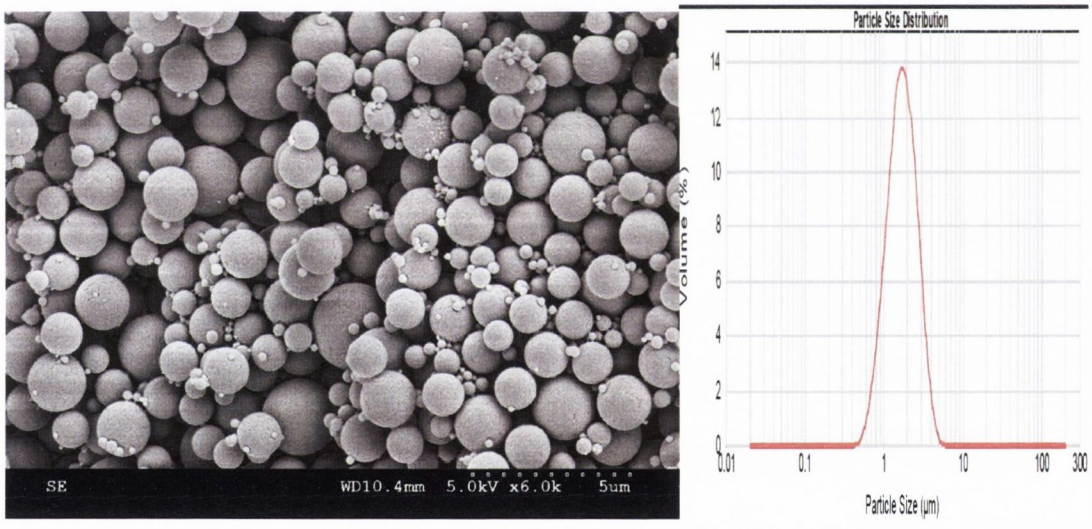


(a) (b)

Figure 5.11 (a) SEM picture, (b) size distribution of PLGA microparticles, batch No.9.

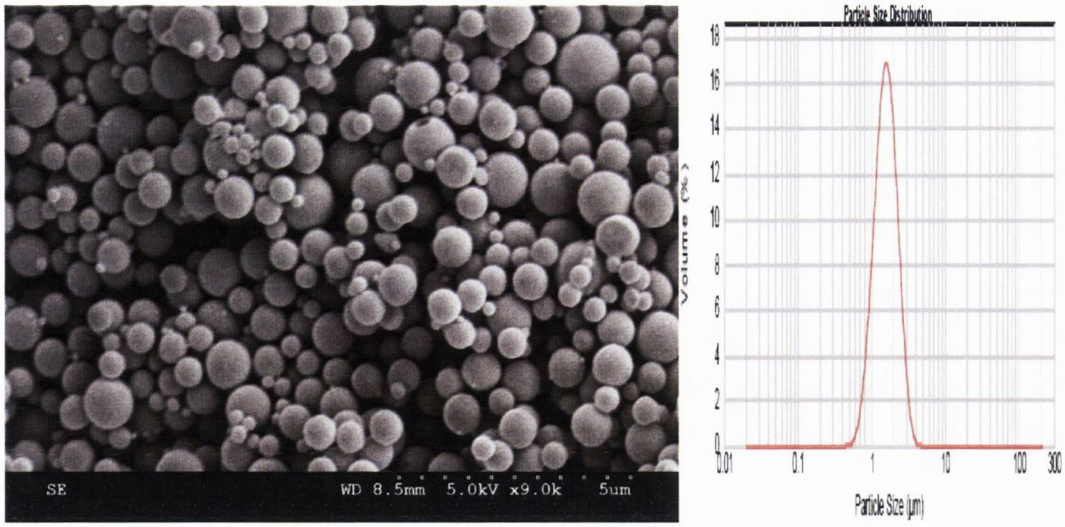


(a) (b)

Figure 5.12 (a) SEM picture, (b) size distribution of PLGA microparticles, batch No.10.

The SEM result indicated that as sonication time and power increased, the particles became more uniform in size. All the microparticles were shown to have relatively smooth surfaces.

On comparison of Table 5.3 and Table 5.2, as the sonication time and amplitude increased from 30s and 2 watts to 1 min and 4 watts, PLGA particles became more uniform in size for both solvents employed (DCM and ethyl acetate). The highest protein loading and encapsulation efficiency (%) were obtained for particles produced with ethyl acetate, and particles made by ethyl acetate showed relatively smaller and evener particle sizes, compared to particles made by DCM (Figure 5.2-5.6, Figure 5.8-5.12). This may due to the different miscibility and density properties of ethyl acetate and DCM. Miscibility is the solubility of one liquid in another. Ethyl acetate has a higher miscibility in water (8.7% w/w, Lide, 1995) than DCM (2.5 % w/w, Lide 1995). When the first water in oil emulsion was formed, the protein molecules in water were able to associate with polymer dissolved in the organic solvent more readily. In the work reported by Liu and Deng (2002),

poly-DL-lactic acid-polyethylene glycol (PELA) was used as a DNA delivery system. PELA microspheres were prepared by emulsion evaporation technique. Pure methylene chloride and methylene chloride/ethyl acetate mixture (volume ratio 1:1) were used to investigate the factors influencing the particle size and DNA loading efficiency. When ethyl acetate was mixed with methylene chloride, a higher loading efficiency (60.8% w/w) and smaller particle size (diameter 1.38 μm) were obtained, compared to the pure methylene chloride as solvent (loading efficiency 49.3% w/w; diameter 1.90 μm) (Liu and Deng, 2002). The miscibility of methylene chloride with water is 2.5% w/w (Lide, 1995). The improved water solubility of the solvent ameliorated the compatibility between the water phase (including DNA molecules and water molecules) and oil phase (including polymer molecules and solvent molecules) (Liu and Deng, 2002). When two immiscible liquids mixed together and are not emulsified yet, the liquid with higher density stands at the bottom and the liquid with lower density at the top. In the current study, the emulsifying process was assisted by the sonication with sonication probe on the surface of the upper liquid. When solvent ethyl acetate was used, since it has a lower density (0.897 g/cm$^3$) than water (1 g/cm$^3$), it settled at the top of water phase with the sonication probe touching at its surface. When sonication power is on, the power blew the solvent into the aqueous phase, forming oil droplets in water. If DCM was used as solvent, since it has a higher density (1.326 g/cm$^3$) compared to water, DCM stood at the bottom, with aqueous phase at the top. When the probe was placed on the surface of upper aqueous liquid, it became difficult to formulate DCM droplets into water, compared to ethyl acetate system. DCM is one of the solvents mostly used in emulsion techniques, however due to its toxicity concern (Martindale, 1996) and better particle characteristics obtained by using ethyl acetate, ethyl acetate was chosen as the solvent for preparation of micro and nanoparticles in further studies.

## 5.3.2 Differential scanning calorimetry (DSC) of PLGA microparticles

DSC is an analytical tool employed to measure a glass transition temperature ($T_g$), which is a thermal characteristic of amorphous substances. An important application of DSC is the determination of possible interactions between a drug substance and polymers used in the formulation. One approach is to produce binary mixtures of each ingredient and to monitor changes in melting endotherms, which would indicate either a physical or chemical interaction between the two components (Souillac and Rytting, 1999).

In order to compare the $T_g$ of H S A loaded PLGA microparticles with the drug free microparticles, two drug free batches of PLGA microparticles were prepared using DCM and ethyl acetate as solvents, respectively. The drug free batch made by DCM was named No.11 and had similar physical properties to the No.5 batch; the drug free sample made by ethyl acetate was named No.12 and had similar physical properties to the No.10 batch. The details are shown in Appendix I.

The thermal characteristics of (a) H S A loaded PLGA microparticles with DCM as solvent (No. 5), (b) H S A loaded PLGA microparticles with ethyl acetate as solvent (No. 10), (c) physical mixture of H S A and PLGA (1:100), (d) drug free PLGA microparticles with DCM as solvent (No. 11), (e) drug free PLGA microparticles with ethyl acetate as solvent (No. 12), (f) pure PLGA polymer are shown in Figure 5.13.

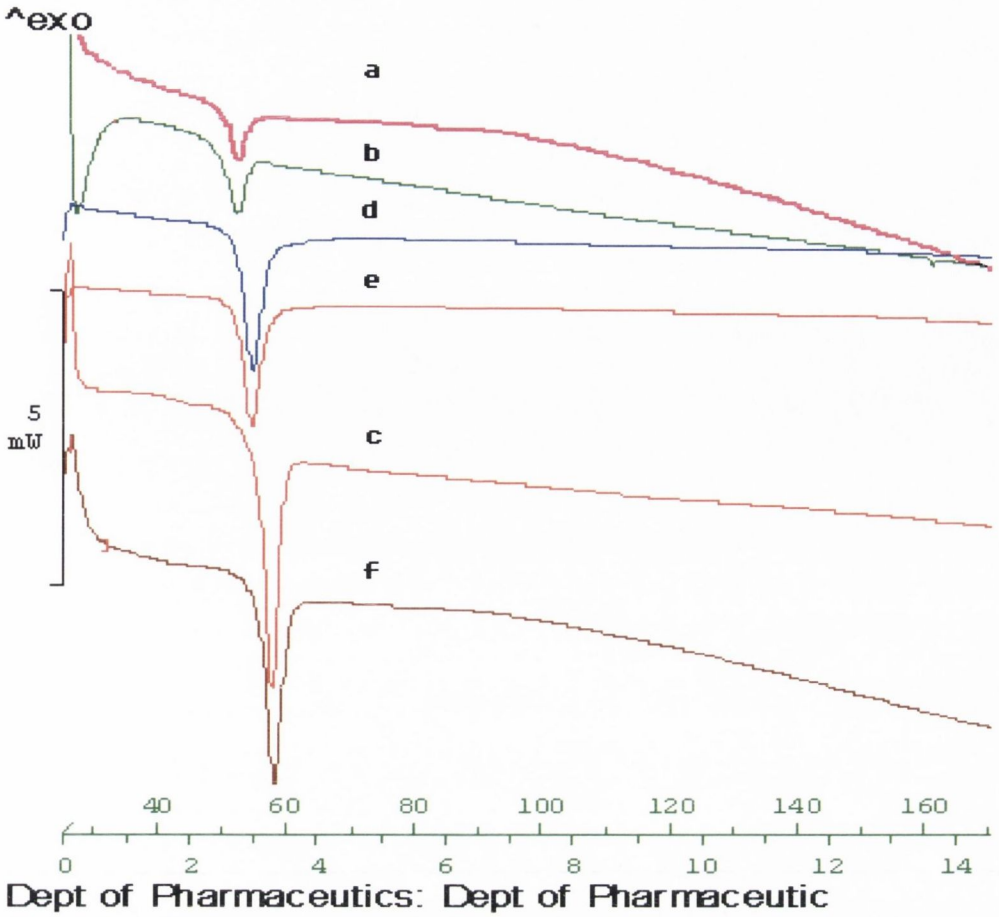


Figure 5.13 DSC results of (a) H S A loaded PLGA microparticles with DCM as solvent (No. 5 with loading 0.711%), (b) H S A loaded PLGA microparticles with ethyl acetate as solvent (No. 10 with loading 0.842%), (c) physical mixture of H S A and PLGA (1:100), (d) drug free PLGA microparticles with DCM as solvent (No. 11), (e) drug free PLGA microparticles with ethyl acetate as solvent (No. 12), (f) pure PLGA polymer.

The $T_g$ values are listed in Table 5.4. From Table 5.4 we can see that the H S A loaded PLGA microparticles had similar $T_g$ values regardless of the solvent used. The same trend was observable for the drug free PLGA microparticles. Using ethyl acetate, the $T_g$ of H S A loaded PLGA particles was 52.45 °C, which was smaller than the $T_g$ of drug free particles with a value of 54.39 °C. There was no protein peak observable with H S A loaded PLGA particles, indicating that the protein was molecularly dispersed in PLGA particles (Souillac and Rytting, 1999) or was not detectable due to the low level of the protein content. Similarly with DCM, the $T_g$ of H S A loaded PLGA particles was 52.33 °C, which was smaller than the $T_g$ of drug

free particles with a value of 54.62 °C, and there was no protein peak observable in the DSC scan of the H S A loaded PLGA particles. The DSC scan of the physical mixture of PLGA and H S A only showed one single peak which may be caused by the low concentration of H S A presented in the mixture (1:100). Many authors have reported that drugs dispersed at the molecular level in such polymeric carriers result in amorphous dispersed drug, combining the benefits of enhanced dissolution capabilities, improved stability and a disordered phase of the drug (Tajber et al., 2005 and Ford, 1986).

Table 5.4 Glass transition temperatures ($T_g$) of PLGA microparticles.

| No. | Name | $T_g$ °C |
|---|---|---|
| (a) | H S A loaded PLGA microparticle with DCM as solvent (No. 5) | 52.33 |
| (b) | H S A loaded PLGA microparticle with ethyl acetate as solvent (No. 10) | 52.45 |
| (c) | Physical mixture of H S A and PLGA | 55.13 |
| (d) | Drug free PLGA microparticles with DCM as solvent (No. 11) | 54.62 |
| (e) | Drug free PLGA microparticles with ethyl acetate as solvent (No. 12) | 54.39 |
| (f) | Pure PLGA polymer | 56.71 |

The thermal characteristic of pure H S A is shown in Figure 5.14. The first broad peak indicated the dehydration of H S A and the second peak indicated the decomposition.

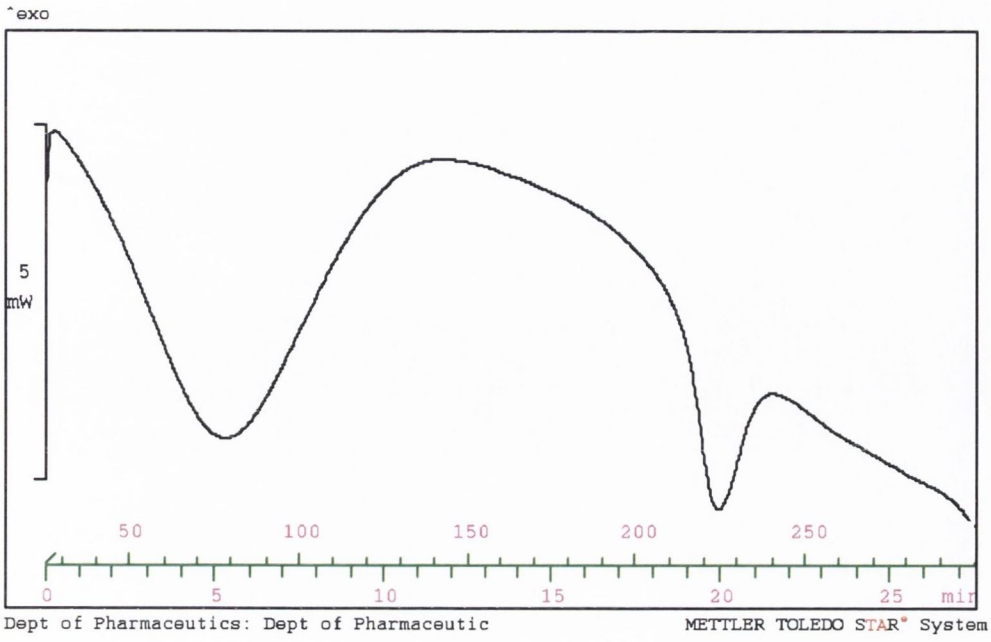


Figure 5.14 DSC result of H S A.

### 5.3.3 Integrity of protein encapsulated

The integrity of protein extracted from PLGA microparticles manufactured by ethyl acetate and DCM was studied by Sodium Dodecyl Sulphate PAGE electrophoresis (SDS-PAGE) (Figure 5.15). Samples were run in lane 3 (PLGA microparticles made with ethyl acetate, No.10) and lane 4 (PLGA microparticles made with DCM, No.5) with a standard H S A sample in lane 2 and a molecular weight marker in lane 1.

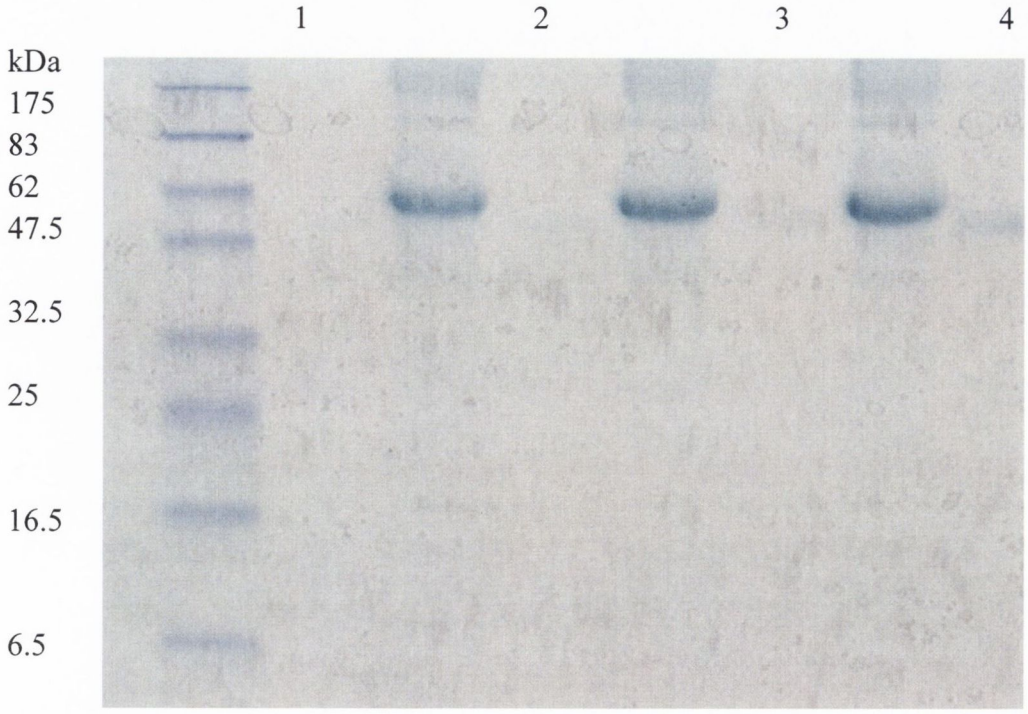


Lane 1: Molecular weight markers (M.W. range: 6.5 kDa-175 kDa)
Lane 2: H S A protein standard (66 kDa)
Lane 3: H S A extracted from microparticles with ethyl acetate as solvent (No. 10)
Lane 4: H S A extracted from microparticles with DCM as solvent (No.5)

Figure 5.15 SDS-PAGE of extracted protein from PLGA microparticles prepared with different solvents.

The molecular weights of H S A extracted from batches No.5 and No.10 were similar to each other as shown on the SDS-page (Figure 5.15) and both of them were similar to the H S A standard which suggests the procedure does not affect the integrity of protein, and the integrity was maintained throughout the production processes.

### 5.3.4 Release study of H S A

The release profiles of H S A from PLGA microparticles prepared with ethyl acetate and dichloromethane are compared in Figure 5.16. The released protein was collected from PBS buffer (pH 7.4) at 37°C and measured by the Pierce Micro BCA™ Protein Assay Reagent Kit as described in Section 4.5.1.

Regardless of the solvent used, *in vitro* release studies showed a burst release, followed by a slower, sustained release of protein. Around 3.5-5.0 μg/mg of protein (50-60 %) was released from PLGA particles by 30 days and this amount remained constant until 45 days. The microparticles used here were particles from the batches No.5 and No.10. The amount and percentage release data at different time points are listed in Appendix II.

The profiles are in agreement with the profiles reported by Gang et al., (2002). In their study, H S A, as a model protein, was encapsulated in PLGA (50:50 molecular weight 40 000-75 000) microparticles by a double emulsion technique with a mean particle size of 6.7 μm, and protein loading of 1.65 %. *In vitro* studies were carried out for 30 days. Around 50-60 % of the encapsulated H S A was released from PLGA particles within 30 days in PBS buffer (pH 7.4) at 37 °C.

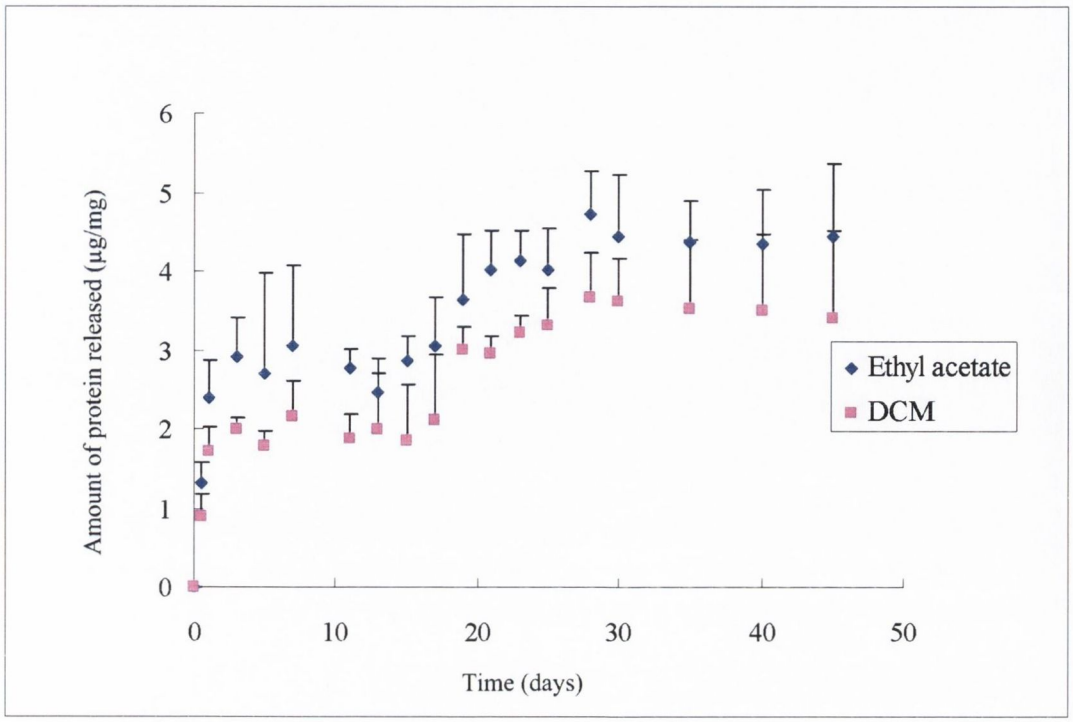


Figure 5.16 Study of H S A release from PLGA microparticles prepared using DCM and ethyl acetate. The medium was PBS (pH 7.4) buffer and the studies were carried out at 37 °C.

The H S A release profiles from PLGA microparticles manufactured by ethyl acetate and DCM were fitted to Equation 1.7 and the fittings are shown in Figure 5.17. The fractional value was calculated by the amount of protein released at that day divided by the average release of the highest release and the releases following. Parameters (estimate ± S.D.) obtained for the degradation controlled release rate and the burst release rate of the model were determined and are shown in Table 5.5. The equation assumes two additive release processes: an exponential fast release phase with a parameter $F_B$ which can be defined as the fraction of drug available for direct surface release and $K_B$ which is the release rate of this part of drug and a degradation controlled release phase with parameters k which is the rate constant and $T_{max}$, the time to the maximum drug release rate. The coefficient of determination (CD) and model selection criterion (MSC) were used as measures of goodness of fit when evaluating the suitability of a model. When judging the fit of a

particular model to experimentally determined data, the most appropriate model is that with the largest MSC.

Table 5.5 Parameters fitted to the model for H S A release study from PLGA microparticles.

| Solvent | $F_B$ | $K_B$ ($day^{-1}$) | k ($day^{-1}$) | $T_{MAX}$ (days) | CD | MSC |
|---|---|---|---|---|---|---|
| Ethyl acetate (No.10) | 0.623 ±0.022 | 1.53 ±0.25 | 0.561 ±0.172 | 19.5 ±0.6 | 0.977 | 3.340 |
| DCM (No.5) | 0.543 ±0.024 | 1.58 ±0.32 | 0.526 ±0.138 | 19.4 ±0.6 | 0.976 | 3.327 |

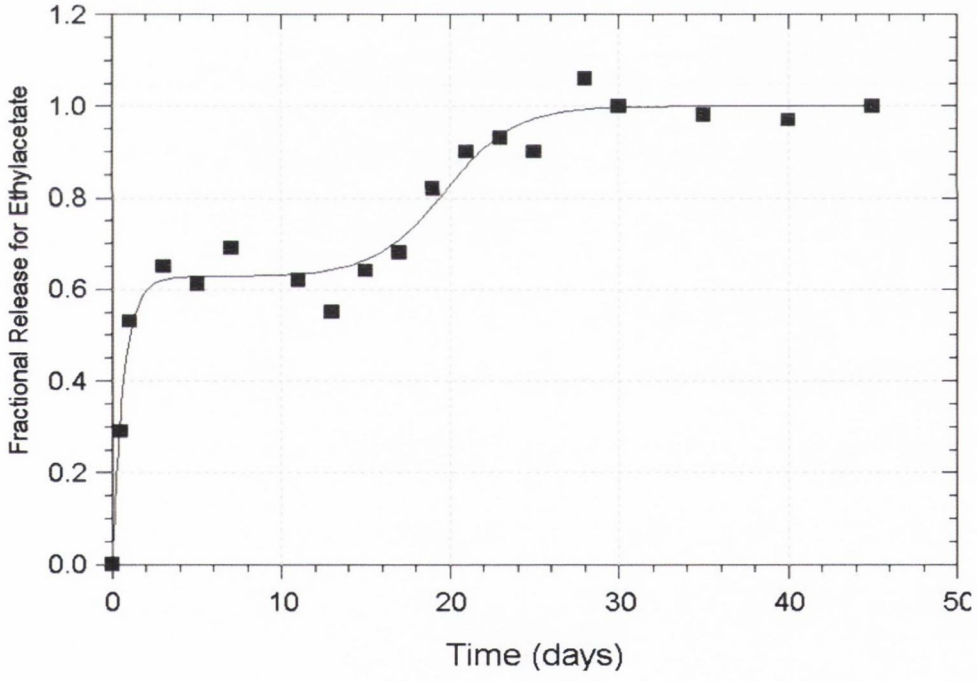


(a)

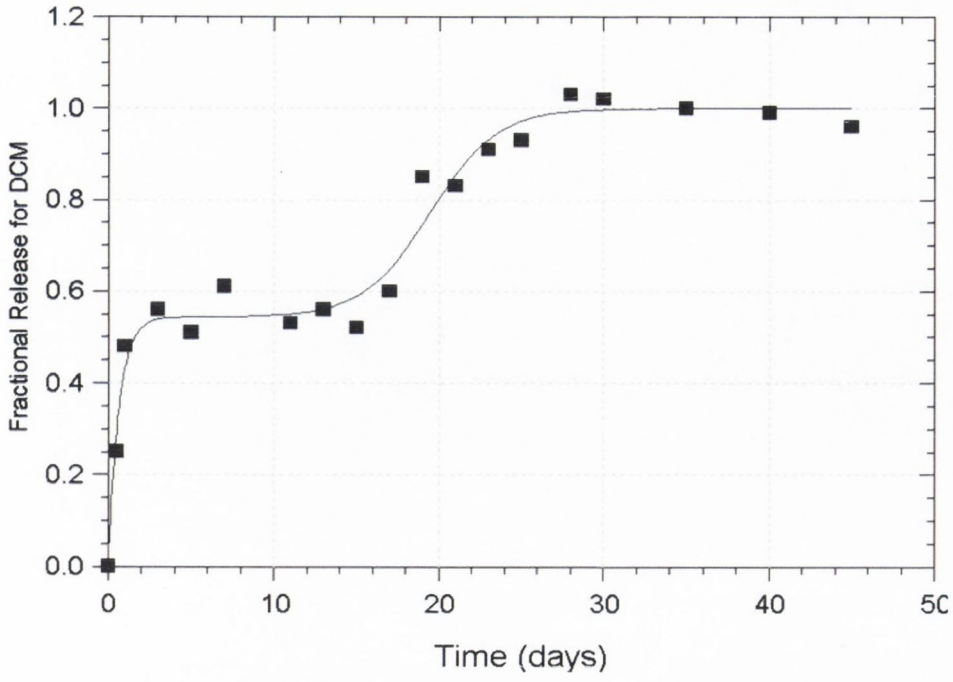


(b)

Figure 5.17 Model fit to protein loaded PLGA microparticles (a) No. 10 made by ethyl acetate, (b) No.5 made by DCM.

PLGA degradation plays an important role in drug release studies from PLGA particles. Dunne and co-workers (2000) studied the degradation behaviour of PLGA and reported that the polymer degradation demonstrated a biphasic profile consisting of an initial fast rate of molecular weight reduction, followed by a slower rate. More than 90% of the molecular weight reduction occurred in the initial fast rate. When incubated in PBS buffer (pH=7.4) at 37°C, the first molecular weight reduction phase of PLGA ended by 30 days of incubation, which is longer than the time of H S A release used to reach the maximum drug release rate (~19 days), which indicated that in the presence of protein, the polymer degradation was accelerated. In the work reported by Dunne and co-workers (2000), fluphenazine hydrochloride was loaded to PLGA microparticles (mean size 4.20 μm) with a drug loading of 8.17% and the time to reach the maximum release rate ($T_{MAX}$) was 15.8 days.

The amount of the protein released and their model fits are compared in Figure 5.18. The graph indicates that the release profiles of H S A from PLGA microparticles prepared with the use of different solvents both fit the model (Equation 1.7) and regardless of the solvent used, there is a burst release on the first day, followed by a slower, sustained, degradation controlled release of protein. The only difference is the larger loading and burst release observed for the ethyl acetate system.

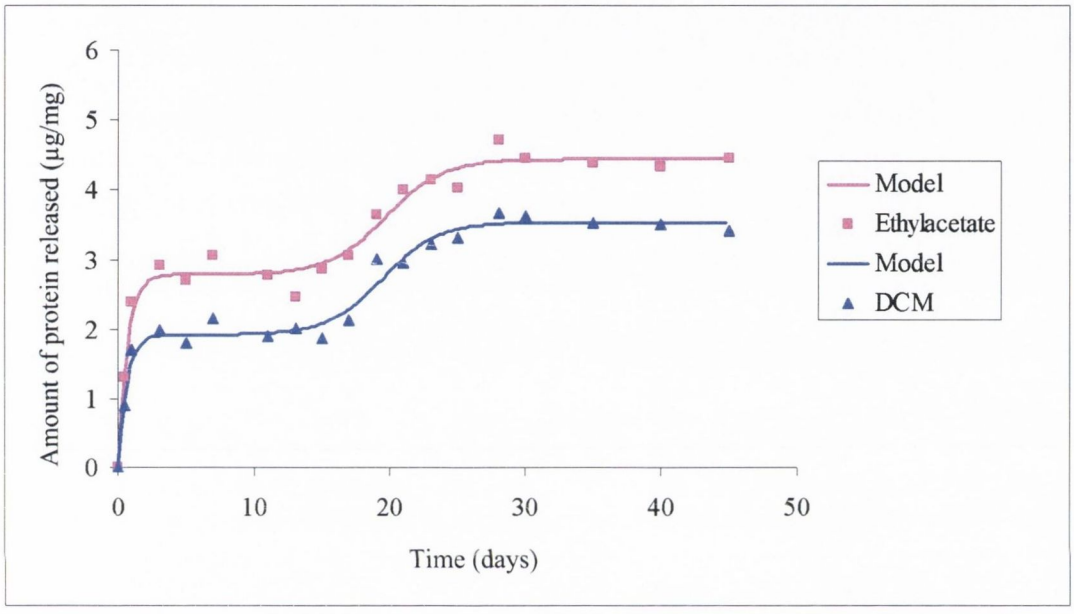


Figure 5.18 Model fit to the H S A released from PLGA microparticles prepared with different solvents (ethyl acetate and DCM).

## 5.3.5 Release studies of proteins other than H S A

To investigate the potential effects of the protein molecular weight on the protein releases from PLGA particles, two proteins, other than H S A ($M_w$, 66,500 Da), were encapsulated into PLGA microparticles. They were ovalbumin (OVA) ($M_w$, 44,300 Da) and OVA coupled F/G peptide ($M_W$, 46,300 Da). OVA coupled F/G peptide (OVA-F/G) was generously supplied by Professor Brian M Adair, Department of Veterinary Science, the Queen's University of Belfast. Ethyl acetate was used as the solvent. OVA coupled F/G peptide loaded PLGA microparticles

were named No.13 and OVA loaded PLGA microparticles-No.14. The characteristics of these three batches of microparticles are presented in Table 5.6.

Table 5.6 Physical properties of proteins loaded PLGA microparticles.

| No. | Protein | Molecular weight (kDa) (manufacturer) | Actual loading (% w/w) | Particle median size (μm) |
|---|---|---|---|---|
| 10 | H S A | 66.5 | 0.842 ±0.018 | 1.74 ±0.21 |
| 13 | OVA-F/G | 46.3 | 0.520±0.070 | 2.26±0.43 |
| 14 | OVA | 44.3 | 0.800±0.110 | 3.44±0.66 |

(Samples represent the mean of three determinations ±standard deviation)

Protein release profiles in PBS buffer (pH 7.4) at 37 °C are shown in Figure 5.19. From Figure 5.19 we can see that regardless of the different proteins used, the release profiles showed a burst release, followed by a slower, sustained release.

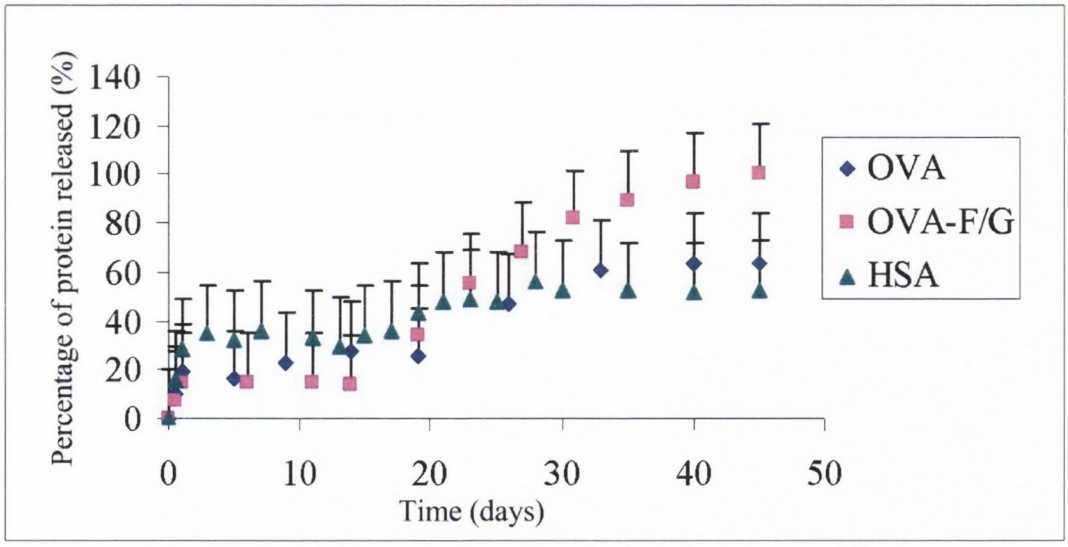


Figure 5.19 Percentage of protein released from PLGA microparticles in PBS buffer (pH 7.4) at 37 °C.

To evaluate the effect of proteins on their release behaviours, the release profiles were fit to Equation 1.7, the parameters were estimated and are shown in Table 5.7.

Table 5.7 Parameters of the release profiles of different proteins obtained from the fitting procedures.

| No. | Protein | $F_B$ | $K_B$ ($day^{-1}$) | k ($day^{-1}$) | $T_{MAX}$ (days) | CD | MSC |
|---|---|---|---|---|---|---|---|
| 10 | H S A | 0.623 | 1.53 | 0.561 | 19.5 | 0.977 | 3.340 |
| | | ±0.022 | ±0.25 | ±0.172 | ±0.6 | | |
| 13 | OVA-F/G | 0.108 | 3.18 | 0.215 | 23.9 | 0.994 | 4.470 |
| | | ±0.029 | ±1.77 | ±0.023 | ±0.6 | | |
| 14 | OVA | 0.290 | 1.24 | 0.495 | 25.4 | 0.997 | 5.204 |
| | | ±0.013 | ±0.16 | ±0.128 | ±0.3 | | |

Equation 1.7 describes the drug release profiles by combining the first order initial burst release and the polymer degradation controlled release. In Table 5.7, OVA loaded microparticles had the highest CD and MSC values of 0.997 and 5.204 compared to other particles (No.10 and No.13). From Table 5.7, we can see that with the decrease in the protein molecular weight from 66.5 kDa to 44.3 kDa, $T_{MAX}$ values were increased from 19.5±0.6 to 25.4±0.3.

PLGA degradation is a process marked by diffusion of water into the polymer matrix, swelling, and subsequent degradation brought about by hydrolysis of covalent bonds (Hutchinson and Furr, 1985). The first rapid release happens when the water initially penetrates into the polymer matrix which initiates release of the protein molecules present close or on the surface of the matrix, and additional protein molecules migrate through the interconnecting channels in the polymer matrix (Pean et al., 1998; Hernadez et al., 1998; Duggirala et al., 1996).

Microspheres encapsulating larger proteins had a preponderance of larger pores close to the surface which might allow the initial release of large protein clusters on the surface. This release would lead to a quicker penetration of the microsphere by water, causing the formation of the interconnecting channels or the release of protein in pre-existing channels within the microsphere (Hernadez et al., 1998; Duggirala et al., 1996). Both of these effects could lead to the continuous release through pores seen for microspheres encapsulating larger proteins. Microspheres encapsulating smaller proteins, however, seemed to have a higher percentage of small pores distributed throughout the microsphere (Sandor et al., 2001). This type of structure might entrap proteins, which would most likely yield a lag effect (Sandor et al., 2001). Sandor and the co-workers studied the effect of protein molecular weight on release from PLGA microparticles. In their work, proteins with different molecular weights (lysozyme 13.4 kDa, carbonic anhydrase 29 kDa, bovine serum albumin 66 kDa, alcohol dehydrogenase 150 kDa, thyroglobulin 669 kDa) were encapsulated in PLGA (50:50 MW 12,068) microspheres with particle sizes of 1-3 μm. At low loadings of 0.5-1.6 % w/w, release appeared to be dependent on the protein molecular weight while independent at high loadings of 4.8-6.9 % w/w. At low loadings, release of the larger proteins was dependent on diffusion through pores for the duration of the study (8 weeks), while for the smaller proteins it seems to depend on diffusion through pores initially and on degradation at later times (Sandor et al., 2001). When the molecular weight of protein decreased from 669 kDa to 13.4 kDa, the time required to reach 'the maximum release rate' was increased from 12 days to 28 days.

Size differences may be another reason that caused the increase of $T_{MAX}$ from H S A microparticles to OVA microparticles. H S A microparticles were smaller particle sizes (1.74 ± 0.96 μm) than OVA proteins (3.44 ± 0.66 μm). Particle size effects on release are discussed in Section 5.5.3. OVA-F/G loaded microparticles had the lowest $F_B$ value of 0.108 ± 0.029, with the greatest $F_B$ value being for H S A. It is in

agreement with a trend of protein loadings on PLGA microparticles (Table 5.6). OVA-F/G had a low actual loading of 0.52 %, compared to the model protein of OVA and H S A with values of 0.80 % and 0.84 %, respectively. Loading effects on protein releases are discussed in Section 5.5.2.

## 5.4 Preparation of PLGA nanoparticles

### 5.4.1 Properties of PLGA nanoparticles

By increasing the sonication time and power, the particle size of PLGA was decreased from micro range to the nano range. In this study, model protein H S A was used as the antigen and ethyl acetate was used as the solvent to prepare PLGA nanoparticles. This batch of particles was named No.15.

The properties of PLGA microparticles (No.10) and nanoparticles (No.15) are compared and shown in Table 5.8.

Table 5.8 Properties of PLGA micro and nanoparticles loaded with H S A.

| No | D50% (μm) | D90% (μm) | Span | Yield% | Protein EE% | Protein loading (% w/w) |
|---|---|---|---|---|---|---|
| 10 | 1.74 ±0.21 | 3.38 ±1.60 | 1.45 ±0.73 | 80.7 ±0.6 | 84.2 ±1.80 | 0.842 ±0.018 |
| 15 | 0.56 ±0.17 | 0.97 ±0.14 | 0.95 ±0.16 | 86.1 ±3.2 | 52.1 ±1.7 | 0.521 ±0.017 |

(Samples represent the mean of three determinations ±standard deviation)

From Table 5.8 we can see that when the sonication time was increased from 1 minute to 10 minute on both emulsifying processes, keeping the sonication power all the same (4 watt), the median particle size of microparticles was decreased from 1.74 $\pm$ 0.21 μm to 0.56 $\pm$ 0.27 μm and the D90% was decreased from 3.38 $\pm$ 1.60 μm to 0.97 $\pm$ 0.34 μm. The difference in the median particle size was significant ($p<0.05$).

From Table 5.8 we can see that when the particle size was decreased by increasing the sonication time, the protein loading and EE% were decreased ($p<0.05$). It may be due to the fact that larger oil droplets prevent leakage of the inner aqueous phase through the oil phase into the outer aqueous phase. The size of oil droplets plays an important role in determining the resultant particle sizes (Yang et al., 2001; Cui et al., 2005).

The morphology of PLGA nanoparticles (No.15) together with the size distribution is shown in Figure 5.20.

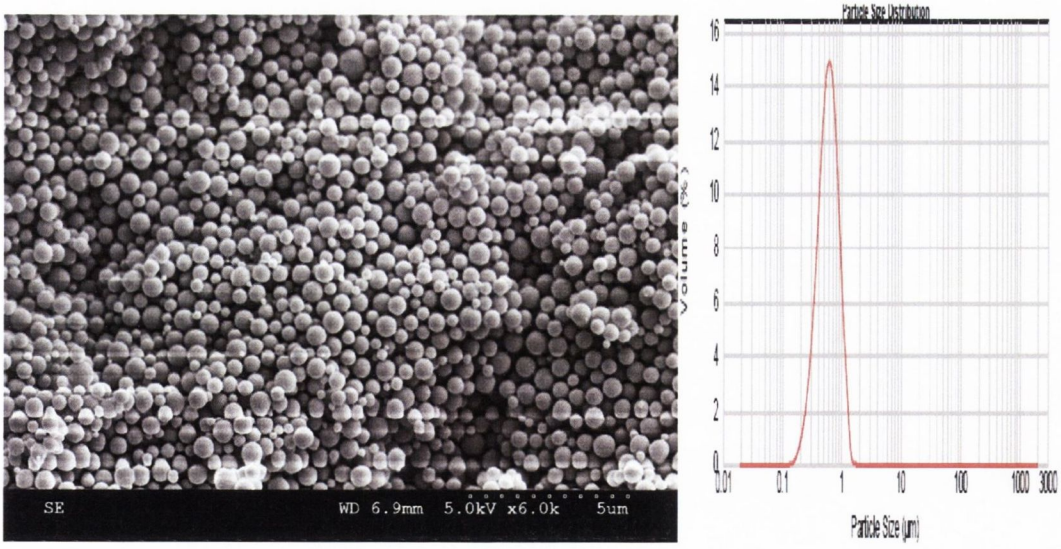


(a) (b)

Figure 5.20 (a) SEM picture, (b) size distribution of PLGA nanoparticles loaded with H S A (No.15).

Figure 5.20 indicates that the nanoparticles presented smooth particle morphology and even range of particle sizes.

## 5.4.2 Integrity of protein encapsulated

The molecular weights of H S A extracted from PLGA nanoparticles (No.15) were compared with those of the protein before encapsulation by SDS-PAGE. H S A extracted from the nanoparticles was similar to H S A standard shown on the SDS-PAGE (Figure 5.21) which suggested that the integrity of the protein conformation of H S A was maintained in PLGA nanoparticles.

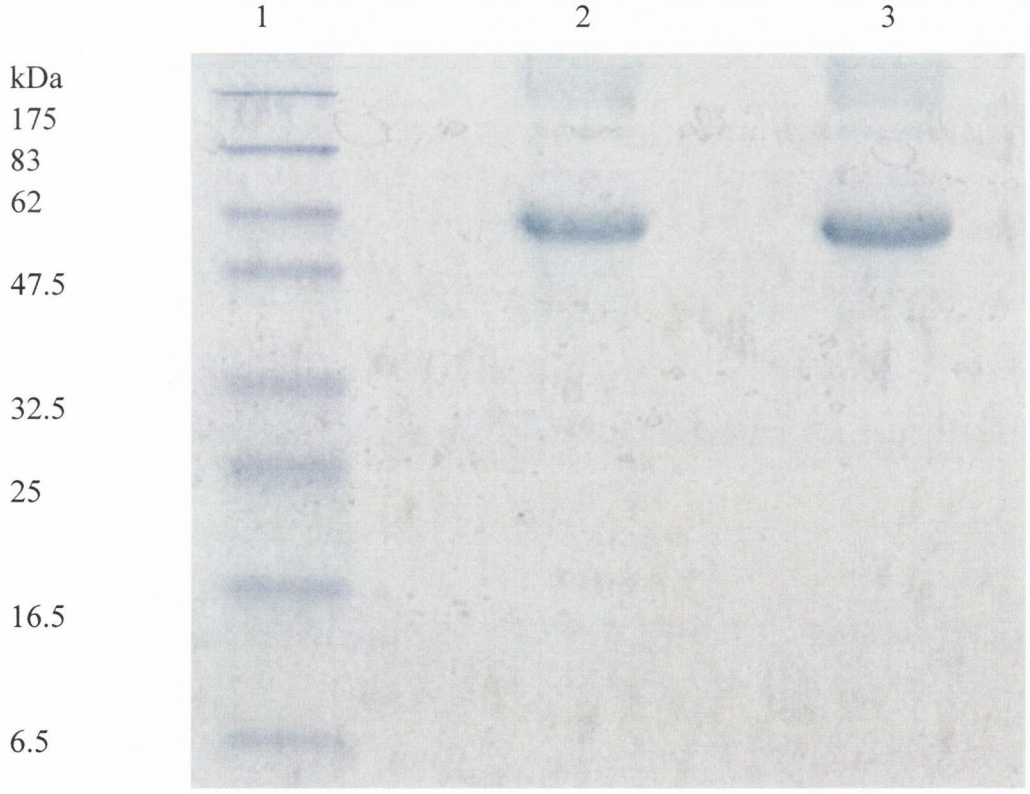


Lane 1: Molecular weight markers (M.W. range: 6.5 kDa-175 kDa)
Lane 2: H S A protein standard (66 kDa)
Lane 3: H S A extracted from nanoparticles (No.15)

Figure 5.21 SDS-PAGE of H S A extracted from nanoparticles (No.15).

The integrity of model proteins such as H S A, BSA and OVA are generally maintained under processing conditions encountered during microencapsulating. In the work reported by Igartua et al. (1998), a model protein bovine serum albumin (BSA, $M_w$ 66,200 Da) was encapsulated within PLGA RG 506 (50:50) microspheres using a double emulsion method. The particles presented a mean size of 1.32 μm, with the protein loading of 8.61% w/w. The SDS-PAGE results showed that there was no apparent effect of the encapsulation conditions on the structural integrity of the protein. The encapsulation conditions include the contact with solvent DCM, probe sonication and vigorous shaking (Igartua et al., 1998). In another work recently reported by Cohen et al. (2007), PLGA (50:50, $M_w$ 123,400 Da) was used to encapsulate pDNA (alkaline phosphatase, AP, a reporter gene) in nanoparticles with a size range of 600 nm. As shown from agarose gel electrophoresis, the entrapped plasmid maintained its structural and functional integrity (Cohen et al., 2007).

### 5.4.3 Drug free PLGA nanoparticles

To exclude the H S A effect on the preparation process, drug free PLGA nanoparticles were prepared using similar conditions as those used to manufacture of PLGA nanoparticles loaded with H S A (Section 5.4). Ethyl acetate was used as solvent. The resultant nanoparticles presented a median particle size of 0.64 ± 0.15 μm (n=3) and D 90% of 1.09 ± 0.54 μm (n=3), which were similar to the sizes of H S A loaded nanoparticles (No.15). The SEM picture and size distribution of the drug free PLGA nanoparticles (No.16) are shown in Figure 5.22. Both of the drug free and H S A loaded batches of nanoparticles showed smooth surfaces and spherical particle shapes.

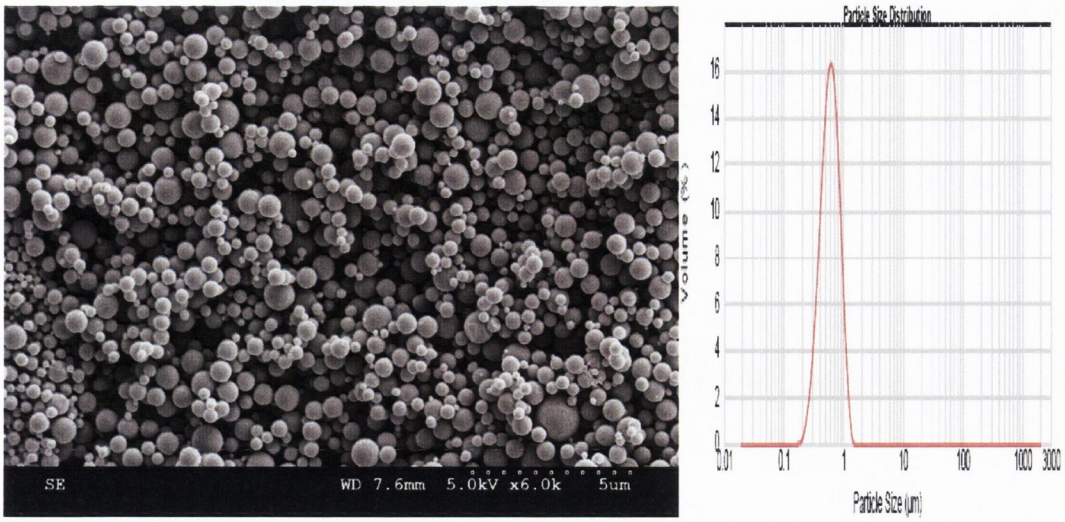


(a) (b)

Figure 5.22 (a) SEM picture, (b) size distribution of drug free PLGA nanoparticles, batch No.16.

### 5.4.4 H S A loaded PLGA nanoparticles stained with coumarin

Coumarin-6 was loaded to PLGA nanoparticles as a lipophilic fluorescence marker to observe the particles under a fluorescence microscope. It is preferred to use coumarin as a fluorescent label because of easier handling, avoiding the problems associated with the use of radioactive material and high marker recovery. It is a common experimental approach to study uptake and particle targeting *in vivo* or *in vitro*.

In this study, coumarin-6 was dissolved in PLGA solution. After the emulsification and collection, the resultant particles encapsulating protein H S A (named No. 17) were freeze dried and their morphologies were observed under a fluorescence microscope. The solvent used to formulate the particles was ethyl acetate. From the microscopic picture (Figure 5.23), we can see that all the nanoparticles showed a

bright green colour, which indicates the feasibility of using them in *in vivo* studies. The properties of the coumarin-6 loaded nanoparticles are presented in Table 5.9.

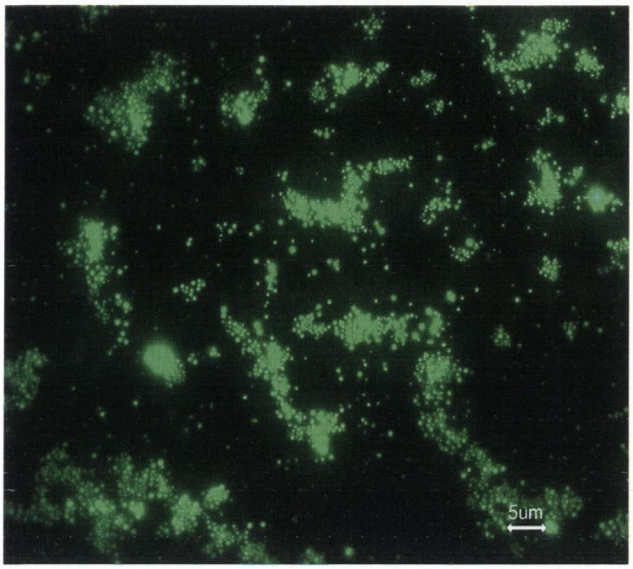


Figure 5.23 Fluorescence microscope picture of H S A loaded PLGA nanoparticles with coumarin-6 (No.17).

Table 5.9 Comparison of properties of PLGA nanoparticles loaded with coumarin-6 (No.17) and particles without coumarin (No.15). Both of the batches were encapsulated with protein H S A.

| No | D50% | D90% | Span | Yield % | Protein Loading (μg/mg) |
|---|---|---|---|---|---|
| 15 | 0.56 ±0.17 | 0.97 ±0.14 | 0.95 ±0.16 | 86.1 ±3.2 | 5.21 ±0.17 |
| 17 | 0.74 ±0.17 | 1.26 ±0.38 | 1.19 ±0.18 | 89.1 ±3.8 | 5.15 ±2.25 |

(Samples represent the mean of three determinations ±standard deviation)

The loading of coumarin-6 in particles (No.17) was 0.25 μg/mg (0.025% w/w), with an encapsulation efficiency of 100 %. These results agree with the work previously reported by Pietzonka et al., (2002). In their work coumarin-6 was loaded onto PLGA (RG 752) nanoparticles with coumarin loading of 1 μg/mg and the resultant

EE% value was over 95%. Coumarin loaded nanoparticles (No.17) had similar particle sizes to particles without coumarin (No.15).

The release of H S A and coumarin from the same batch of nanoparticles (No.17) were carried out for 45 days separately. The release medium used was PBS buffer (pH=7.4) at 37°C. The release profile of coumarin-6 is shown in Figure 5.24 and the amount and percentage release data collected over time is listed in Appendix II. The release data from these coumarin loaded PLGA nanoparticles is also shown in Figure 5.243.

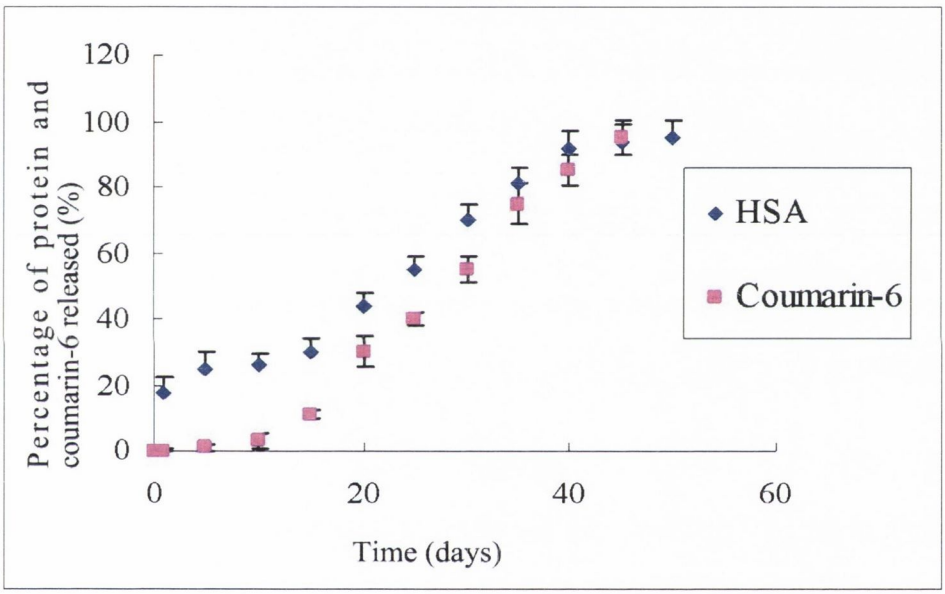


Figure 5.24 Percentage of coumarin-6 and H S A released from PLGA nanoparticles.

From Figure 5.24 we can see that coumarin-6 showed a very low burst release at the first day, with a value of no more than 1%, and then the coumarin release was sustained until the end of the study, which was 45 days. In the work previously reported by Qaddoumi et al. (2003), coumarin-6 was loaded into PLGA (50:50 RG752) nanoparticles with a loading of 0.50 μg/mg and particle size of 100 nm to study the coumarin release from PLGA particles *in vitro*. BSA was encapsulated as a model protein with loading of 5%. As a result, no more than 0.32% of coumarin-6

was released within the first 24 hours in bicarbonate Ringer's solution (BRS) at 37 °C. H S A showed a burst release around 20% of the total encapsulated protein, and followed by a sustained release until the end of the study.

Both of the release profiles of coumarin-6 and H S A were fitted to Equation 1.7 to evaluate the release parameters and the results are listed in Table 5.10. The model fits are presented in Figure 5.25.

Table 5.10 Parameters obtained by fitting the experimental points of the release profiles to Equation 1.7 (Batch number 17).

| Release | $F_B$ | $K_B$ ($day^{-1}$) | k ($day^{-1}$) | $T_{MAX}$ (days) | MSC | CD |
|---|---|---|---|---|---|---|
| Coumarin-6 | 0.006 | 0.786 | 0.167 | 27.5 | 4.062 | 0.990 |
| | ±0.001 | ±0.050 | ±0.070 | ±5.5 | | |
| H S A | 0.206 | 1.565 | 0.148 | 26.8 | 4.245 | 0.991 |
| | ±0.020 | ±0.503 | ±0.009 | ±0.6 | | |

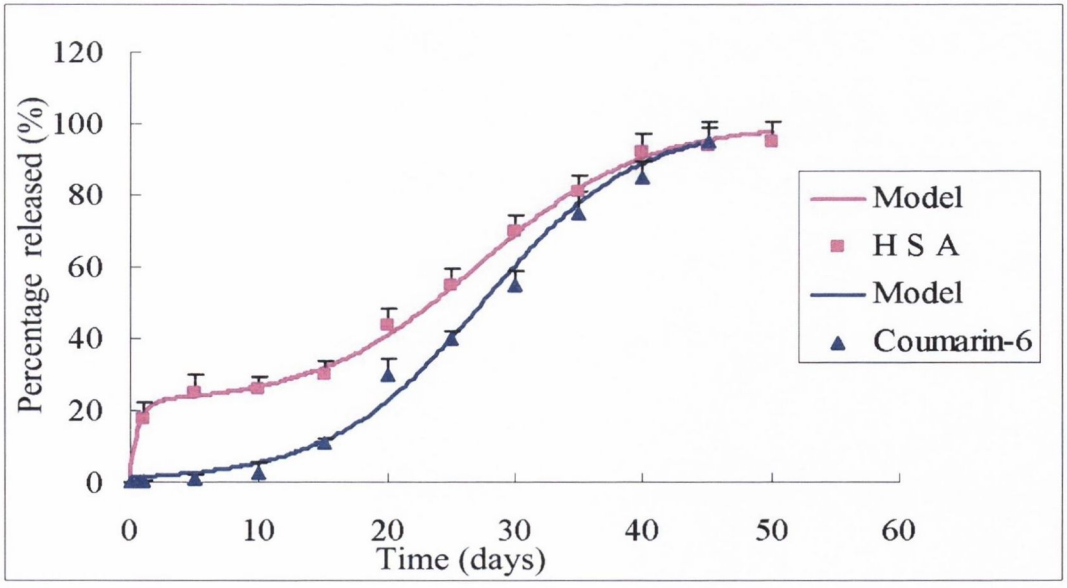


Figure 5.25 Model fit to the percentage of H S A and coumarin-6 released from PLGA nanoparticles.

From Table 5.10 we can see that the time to reach the maximum release rate of coumarin-6 ($T_{MAX}$) was 27.5 days. Compared to the degradation results reported by Dunne (2000), the presence of H S A and coumarin-6 accelerated the degradation of PLGA nanoparticles. The degradation results of PLGA nanoparticles with sizes of 0.5 μm presented $T_{MAX}$ time of 59.7 days and k of 0.045 (Dunne, 2000). Compared to the release of protein H S A, coumarin-6 showed a lower burst release ($F_B$ 0.006 ±0.001) than H S A ($F_B$ 0.218 ±0.034). This may due to the fact that low loading of coumarin-6 (0.25 μg/mg) leads to a low burst release, compared to H S A with loading of 5.15 μg/mg. The loading effects on the drug release are discussed in Section 5.5.2.

Coumarin-6 could be a useful probe for fluorescence microscopic studies. About 0.025% w/w dye loading in the particles results in bright fluorescent nanoparticles (Figure 5.23). Coumarin-6 can also be quantified by HPLC. Researchers have reported a sensitive HPLC method to quantify 6-coumarin in both cell lysates and in tissue samples (Panyam et al., 2002; Davda and Labhasetwar, 2002). As a marker, coumarin-6 loaded nanoparticles can be used in *in vivo* pharmacokinetics and tissue distribution studies.

Under the same sonication time and power, the concentration of PLGA RG 504 in ethyl acetate was increased from 100 mg/ml to 200 mg/ml to investigate the effect of coumarin on the particle size. No additional excipients like coumarin-6 were incorporated. As a result, the median particle size was increased from 0.75 μm to 3 μm with an increasing protein loading from 7 μg/mg to 8 μg/mg. This batch was named No.18 and the properties of the particles are listed in Appendix I. The results agreed with the previous work reported by Cui et al., 2005. It was considered that the higher concentration of PLGA, at a fixed sonication force, results in a higher viscosity of the oil phase, which makes the formation of small oil droplets difficult and, as a result, larger particles. The increased encapsulation efficiency of protein

can also be attributed to the increase in both oil phase viscosity and the larger size of the oil droplets, which prevent leakage of the inner aqueous phase through the oil phase into the outer aqueous phase (Yang et al., 2001; Cui et al., 2005).

### 5.4.5 Particle preparations with Digital Sonifier

Digital Sonifier 250 (Branson) is a more powerful sonicator compared to SONICS VC130PB and may provide ten times higher power output than SONICS VC130PB. A Branson 250 sonifier was used in this study to investigate the effect of sonication power on the particle size. The particle sizes did not decrease when the output power was increased from 4 watts to 40 watts, and furthermore, aggregation of the product was observed after emulsification. This batch was named No.19 and the properties of the particles are listed in Appendix I. The emulsification process under high power of sonication would result in a large and rapid rise in the emulsion temperature. When 40 watts of sonication power was applied to the system for more than 30 seconds, the emulsion boiled, which may have caused polymer aggregation.

## 5.5 PLGA nanoparticles loaded with OVA

In this study, ovalbumin (OVA) was used as the model protein and encapsulated into PLGA nanoparticles to observe the loading effects on the properties of particles and protein release from nanoparticles. Ethyl acetate was used as solvent.

### 5.5.1 Loading effects on the properties of nanoparticles

Three batches of nanoparticles with different OVA loadings, named No.20, 21 and 22, were prepared by the double emulsion technique and their characteristics are shown and compared in Table 5.11.

Table 5.11 Properties of PLGA nanoparticles with different loading of OVA.

| No. | Theoretical loading% | Actual protein loading% | Protein EE% | D50% (μm) | D90% (μm) | Span |
|---|---|---|---|---|---|---|
| 20 | 1 | 0.71 ±0.03 | 70.8 ±2.8 | 0.42 ±0.17 | 1.03 ±0.51 | 1.47 ±0.46 |
| 21 | 10 | 2.95 ±0.50 | 29.7 ±5.0 | 0.44 ±0.12 | 1.10 ±0.77 | 2.14 ±0.97 |
| 22 | 20 | 5.45 ±0.40 | 27.3 ±2.0 | 0.67 ±0.24 | 1.19 ±0.58 | 1.35 ±0.32 |

(Samples represent the mean of three determinations ± standard deviation)

The protein loadings in these three nanoparticle batches were 0.71 %, 2.95 % and 5.45 %, respectively. The encapsulation efficiency% (EE %) was determined and was expressed by relating the actual OVA entrapment to the theoretical OVA entrapment. The EE% tended to decrease from batch No.20 to 22 and the difference was significant when comparing No.20 with No.22 ($p<0.05$), which indicated a decrease in loading capacity of proteins when the initial theoretical loading of the protein was increased. This is in agreement with the work previously reported by Yang et al., (2001). In their work, BSA was encapsulated in PLGA (65:35 $M_w$ 40 000-75 000) microparticles with different loadings. An increase in BSA loading reduced the encapsulation efficiency (EE%) of BSA. When the theoretical protein loading was 0.57 %, the EE% was 79.1 %; when the theoretical loading was increased to 4.80 %, the EE% was decreased to 55.0 %. A higher loading provides a higher BSA concentration in the emulsion droplets. This increase in the

concentration gradient of BSA between the emulsion droplets and the continuous water phase increases the amount of BSA dissolving into the continuous water phase (Yang et al., 2001).

The morphologies of these three batches of nanoparticles are shown in Figure 5.26, 5.27 and 5.28.

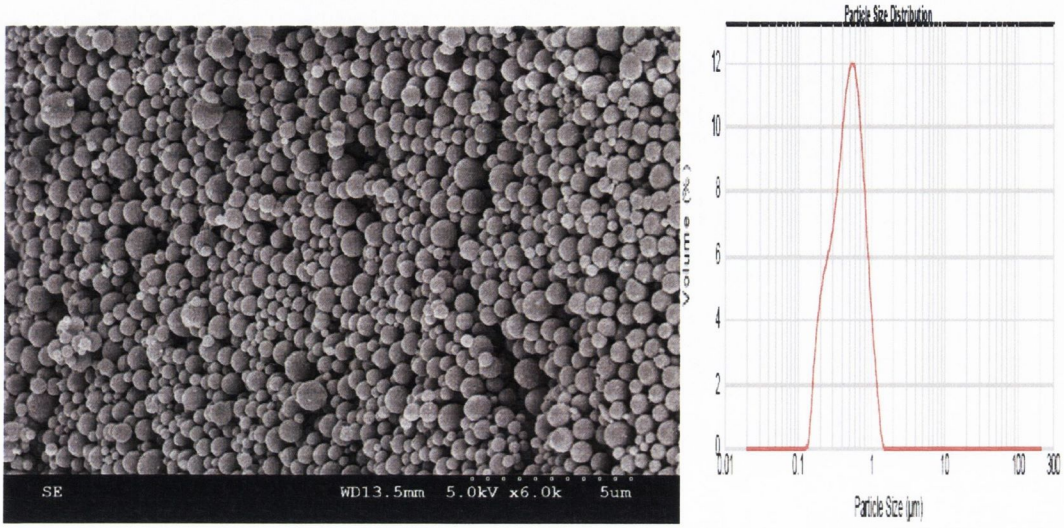


(a) (b)

Figure 5.26 (a) SEM picture, (b) size distribution of PLGA nanoparticles loaded with OVA (No.20).

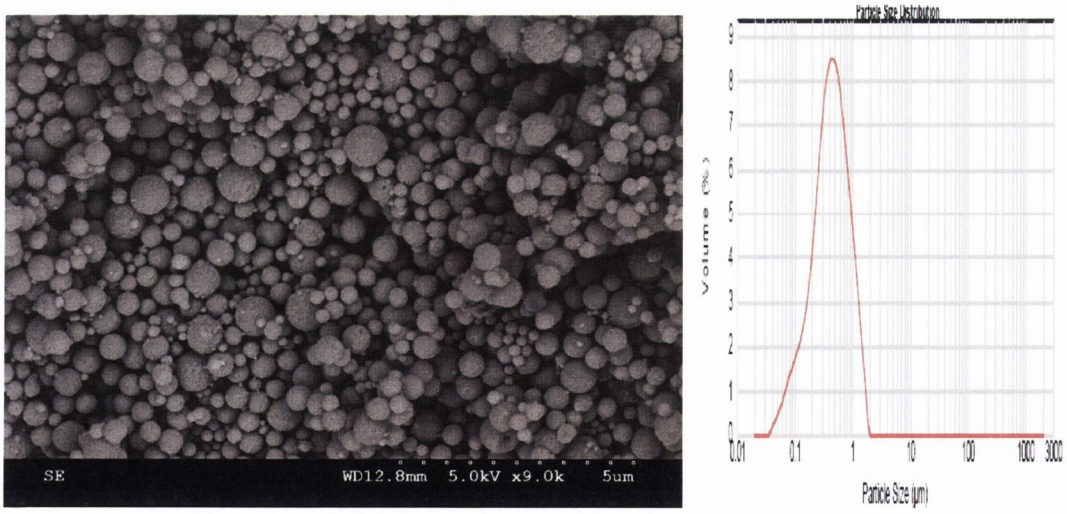


(a) (b)

Figure 5.27 (a) SEM picture, (b) size distribution of PLGA nanoparticles loaded with OVA (No.21).

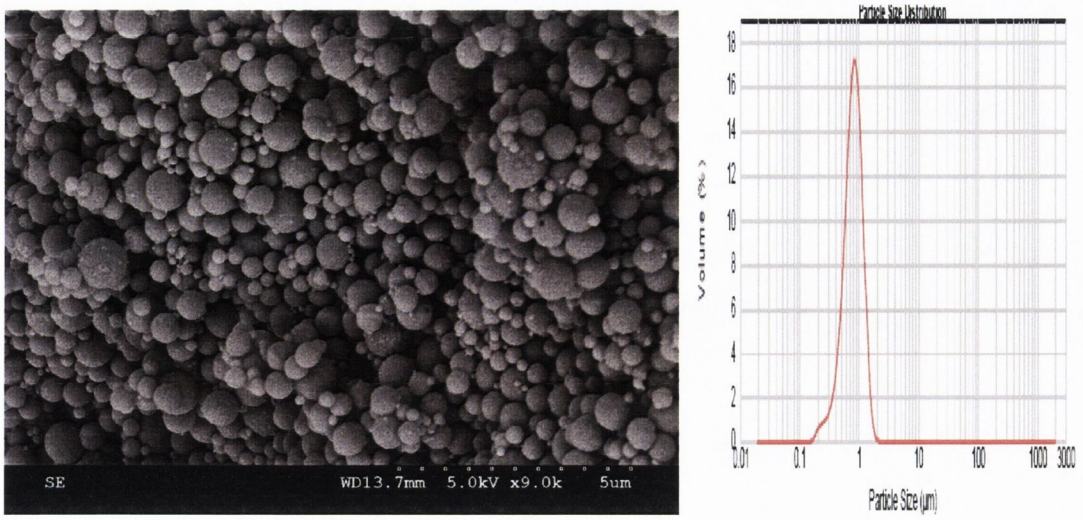


(a) (b)

Figure 5.28 (a) SEM picture, (b) size distribution of PLGA nanoparticles loaded with OVA (No.22).

From Figure 5.26, 5.27 and 5.28, it can be seen that all the particles are spheres with relatively even particle sizes. Particles from batch No.20 showed smoother surfaces than those of batch No.22. It might be due to the fact that more protein was loaded into No. 22, leading to more protein available on the surface compared to the one with a low loading (No.20). As mentioned previously, OVA may be physically dispersed in PLGA particles when manufactured by double emulsion method (Chapter 5.3.2).

## 5.5.2 Loading effects on OVA release

*In vitro* release study of OVA from the three PLGA batches of nanoparticles with different loadings was carried out over 70 days in PBS buffer (pH 7.4) at 37 °C (Figure 5.29). All the three release profiles showed a burst release on the first day, followed by a sustained release. Nanoparticles No.22 with the highest loading (5.45

%) gave the highest protein release throughout the incubation period, followed by No.21 and No.20.

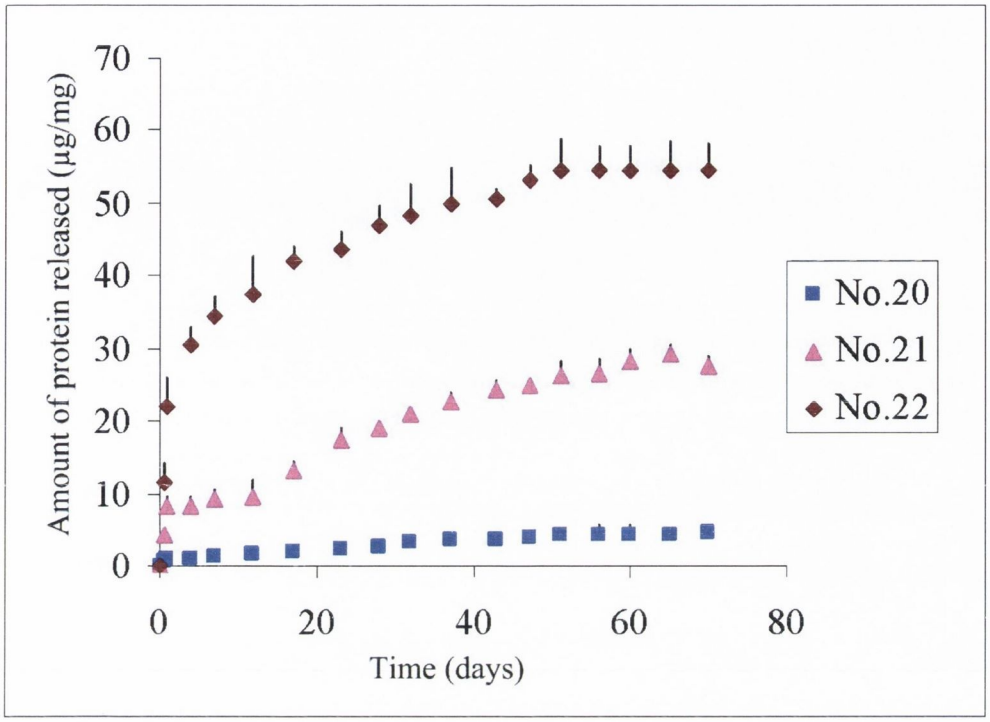


Figure 5.29 Release profiles of OVA from PLGA nanoparticles with different loadings (loading of 0.71%- No.20; loading of 2.95%- No.21; loading of 5.45%- No.22).

At the first day, the OVA presented a burst release with a value of 22.2 μg/mg from nanoparticles No.22, followed by 8.17 μg/mg (No.21) and 1.28 μg/mg (No.20). At the end of the incubation period (day 70), there was in total 46.5 μg/mg of protein released from No.22 PLGA nanoparticles, followed by 27.4 μg/mg and 4.49 μg/mg from No.21 and No.20, respectively. The amount and percentage release data at the different time points are listed in Appendix II.

The percentage values of OVA released from the particles are shown in Figure 5.30. Particles with loading of 5.45% presented a complete OVA release over 51 days, and particles with loading of 2.95% presented a complete release over 65 days.

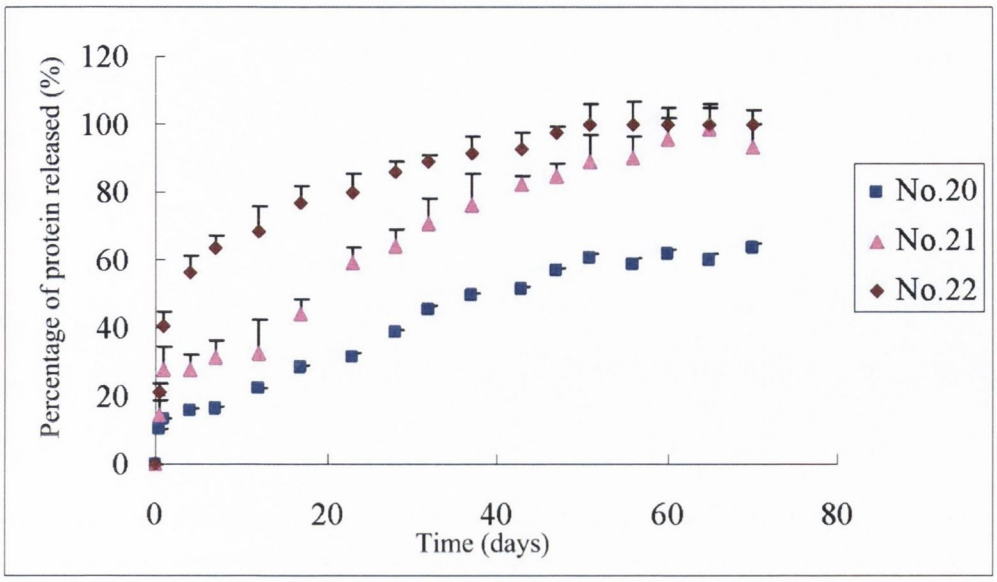


Figure 5.30 Release profiles of OVA from PLGA nanoparticles with different loadings (loading of 0.71%- No.20; loading of 2.95%- No.21; loading of 5.45%- No.22).

The release profiles of OVA from PLGA nanoparticles with the different loadings were fitted to Equation 1.7. Parameters relating to the burst release and degradation controlled release were estimated and summarised in Table 5.12.

Table 5.12 Fitting parameters of OVA release from PLGA nanoparticles with different protein loadings.

| NP No. | Drug loading% | $F_B$ | $K_B$ ($day^{-1}$) | k ($day^{-1}$) | $T_{MAX}$ (days) | CD | MSC |
|---|---|---|---|---|---|---|---|
| 20 | 0.71 | 0.192 ±0.036 | 1.61 ±0.58 | 0.099 ±0.008 | 27.2 ±1.3 | 0.994 | 4.622 |
| 21 | 2.95 | 0.235 ±0.045 | 1.69 ±0.61 | 0.102 ±0.011 | 25.9 ±1.7 | 0.990 | 4.210 |
| 22 | 5.45 | 0.569 ±0.037 | 0.89 ±0.10 | 0.113 ±0.015 | 21.7 ±2.1 | 0.994 | 4.644 |

(Samples represent the mean of three determinations ±standard deviation)

Equation 1.7, combining contributions from a first-order initial release phase and a polymer degradation controlled drug release phase, gave a relatively good fit with all three data sets.

$F_B$ is the fraction of the drug released in the burst phase. In this study, $F_B$ increased from 0.192±0.036 to 0.569±0.037 when protein loadings were increased from 0.71 % to 5.45 % (Table 5.12). It is consistent with the results reported by Gallagher and Corrigan (2000) that the burst of drug released from PLGA (50:50 RG504) discs is increased with the increase in the drug loading. In their studies, the release of levamisole hydrochloride from PLGA discs prepared at 5, 10 and 20% drug loading was investigated. The disks were prepared from films obtained by solvent evaporation from PLGA solution containing the suspended drug particles. Release was found to occur in a biphasic manner, with an initial fast release phase followed by a slower polymer degradation controlled release phase. When the levamisole hydrochloride particles were in the size ranged of drug 90-125 μm, the $F_B$ value was increased from 0.111 to 0.188 and 0.350 when the drug loading was increased from 5% to 10% and 20%, respectively; when the levamisole hydrochloride particles ranged 125-250 μm, the $F_B$ value was increased from 0.131 to 0.193 and 0.259 when the drug loading was increased from 5% to 10% and 20%, respectively. The increase in $F_B$ with increased loading was attributed to the higher concentration of drug dispersed in particles which effectively increased the proportion of drug linked to the particle surface. It is consistent with the model proposed by Gallagher and Corrigan (2000).

$T_{MAX}$ is the time to the maximum drug release rate. In this study, $T_{MAX}$ decreased from 27.2±1.3 to 21.7±2.1 days when the loading was increased from 0.71% to 5.45% (Table 5.12), while the rate constant k remains relatively constant. In the work reported by Gallagher and Corrigan (2000), $T_{MAX}$ decreased when the drug

loading was increased from 5% to 10% and 20%. The reason that discs with higher loadings had rapid release, may be due to the fact that high density of interconnecting channels, as opposed to that of discs with lower loadings, increase polymer permeability in the presence of drug and as a result increase PLGA degradation. It is consistent with the model proposed by Gallagher and Corrigan (2000).

The amount of protein released and their model fits are shown in Figure 5.31 and indicate that the release profiles from different loadings of nanoparticles can all fit to the model (Equation 1.7). The fraction of the initial burst release increases with increasing drug loadings. The time to reach the highest release rate tends to decrease with increasing drug loading, while the rate constant k remains relatively constant.

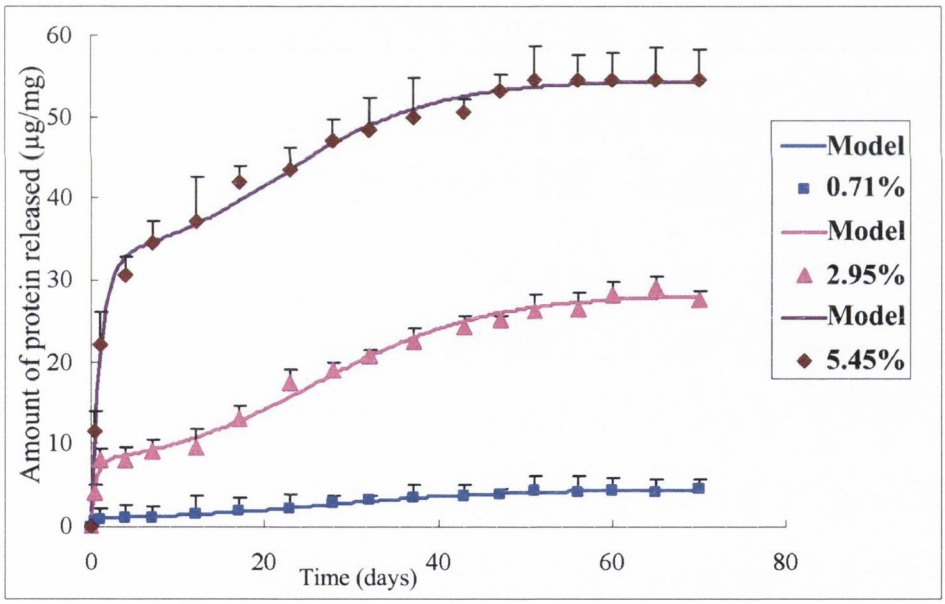


Figure 5.31 Model fit to amount released of OVA from PLGA nanoparticles with different loadings (loading 0.71%- No.20; loading 2.95%- No.21; loading 5.45%- No.22).

### 5.5.3 Particle size effects on OVA release

In order to illustrate the particle size effects on the protein release from particles, two release profiles of OVA loaded particles were chosen for comparisons. They had similar drug loadings and different median sizes. They are batches No.14 and No.20 and their properties are listed in Table 5.13.

Table 5.13 Properties of OVA loaded PLGA micro and nano particles.

| No. | Type | Protein | Loading % | Median size (μm) |
|---|---|---|---|---|
| 14 | Microparticles | OVA | 0.80 | 3.44 |
| 20 | Nanoparticles | OVA | 0.71 | 0.42 |

The release profiles are shown in Figure 5.32 and the parameters fitted to Equation 1.7 are shown in Table 5.14.

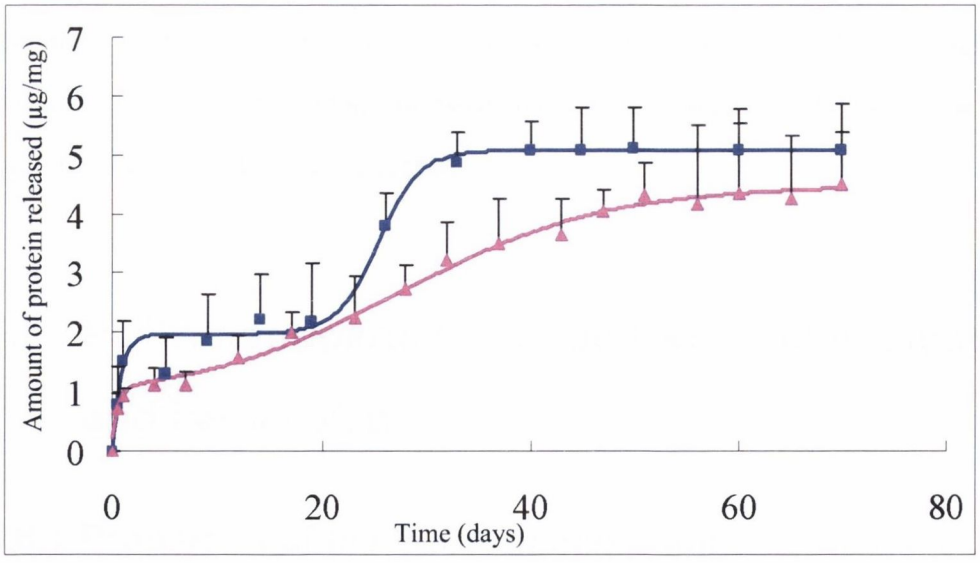


Figure 5.32 Amount of OVA released from PLGA microparticles (No.14) and nanoparticles (No.20).

Table 5.14 Parameters of fittings to Equation 1.7.

| No | Median size (μm) | $F_B$ | $K_B$ ($day^{-1}$) | k ($day^{-1}$) | $T_{MAX}$ (days) | CD | MSC |
|---|---|---|---|---|---|---|---|
| 14 | 3.44 ±0.66 | 0.290 ±0.013 | 1.24 ±0.16 | 0.495 ±0.128 | 25.4 ±0.3 | 0.997 | 5.204 |
| 20 | 0.42 ±0.17 | 0.192 ±0.036 | 1.61 ±0.58 | 0.099 ±0.080 | 27.2 ±1.3 | 0.994 | 4.622 |

From Table 5.14 we can see that when the median particle size was decreased from 3.44 to 0.42 μm, the release rate k was decreased from 0.495 to 0.099 and $T_{MAX}$ was increased from 25.4 ±0.3 days to 27.2 ±1.3 days. In the work previously reported on the study of PLGA degradation by Dunne et al., (2000), a linear relationship between the degradation rate and particle size existed, with the larger particles degrading faster. In smaller particles degradation products formed within the particle can diffuse easily to the surface while in larger particles degradation products have a longer path to the surface of the particle, during which autocatalytic degradation of the remaining polymer material can occur (Dunne et al., 2000). It may help to explain the results obtained with the batch having smaller particles (No. 20) that, the release rate from the particles was decreased and the time to reach the maximum release rate was increased.

## 5.6 PLGA nanoparticles loaded with indomethacin and ketoprofen

### 5.6.1 Properties of the PLGA nanoparticles

Indomethacin and ketoprofen are two nonsteroidal anti-inflammatory drugs (NSAID) with molecular weight of 357.79 and 254.28 Da, respectively and low water

solubility. Since they have small molecular weight and low aqueous solubility, it was of interest to compare their releases with the releases of protein from PLGA nanoparticles. Indomethacin and ketoprofen were encapsulated in PLGA nanoparticles by a single emulsion technique as described in Section 4.3.4. The resulting nanoparticles were named No. 23 and No.24, and their physical properties are shown in Table 5.15

Table 5.15 Properties of indomethacin and ketoprofen loaded PLGA nanoparticles.

| No. | Drug name | D 50% | D 90% | Size span | Drug loading (% w/w) | EE% |
|---|---|---|---|---|---|---|
| 23 | Indomethacin | 0.68 ±0.06 | 1.73 ±1.16 | 2.59 ±0.19 | 6.52 ±0.06 | 65.2 ±0.6 |
| 24 | Ketoprofen | 0.54 ±0.13 | 1.65 ±1.65 | 1.98 ±0.76 | 4.02 ±0.03 | 40.2 ±0.3 |

(Samples represent the mean of three determinations ± standard deviation)

Compared to the drug free PLGA nanoparticles (No.16), indomethacin and ketoprofen did not significantly affect the sizes of the particles. The loading of indomethacin and ketoprofen in PLGA nanoparticles were 6.52 ± 0.06% and 4.02 ± 0.03 % w/v, respectively.

The drug encapsulation efficiency% (EE%) of ketoprofen was lower than that of indomethacin. The EE% were 40.2 ± 0.3% and 65.2 ± 0.6% for ketoprofen and indomethacin, respectively ($p<0.05$), which may be related to the higher aqueous solubility of ketoprofen. Ketoprofen has a solubility of 0.5 mg/ml at 25 °C (Levis, 2003) in water and indomethacin is practically not soluble in water. Indomethacin does not suffer from problems of drug leakage to the external aqueous medium, resulting in improved drug content in the nanoparticles. Barichell and co-workers (1999) assessed the relative advantages and drawbacks of the emulsion technique

for a range of drugs with respect to the drug encapsulation in PLGA (75:25 10kDa) nanoparticles with a mean diameter of 160-170 nm. The theoretical drug loading was 3.3% w/w. The results of the encapsulation efficiency analysis demonstrated that more lipophilic drugs, such as indomethacin, do not suffer from the problems of drug leakage to the external medium. In the work reported by Barichell et al. (1999), indomethacin presented a drug EE% of 93.9 ± 1.3% and ketoprofen demonstrated lower values of encapsulation of 46.2 ± 1.2%. The solvent used was acetone. In another work recently reported by Joung et al. (2007), PLGA particles encapsulating indomethacin were prepared by an oil-in-water (o/w) emulsion method and the solvent ethyl acetate was eliminated by extraction. The loading amount and loading efficiency of indomethacin were 0.023 ± 0.01 mg/mg and 14.8 ± 0.67%, respectively. The low indomethacin encapsulation efficiency may be caused by the different methods used to eliminate solvent. When the o/w emulsion was diluted with isopropyl alcohol, indomethacin may have transferred to isopropyl alcohol with solvent, and resulted in lower encapsulation efficiency. Drug encapsulation efficiency could be different when different manufacture conditions and processes are used.

The SEM picture and particle size distribution of indomethacin loaded PLGA nanoparticles (No.23) are shown in Figure 5.33, and the SEM picture of ketoprofen loaded PLGA nanoparticles (No.24) with the particle size distribution are shown in Figure 5.34. From the SEM pictures we can see that both the indomethacin and ketoprofen loaded PLGA nanoparticles were spherical with smooth surfaces.

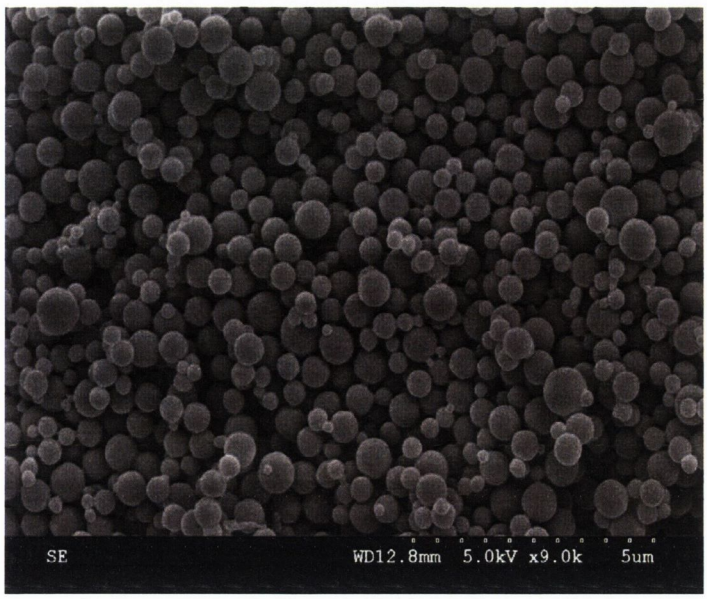


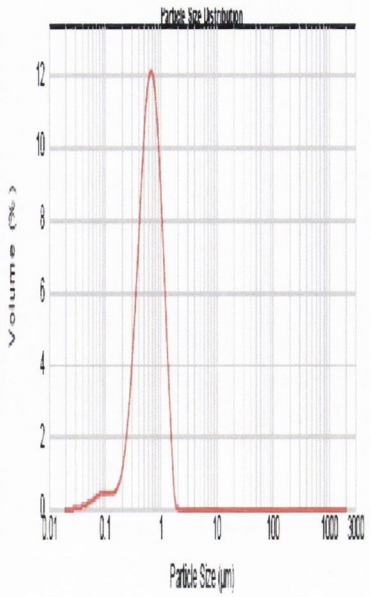


(a) (b)

Figure 5.33 (a) SEM picture, (b) particle size distribution of indomethacin loaded PLGA nanoparticles (No.23).

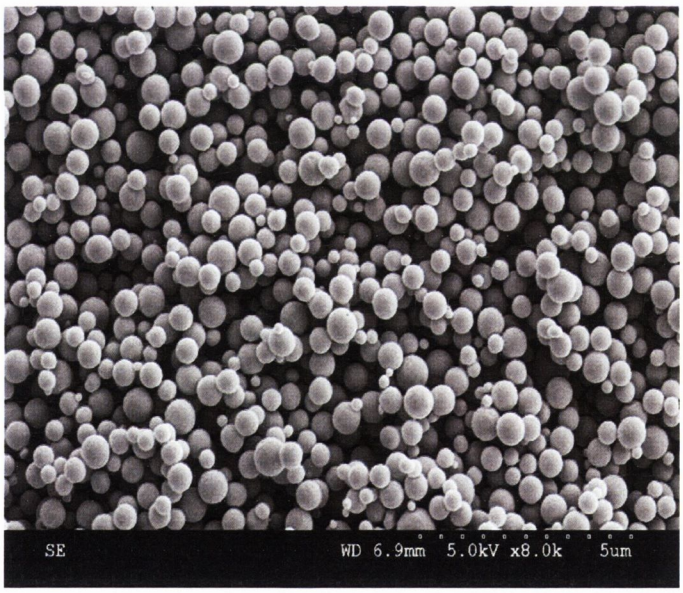


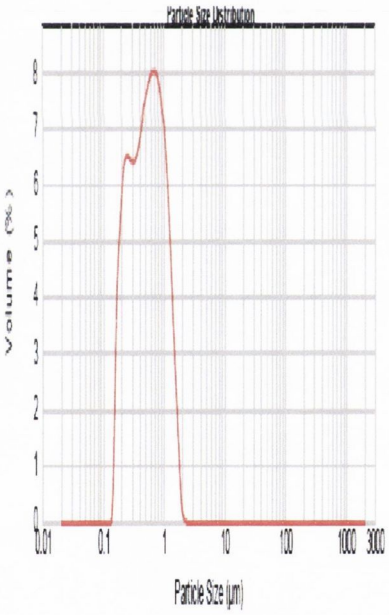


(a) (b)

Figure 5.34 (a) SEM picture, (b) particle size distribution of ketoprofen loaded PLGA nanoparticles (No.24).

## 5.6.2 Differential scanning calorimetry (DSC)

The thermal characteristics of (a) indomethacin loaded PLGA nanoparticles (No. 23), (b) drug free PLGA nanoparticles (No. 16), (c) pure PLGA polymer, (d) physical mixture of indomethacin and PLGA with a ratio the same as the indomethacin loading in particles, are shown in Figure 5.35. The glass transition temperature ($T_g$) values are listed in Table 5.16.

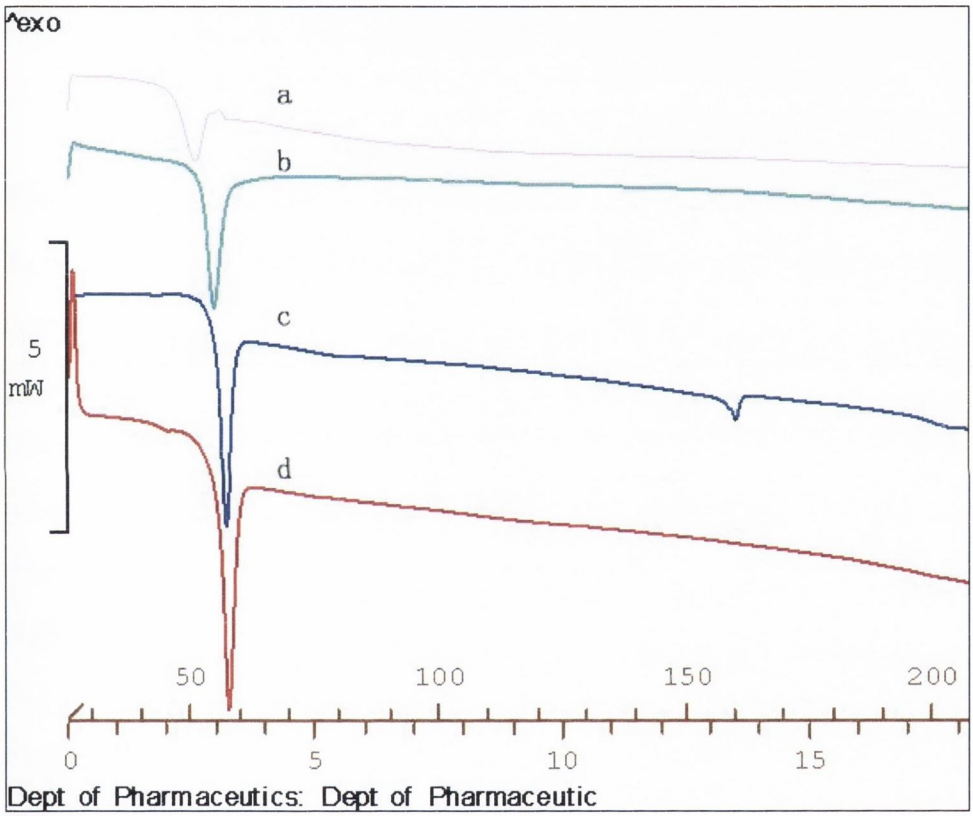


Figure 5.35 DSC results of (a) indomethacin loaded PLGA nanoparticles (No. 25), (b) drug free PLGA nanoparticles (No. 20), (c) physical mixture of indomethacin and PLGA (6.5:100), (d) pure PLGA polymer.

Table 5.16 Glass transition temperatures ($T_g$) of polymer and indomethacin PLGA particles.

| No. | Name | $T_g$ °C |
|---|---|---|
| (a) | Indomethacin loaded PLGA NPs (No.25) | 50.62 |
| (b) | Drug free PLGA NPs (No.21) | 54.39 |
| (c) | Physical mixture of PLGA and indomethacin | 56.69 |
| (d) | Pure PLGA polymer | 56.71 |

The $T_g$ of indomethacin loaded PLGA NPs was 50.62 °C, which was lower than the $T_g$ of the drug free PLGA nanoparticles occurring at 54.39 °C. There was no drug melting peak observable in the DSC curve of indomethacin loaded PLGA particles indicating that the drug was molecularly dispersed within the PLGA particles (Souillac and Rytting, 1999). Compared to Table 5.4, protein H S A loaded PLGA microparticles with DCM as solvent presented a $T_g$ of 52.33 °C, which is higher than the $T_g$ of indomethacin loaded PLGA particles. This may be caused by the higher loading of indomethacin in PLGA particles (6.52%) than H S A loading (0.711%). Drug free PLGA nanoparticles presented a $T_g$ lower than that of pure PLGA polymer which was 56.71°C. This decrease may be caused by the manufacturing process. The glass transition temperature is determined when the polymer state is changed from hard to rubbery state. It indicates how easily the molecular chains of the polymer move. Manufacturing process and molecular dispersion with another molecule would affect conformation of the chains of polymer and as a result decrease in the $T_g$ temperature.

Many authors have reported that drug dispersed at a molecular level in polymeric carriers result in amorphous dispersed drug, combining the benefits of enhanced

dissolution capabilities, improved stability and a disordered phase of the drug (Tajber et al., 2005 and Ford, 1986). The DSC curve of the physical mixture of PLGA and indomethacin had another peak at 159.86 °C (Figure 5.35), indicating the physical presence of indomethacin. The melting point of indomethacin is 155-161 °C (British Pharmacopoeia).

The thermal characteristics of (a) ketoprofen loaded PLGA nanoparticles (No. 24), (b) drug free PLGA nanoparticles (No. 16), (c) physical mixture of PLGA and ketoprofen with a ratio the same as the ketoprofen loading in nanoparticles, (d) pure PLGA polymer, are shown in Figure 5.36.

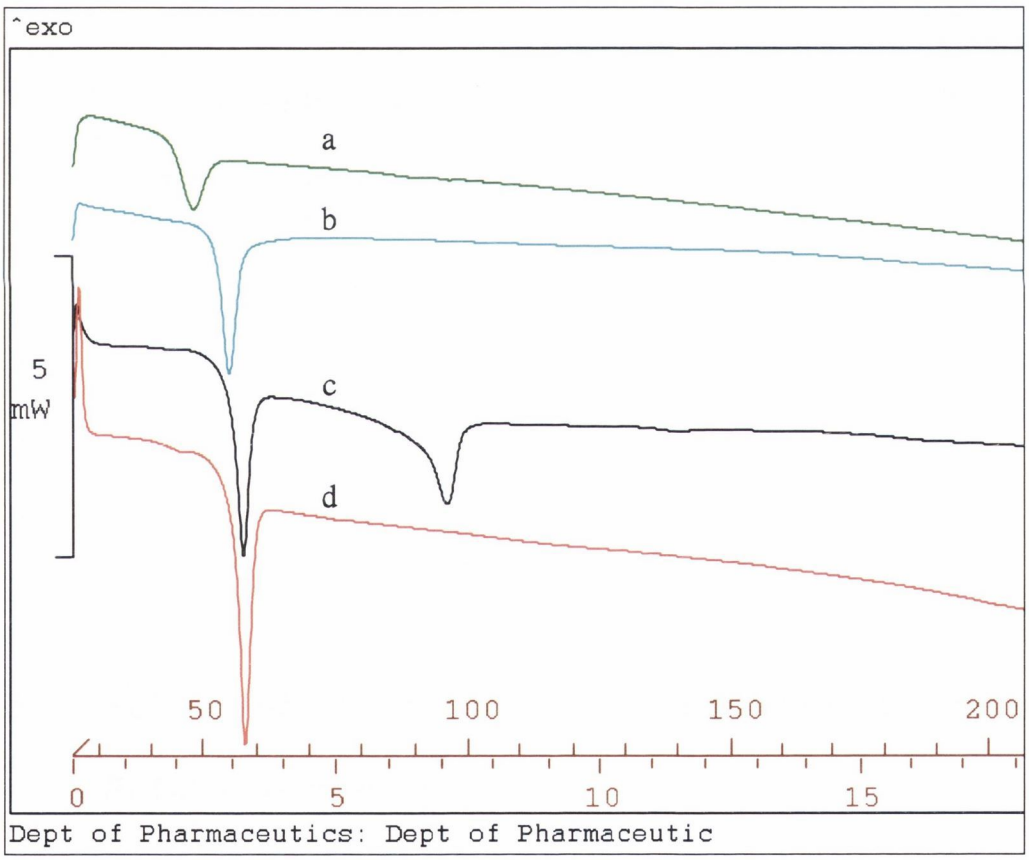


Figure 5.36 DSC results of of (a) ketoprofen loaded PLGA nanoparticles (No. 24), (b) drug free PLGA nanoparticles (No. 16), (c) physical mixture of ketoprofen and PLGA (4:100), (d) pure PLGA polymer.

The glass transition temperature ($T_g$) values of the systems are listed in Table 5.17. The $T_g$ of ketoprofen loaded PLGA NPs was 47.93 °C, which was lower than the $T_g$ of the drug free PLGA nanoparticles seen at 54.39 °C and there was no drug melting peak observable in the DSC curve of the ketoprofen loaded PLGA particles indicating that drug was molecularly dispersed in PLGA particles (Souillac and Rytting, 1999). Drug free PLGA nanoparticles presented a $T_g$ temperature lower than pure PLGA polymer. This decrease may be caused by the manufacturing process, including the dissolution of PLGA and evaporation of the solvent. DSC curve of the physical mixture of PLGA and ketoprofen had another peak at 93.78 °C (Figure 5.36), indicating the physical presence of ketoprofen. The melting point of ketoprofen is 92-95 °C (British Pharmacopoeia).

Table 5.17 Glass transition temperatures ($T_g$) of PLGA and ketoprofen-PLGA particles.

| No. | Name | $T_g$ °C |
|---|---|---|
| (a) | Ketoprofen loaded PLGA NPs (No.26) | 47.93 |
| (b) | Drug free PLGA NPs (No.21) | 54.39 |
| (c) | Mixture of PLGA and ketoprofen | 56.70 |
| (d) | Pure PLGA polymer | 56.71 |

### 5.6.3 Release studies of indomethacin and ketoprofen from PLGA nanoparticles

Indomethacin and ketoprofen loaded PLGA nanoparticles were dispersed in PBS buffer (pH=7.4) under sink conditions. The amount of drug released and percentage (%) release profiles are shown in Figure 5.37 and Figure 5.38, respectively.

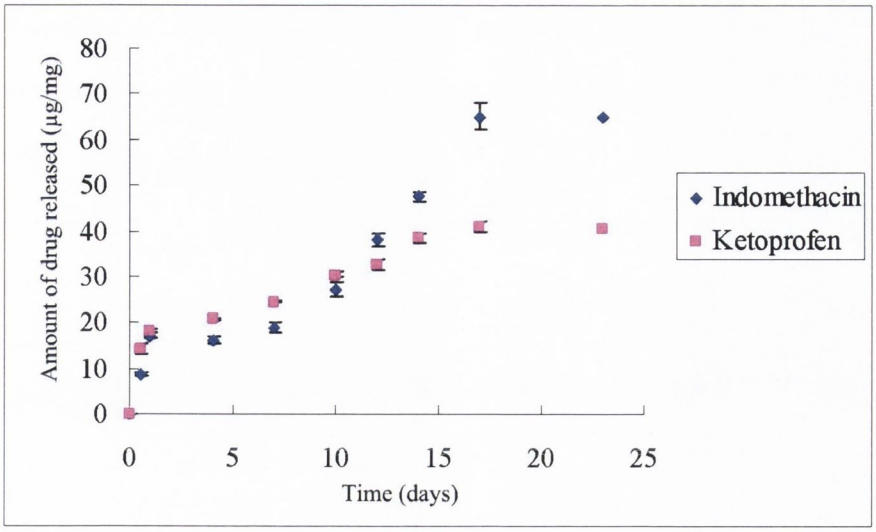


Figure 5.37 Amount of indomethacin and ketoprofen released from PLGA NPs (No.23, No.24 respectively) in PBS buffer (pH=7.4) at 37 °C.

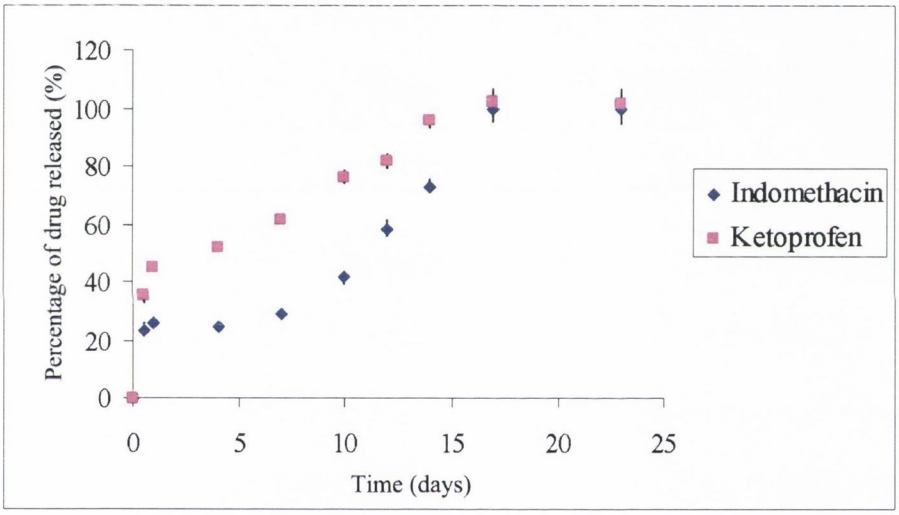


Figure 5.38 Percentage of indomethacin and ketoprofen released from PLGA NPs (No.23, No.24, respectively) in PBS buffer (pH=7.4) at 37 °C.

From Figures 5.37 and 5.38 we can see that both drugs showed an initial burst release in the first day followed by a sustained release. Ketoprofen nanoparticles (No.24) gave a burst release value of 42.2% after 24 hours and indomethacin gave a release value of 26.3 % over the same period of time. Most of the drugs had been released within 25 days. The amount and percentage (%) released values data versus time are listed in Appendix II.

Puebla and co-workers (2005) indicated that encapsulation of non-dissolved drug within the polymeric matrix results in rapid release. In their work, indomethacin was encapsulated within PLGA (RG 503, 50:50, $M_w$ = 34,000 Da) by solvent evaporation to obtain biodegradable indomethacin microspheres for intra-articular administration in rheumatoid arthritis. With a drug loading of 7.29% w/w and mean particle size around 5 μm, the indomethacin microspheres prepared showed an initial burst of 21.19 ±0.42% during the first 24 hours, followed by a sustained release until day 16, when most of the indomethacin had been released. The release medium was PBS buffer at pH=7.4 (sink conditions).

Gabor and co-workers (1999) reported biphasic release profiles of ketoprofen from PLGA microspheres. When polymer PLGA RG502 (50:50, $M_w$ = 12,000 Da) was used to make microspheres and ketoprofen was encapsulated with a loading of 3.9% w/w, the release of ketoprofen had a first burst release of 40% at the end of 24 hours, followed by a sustained release and at the end of the 19$^{th}$ day, most of the ketoprofen was released. The median particle size of these microspheres was 43.7 μm. When PLGA RG 503 (50:50, $M_w$ = 34,000 Da) was used, under similar ketoprofen loadings and microsphere sizes, there was a first release of 51% of ketoprofen at the end of 24 hours, followed by a sustained and complete release until the end of the measurements (day 19). The first burst release was found to increase with the drug content and increased inherent viscosity (Gabor et al., 1999). The inherent viscosity is increased with polymer molecular weight.

The fractional release of indomethacin and ketoprofen over 23 days were fitted to Equation 1.7 (Figure 5.39). Parameters relating to the burst release and degradation controlled release are estimated and summarised in Table 5.18.

Table 5.18 The parameters of release from PLGA nanoparticles loaded with indomethacin and ketoprofen.

| No. | Drug | $F_B$ | $K_B$ ($day^{-1}$) | k ($day^{-1}$) | $T_{MAX}$ (days) | CD | MSC |
|---|---|---|---|---|---|---|---|
| 23 | Indomethacin | 0.271 ±0.044 | 1.76 ±0.90 | 0.615 ±0.153 | 12.5 ±0.4 | 0.985 | 3.394 |
| 24 | Ketoprofen | 0.493 ±0.036 | 2.33 ±0.42 | 0.444 ±0.074 | 10.9 ±0.5 | 0.996 | 4.863 |

(Samples represent the mean of three determinations ±standard deviation)

$F_B$ and $K_B$ in this model represent the fraction of the drug released in the burst phase and release constant. In this study, when ketoprofen was loaded, the estimated $F_B$ and $K_B$ were 0.493±0.036 and 2.33±0.42 respectively, which were both higher than the values estimated from the nanoparticles loaded with indomethacin (Table 5.18). From Equation 1.5 we can see that solubility of the drug encapsulated has an effect on the burst release constant $K_B$. Higher drug solubility leads to higher $K_B$. This might help to explain why ketoprofen presented higher burst release.

$$K_B = DAC_s / W_L F_B h_l \qquad \text{Equation 1.5}$$

D and $C_s$ are the diffusion coefficient and solubility of the drug, respectively. A is the surface of drug available for dissolution. $W_L$ is the total quantity of drug in the compact and $h_l$ is the apparent aqueous diffusion boundary layer thickness.

In the work previously reported by Siegel and the co-workers (2006), different drugs with different water solubility were loaded into PLGA (50:50 63 kDa) pellets. The drug loading was 20% and the effects of drug solubility on drug release were studied. To make the pellets, the polymer and drug were dissolved in acetone and

the mixture was evaporated under vacuum. The *in vitro* drug release studies were carried out in PBS buffer (pH=7.4) at 37 °C. The solubility of haloperidol is 0.13 mg/ml in water. When it was loaded to PLGA pellets, no more than 1% of drug was released on the first incubation day. When ibuprofen was loaded, with a solubility of 0.47 mg/ml in water, there was 10% of the drug released from the PLGA pellets on the first day (Siegel et al., 2006).

The percentage (%) release of indomethacin and ketoprofen and their model fits are presented in Figure 5.39.

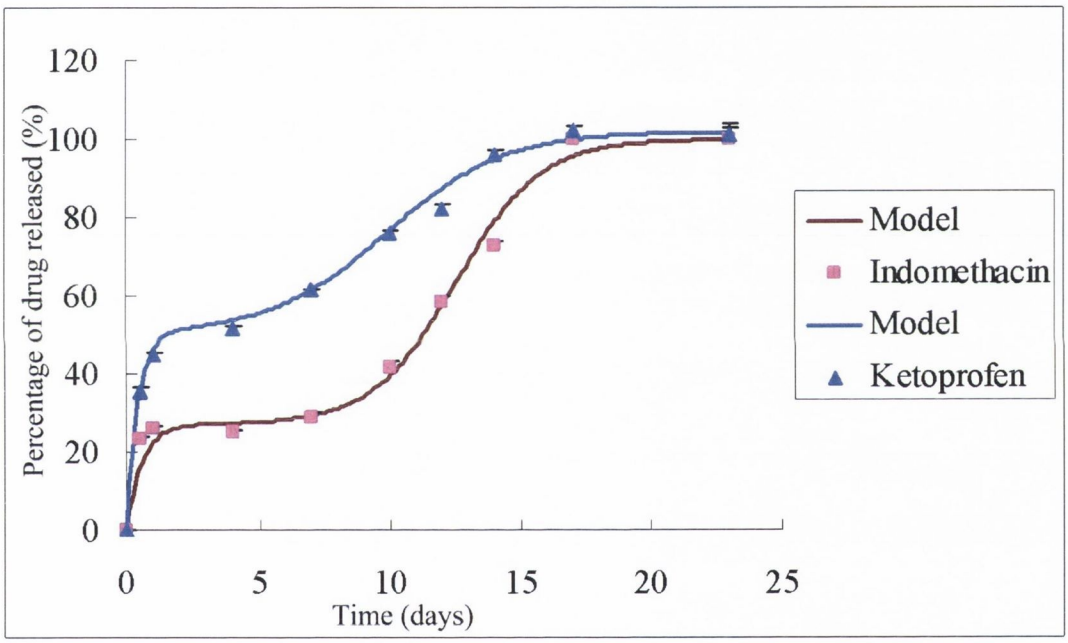


Figure 5.39 Model fit of indomethacin and ketoprofen percentage (%) release from PLGA nanoparticles.

Figure 5.39 indicates that the release profiles of indomethacin and ketoprofen from PLGA nanoparticles can fit to the model (Equation 1.7), with an initial fast release phase followed by slower polymer degradation controlled release.

## 5.6.4 Comparison of ketoprofen and OVA release

Release profiles of ketoprofen and protein OVA from PLGA nanoparticles were compared. Both the ketoprofen and OVA loaded PLGA nanoparticles presented particle sizes smaller than 0.8 μm, and the loadings of ketoprofen and OVA were 4.02% and 5.45%, respectively. Both release studies were carried out in PBS buffer (pH=7.4) at 37 °C, with a shaking speed of 65 rpm. Ketoprofen has a much smaller molecular weight of 254 Da, compared to OVA whose molecular weight is 44,287 Da. The release profiles of both drug and protein are shown in Figure 5.40 and the percentage releases are shown in Figure 5.41.

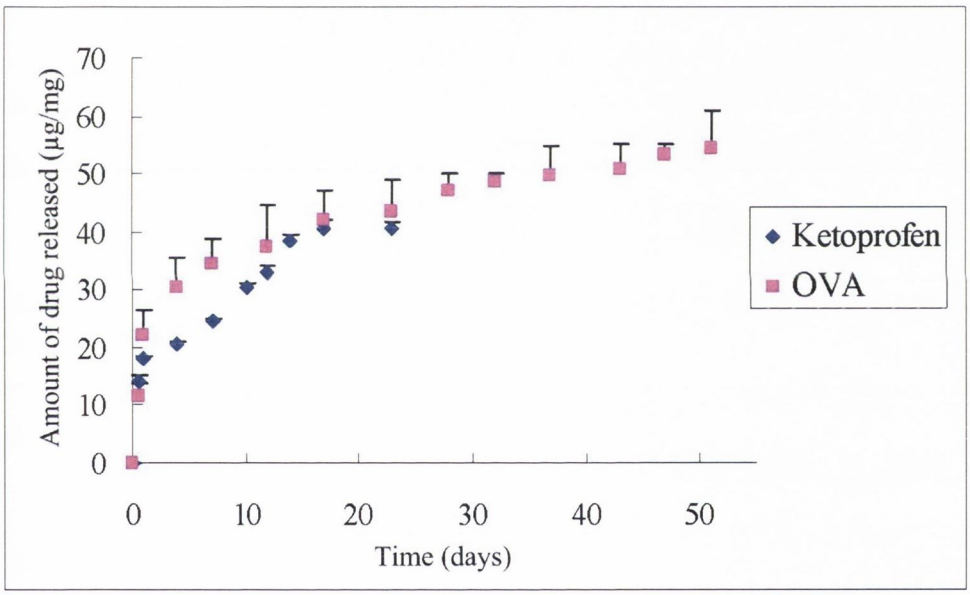


Figure 5.40 Release profiles of ketoprofen and OVA from PLGA nanoparticles (No.24 and No.22).

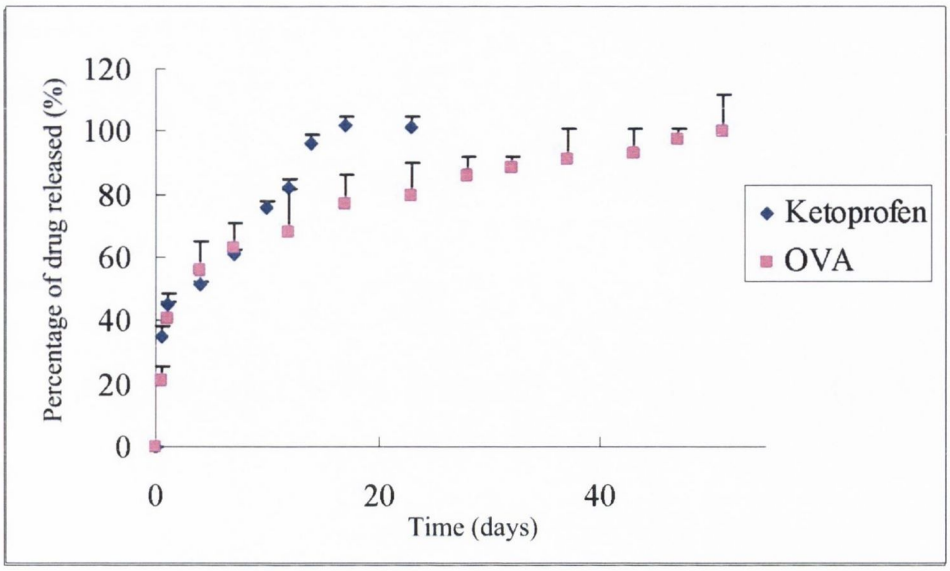


Figure 5.41 Percentage (%) releases of ketoprofen and OVA from PLGA nanoparticles (No. 24 and No. 22).

The parameters estimated from fitting of the data points to the release model (Equation 1.7) are shown in Table 5.19.

Table 5.19 The fitted parameters for ketoprofen and OVA release studies from PLGA nanoparticles.

| No. | Drug | $F_B$ | $K_B$ ($day^{-1}$) | k ($day^{-1}$) | $T_{MAX}$ (days) | CD | MSC |
|---|---|---|---|---|---|---|---|
| 24 | Ketoprofen | 0.493 ±0.036 | 2.33 ±0.42 | 0.444 ±0.074 | 10.9 ±0.5 | 0.996 | 4.863 |
| 22 | OVA | 0.569 ±0.037 | 2.89 ±0.10 | 0.113 ±0.015 | 21.7 ±2.1 | 0.994 | 4.644 |

From Table 5.19 we can see that $T_{MAX}$ time for OVA release was 21.7 days, which was longer than that of ketoprofen of 10.9 days. This indicated that the protein needs longer time to achieve the complete release. K, which is the release rate, was

0.444 for ketoprofen. It was higher than that of OVA of 0.113, indicating a higher release rate of ketoprofen from nanoparticles.

The difference between ketoprofen and OVA are their different molecular weights and chemical structures. As discussed in section 5.3.5, at protein loadings lower than 1%, the mechanism of release from PLGA microparticles appeared to be dependent on the protein molecular weight. This is in agreement with the work reported by Sandor et al., (2001) in which smaller proteins needed a longer time to achieve complete release. While at high loadings, Sandor et al., (2001) reported that when protein loading was at 4.8-6.9%, the release was independent of the protein molecular weight. In the current work, ketoprofen and OVA loadings of PLGA nanoparticles were 4.02% and 5.45% respectively. The higher release rate of ketoprofen indicated that the PLGA degradation was accelerated in the presence of the drug compared to protein H S A.

## 5.7 Conclusions

H S A loaded PLGA microparticles were manufactured by a double emulsion technique. When sonication time and power was increased, the median particle size of PLGA particles was decreased and the size ranges became more uniform, regardless of the solvent (DCM, ethyl acetate) used for preparation. The highest yield was obtained for microparticles produced with ethyl acetate. Encapsulation efficiency was also generally higher for all batches produced with ethyl acetate (84.2 ± 1.80 %) than with dichloromethane (71.1 ± 9.1 %). Higher miscibility of ethyl acetate may ameliorate the compatibility between the water phase containing proteins and oil phase containing polymer PLGA and as a result the encapsulation efficiency is improved (Liu and Deng, 2002). Microparticles prepared with ethyl acetate were observed to be more homogenous in size than microparticles prepared

with dichloromethane. This may be attributed to the fact that ethyl acetate has lower density, which assists the formation of oil droplets in the water phase. Regardless of the solvent used, *in vitro* release studies showed a burst release of the loaded substance, followed by a slower, sustained and degradation controlled release of protein. The integrity of the protein conformation of H S A was maintained for the manufacturing processes employing both solvents as determined by SDS-PAGE analysis.

H S A loaded PLGA nanoparticles were successfully manufactured with the particle size of 0.56 ± 0.17 μm and D 90% of 0.97 ± 0.14 μm by a double emulsion technique. The integrity of the protein conformation of H S A was maintained in both micro and nano particles as determined by SDS-PAGE analysis. Coumarin-6 was loaded into the PLGA nanoparticles with a loading of 0.25 μg/mg. Its low burst release made it feasible to be used in animal or cell studies in the future.

Protein OVA and OVA-coupled F/G peptide was encapsulated into PLGA microparticles by a double emulsion technique and their release profiles were compared with H S A microparticles to see the effects of the protein molecular weights on releases (Sandor et al., 2001). At low loadings (<1%), the smaller protein had relatively longer $T_{MAX}$ time than the larger proteins H S A, which has the highest molecular weight of 66.5 kDa, had a $T_{MAX}$ time of 19.5 days, followed by OVA-coupled F/G peptide ($M_w$ 46.3 kDa) of 23.9 days and OVA ($M_w$ 44.3 kDa) of 25.4 days. Microspheres encapsulating larger proteins allow the initial release of large protein, which would lead to a quicker penetration of the particles by water, causing the formation of the interconnecting channels or the release of protein in pre-existing channels within the particles (Hernadez et al., 1998; Duggirala et al., 1996).

When increasing the protein loading on PLGA nanoparticles, the size remained relatively constant, while the encapsulation efficiency% (EE %) was significantly decreased from 70.8 ± 2.8% to 27.3 ± 2.0%, which indicated a decrease in loading capacity of proteins when the initial protein concentration was increased. Nanoparticles with the lowest loading showed the smoothest particle surface. All the protein release profiles of nanoparticles with different loadings showed an initial fast release phase followed by sustained, polymer degradation controlled release phase. With the increasing loading, the $F_B$ was increased and the $T_{MAX}$ was decreased. The increase in $F_B$ with increased loading was attributed to the higher concentration of protein dispersed in particles which effectively increased the proportion of protein linked to the particle surface. The reason that highly loaded particles have rapid release, may be due to the fact that high density of interconnecting channels, as opposed to that of low loaded particles, increase polymer permeability in the presence of drug and as a result increase the PLGA degradation. The trends are in agreement with the model proposed by Gallagher and Corrigan (2000).

Release profiles of OVA loaded PLGA nanoparticles and microparticles with similar protein loadings were compared to see the effect of particle size on protein release. PLGA nanoparticles with the median size of 0.42 μm indicated a longer $T_{MAX}$ time, compared to microparticles. In smaller particles degradation products formed within the particle can diffuse easily to the surface while in larger particles degradation products have a longer path to the surface of the particle during which degradation of the remaining polymer material can occur (Dunne et al., 2000)

Indomethacin and ketoprofen were encapsulated into PLGA nanoparticles by a single emulsion technique. The drug encapsulation efficiency% of ketoprofen was lower than indomethacin. EE% was 40.2 ± 0.3 % and 65.2 ± 0.6% for ketoprofen and indomethacin, respectively. The release profiles of indomethacin and

ketoprofen from PLGA nanoparticles were compared. Both of drugs presented complete release by 23 days and ketoprofen indicated a higher burst release with $K_B$ value of 2.33, compared to the $K_B$ value of 1.76 for indomethacin. From Equation 1.6 we can see that solubility of the drug encapsulated has an effect on the burst release constant, $K_B$. Higher drug solubility leads to higher $K_B$ values. It might help to explain why ketoprofen presented a higher burst release rate constant and release fraction than indomethacin.

# RESULTS AND DISCUSSION

## Chapter 6 Chitosan-PLGA micro and nano particles

## 6.1 Introduction

Chitosan (CS) was selected as excipients because of its properties of cationic charge, mucoadhesion and biodegradability (Paul and Sharma, 2000; Pangburn et al., 1982; Dornish et al., 1996; Yang et al., 2003). Kawashima et al., (2000) prepared PLGA nanospheres with elcatonin, a calcitonin derivative, by coating the surface of the resultant nanospheres with mucoadhesive polymers such as chitosan, poly(acrylic acid), and sodium alginate. A single emulsion technique was used and the coating polymer was dissolved in PVA water phase to prepare the particles. The chitosan-coated nanospheres showed higher mucoadhesion to the reverted intestinal tract in saline than other polymer-coated nanospheres. There was no mucoadhesion site-specificity of the chitosan-coated nanospheres between duodenal, jejunal, and ileal sacs. Kumbar et al., (2002) formulated cationically modified PLGA nanoparticles that can efficiently bind DNA, by using chitosan as excipient. From the gel electrophoresis studies, the charge on the resultant nanoparticles was sufficient to efficiently bind the negatively charged DNA electrostatically.

CS-PLGA nanoparticles were prepared by dissolving chitosan with PVA (polyvinyl alcohol) in aqueous solution. PVA is one of the emulsifiers most frequently used to stabilise the emulsion since it forms particles of relatively small size and uniform size distribution (Scholes et al., 1993; Zambaux et al., 1998).

Chitosan loadings on PLGA nanoparticles were increased to see its effects on the properties of particles, such as particle size and morphology. It has been known that a fraction of PVA remains associated with the particles despite repeated washing because PVA forms an interconnected network with the polymer at the interface (Sahoo et al., 2002). The binding of PVA on the particle surface is likely to happen when the organic solvent is removed from the interface in which interpenetration of

PVA and PLGA molecules takes place (Boury et al., 1995). PVA has both structures of poly(vinyl acetate) and poly(vinyl alcohol) and the hydrophobic vinyl acetate part serves as an anchor polymer at the oil interface for binding to the surface of PLGA polymer during the formation of particles (Sahoo et al., 2002). The structure of PVA is shown in Figure 6.1. PVA is prepared by hydrolysing polyvinyl acetate in ethanol with potassium hydroxide (Kibbe, 2000).

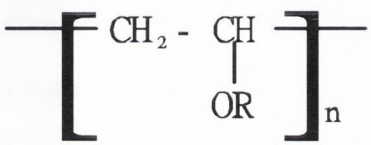

where R= H or $COCH_3$

Figure 6.1 Chemical structure of PVA (polyvinyl alcohol) (Kibbe, 2000)

It has been reported that PVA content in particles affects the cellular uptake properties of particles, with particles containing lower amounts of PVA demonstrating higher uptake (Sahoo et al., 2002).

Protein OVA was encapsulated into chitosan-PLGA nanoparticles to study its release properties and the release profile was compared with that of PLGA nanoparticles without chitosan.

Matrices composed of chitosan and PVA blends have been reported to be highly compatible with blood (Chandy and Sharma, 1992) and are good candidates for the controlled delivery of drugs (Kim et al., 1992). In the current study, chitosan-PVA nanoparticles were prepared and their physicochemical properties were analysed to exam their potential in drug delivery system.

## 6.2 Characterisation of chitosan

### 6.2.1 Molecular weight

The molecular weight of chitosan was determined by gel permeation chromatography (GPC) and the weight average molecular weight of a polymer ($M_w$), the number average molecular weight ($M_n$), the ratio of the weight average to the number average (polydispersity) and the manufacturer data (Fluka, low molecular weight) are listed in Table 6.1.

Table 6.1 Molecular weight characteristics of chitosan (Fluka)

| Chitosan (Fluka) | $M_w$ (kDa) | $M_n$ (kDa) | Polydispersity | Manufacturer data ($M_w$) (kDa) |
|---|---|---|---|---|
| Low molecular weight | 179 ± 11.6 | 160 ± 7.58 | 1.12 ± 0.03 | ~150 |

(Samples represent the mean of three determinations ±s tandard deviation)

From Table 6.1, we can see that the $M_w$ of chitosan (Fluka) is 179 ±11.6 kD. This result agrees with the data supplied by the manufacturer (~ 150 kDa).

Bozkir and Saka (2004) measured the molecular weight of chitosan (Fluka) (low, medium and high) using the viscometric method. The average molecular weight was calculated using suitable parametric values based on the Mark-Houwink equation. According to the equation, the molecular weight of chitosan (Fluka, low) was found to be 137 kDa. In the work previously reported by Corrigan (2003), the molecular weight of chitosan with the same batch number (40756811 50100) was measured by gel permeation chromatography (GPC) and the resultant number average molecular weight was 164,651±59,154 Da.

## 6.2.2 Determination of degree of deacetylation of chitosan

$^1$H-Nuclear Magnetic Resonance Spectroscopy ($^1$H-NMR) was used to measure deacetylation of chitosan and the degree of deacetylation was determined by Equation 6.1 (Hirai et al., 1991) using the integral intensity, $ICH_3$, of the $CH_3$ residue and the sum of integral intensities $IH_2$-$H_6$ of the $H_2$, $H_3$, $H_4$, $H_5$, and $H_6$ protons.

$$\text{Degree of deacetylation (\%)} = \{1-(\frac{1}{3}ICH_3 / \frac{1}{6}ICH_2 - H_6)\} \times 100$$

Equation 6.1

After calculation, the sample was found to have a degree of deacetylation of 84.6 ±5.4%, which was in agreement with the data supplied by the manufacturer. According to the data supplied, this sample had a degree of deacetylation in the range of 75-85 %. The $^1$H-NMR scan is shown in Figure 6.2 and the integral intensities are shown in Table 6.2.

Table 6.2 $^1$H-NMR results of chitosan (Fluka)

| Protons | Chemical Shifts (ppm) |
|---|---|
| H2 | 3.02 |
| H3~6 | 3.57~3.76 |
| CH3 | 2.06 |

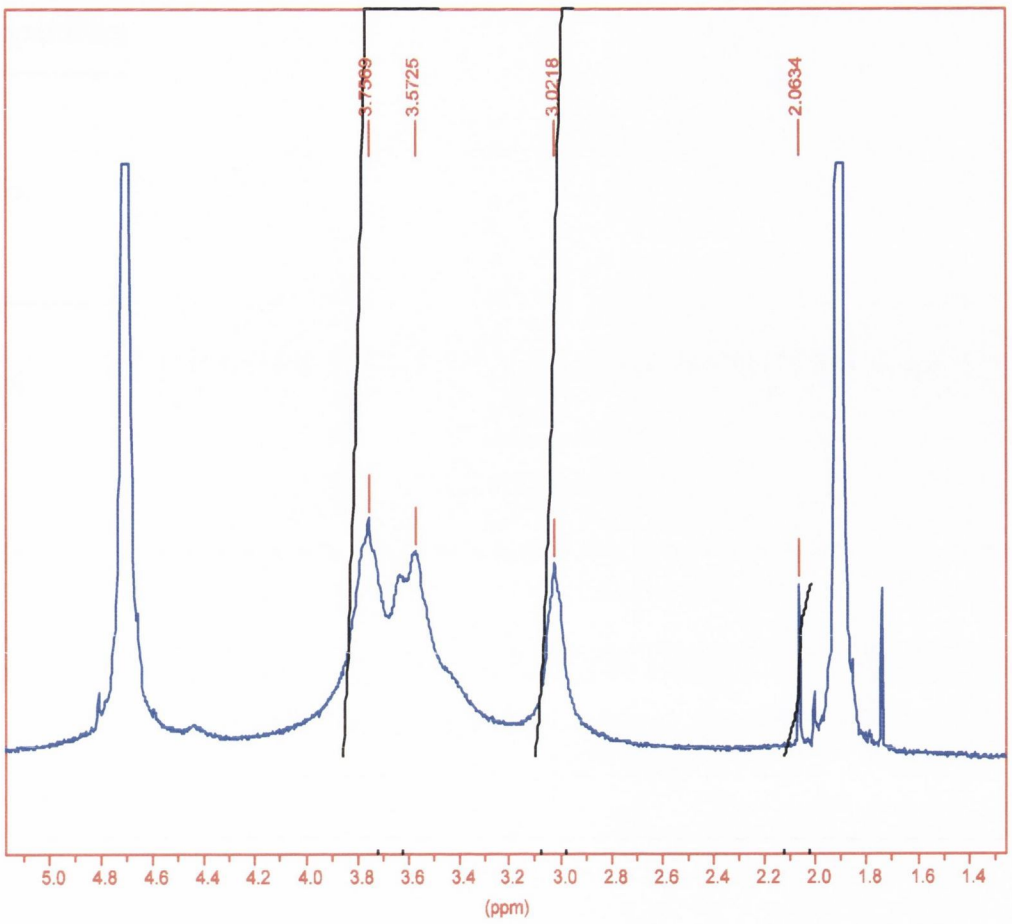


Figure 6.2 $^{1}$H-NMR scan of chitosan (Fluka)

## 6.3 Drug free chitosan-PLGA nano and micro particles

### 6.3.1 Drug free chitosan-PLGA nanoparticles

Drug free chitosan-PLGA nanoparticles were prepared and named No.25. The following properties of these particles were measured: particle size, PVA content and zeta potential. These properties were compared with those of the drug free PLGA nanoparticles (No.16) described in the previous chapter, to see how chitosan effects these properties. The results are listed in Table 6.3

Table 6.3 Size and zeta potential data of drug free PLGA and CS-PLGA nanoparticles.

| No. | Drug free particles | D 50% (μm) (n=3) | D 90% (μm) (n=3) | "Chitosan content" (% w/w) (n=3) | "PVA content" (% w/w) (n=3) | Zeta potential (mV) (n=5) |
|---|---|---|---|---|---|---|
| 16 | PLGA | 0.64 ±0.15 | 1.09 ±0.54 | ------ | 10.89 ±0.16 | -17.4 ±0.55 |
| 25 | CS-PLGA | 0.58 ±0.23 | 1.23 ±0.26 | 1.77 ±0.12 | 8.58 ±0.67 | -5.66 ±0.76 |

(Samples represent the mean values ± standard deviation)

The loading of chitosan on CS-PLGA (No.25) was 1.77 ± 0.12% w/w and the efficiency was 44.2 ± 2.99 %.

PVA was determined by a colorimetric method which was described in Section 4.4.12. From Table 6.3 we can see that the PVA content in drug free PLGA nanoparticles was 10.89 ± 0.16% w/w. In the work reported by Sahoo et al. (2002), the PVA content left in PLGA nanoparticles was 5% w/w. Their particles were prepared by emulsion technique with DCM as solvent. Compared to particles made by Sahoo and co-workers, the PVA content in the current study is higher. This may be due to the use of different solvents in both of the studies. Solvent miscibility in water is one of the parameters that affect the content of PVA in PLGA particles. Solvents having higher solubilities in water resulted in higher PVA content in particles (Sahoo et al., 2002). In the work of Sahoo et al. (2002), when chloroform was used, which has a solubility of 0.5% w/w with water, the PVA content of particles was 4.87% w/w; while when DCM was used, which has a solubility of 2% w/w, the content of PVA on PLGA particles was increased to 6.15% w/w. Ethyl

acetate, which was used in the current work, has a solubility with water of 8.7% w/w (Merck index), the increased solubility of ethyl acetate compared to DCM may be the reason for the higher PVA content in PLGA nanoparticles in the current work.

The PVA content in CS-PLGA nanoparticles was 8.58 ± 0.67% w/w. The decrease in residual PVA in CS-PLGA nanoparticles compared to PLGA nanoparticles without chitosan may be attributed to the involvement of chitosan in the aqueous phase during manufacture. The blending of positively charged polymer chitosan with negatively charged PVA may affect the interaction of PVA with PLGA solution, and as a result, decrease the residual content of PVA associated with PLGA particles.

The zeta potential of PLGA (No.16) and CS-PLGA (No.25) nanoparticles were measured at 25°C in deionised water. In this study, the zeta potential of PLGA nanoparticles showed a significantly greater negative charge of -17.4 ± 0.55 mV than CS-PLGA nanoparticles, whose charge was -5.66 ± 0.76 mV. This difference indicated the presence of positively charged chitosan in CS-PLGA nanoparticles. The SEM picture and particle size distribution of these nanoparticles (batch No.25) is shown in Figure 6.3.

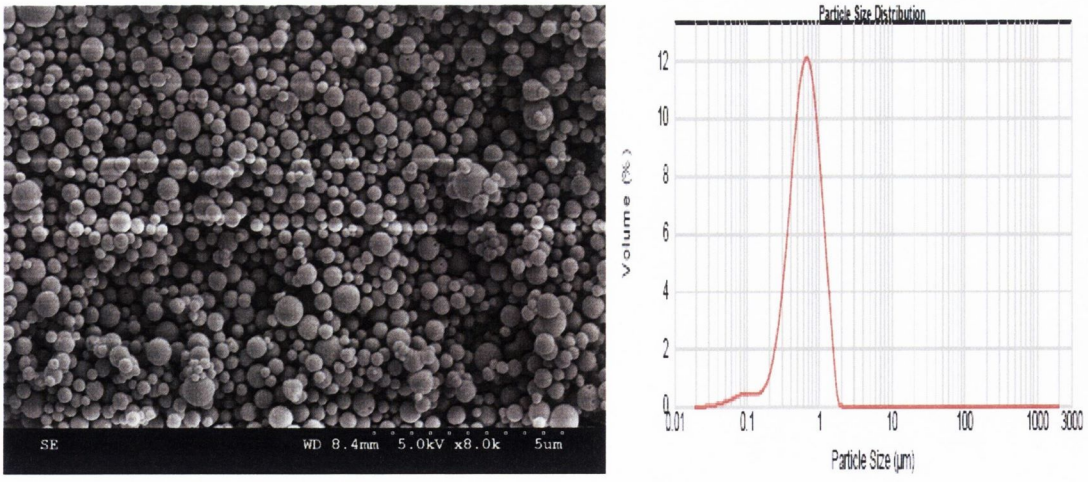


(a) (b)

Figure 6.3 SEM picture and particle size distribution of drug free CS-PLGA (No.25) nanoparticles.

From Figure 6.3, we can see that the loading of chitosan onto PLGA nanoparticles did not dramatically affect the morphology of PLGA nanoparticles compared to nanoparticles No.16. The particles from both of the batches were shown to have relatively smooth surfaces.

### 6.3.2 Chitosan effects on chitosan-PLGA particles

CS-PLGA nanoparticles (No.25) were prepared by dissolving 0.2% (w/v) chitosan with PVA in a ratio of 1:5. Higher concentrations of chitosan solutions, like 0.5% w/v (CS:PVA 1:2) and 1.0% w/v (CS:PVA 1:1) were used to prepare nanoparticles, to increase chitosan loading on nanoparticles. PVA concentration was kept the same e.g. 1% w/v during the preparations. The resultant particles were named No.26 and No.27 and their properties are shown in Table 6.4.

Table 6.4 Properties of CS-PLGA particles.

| No. | Ratio of PVA:CS | Median size (μm) (n=3) | "PVA content" (% w/w) (n=3) | "CS content" (% w/w) (n=3) | "Chitosan EE%" (n=3) |
|---|---|---|---|---|---|
| 25 | 5:1 | 0.58 ±0.23 | 8.58 ±0.67 | 1.77 ±0.12 | 44.2 ±2.99 |
| 26 | 2:1 | 5.15 ±0.78 | 6.28 ±0.78 | 3.15 ±0.24 | 31.5 ±2.40 |
| 27 | 1:1 | 5.56 ±0.92 | 4.31 ±0.53 | 4.20 ±0.16 | 23.8 ±1.91 |

(Samples represent the mean values±standard deviation)

The yield of the resultant CS-PLGA particles (No.25, 26 and 27) ranged from 85% to 95%. From Table 6.4 we can see that with increasing ratio of chitosan to PVA, the

particle sizes were increased from 0.58 ± 0.23 μm to 5.15 ± 0.78 and 5.56 ± 0.92 μm, respectively. This significant increase ($p<0.05$) may be attributed to the inclusion of increasing amount of chitosan to PVA. Kawashima et al. (2000) prepared different concentrations of chitosan (0.40 to 1.0 % w/v) at constant concentration of PVA (1% w/v) to form PLGA nanoparticles with elcatonin by the emulsion solvent diffusion method to coat the surface of the resultant nanospheres with a mucoadhesive polymer. Aggregation of the nanospheres occurred when higher concentrations of chitosan (>0.5%) was used, indicating the difficulties of formation of nanoparticles.

The SEM pictures and particle size distributions of No. 26 and No.27 are shown in Figure 6.4 and 6.5.

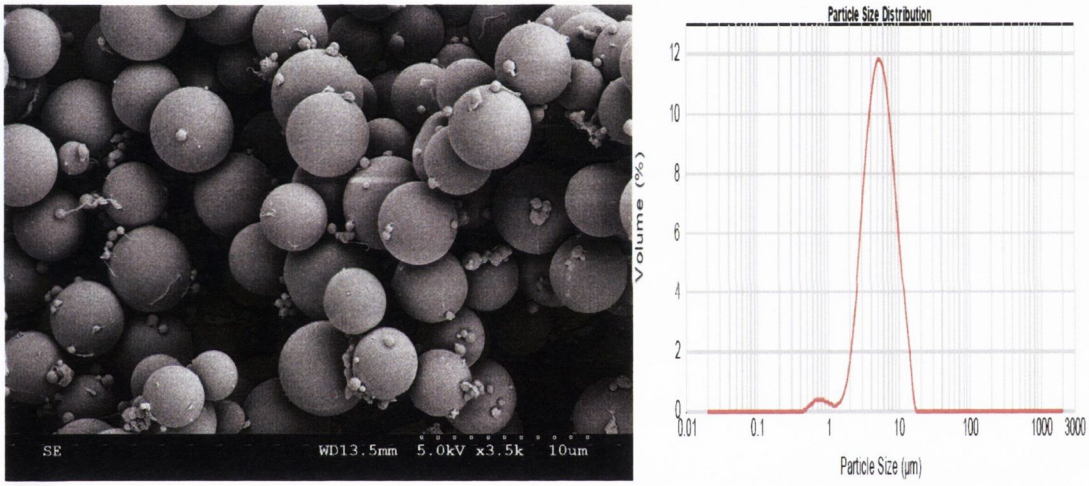


(a) (b)

Figure 6.4 SEM picture and particle size distribution of CS-PLGA microparticles with chitosan loadings of 3.15% w/w (No.26).

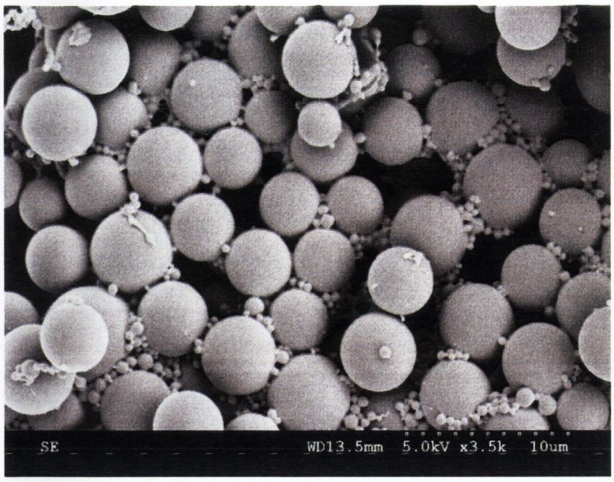


(a)

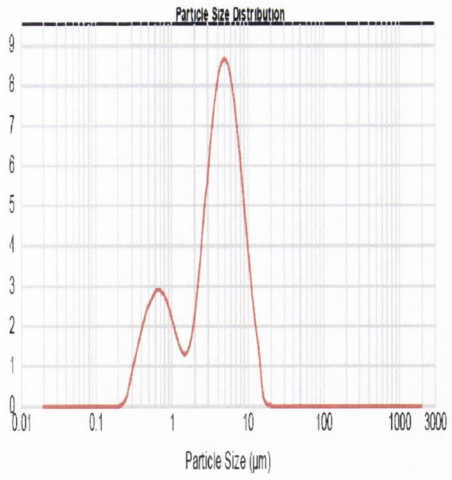


(b)

Figure 6. 5 SEM picture and particle size distribution of CS-PLGA microparticles with chitosan loadings of 4.20% w/w (No.27).

Comparing to the drug free CS-PLGA nanoparticles (No.25, Figure 6.3), the PLGA particle prepared by higher chitosan ratios (to PVA) presented higher particle median sizes with the presence of some tiny particles in the nano range.

As a polymeric surfactant, PVA contains both hydrophobic groups (vinyl acetate part) and hydrophilic groups (vinyl alcohol part). When surfactant is dissolved in some solvents, it may aggregate under certain conditions like concentrations, temperature and addition of polymer to form spherical micelles (Clint, 1991; Jonsson et al., 1998). Micelles consist of a core of the insoluble part of the polymer molecule surrounded by a corona of the soluble fragments. Since the addition of polymer can induce surfactant aggregation by polymer-surfactant interactions (Clint, 1991; Jonsson et al., 1998), the addition of chitosan to PVA solution may cause the formation of PVA-chitosan aggregates and chitosan-PVA particles may be formed.

Chitosan-PVA nanoparticles were produced by emulsion technique under the same conditions as batch No.26, without PLGA. The resultant particles were analysed to see the composition. By using the colorimetric method mentioned in Section 4.4.12,

there was 69.2±6.9 % w/w of PVA and 30.2±9.5% w/w of chitosan. These particles were named No.28. This result suggests that the small particles were chitosan-PVA composites. After the size measurement, these chitosan-PVA particles presented median particle size of 0.478 ±0.085 μm. The SEM picture and size distribution are shown in Figure 6.6.

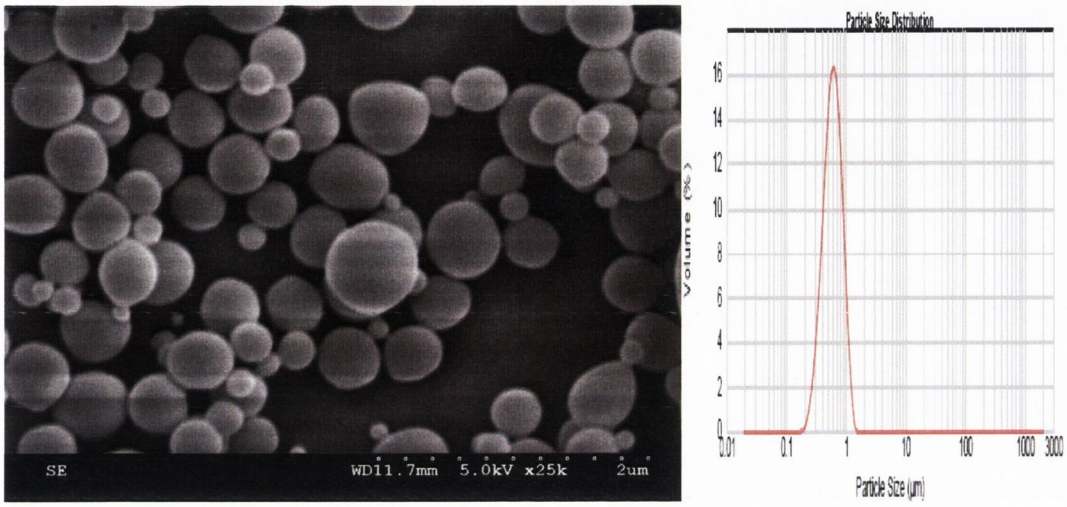


(a) (b)

Figure 6.6 SEM picture and particle size distribution of CS-PVA nanoparticles (No.28).

Chitosan was conjugated with PVA because of their different electrical charges. In the work previously reported by Koyano et al., (2000), different initial concentrations of chitosan were used to prepared hydrogels containing both of chitosan and PVA. The proportion of chitosan contained in the hydrogels was determined. The chitosan contents calculated from the results of the spectroscopy analysis were lower than those calculated from the initial amount of chitosan added during the preparation process of the matrices. For example, when the initial content of chitosan was 33.3% (PVA:CS 2:1), the chitosan content found from spectroscopy analysis was 28.1% (Koyano et al., 2000). It is in agreement with the work in the current study, that when the initial content of chitosan was 33.3% (PVA:CS 2:1), the chitosan content in the particles was 30.2 %.

When the content of chitosan to PVA was increased to 1:1 (Table 6.4), the chitosan-PLGA particles contained more small particles with size range around 500nm (Figure 6.5). It may be attributed to the increased addition of chitosan which may induce more PVA-chitosan aggregation. The chitosan-PVA nanoparticles were reproduced by emulsion technique under the same conditions as batch No.27, without PLGA. By using the colorimetric method mentioned in Section 4.4.12, there was 57.1±9.2% w/w of PVA and 41.3 ±8.9% w/w of chitosan. The median particle size was 0.516±0.091 μm. These particles were named No.29. The SEM picture and size distribution are shown in Figure 6.7.

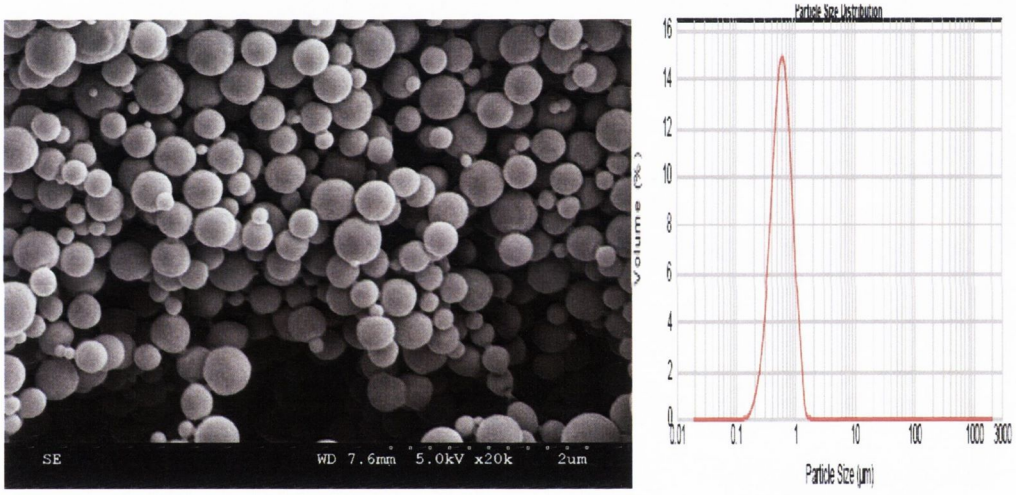


(a) (b)

Figure 6.7 SEM picture and particle size distribution of CS-PLGA nanoparticles (No.29).

With increasing ratio of chitosan to PVA from 1:2 to 1:1, the chitosan loadings on PLGA particles were increased from 1.77 ± 0.12% to 4.20 ± 0.16% w/w (Table 6.4). The loading efficiency% (EE %) of chitosan during the manufacture was decreased from 44.2 ± 2.99% to 23.8 ± 1.91%, which indicated a decrease of loading capacity of chitosan when the initial theoretical chitosan loading was increased, while the content of PVA decreased from 8.58 ± 0.67% to 4.21 ± 0.53% w/w. This decrease

may be caused by the increased addition of chitosan which interact with PVA since their different static charges. This interaction may affect the interaction of PVA with PLGA, and decrease in the residual content of PVA associated with PLGA particles. A graph comparing PVA and chitosan contents on PLGA particles manufactured with different blending ratios of PVA:CS is shown in Figure 6.8.

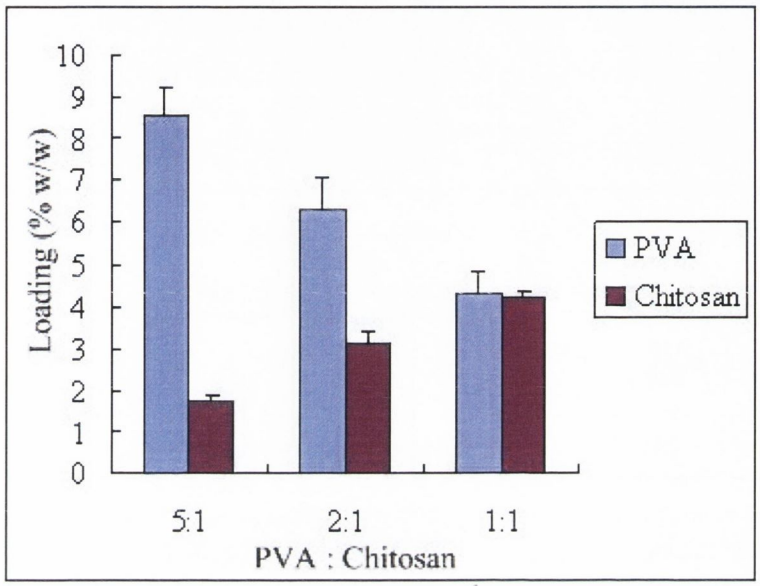


Figure 6.8 PVA and chitosan contents in PLGA particles prepared by different ratios of PVA to chitosan (5:1 No.25; 2:1 No.26; 1:1 No.27).

## 6.4 OVA release from chitosan-PLGA nanoparticles

### 6.4.1 OVA loaded chitosan-PLGA nanoparticles

OVA loaded chitosan-PLGA nanoparticles were made by double emulsion technique and the solvent used was ethyl acetate. The blending ratio of PVA to chitosan was 5:1 and the resultant OVA loaded CS-PLGA nanoparticles batch was named No.30. The physical properties, including protein loading, size, contents of chitosan and PVA, and zeta potential are listed in Table 6.5.

Table 6.5 Properties of OVA loaded CS-PLGA nanoparticles and comparison with drug free nanoparticles.

| No | Name of NPs | OVA loading (%w/w) (n=3) | Size D50% (μm) (n=3) | Size D90% (μm) (n=3) | "Chitosan content" (%w/w) (n=3) | "PVA content" (%w/w) (n=3) | Zeta potential (mV) (n=5) |
|---|---|---|---|---|---|---|---|
| 30 | CS-PLGA | 5.32 ±0.42 | 0.503 ±0.21 | 1.48 ±0.41 | 1.63 ±0.42 | 7.91 ±0.92 | -8.89 ±0.55 |
| 25 | Drug free CS-PLGA | ------ | 0.581 ±0.23 | 1.23 ±0.26 | 1.77 ±0.12 | 8.58 ±0.67 | -5.66 ±0.76 |

(Samples represent the mean of three or five determinations ±standard deviation)

OVA loaded CS-PLGA nanoparticles (No.30) had a median size of 0.503 ±0.21 μm and D90% size of 1.48 ± 0.41 μm. Compared to drug free CS-PLGA particles (No.25) with a median size of 0.581 ± 0.23 μm and D90% of 1.23 ± 0.26 μm, the presence of OVA did not dramatically affect the particle sizes. The OVA loading on CS-PLGA nanoparticles was 5.32 ± 0.42% (w/w). The contents of chitosan and PVA remained relatively constant between both of the CS-PLGA batches of nanoparticles. The zeta potential of OVA loaded CS-PLGA nanoparticles was -8.89 ± 0.55 (mV) (n=5), which is more negative than the drug free CS-PLGA nanoparticles (-5.66 ± 0.76 mV, n=5) ($p<0.05$). This difference may be caused by the loading of negatively charged protein OVA on nanoparticles. The encapsulation efficiency of OVA on CS-PLGA nanoparticles was 26.6 ± 2.1% and the yield of the resultant nanoparticles was (No.30) 89.1 ± 4.3%.

The SEM picture of the OVA loaded CS-PLGA nanoparticles is shown in Figure 6.9.

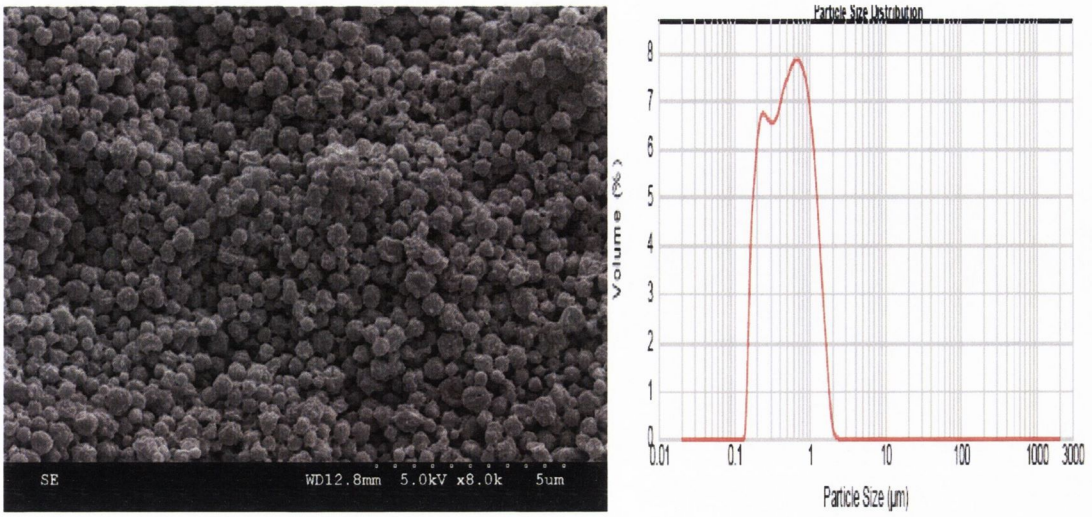


(a) (b)

Figure 6.9 (a) SEM picture, (b) size distribution of OVA loaded CS-PLGA nanoparticles.

Compared to the drug free chitosan-PLGA nanoparticles (Figure 6.3 b, No. 25), the shapes of the OVA loaded chitosan-PLGA nanoparticles were more irregular with rough surfaces. This may be attributed to the involvement of water soluble OVA during the manufacture.

## 6.4.2 OVA release from chitosan-PLGA nanoparticles

The amount of OVA released from CS-PLGA nanoparticles (No. 30) is shown in Figure 6.10.

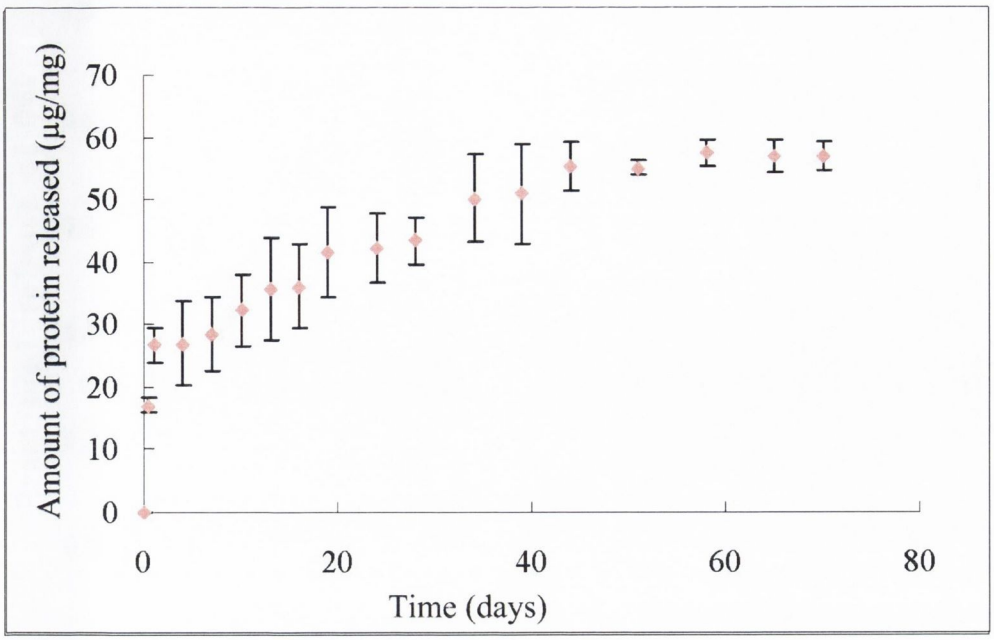


Figure 6.10 OVA release profile from chitosan-PLGA nanoparticles (No.30).

From Figure 6.10 we can see that the release profile showed a burst release, followed by a slower, sustained release of OVA. At the first day, OVA with a content of 26 (μg/mg) was released, and by 44 days, the release was increased to 55 μg/mg and remained constant until 70 days. The amount and percentage release data corresponding to time are listed in Appendix II.

The fractional release values of OVA from CS-PLGA nanoparticles were fitted to the previously described Equation 1.7, which combines the contribution from first order burst release and polymer degradation release. The fitting result is shown in Figure 6.11.

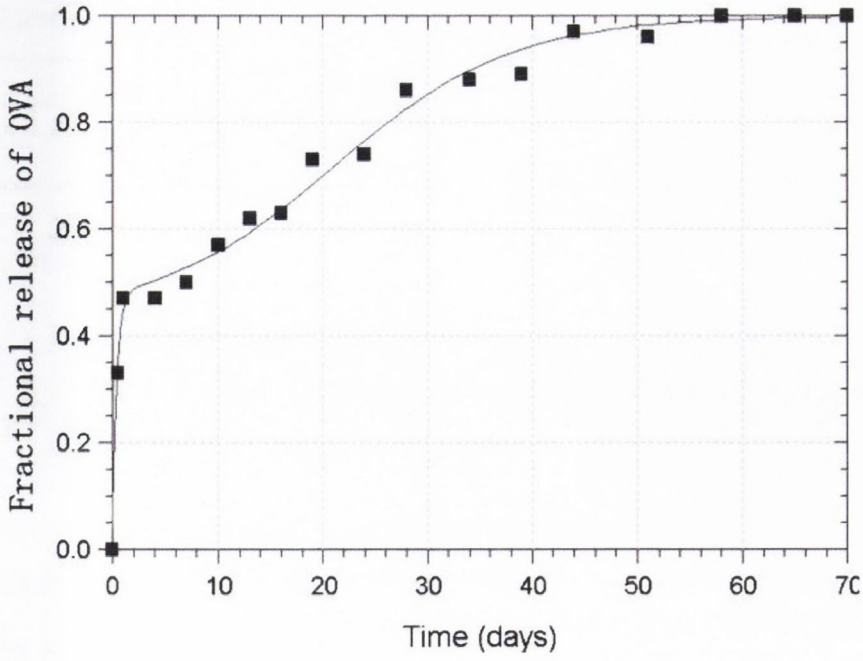


Figure 6.11 Model fit of fractional release of OVA from chitosan-PLGA nanoparticles (No.30).

Parameters estimated for the burst release rate and degradation controlled release rate of the model (Equation 1.7) were determined and are shown in Table 6.6. To compare chitosan effects on OVA release from nanoparticles, OVA loaded PLGA nanoparticles assigned as No.22 were selected, since they have similar particle size and OVA loadings to CS-PLGA particles (No.30). As discussed in Chapter 5, OVA release from the particle batch No.22 was fitted to a model (Equation 1.8) and the estimated parameters of this model are also listed in Table 6.6 for comparison. The median particle size of No.22 was 0.671 ± 0.24 μm, compared with the size of the particles No.30 of 0.503 ± 0.21 μm; the OVA loading of No.22 was 5.45 ± 0.40 μg/mg, compared with No.30, whose OVA loading was 5.32 ± 0.42 μg/mg. The parameters are shown in Table 6.6.

Table 6.6 Estimated parameters of the release model.

| NO. | Name | $F_B$ | $K_B$ ($day^{-1}$) | k ($day^{-1}$) | $T_{MAX}$ (days) | CD | MSC |
|---|---|---|---|---|---|---|---|
| 30 | CS-PLGA | 0.436 ±0.041 | 1.08 ±0.32 | 0.116 ±0.014 | 21.1 ±1.77 | 0.990 | 4.172 |
| 22 | PLGA | 0.569 ±0.037 | 0.893 ±0.099 | 0.113 ±0.015 | 21.7 ±2.1 | 0.994 | 4.644 |

From the Table 6.6 we can see that there was no large difference between both of the batches of nanoparticles (No.22 and No.30), regarding estimated parameters $F_B$, $K_B$, k and $T_{MAX}$. It indicates similar release profiles of OVA from the CS-PLGA and PLGA nanoparticles. The two release profiles are shown in Figure 6.12. Both of the release tests were carried under the same conditions in which the particles were incubated in PBS buffer (pH=7.4) at 37 °C, with a shaking speed of 65 rpm.

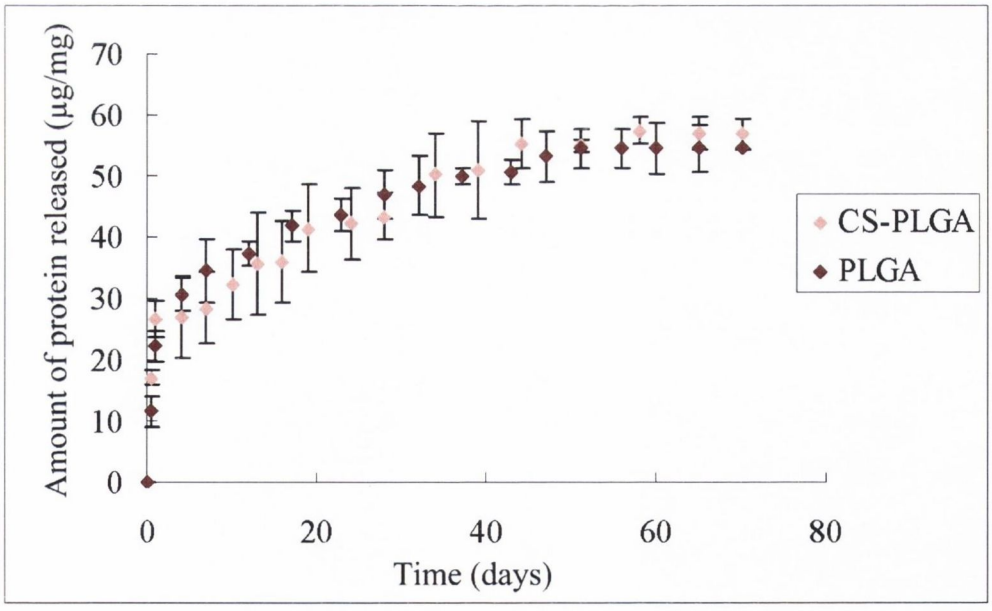


Figure 6.12 OVA release from CS-PLGA nanoparticles (No.30) and PLGA nanoparticles (No.22).

From Figure 6.12 we can see there is no significant difference between OVA release profiles from CS-PLGA and PLGA nanoparticles. This is in agreement with the work previously reported by Kawashima and co-workers (2000). In their study, elcatonin loaded PLGA (75:25) nanospheres with a mean size of 650 nm were prepared by coating the surface with the mucoadhesive polymer chitosan, to improve their mucoadhesive properties. The release behaviour of elcatonin from CS-PLGA and PLGA nanospheres were compared and the conclusion was that the pattern of drug release of the nanospheres did not differ markedly from that of uncoated nanospheres (Kawashima et al., 2000).

## 6.5 Conclusions

Drug free CS-PLGA nanoparticles were successfully prepared by the emulsion technique with a chitosan loading of 1.77 ± 0.12% w/w. The presence of chitosan in particles did not significantly affect the physical properties of the resultant nanoparticles, including size and morphology. The median particle size of the CS-PLGA and PLGA nanoparticles were 0.58 ± 0.23 μm and 0.64 ± 0.15, respectively. The significantly different zeta potentials of PLGA and CS-PLGA nanoparticles indicate the presence of positively charged chitosan in CS-PLGA nanoparticles. The zeta potential of PLGA nanoparticles showed a significantly more negative charge of -17.4 ± 0.55 mV than that of CS-PLGA nanoparticles, whose charge was -5.66 ± 0.76 mV.

PVA is necessary to stabilise PLGA particles which lead to negatively charged particles and heterogeneous size distribution. In this work, the residual content of PVA in CS-PLGA nanoparticles was decreased compared to the content in PLGA nanoparticles. This decrease may be attributed to the inclusion of chitosan during

manufacture and its interaction with PVA. The blending of positively charged polymer chitosan with negatively charged PVA in the aqueous phase may affect the interaction of PVA with PLGA, and as a result, a decrease in the residual content of PVA associated with PLGA particles.

When increasing the ratio of chitosan to PVA, the sizes of the resultant chitosan-PLGA particles were increased. Chitosan-PVA nanoparticles were prepared using emulsion technique under the same conditions to CS-PLGA nanoparticles without the presence of PLGA. The resultant particle sizes were around 500 nm.

OVA encapsulated CS-PLGA nanoparticles were prepared and the protein profile was compared with OVA loaded PLGA nanoparticles. There were no significant differences between OVA release profiles from CS-PLGA and PLGA nanoparticles.

# RESULTS AND DISCUSSION

## Chapter 7 Chitosan micro and nano particles

## 7.1 Introduction

Various methods have been reported on preparation of chitosan microparticles, including precipitation (Berthold et al., 1996) and spray drying (Corrigan et al., 2005). Chitosan nanoparticles prepared on the principle of precipitation/coacervation were reported by Nagamoto et al. (2004). Although chitosan nanoparticles have widely been studied in both of animal and cell models (Chapter 1.3), their properties, such as morphologies of dry products and manufacture processes have not received much attention.

In the current study, chitosan microparticles (CL213 and CL213/GLU) were prepared by spray drying with and without a crosslinking agent glutaraldehyde. CL213 is a highly purified water-soluble chloride salt of chitosan with high molecular weight. CL213/GLU is the chitosan microparticles with a crosslinking agent gluraraldehyde.

Four different batches of chitosan nanoparticles (CS-F NP, CL113 NP, CL213 NP and G213 NP) were prepared by modification of the methods previously reported by Berthold et al., (1996) and Nagamoto et al., (2004). CS-F NP are chitosan nanoparticles prepared with the chitosan material (low molecular weight) from Fluka; CL113 is a highly purified water-soluble chloride salt of chitosan with low molecular weight; G213 is a highly purified water-soluble glutamate salt with high molecular weight.

The morphologies and the manufacture processes of these nanoparticles are discussed. OVA, as a model protein, was adsorbed onto the chitosan nanoparticles to study its release from chitosan nanoparticles prepared by the precipitation/coacervation technique.

## 7.2 Physicochemical properties of chitosan salts

### 7.2.1 Measurement of molecular weights

The molecular weights of the series of chitosan salts, including CL113, CL213 and G213, were determined by gel permeation chromatography (GPC) and the results together with the manufacturer data (NOVAMATRIX, Norway) are listed in Table 7.1.

Table 7.1 Molecular weight characteristics of chitosan salts of CL113, CL213 and G213.

| Chitosan salts (NOVAMATRIX) | Mw (kDa) | Mn (kDa) | Polydispersity | Manufacturer data (kDa) |
|---|---|---|---|---|
| CL 113 | 71.5 ± 67.8 | 65.4 ± 60.8 | 1.09 ± 0.04 | <150 |
| CL 213 | 194 ± 89.1 | 169 ± 72.7 | 1.14 ± 0.03 | 150-400 |
| G 213 | 443 ± 66.1 | 387 ± 57.7 | 1.15 ± 0.00 | 200-600 |
| Chitosan (Fluka) | 179 ± 11.6 | 160 ± 7.58 | 1.12 ± 0.03 | ~150 |

(Samples represent the mean of three determinations ± standard deviation)

From Table 7.1 we can see that the chitosan chloride salt CL213 has a higher molecular weight of 194 ± 89.1 kDa, compared to the chloride salt CL113, which is 71.5 ± 67.8 kDa. Chitosan glutamate salt G213 has the highest molecular weight of 443 ± 66.1 kDa. All of the results measured by GPC agree with the manufacturer data supplied by NOVAMATRIX (Norway), however the methodology employed by the manufacturer in the determination of the molecular weight was not specified. The viscosity of CL 113, CL213 and G213 supplied by the manufacturer are <20, 20-200 and 20-200 mPa·s, respectively under condition of 1% in 1% acetic acid. The methodology employed in the determination of viscosity was not specified. Compared to chitosan chloride salts CL213 and CL113, the molecular weight of

chitosan (Fluka) characterised in Chapter 6 (179 ± 11.6 kDa) is higher than CL113 and smaller than CL213.

## 7.2.2 Measurement of degree of deacetylation

The degree of deacetylation of chitosan affects many inherent qualities of the polymer itself such as solubility, degradation rate, efficiency of gene carrier, and stability of particle size (Bozkie and Saka, 2004b). Also Kiang et al. (2002) reported that chitosan can bind DNA with high efficiency when the degree of deacetylation is high. Thus it is very important to determine the degree of deacetylation while studying series of chitosan and chitosan salts.

$^1$H-Nuclear Magnetic Resonance Spectroscopy ($^1$H-NMR) was used to measure the deacetylation of series of chitosan salts and the degree was determined by Equation (6.1) discussed in Chapter 6. The equation involves the integral intensity of $CH_3$ residue and the sum of integral intensities of $H_2$, $H_3$, $H_4$, $H_5$, and $H_6$ protons.

The NMR results for CL113 and CL213 are shown in Figure 7.1, 7.2 and the chemical shifts of protons are listed in Table 7.2.

Table 7.2 Chemical shifts of protons related to chitosan CL 113 and CL 213.

| Protons | CL 113 | CL 213 |
|---|---|---|
| $H_2$ | 3.01 | 3.04 |
| $H_{3\sim6}$ | 3.62~3.77 | 3.62~3.79 |
| $CH_3$ | 1.96 | 1.96 |
| Degree of deacetylation% | 86.3 | 88.0 |

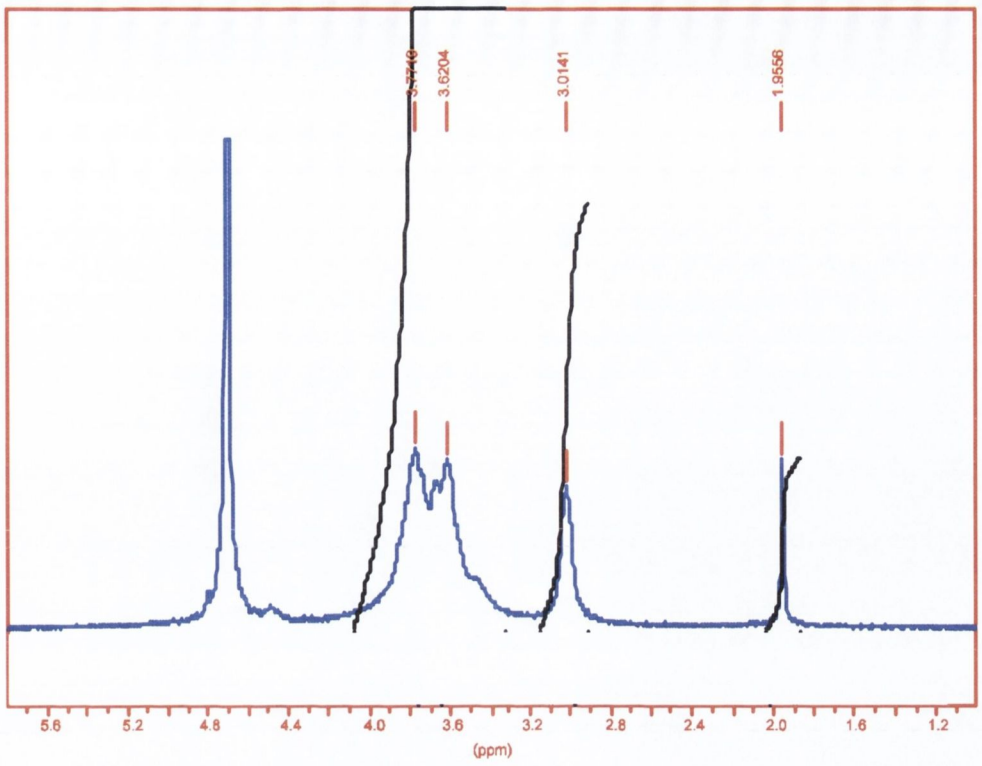


Figure 7.1 NMR spectra of chitosan chloride CL113.

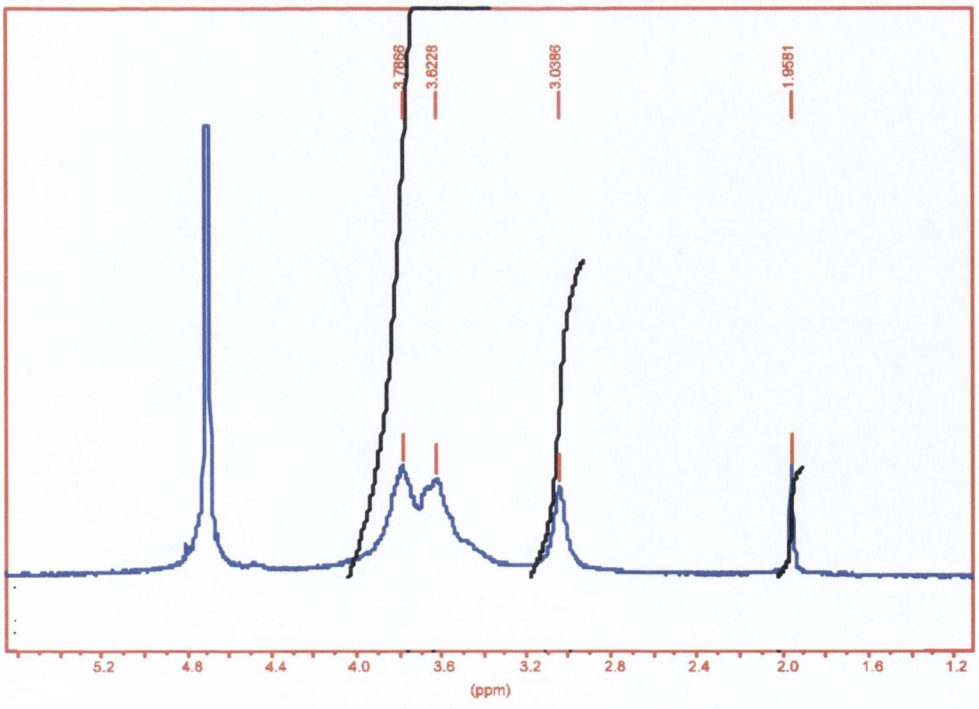


Figure 7.2 NMR spectra of chitosan chloride CL213.

The NMR pictures of CL113 and CL213 are similar to each other indicating their similar chemical structures. CL113 and CL213 are both chloride salts of chitosan with different molecular weights. After calculations, the degree of deacetylation of CL113 and CL213 are 86.3 ± 3.5 % and 88.0 ± 5.1 %, respectively. These results are in a good agreement with the data supplied by the manufacturer NOVAMATRIX, which quotes that the values should be between 75-90%.

The NMR result of G213 is shown in Figure 7.3. Compared to NMR results of CL113 and CL213, the differences between (2.2 to 2.5 ppm) are caused by the involvement of glutamate groups as G213 is a glutamate salt of chitosan. Due to the presence of the glutamate moiety, the integral intensity of $CH_3$ was affected at the chemical shift around 2 ppm (Figure 7.3). In this case $^1H$ NMR is unsuitable to determine the degree of deacetylation.

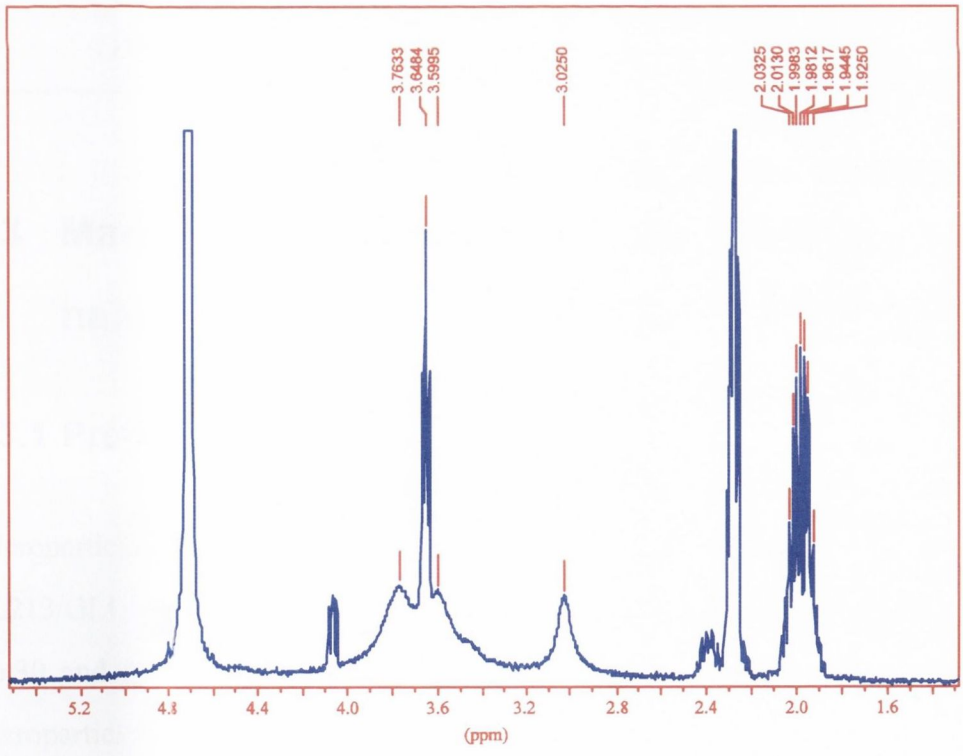


Figure 7.3 NMR result of glutamate chitosan G213.

Ninhydrin assay is a ninhydrin colorimetric test that was used to determine the percentage of free amino groups (Curotto and Aros 1993; Corrigan 2003). In the current study, the degree of deacetylation of G213 was measured by ninhydrin assay and the result was 90.3 ± 4.1 %. The deacetylation values for CL113, CL213 and G213 measured by NMR and ninhydrin assay agreed with the data supplied by the manufacturer which was 75-90 %. The deacetylation degrees of CL113, CL213 and G213 are listed in Table 7.3.

Table 7.3 Deacetylation degree of chitosan.

| Material | Degree of deacetylation % | Manufacturer (Novamatrix) data % |
|---|---|---|
| CL113 | 86.3 ±3.5 | 75-90 |
| CL213 | 88.0 ±5.1 | 75-90 |
| G213 | 90.3 ±4.1 | 75-90 |

## 7.3 Manufacture of chitosan micro and nanoparticles

### 7.3.1 Preparation of chitosan microparticles by spray drying

Microparticles of chitosan CL213 and chitosan cross-linked microparticles CL213/GLU were prepared by spray drying and the resultant particles were named No.30 and No.31, respectively. The physical properties of these two batches of microparticles with and without cross-linking agent are shown in Table 7.4. The median sizes of both of chitosan particles ranged from 3 to 5 μm and there was no significant difference between the D90% sizes and size spans.

Table 7.4 Physical properties of chitosan microparticles spray dried with and without cross linking agent.

| No. | Name | D50% (μm) (n=3) | D90% (μm) (n=3) | Span (n=3) |
|---|---|---|---|---|
| 31 | CL213 MP | 3.15 ±0.27 | 6.08 ±0.68 | 1.41 ±0.49 |
| 32 | CL213/GLU MP | 2.95 ±0.51 | 5.16 ±0.96 | 1.18 ±0.77 |

(Samples represent the mean values ±standard deviation)

The SEM pictures of chitosan microparticles with and without cross-linking agent glutaraldehyde are shown in Figure 7.4 and Figure 7.5.

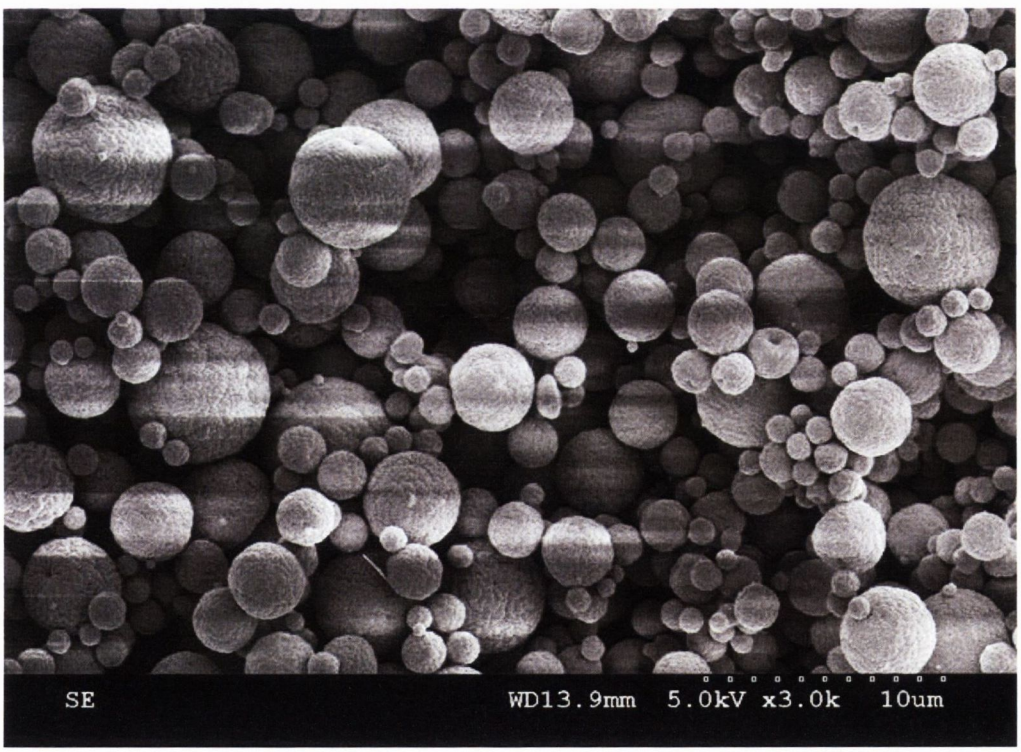


Figure 7.4 The SEM picture of chitosan microparticles (No.31) prepared by spray drying.

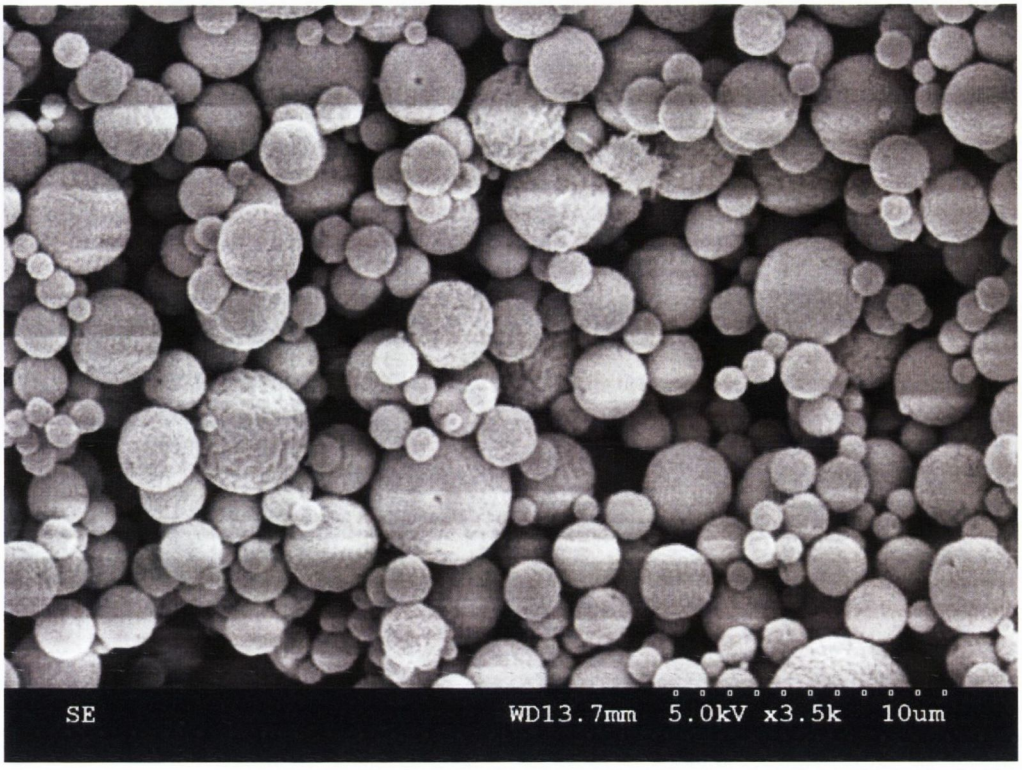


Figure 7.5 The SEM picture of chitosan microparticles (No.32) prepared by spray drying with glutaraldehyde.

From SEM pictures, we can see that no visible changes in the morphologies of the spray dried chitosan microparticles due to the cross-linking were observed, compared to the non-cross-linked microparticles. This agrees with the work previously reported by Corrigan et al. (2005) and Oliveira et al. (2005). In the work reported by Corrigan and co-workers (2005), co-spray drying of salbutamol sulphate/chitosan systems with the cross-linking agent formaldehyde (0.08 % w/w) had no detectable effect on the particle morphology. The concentration of the chitosan solution used for spray drying was 0.2% w/v in 1% v/v acetic acid solution and the diameter of the particles was approximately 5 μm (Corrigan et al., 2005). In the work reported by Oliveira and the co-workers (2005), two cross-linking agent, d,l-glyceraldehyde (0.15% w/w) and glutaraldehyde (0.15% w/w) were used to make chitosan microspheres by spray drying. The concentration of chitosan solution used was 0.5% w/v in 0.7% v/v acetic acid solution. Compared to the

non-cross-linked microspheres, there was no visible change in the morphology of the spray dried chitosan microspheres due to the chemical cross-linking. The mean particle sizes of d,l-glyceraldehyde cross-linked and glutaraldehyde cross-linked microparticles were similar to non-cross-linked particles with a mean size of 3.42 μm (Oliveira et al., 2005).

## 7.3.2 Preparation of chitosan nanoparticles

Chitosan nanoparticles were prepared by a coacervation/precipitation method using chitosan (Fluka) and series of chitosan salts (CL113, CL 213 and G213). The physical properties of these chitosan nanoparticles are listed in Table 7.5.

Table 7.5 Physical properties of chitosan nanoparticles.

| No. | Name | D50% (μm) (n=3) | D90% (μm) (n=3) | Zeta potential (mV) (n=5) |
|---|---|---|---|---|
| 33 | CS-F NP | 0.43 ±0.07 | 1.13 ±0.11 | 14.1 ±0.64 |
| 34 | CL113 NP | 0.58 ±0.05 | 1.26 ±0.20 | 12.1 ±0.44 |
| 35 | CL213 NP | 0.51 ±0.07 | 1.09 ±0.94 | 13.4 ±0.78 |
| 36 | G213 NP | 0.53 ±0.09 | 1.18 ±0.24 | 11.4 ±0.89 |

(Samples represent the mean values ± standard deviation)

The median sizes of chitosan nanoparticles ranged from 0.43 ±0.07 μm to 0.58 ±0.05 μm. There was no dependence of particle size on the molecular weight of chitosan, which is in agreement with the work previously reported by Berthold et al. (1996). In their work, low, median and high molecular weight chitosan samples ($M_r$ 70 000, 750 000 and 2 000 000) were used to prepare chitosan particles and the resultant particle sizes ranged from 1.5 μm to 2.5 μm, without dependence of the molecular weights on the microsphere sizes.

Zeta potentials of the four batches of nanoparticles were measured and the values are presented in Table 7.5. From the table we can see that there was no significant difference between the zeta potential values.

The SEM pictures of chitosan nanoparticles No.33, No.34, No. 35 and No.36 are shown in Figure 7.6, 7.7, 7.8 and 7.9, respectively.

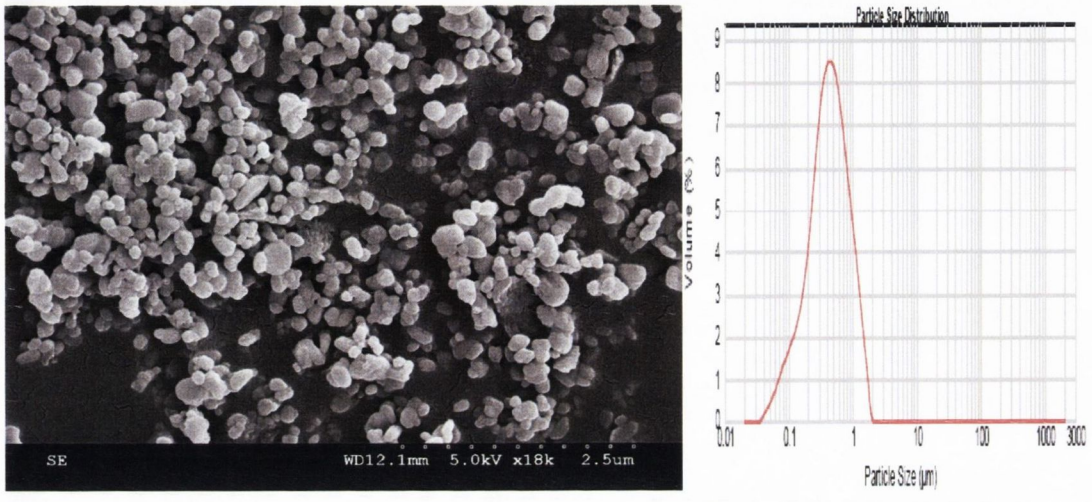


(a) (b)

Figure 7.6 The SEM picture and particle size distribution of chitosan (Fluka) nanoparticles (No.33).

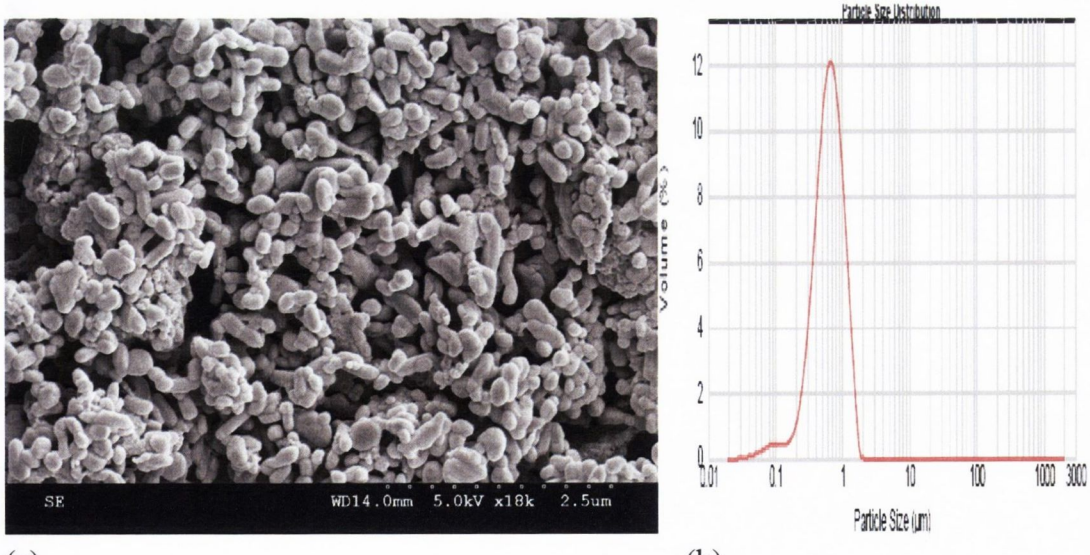


(a) (b)

Figure 7.7 The SEM picture and particle size distribution of chitosan CL113 nanoparticles (No.34).

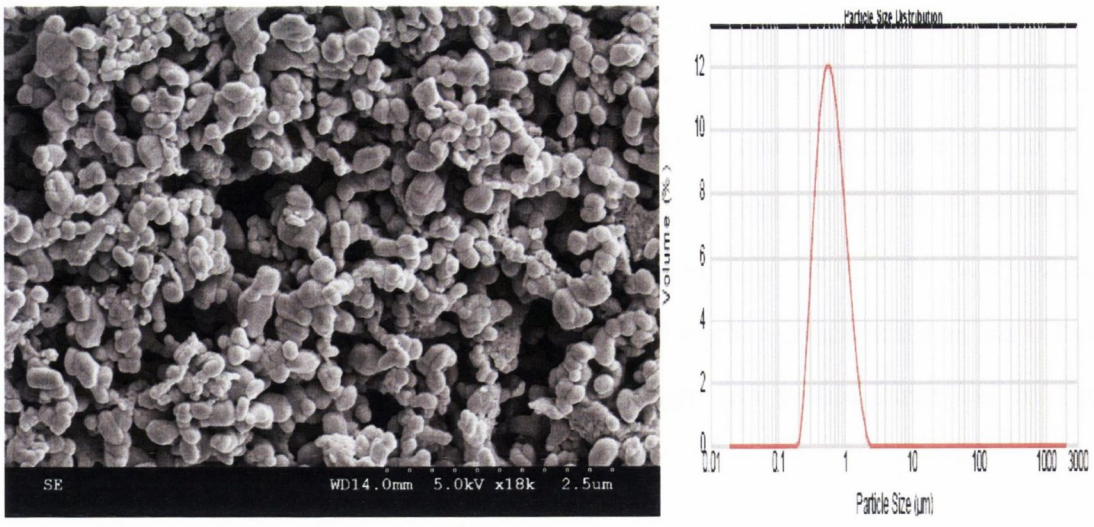


(a) (b)

Figure 7.8 The SEM picture and particle size distribution of chitosan CL213 nanoparticles (No.35).

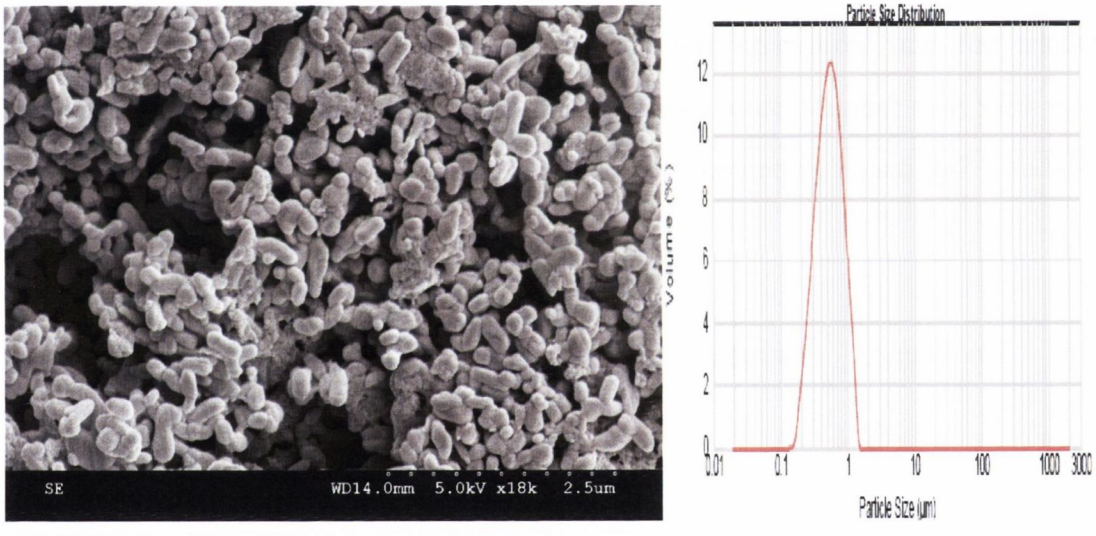


(a) (b)

Figure 7.9 The SEM picture and particle size distribution of chitosan G213 nanoparticles (No.36).

From the SEM pictures we can see that all the chitosan particles are in the nano range, and they have relatively irregular shapes. There was no visible difference in the morphology of the chitosan nanoparticles made from the chitosan glutamate and chloride salts.

All the original concentrations of chitosan solutions used to prepare the nanoparticles (No. 33 - No. 36) were 0.2% w/v. Solutions with higher concentrations would increase the solution viscosity and could have led to the formation of agglomerates. In the work previously reported by Berthold et al. (1996), chitosan was always employed at a concentration of 0.25 % (w/v) when used to prepare particles by the same technique. Higher concentrations were not practical, because the viscosity became too high and would have led to the formation of agglomerates (Berthold et al., 1996).

Sodium sulphate was included as a desolvating reagent to facilitate the phase separation, since it has greater affinity for water and facilitates the removal of the associated water layer from around the dissolved colloidal chains (Mao et al., 2001). The contents of chitosan in the nanoparticles were measured and the results indicated that all of the four batches had the chitosan content higher than 97% w/w (Table 7.6). Residual contents, like sulphate were estimated by equation 7.1 and the data is shown in Table 7.6.

Residual content% (w/w) = 100% - Chitosan content% (w/w) Equation 7.1

Table 7.6 Chitosan and residual contents in chitosan nanoparticles.

| No. | Name | Chitosan content% (w/w) | Residual content% (w/w) |
|---|---|---|---|
| 33 | CS-F NP | 97.4±2.4 | 2.6±2.4 |
| 34 | CL113 NP | 97.3±3.7 | 2.7±3.7 |
| 35 | CL213 NP | 98.2±2.7 | 1.8±2.7 |
| 36 | G213 NP | 97.9±3.1 | 2.1±3.1 |

(Samples represent the mean of three determinations ± standard deviation)

The formation of nanoparticles was monitored by turbidity. Figure 7.10 presents the transmission in relation to the amount of added sodium sulphate.

$$\text{Transmission \%} = \frac{a_{max} - a_n}{a_{max} - a_{min}} \ 100\% \qquad \text{Equation 7.2}$$

Transmission% at different concentrations of sodium sulphate was calculated by Equation 7.2. 'a' in equation is the spectrophotometer absorbance reading; $a_n$ is the sample reading; $a_{min}$ is the minimum reading and $a_{max}$ is the maximum reading when the turbidity was examined by transmission measurements at 500 nm.

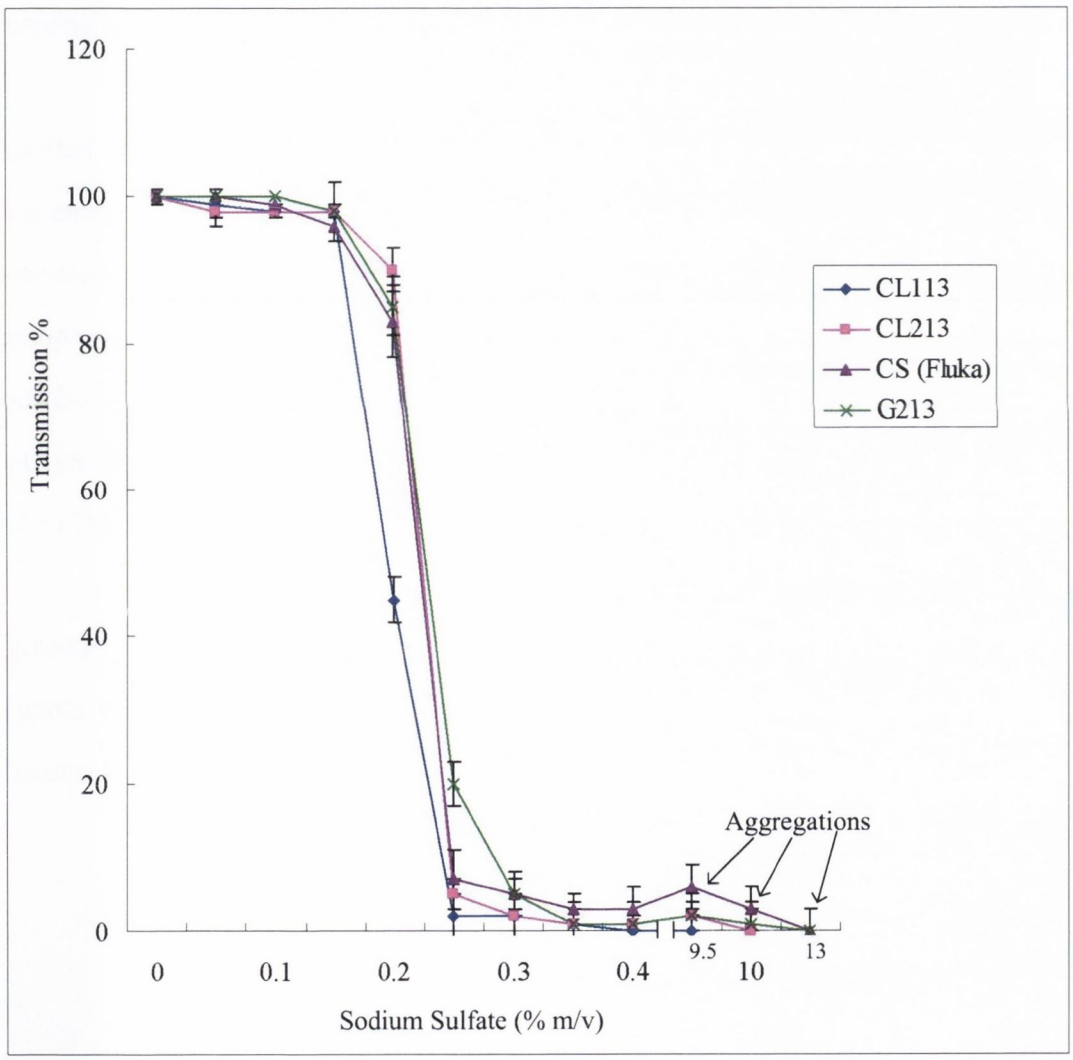


Figure 7.10 Turbidity monitoring during the precipitation employed to produce chitosan particles of CS (Fluka) (No.33), CL113 (No.34), CL213 (No.35) and G213 (No.36).

The transmissions% of four chitosan solutions (CL113, CL213, Chitosan-Fluka and G213) decreased dramatically when the concentrations of sodium sulphate were higher than 0.25% w/v, reflecting the formation of nanoparticles. The arrows (↑↑↑↑) indicate the concentrations where the aggregates were evident during the addition of sodium sulphate. When sodium sulphate reached the concentration of 9.5% w/v, aggregates of chitosan CL113 were present, followed by CL213, Chitosan (Fluka) and G213 with concentrations of sodium sulphate of 10%, 13% and 13% w/v, respectively. The aggregates presented fibre-like aggregates on the top of suspensions.

Another batch of chitosan nanoparticles (CL113.2) was collected when the concentration of sodium sulphate reached 10% w/v, and the CL213.2 particles were collected when sodium sulphate reached 13% w/v. These two batches of nanoparticles were named No.37 and No.38 and they presented similar size and morphology to the nanoparticles No.34 and No.35. The difference was that the batches No.37 and No.38 presented higher residual contents of 7.4 ±2.4 % w/w and 6.5±3.7% w/w, respectively. Residual contents% was calculated by equation 7.1.

Chitosan nanoparticles (from No. 33 to No. 38) were studied and compared as regards their bio-interactions with dendrite cells and the details are discussed in Chapter 10.

## 7.4 In vitro release studies of OVA

### 7.4.1 Physical properties of OVA loaded chitosan nanoparticles

OVA was encapsulated in chitosan nanoparticles by complex coacervation between chitosan and OVA. Although a considerable amount of work has been reported on the formation of antigen encapsulated chitosan nanoparticles (Maclauglin et al., 1998; Lee et al., 1998; Lee et al., 2001; Mao et al., 2001; Hirosue et al., 2001), there is limited work on the study of the *in vitro* antigen release from the nanoparticles made by complex cooperation. In this section, work is focused on the release study of OVA from a series of chitosan nanoparticles, made from chitosan (Fluka), CL113, CL213 and G213.

In the current study, the ratio of OVA to chitosan used to prepare OVA-chitosan nanoparticles was 1:2, because of its high resultant loading efficiency (EE%). In the work previously reported by Bozkir and Saka (2004b), DNA-chitosan nanoparticles were prepared with the weight ratio of 1:2 (DNA:chitosan), and with different molecular weight of chitosans (LMW 137,000; MMW 415,000 and HMW 620 000). As a result the loading efficiency% (EE%) of DNA ranged from 87% to 95%. By increasing the ratio to 1:1 (DNA:chitosan), the loadings of DNA were not significantly increased with all the chitosans (LMW, MMW and HMW), compared to the ratio of 1:2 for DNA/chitosans nanoparticles (Bozkir and Saka, 2004b).

The resultant nanoparticles made with chitosan (Fluka), CL113, CL213 and G213 were named No. 39, No.40, No.41 and No.42, and their physical properties are listed in Table 7.7.

Table 7.7 Physical properties of OVA loaded chitosan nanoparticles.

| No. | Name | Median size (n=3) | OVA loading% (n=3) | OVA EE% (n=3) | Zeta potential mV (n=5) |
|---|---|---|---|---|---|
| 39 | OVA-CS | 0.545 ±0.078 | 30.2 ±1.5 | 90.6 ±4.6 | 5.02 ±0.35 |
| 40 | OVA-CL113 | 0.468 ±0.024 | 30.8 ±1.1 | 92.3 ±3.2 | 4.18±0.56 |
| 41 | OVA-CL213 | 0.534 ±0.081 | 28.6 ±2.6 | 85.7 ±7.9 | 4.79 ±0.91 |
| 42 | OVA-G213 | 0.619 ±0.092 | 30.0 ±2.4 | 89.8 ±7.1 | 3.37 ±0.66 |

(Samples represent the mean values ± standard deviation)

The encapsulation efficiency (%) of OVA in chitosan nanoparticles was 90.6 ± 4.6%, 92.3 ± 3.2%, 85.7 ± 7.9% and 89.8 ± 7.1% for chitosan (Fluka), CL213, CL113 and G213 nanoparticles, respectively. The zeta potential of the four OVA loaded nanoparticles ranged from 5.02 to 3.37 mV. Compared to the drug free chitosan nanoparticles (No.33, No.34, No.35 and No.36, Table 7.4), the zeta potential was decreased from 14.1 ± 0.64 mV to 5.02 ± 0.35mV for chitosan (Fluka) nanoparticles, 12.1 ± 44 mV to 4.18 ± 0.56 mV for CL213 nanoparticles, 13.4 ± 0.78 mV to 4.79 ±0.91 mV for CL113 nanoparticles and 11.4 ± 0.89 to 3.37 ± 0.66 mV for G213 nanoparticles. The median sizes of these four chitosan nanoparticles ranged from 0.468 ± 0.024 μm to 0.619 ± 0.092 μm. Compared to the drug free nanoparticles, the loading of OVA did not significantly affect the sizes of nanoparticles.

The amino groups on the chitosan structure are protonated at pH 5.5 and are responsible for the solubility of chitosan in acetic solution (Aiba, 1992). While at the physiological pH, most of the positive charges would be neutralised, and the hydrophobic chitosan becomes insoluble. This unique property ensures that

nanoparticles could remain physically stable at the physiological pH without chemical cross-linking (Truong-Le et al., 1998; Truong-Le et al., 1999; Mao et al., 2001). In the current work, CL213 NP (1.0% w/v) were suspended in water and the resultant pH was 5.87. At the same concentration, CL213 NP was suspended in PBS buffer with pH of 7.4. The turbidities of these two suspensions were measured and compared. There was no significant change of the turbidities, indicating that there were no fresh particles forming under pH of 7.4.

## 7.4.2 Release studies of OVA from chitosan nanoparticles

The release studies of OVA from the four chitosan batches of nanoparticles (CS-F NP, CL113 NP, CL213 NP and G213 NP) were carried out in PBS buffer (pH=7.4) at 37°C. The results are shown in Figure 7.11.

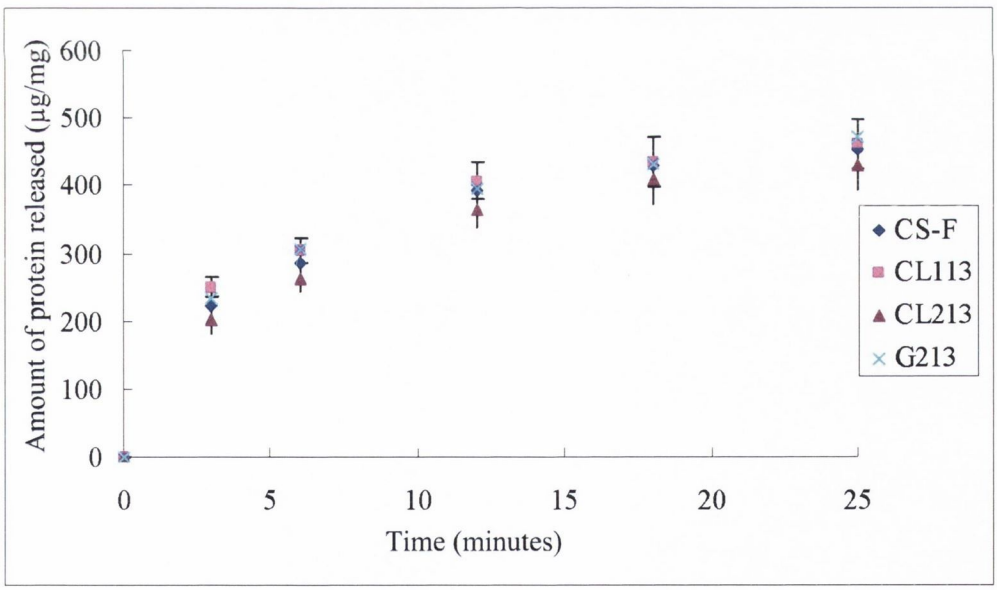


Figure 7.11 Release profiles of OVA from chitosan (Fluka) nanoparticles (No.39), CL113 nanoparticles (No.40), CL213 nanoparticles (No.41) and GL213 nanoparticles (No.42).

From Figure 7.11 we can see that releases for all the four chitosan nanoparticles were complete by 25 minutes. The amount and percentage release data corresponding to time are listed in Appendix I.

The experimental release profiles were fitted to a 'general power law expression' (Equation 1.3) described by Sinclair and Peppas (1984) and Ritger and Peppas (1987). The model is introduced to describe the general solute release behaviour from polymer devices.

It was shown that in cases of pure Fickian release the exponent n has the limiting values of 0.50, 0.45 and 0.43 for release from slabs, cylinders and spheres, respectively (Ritger and Peppas, 1987). As described in Section 1.4, Fickian diffusional release considers one-dimensional, isothermal solute release from a thin polymer slab of thickness L where the system is initially maintained at a constant uniform drug concentration and its surfaces are kept at a constant drug concentration (Ritger and Peppas, 1987; Crank, 1975). Setting the value of n to 0.43 in the equation, the release data were fitted to Equation 1.3 and the estimated parameters of K are listed in Table 7.8. The coefficient of determination (CD) and model selection criterion (MSC) were used as measures of goodness of fit when evaluating the suitability of a model. From Table 7.8, we can see that MSC values ranged from 3.137 to 3.807, which indicated a good fit of the release data to the model (Equation 1.3). There is no significant difference between estimated values of K, which indicated limited differences between the release profiles of OVA from the four chitosan nanoparticles.

Table 7.8 Estimated values to release model of general law expression (Equation 1.3, n=0.43).

| No. | Name | K | MSC | CD |
|---|---|---|---|---|
| 39 | OVA-CS NP | 0.276 ±0.008 | 3.547 | 0.979 |
| 40 | OVA-CL113 NP | 0.275 ±0.010 | 3.137 | 0.969 |
| 41 | OVA-CL213 NP | 0.274 ±0.007 | 3.807 | 0.984 |
| 42 | OVA-G213 NP | 0.286 ±0.009 | 3.508 | 0.979 |

The amount of protein release and their model fits are collected in Figure 7.12

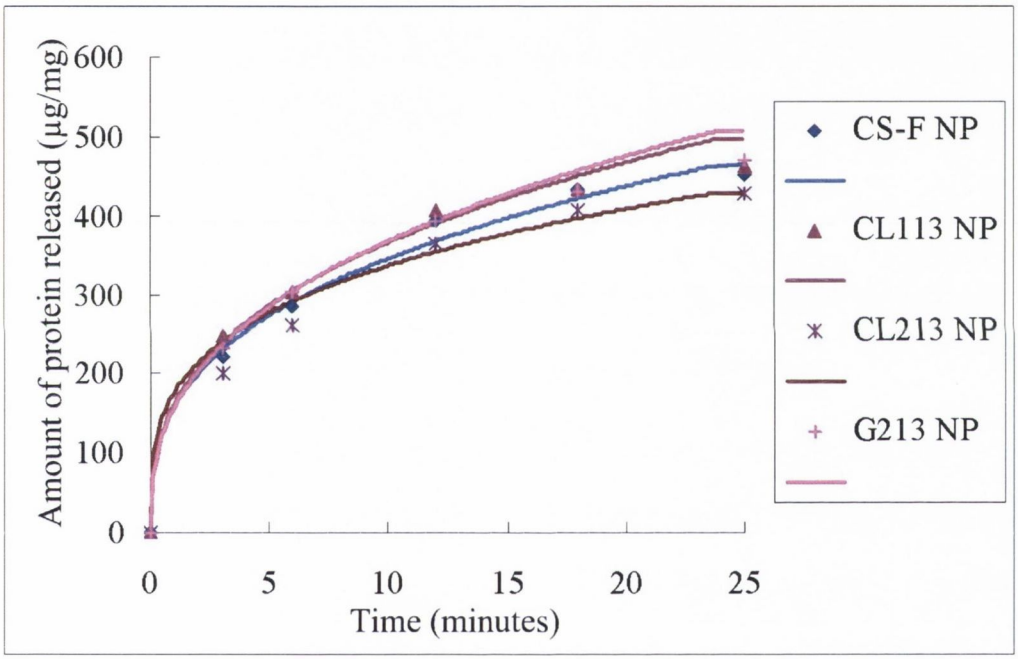


Figure 7.12 Release and model fit of OVA from chitosan nanoparticles (No. 39, No 40, No.41 and No.42).

The release data were fitted to another model, the first order model, to see its suitability to model the data in these release studies. The first order model was first used by Schwartz et al., (1968), to fit the release of drug into aqueous media from wax matrices. The data was examined from the viewpoint of the first order kinetic

theory and that of a diffusion controlled process. It was found that the experimental data were well analysed using this diffusion-controlled model

$$W = W_{\infty}(1 - e^{-kt}) \qquad \text{Equation 7.3}$$

where W is weight released at time t, $W_{\infty}$ is the weight released at infinity and k is the release rate constant. The estimated parameters and related statistics are summarised in Table 7.9.

Table 7.9 Estimated parameters to model fit of first order model.

| No. | Name | k ($min^{-1}$) | $W_{\infty}$ | MSC | CD |
|---|---|---|---|---|---|
| 39 | OVA-CS | 0.191±0.021 | 298 ±9.6 | 4.060 | 0.991 |
| 40 | OVA-CL113 | 0.224 ±0.029 | 298 ±10.8 | 3.630 | 0.986 |
| 41 | OVA-CL213 | 0.177 ±0.020 | 284 ±9.8 | 4.053 | 0.991 |
| 42 | OVA-G213 | 0.204 ±0.026 | 302 ±11.0 | 3.742 | 0.988 |

The rate constant k of OVA release remained relatively constant from all chitosan nanoparticles. The MSC (model selection criterion) values ranged from 3.630 to 4.060, which were relatively higher than the values to the model of general power law expression (Equation 1.3, Table 7.8). For example, the MSC value of OVA-CS NP to Equation 1.3 was 3.547, which was smaller than the value of 4.060 when fitted to Equation 7.3.

It has been known that the most appropriate model is that with the largest MSC, when judging the fit of a particular model to experimentally determined data. The first order model is the model that best fit to OVA release data from chitosan

nanoparticles (CS-F NP, CL113 NP, CL213 NP and G213 NP) with relatively high values of MSC, compared to the general power law expression model.

## 7.5 Conclusions

Chitosan microparticles were successfully prepared by spray drying with and without crosslinking agent, glutaraldehyde. There was no visible change in morphology of the spray dried chitosan microparticles due to the chemical crosslinking. The median particle sizes of both microparticle batches samples ranged from 3 to 5 μm. Oliverira et al., (2005) prepared their chitosan microparticles by spray drying using glutaraldehyde or d,l-glyceraldehyde as crosslinking agent. Compared to their non-crosslinked microparticles, there was no visible change in the morphology (Oliverira et al., 1005).

Chitosan nanoparticles were successfully prepared by coacervation/precipitation methods, by using chitosan or chitosan salts (CL113, CL213 and G213). Coacervation/precipitation was firstly used by Berthold and the co-workers (1996) to prepared chitosan particles by using sodium sulphate as precipitation agent. In the current study, there was no visible difference in the morphology of the chitosan nanoparticles made from chitosan chloride and chitosan glutamate. All the particles presented irregular particulate shapes in the nano size range (median size from 0.43 ± 0.07 μm to 0.58 ± 0.05 μm).

Protein OVA was loaded onto chitosan nanoparticles by adsorption with encapsulation efficiency (%) ranging from 85.7% to 92.3%. The range of zeta potential was 3.37 ± 0.66 mV to 5.02 ± 0.35 mV, which is smaller than that of drug free nanoparticles (11.4 ± 0.89 mV to 14.1 ± 0.64 mV). This decrease indicated the presence of negatively charged OVA. Release was completed for all the four

batches of particles by 25 minutes. The release data was fit to models of general power law expression and first order models. First order model gave the best fit to the release profiles. There is no significant difference between release profiles of OVA from chitosan nanoparticles of CS-F, CL113, CL213 and G213.

# RESULTS AND DISCUSSION

## Chapter 8 Hyaluronate micro particles and hyaluronate-chitosan nano particles

## 8.1 Introduction

Because of its various functions and physicochemical properties (described in Chapter 1), hyaluronic acid (HA) and modified HA have been investigated and used for ophthalmic surgery (Balazs, 1983), arthritis treatment (Balazs and Denlinger, 1993) and drug delivery (Joshi et al., 1992). Most of the strategies for the modification of HA have been focused on chemical modifications through carboxyl and hydroxyl groups, like esterification (Illum et al., 1994), derivatisation with carbodiimide (Kuo et al., 1991), and cross-linking of HA using divinyl sulfone (Balazs and Leshchiner, 1986), glycidyl ether (Balazs and Leshchiner, 1987), or dialdehyde after modification of HA with adipic dihydrazide (Luo et al., 2000). These chemical modifications were generally carried out in highly alkaline or acidic solutions and at elevated temperatures, which are not suitable for the inclusion of sensitive molecules such as proteins. On the other hand, although polymeric particles have been widely studied for drug delivery systems, there is little work which has reported on HA particulate systems, especially HA nanoparticles. As a biodegradable, biocompatible and viscoelastic polymer (Zhong et al., 1994; Prestwitch et al., 1998; Balazs, 1998; Brown and Jones, 2004; Hahn et al., 2004), particulate HA has potential as a nano sized drug delivery carrier. Chitosan was used to combine with HA during the manufacture process to aid the formation of the nanoparticles.

In the current work, sodium hyaluronate microparticles were manufactured by spray drying. HA/chitosan nanoparticles were manufactured by coacervation/precipitation. Two sodium hyaluronates and four chitosans (CL113, CL213, G113 and G213) were used to prepare a range of HA-chitosan nanoparticles. The physical properties of the resultant nanoparticles were measured and compared. The two sodium hyaluronates were sodium hyaluronate (Fluka) and ultrapure sodium hyaluronate

(NovaMatrix). Ultrapure sodium hyaluronate (NovaMatrix) presents a low endotoxin level smaller than 2.5 EU/g, as supplied by the manufacturer.

## 8.2 Hyaluronic acid particles

### 8.2.1 Hyaluronic acid microparticles prepared by spray drying

Sodium hyaluronate microparticles were made by spray drying by using sodium hyaluronate (Fluka) and lecithin. Lecithin was used as a surfactant. The physical properties of the resultant sodium hyaluronate microparticles are listed in Table 8.1 and the SEM picture is shown in Figure 8.1. HA-Na represents the sodium hyaluronate.

Table 8.1 Physical properties of sodium hyaluronic microparticles made by spray drying.

| No. | Name | D50% (μm) (n=3) | D90% (μm) (n=3) | Span |
|---|---|---|---|---|
| 43 | HA-Na MP | 2.69 ± 0.53 | 6.23 ± 0.79 | 2.12 ± 0.88 |

(Samples represent the mean value ± standard deviation)

Figure 8.1 SEM picture of HA microparticles (No.43).

The median size of the spray dried microparticles was 2.69 ± 0.53 μm. From the SEM picture (Figure 8.1) we can see that the particles present relatively spherical shapes with rough surfaces.

Lecithin is a surfactant widely used in pharmaceutical and food manufacturing. It can be used as a surfactant in large volume parenterals and is used for the preparation of intravenous fat emulsions (Washington, 1990). It behaves as a charge-stabilising surfactant in lactose and salbutamol dispersions (Sidhu et al., 1993). When making chocolate, lecithin is added to the cocoa butter and adsorbs to the particles' surfaces reducing inter-particle interaction. In the current work, lecithin was dispersed with sodium hyaluronate solution with a ratio of 1:8 w/w (lecithin:sodium hyaluronate) as a surfactant.

## 8.2.2 Hyaluronic acid (Fluka)/chitosan nanoparticles

Hyaluronic acid is a high molecular mass linear, anionic polysaccharide with a rich presence of carboxyl groups (Sall and Ferard, 2007; Chen et al., 2005; Gold, 1981 and 1979), while chitosan is a polysaccharide with cationic properties. The charge difference between these two biomaterials makes possible preparation of HA/CS particles. The hyaluronate and chitosan used in this preparation were sodium hyaluronate (Fluka) and CL213.

The particle size of the resultant HA(F)/CL213 particles (No.44) was measured with a Malvern Zetasizer and it was 198 ±11 nm and the size width (width of the peak in the size distribution Figure 8.2) was 99.1 ±14.3 nm. The zeta potential was 1.64 ± 0.52 mV. The chitosan loading on the HA(F)/CL213 nanoparticles was 42.7 ± 9.7 % w/v, determined by ninhydrin (Section 4.2.2) analysis. The physical properties of

HA(F)/CL213 nanoparticles are listed in Table 8.2 and the SEM picture is shown in Figure 8.2.

Table 8. 2 Physical properties of HA/CS nanoparticles.

| No. | Name | z-Average size (nm) (n=3) | Size width (nm) (n=3) | Chitosan content% (w/w) (n=3) | Zeta potential (mV) (n=5) |
|---|---|---|---|---|---|
| 44 | HA(F)/CL213 NP | 198 ± 11 | 99.1 ± 14.3 | 42.7 ± 9.7 | 1.64 ± 0.52 |

(Samples represent the mean value ± standard deviation)

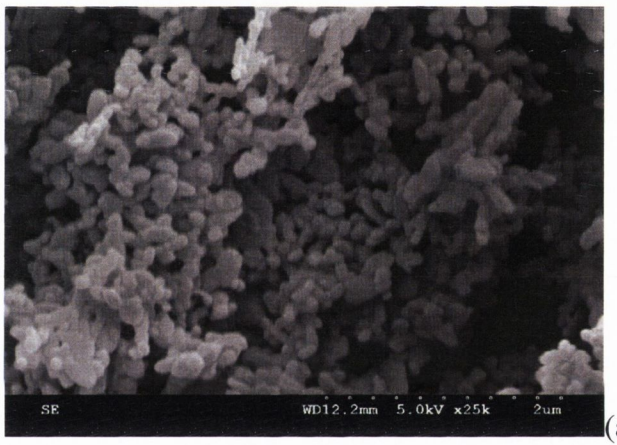


(a)

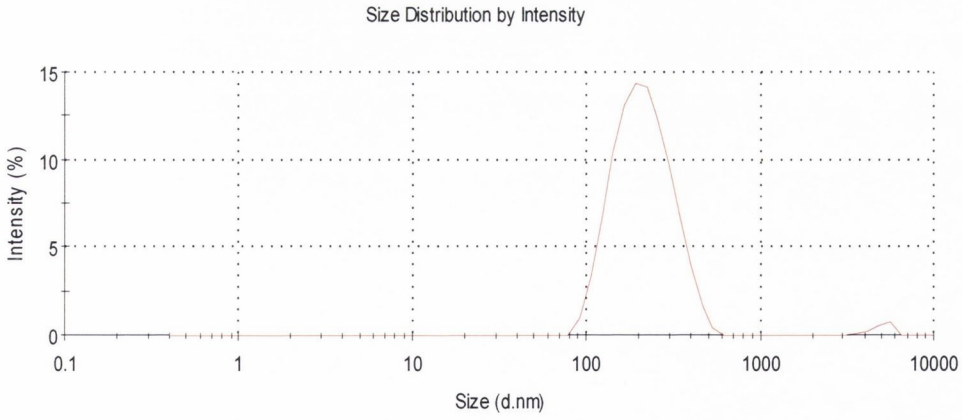


(b)

Figure 8.2 SEM picture and particle size distribution of HA/CS nanoparticles (No.44).

From SEM picture we can see that the particles are in the nano size range with relatively irregular shapes. The particles look to be fused. This may be due to the

coating procedure used for sample preparation for SEM, which may have caused fusion of small particles, especially in the nano-range. Gold coating is a necessary step when preparing samples for SEM analysis. From the size distribution we can see that there might be some aggregates present in the nanoparticles as well.

When HA solution was mixed with CS solution while stirring, large aggregates were produced which may be caused by the high molecular weight of HA and CS polymers. The large aggregates were eliminated by filtration through a 0.2 μm filter. This filtration process may have affected the resultant particles sizes by decreasing the viscosity of the mixture solution and decreased the mean sizes to 198 nm. The primary concentrations of HA and CS solutions used to make mixtures were both 0.2 % w/v. Solutions with lower concentrations (0.02% w/v) of HA and chitosan were also prepared, and the mixture of both solutions produced aggregates, therefore filtration is a necessary step in the preparation process.

Without the presence of chitosan, the hyaluronic acid in solution was not precipitated by the addition of sodium sulphate. The mixture remains clear under stirring. Consequently, chitosan is necessary in the preparation of nanoparticles containing hyaluronic acid by precipitation/coacervation method. The formation of HA/CS nanoparticles was monitored by turbidity. Figure 8.3 shows the transmission in relation to the added amount of sodium sulphate.

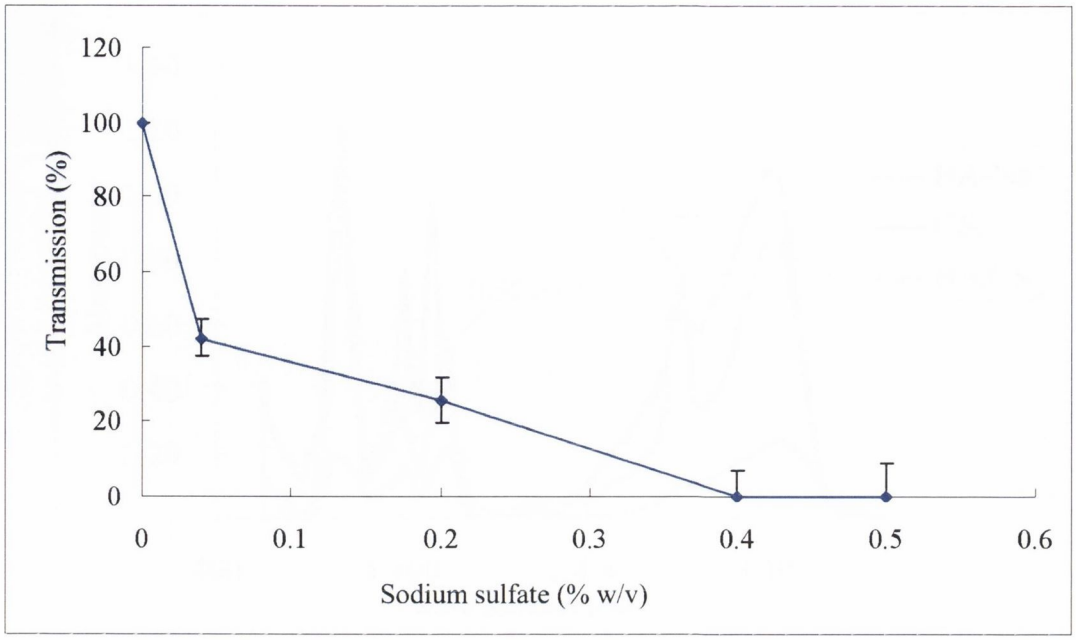


Figure 8.3 Turbidity monitoring during the precipitation employed to produce HA/CS nanoparticles (No.44).

Transmission (%) at the different concentrations of sodium sulphate was calculated by Equation 7.2 in Chapter 7. From Figure 8.3 we can see that the transmission (%) decreased dramatically when the concentrations of sodium sulphate were higher than 0.4% w/v, facilitating the formation of nanoparticles.

The FTIR analysis of the resultant HA/CS nanoparticles was performed and compared to pure sodium hyaluronate and chitosan CL213 (CS) (Figure 8.4) to identify the presence of HA and chitosan in nanoparticles.

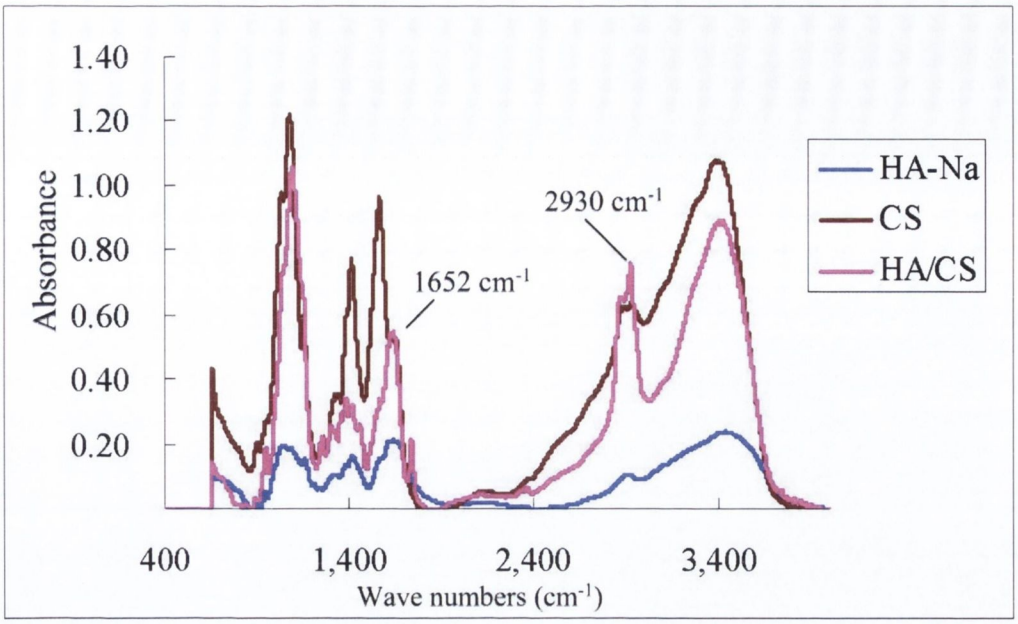


Figure 8. 4 FTIR of sodium hyaluronate, chitosan CL213 polymers and HA/CS particles.

From Figure 8.4 we can see that sodium hyaluronate have an absorption peak at 1652 $cm^{-1}$, which is characteristic of C=O stretch of carboxylic acid in HA polymers (Hill and Holman, 2000). HA/CS system also has this absorption peak at 1652 $cm^{-1}$ which indicated the presence of HA in HA/CS particles. The absorption at 2930 $cm^{-1}$ is characteristic of a stretch of $-CH_3$ groups (Hill and Holman, 2000). The increased intensity of this band in the HA/CS system at 2930 $cm^{-1}$ compared to sodium hyaluronate and chitosan CL213 on their own could be attributed to the interactions between the polymers and as a result, shifting peaks exposing at the band 2930 $cm^{-1}$. The FTIR result indicated the presence of HA and CS in HA/CS nanoparticles.

Sodium sulphate was included as a desolvation reagent to facilitate the phase separation, since it has a greater affinity for water and facilitates the removal of the associated water layer from around the dissolved colloidal chains (Mao et al., 2001). In the current study, HA/CS particle were prepared with or without the addition of

sodium sulphate. Without the sodium sulphate, there was no obvious indication of the formation of nanoparticles in the resultant products. The SEM picture of resultant products is shown in Figure 8.5.

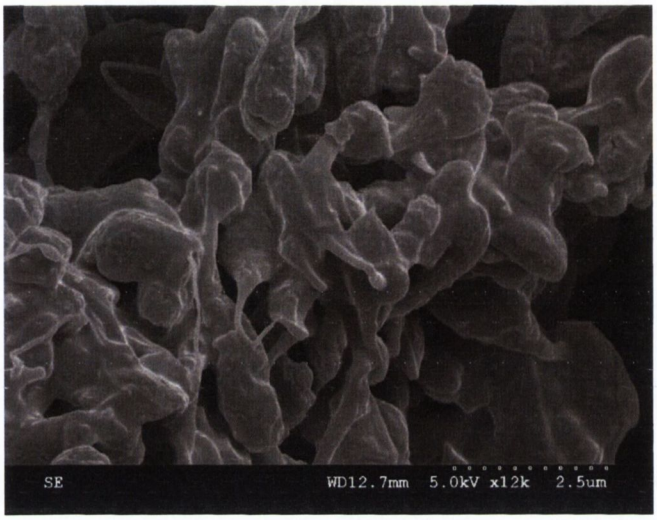


Figure 8. 5 SEM picture of the HA-CS system without addition of sodium sulphate.

The HA and CS solutions at the concentration of 0.2% w/v have pH values of 6.71 and 5.45, respectively. A concentration value of 0.2% w/v was chosen for the manufacture of primary solutions because a solution with higher concentration would increase the solution viscosity and as a result lead to the formation of agglomerates (Berthold et al., 1996).

## 8.2.3 Hyaluronic acid (NovaMatrix)/chitosan nanoparticles

Highly purified sodium hyaluronate (NovaMatrix) was used to prepare nanoparticles with chitosan CL213, CL113, G213 and G113. The difference with sodium hyaluronate (Fluka) is the low LPS level of the NovaMatrix grade which is smaller than 2.5 EU/g (endotoxin units per gram) as claimed by the manufacturer.

According to the U.S. Food and Drug Administration guideline, the upper limit of the pyrogen level is 5.0 endotoxin units (EU)/kg (body weight) per injection.

The resultant nanoparticles were named with No.45 to No.48 and their physical properties are listed in Table 8.3.

Table 8. 3 Physical properties of HA/CS nanoparticles

| No. | Name | z-average size (nm) (n=3) | Size width (nm) (n=3) | Chitosan content% (w/w) (n=3) | Zeta potential (mV) (n=5) |
|---|---|---|---|---|---|
| 45 | HA/CL113 NP | 171.2 ±21.3 | 70.2±12.1 | 43.2 ±5.1 | 1.55±0.44 |
| 46 | HA/CL213 NP | 183.8 ±31.2 | 85.6±27.3 | 45.8±6.7 | 2.12±0.29 |
| 47 | HA/G113 NP | 169.8 ±50.7 | 71.6±16.6 | 45.1±3.3 | 1.34±0.72 |
| 48 | HA/G213 NP | 176.5 ±38.8 | 78.4±12.2 | 44.8 ±7.9 | 1.28±0.31 |

(Samples represent the mean value ± standard deviation)

The SEM pictures of No.44 to No.47 are shown in Figure 8.6, 8.7, 8.8 and 8.9 respectively. From the size distributions we can see that there might be some aggregates present.

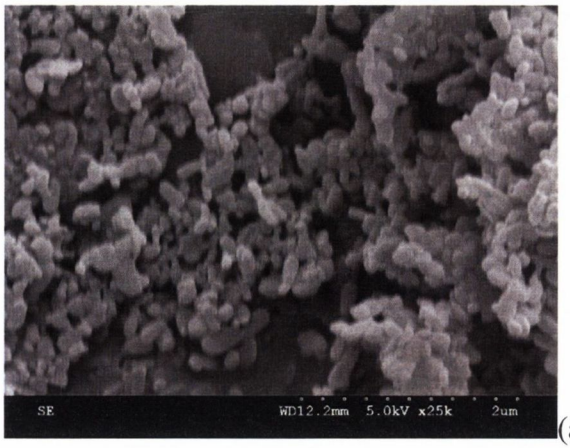

(a)

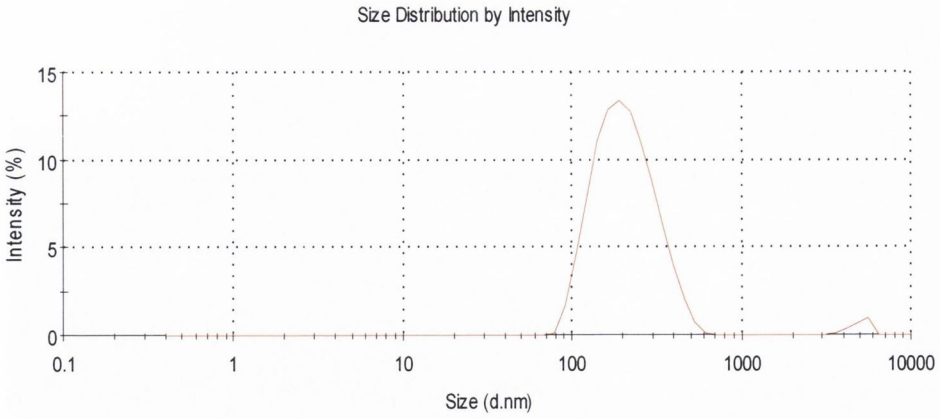


(b)

Figure 8.6 (a) SEM picture (b) size distribution of HA/CL113 nanoparticles.

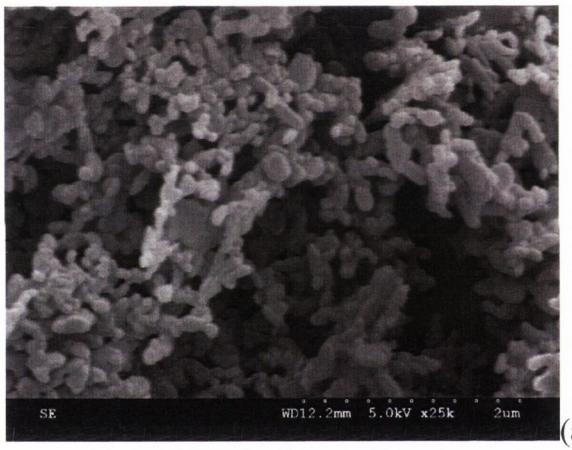


(a)

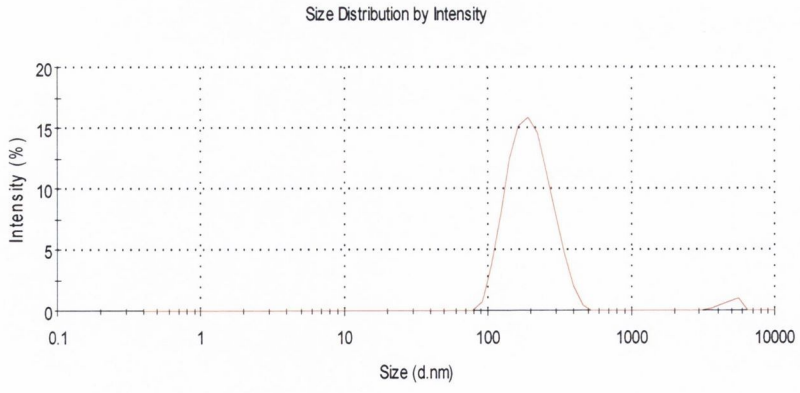


(b)

Figure 8.7 (a) SEM picture (b) size distribution of HA/CL213 nanoparticles.

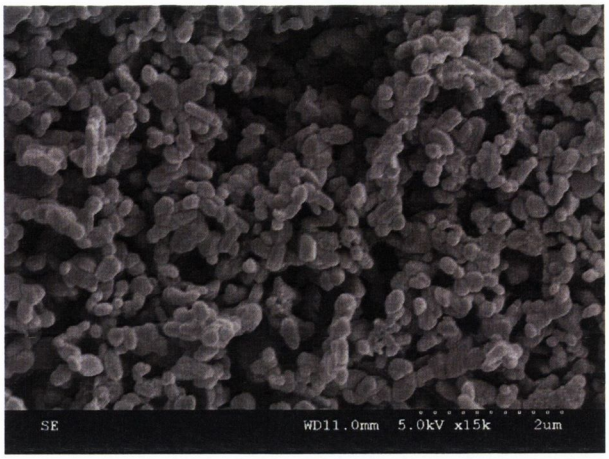


(a)

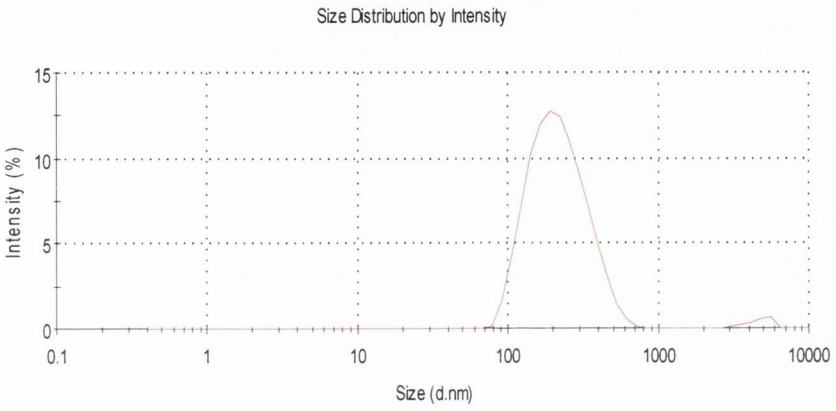


(b)

Figure 8.8 (a) SEM picture (b) size distribution of HA/G113 nanoparticles.

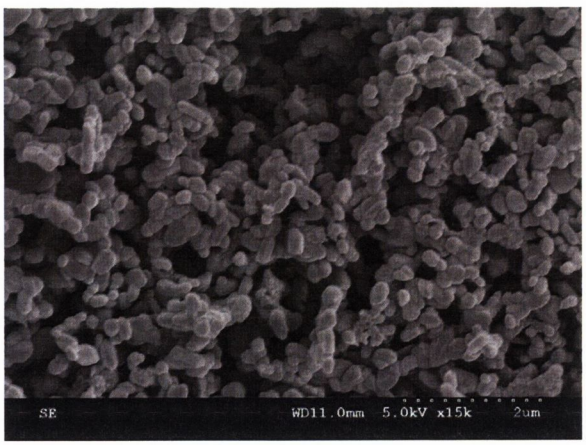


(a)

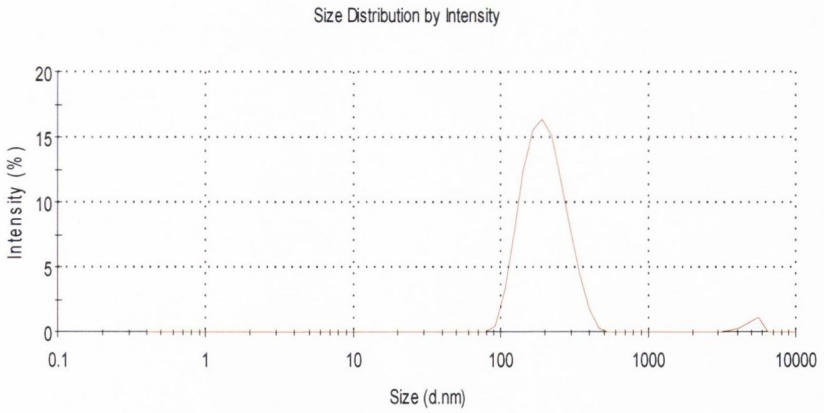


(b)

Figure 8.9 (a) SEM picture (b) size distribution of HA/G213 nanoparticles.

## 8.3 Physicochemical properties of sodium hyaluronate

### 8.3.1 Measurement of molecular weights

The molecular weight of sodium hyaluronate (Fluka) and ultrapure sodium hyaluronate (NovaMatrix) used in this study were characterised by gel permeation chromatography (GPC). The results of the $M_w$, $M_n$, polydispersity are listed in Table 8.4.

Table 8.4 Molecular weight characteristics of sodium hyaluronate

| Chitosan | $M_w$ (kDa) | $M_n$ (kDa) | Polydispersity | Manufacturer (kDa) |
|---|---|---|---|---|
| Fluka | 1,590±720 | 1,410±540 | 1.12±0.02 | ------ |
| NovaMatrix | 1,010±850 | 909±790 | 1.11±0.02 | 620-1200 |

(Samples represent the mean of three determinations ± standard deviation)

The molecular weight of sodium hyaluronate (Fluka) is 1,590±720 kDa, which agreed with the work reported by Moller et al., (2007). In their work, hyaluronic acid sodium salt (Fluka) had a molecular weight of 1500-1800 kDa. The ultrapure sodium hyaluronate (NovaMatrix) presented a molecular weight of 1,010±850 kDa, which agrees with the data supplied by the manufacturer. The approximate ranges of molecular weights were determined by intrinsic viscosity measurement (NovaMatrix). From Table 8.4 we can see that sodium hyaluronate (Fluka) presented relatively higher molecular weight than ultrapure sodium hyaluronate (NovaMatrix).

## 8.3.2 Powder X-ray diffraction (XRD)

XRD scans of sodium hyaluronate starting material and the processed particles are shown in Figure 8.10.

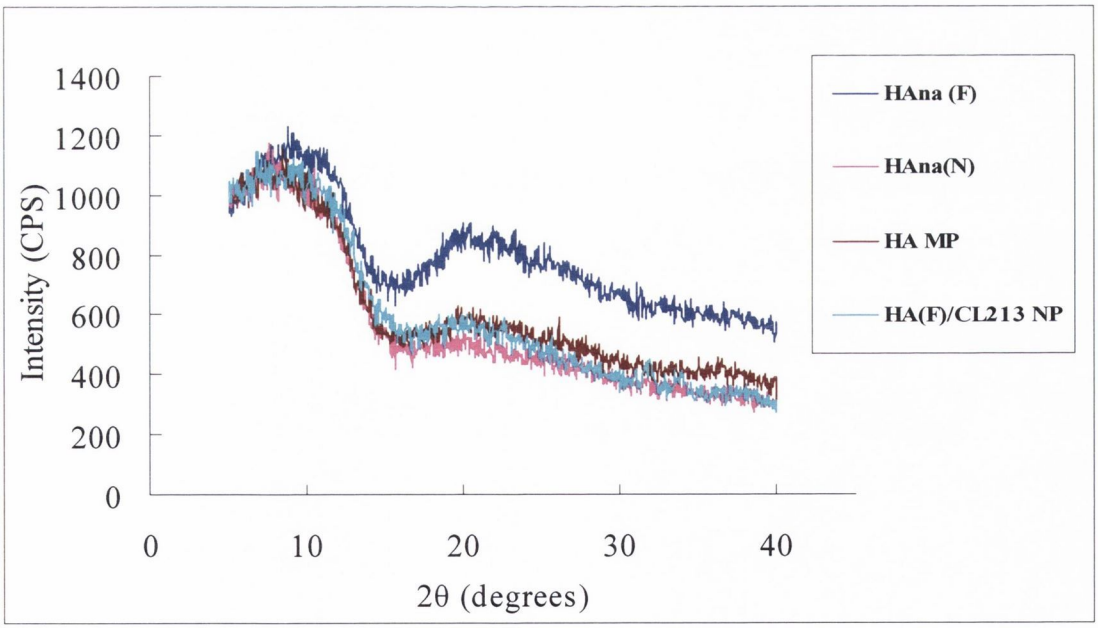


Figure 8.10 XRD scans of sodium hyaluronate (Fluka) (HAna(F), sodium hyaluronate (NovaMatrix) (HAna(N), HA spray dried microparticles (HA MP) and HA/CL213 nanoparitcles (HA(F)/CL213 NP).

In the XRD scans, crystalline materials give sharp narrow diffraction peaks and the amorphous component gives a very broad curve without sharp peaks. From Figure 8.10 we can see that all the systems showed broad peaks without the diffraction peaks indicating that both of the starting sodium hyaluronates were amorphous and the particles which had been processed by spray drying and precipitation/coacervation were also amorphous compounds. The processes did not change the amorphous nature of the materials.

## 8.4 Conclusions

Sodium hyaluronate microparticles were manufactured by spray drying and the median particle size of these particles was 2.69 ± 0.53 μm. Lecithin was used as a surfactant. All the particles presented relatively spherical shapes with rough surfaces.

HA/CS nanoparticles were manufactured by coacervation/precipitation. The particle size dramatically decreased to 198 ± 11 nm, compared to HA microparticles made by spray drying. The FTIR scan indicated the presence of HA in the system. Without the presence of chitosan, sodium hyaluronate was not precipitated by sodium sulphate alone and without addition of sodium sulphate; mixture of hyaluronic and chitosan did not formed particulate forms.

The possibility of formations of hyaluronic acid micro and nanoparticles indicate its potential use in future drug delivery studies.

# RESULTS AND DISCUSSION

## Chapter 9 Effects of nanoparticles on platelet aggregations

## 9.1 Introduction

When damage to small blood vessels occurs, platelet aggregation will be responsible for maintaining the haemostasis. Following damage, the blood vessel reflexes and promote vasoconstriction. At this time, platelets flowing by adhere to the exposed collagen from the damage site. Collagen stimulates phospholipase $A_2$ within the platelets. This reaction in turn releases arachidonic acid which is converted through the action of cyclooxgenase enzyme to thromboxane $A_2$ (Grette, 1962). Other cytoplasmic granules released are serotonin and ADP. ADP attracts more platelets to the area and thromboxane $A_2$ promotes platelet aggregation (Grette, 1962). Then damaged tissue releases factor III, which together with $Ca^{2+}$ will activate factor VII as well as platelets release factor XII, which in turn activates factor XI (Grette, 1962). Both activated factor VII and XI will promote cascade reactions and activate factor X. Active factor X, along with factor III, factor V, $Ca^{2+}$ and platelet thromboplastic factor ($PF_3$) are able to activate prothrombin activator. Prothrombin activator converts prothrombin to thrombin and thrombin converts fibrinogen to fibrin. Fibrin initially forms a loose mesh, however factor XIII causes the formation of covalent cross links and forms a blood clot (Grette, 1962).

The delivery of pharmacological antigens using nanotechnology gives rise to the possibility of the interactions of nanoparticles with blood and its elements (Radomski et al., 2005). The potential of nanoparticles to induce platelet aggregation and precipitate thrombosis was reviewed in Section 2.2. It is important to screen nanoparticles to establish their safety in this regard, especially when there are very limited published studies on these particles in record. In this section therefore, the effect of the drug free PLGA, chitosan-PLGA and chitosan nanoparticles on human platelet aggregation and their effects on inhibition of the collagen induced aggregation *in vitro* were investigated.

Indomethacin and ketoprofen are drugs used for the treatment of inflammation (NSAID). It has been reported that both indomethacin and ketoprofen inhibit platelet aggregation (Leach and Thorburn, 1982; Gursoy et al., 1987; Petrusewicz et al., 1995), and can cause dose related side effects on gastrointestinal and neurological systems, such as nausea, headache, abdominal distress or pain etc. In this section the effect of indomethacin and ketoprofen encapsulated into PLGA nanoparticles on platelet aggregation were also studied.

## 9.2 Effects of nanoparticles on human platelet aggregations

### 9.2.1 PLGA and CS-PLGA nanoparticles

Drug free PLGA nanoparticles (No.16) and CS-PLGA nanoparticles (No.25) were used to study their effects on platelet aggregation. The light transmittance (%) changes of platelets when incubated with PLGA and CS-PLGA nanoparticles at different concentrations of 1, 10, 100, and 500 μg /ml were determined and the results are shown in Figure 9.1, 9.2, 9.3 and 9.4.

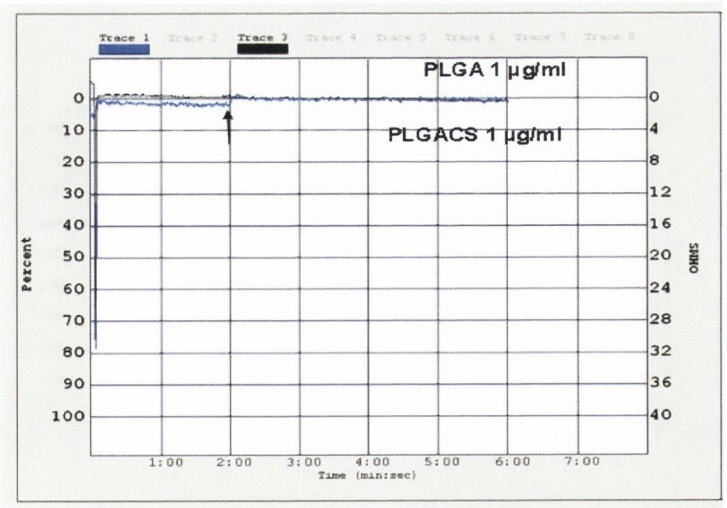


Figure 9.1 Aggregation of platelets by PLGA and CS-PLGA nanoparticles at concentrations of 1 μg/ ml.

Indomethacin and ketoprofen are drugs used for the treatment of inflammation (NSAID). It has been reported that both indomethacin and ketoprofen inhibit platelet aggregation (Leach and Thorburn, 1982; Gursoy et al., 1987; Petrusewicz et al., 1995), and can cause dose related side effects on gastrointestinal and neurological systems, such as nausea, headache, abdominal distress or pain etc. In this section the effect of indomethacin and ketoprofen encapsulated into PLGA nanoparticles on platelet aggregation were also studied.

## 9.2 Effects of nanoparticles on human platelet aggregations

### 9.2.1 PLGA and CS-PLGA nanoparticles

Drug free PLGA nanoparticles (No.16) and CS-PLGA nanoparticles (No.25) were used to study their effects on platelet aggregation. The light transmittance (%) changes of platelets when incubated with PLGA and CS-PLGA nanoparticles at different concentrations of 1, 10, 100, and 500 μg /ml were determined and the results are shown in Figure 9.1, 9.2, 9.3 and 9.4.

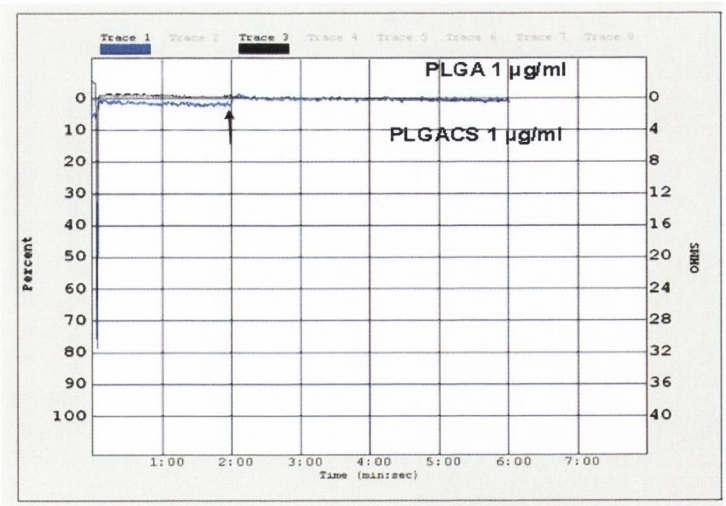


Figure 9.1 Aggregation of platelets by PLGA and CS-PLGA nanoparticles at concentrations of 1 μg/ ml.

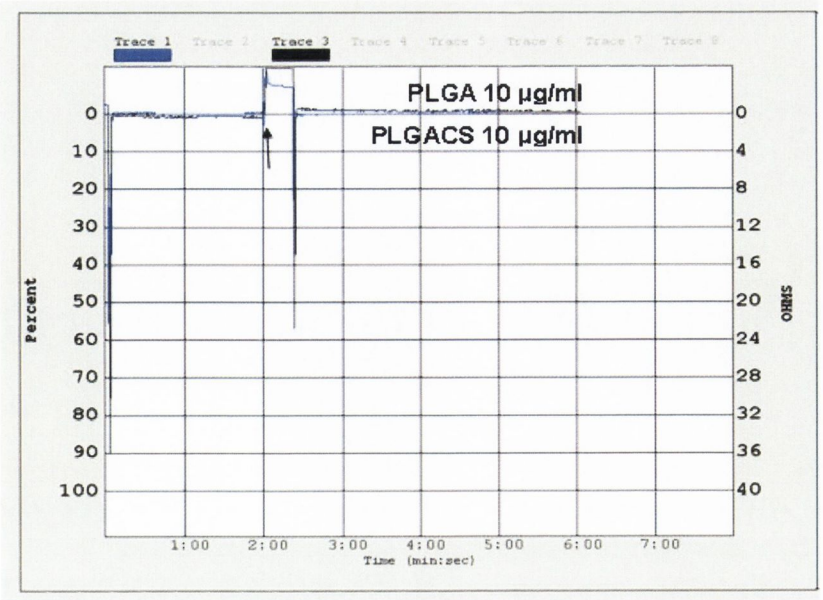


Figure 9.2 Aggregation of platelets by PLGA and CS-PLGA nanoparticles at concentrations of 10 µg/ ml.

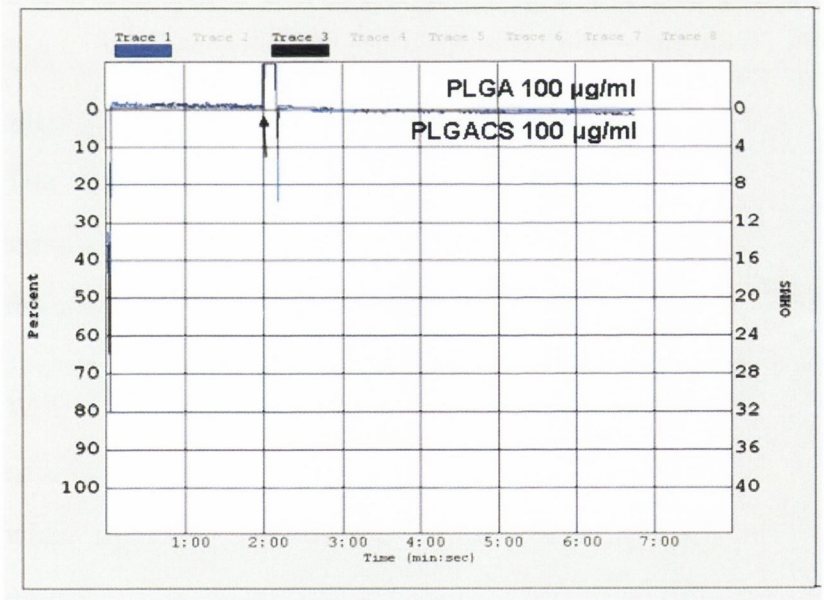


Figure 9.3 Aggregation of platelets by PLGA and CS-PLGA nanoparticles at concentrations of 100 µg/ ml.

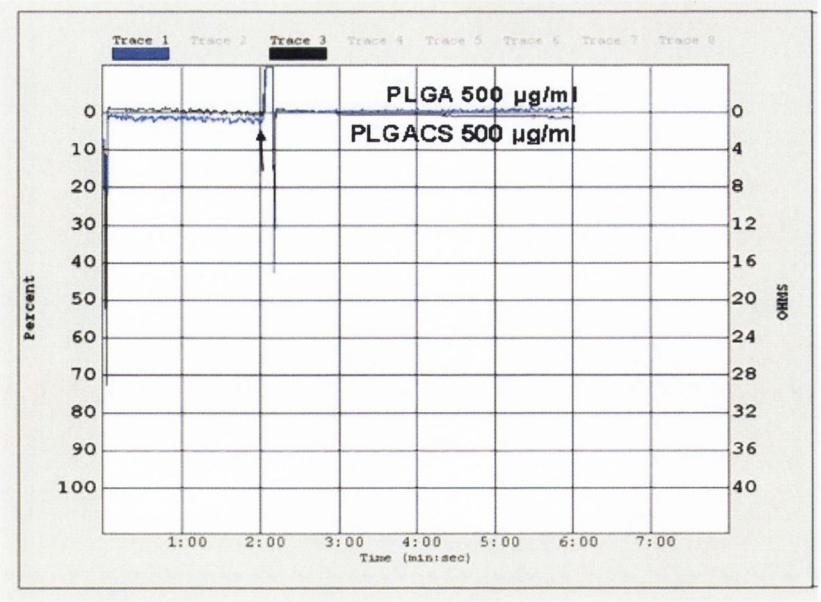


Figure 9.4 Aggregation of platelets by PLGA and CS-PLGA nanoparticles at concentrations of 500 µg/ ml.

The arrows (↑) indicate the time at which sample was added at the dose indicated. The increase in light transmittance is associated with the formation of platelet aggregates while the return to the base line represents deaggregation of the platelets. The scan lasts at least 6 minutes for each measurement. PLGA and CS-PLGA samples were added to human platelets simultaneously in two different channels of the aggregometer.

With these aggregation traces, it can be seen that PLGA and CS-PLGA nanoparticles did not induce platelet aggregation (0±2% light transmittance, n=4) when incubated with platelet-rich plasma at concentrations of 1, 10, 100 and 500 µg/ml.

Collagen is a physiological aggregating agent. In the current platelet study, collagen (0.3-5 µg/ml) was used as an agent to induce platelet aggregation. From Figure 9.5 it can be seen that collagen at concentrations of 2 µg/ml, 3 µg/ml and 5 µg/ml induced platelet aggregations.

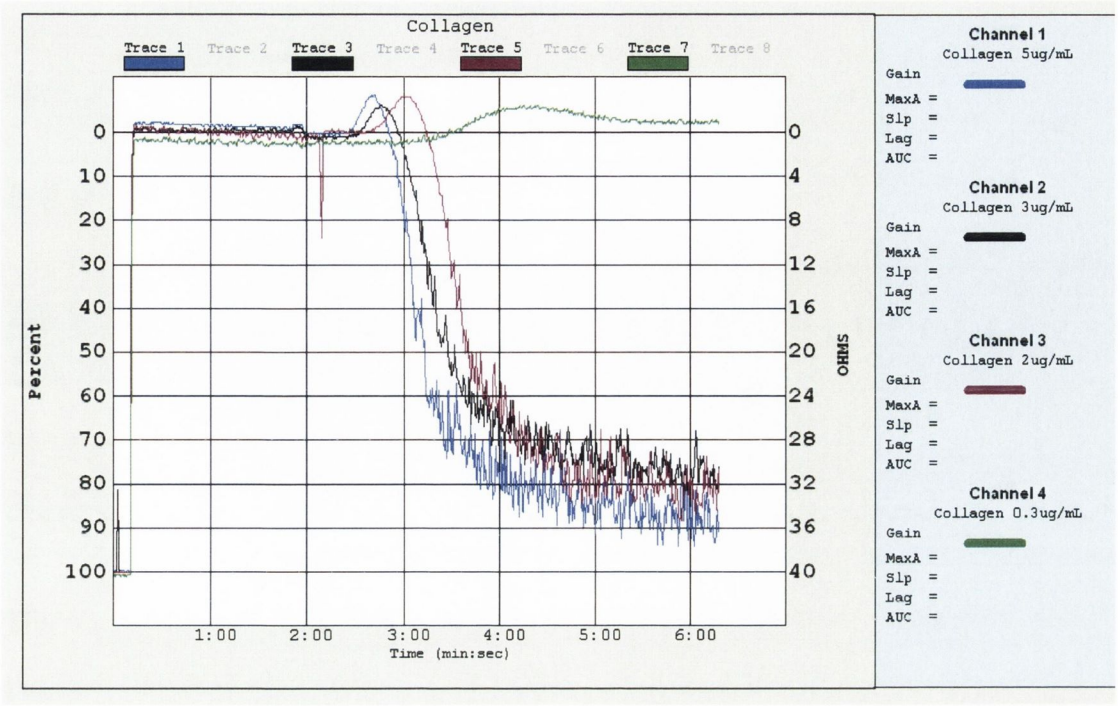


Figure 9.5 Aggregation of platelets by collagen with different concentrations.

The aggregation effects of nanoparticles (500 μg /ml) and collagen (5 μg/ml) on platelets is shown in Figure 9.6.

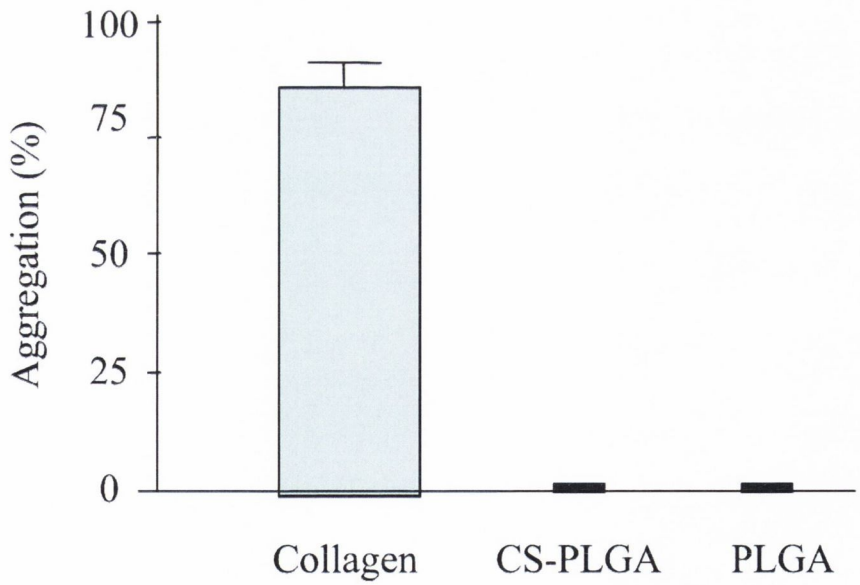


Figure 9.6 Effects of collagen, PLGA and CS-PLGA nanoparticles on platelet aggregation.

Figure 9.6 indicates that there is no significant difference between aggregation effects of drug free PLGA and CS-PLGA nanoparticles on human platelet aggregation.

## 9.2.2 Chitosan nanoparticles

The effects of chitosan nanoparticles on human platelet were measured to compare their effects on platelet aggregations. Platelet-rich plasma (PRP) was obtained from blood of healthy volunteers and the nanoparticles used were drug free nanoparticles of CS-F NP (No. 33), CL113 (No.34), CL 213 (No.35) and G 213 (No. 36).

The aggregative properties of nanoparticles (500 μg /ml) and collagen (5μg/ml) in platelets are shown in Figure 9.7.

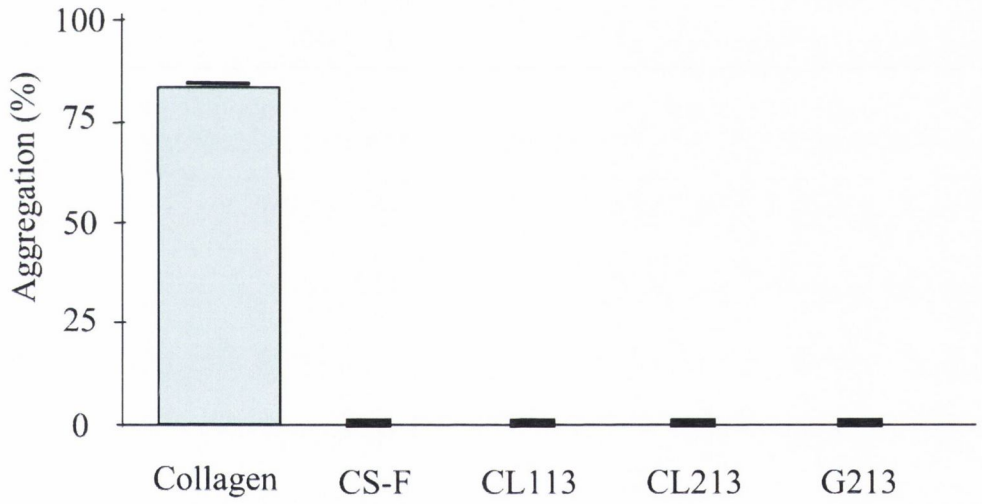


Figure 9.7 Platelet aggregation effects by chitosan nanoparticles: CS-F, CL113, CL213 and G213

From Figure 9.7, we can see that all the chitosan nanoparticles (No.33 – No.36) did not induce platelet aggregation (0±2% light transmittance, n=4) when incubated with human platelets.

It has been reported that chitosan can endorse hemostasis and allow the promotion

of normal tissue regeneration (William and Herbert, 1985). Due to these properties, chitosan has been examined for use in a wide range of biomedical applications, such as surgical thread, bone healing materials and wound dressing (Biagini et al., 1991; Abhay, 1998). The mechanism of action of chitosan may be associated with the increasing $[Ca^{2+}]_i$ mobilisation which assists the activation of platelets (Chou et al., 2003). The inhibition effects presented by chitosan nanoparticles in the current study may be due to the presence of sulphate anion as in the particles. The content details of chitosan nanoparticles are discussed in Chapter 7. In the work reported by Sheu et al. (2003), the inhibitory mechanisms of magnesium sulphate on platelet aggregation was studied. Magnesium sulphate concentration-dependently inhibited platelet aggregation in human platelets stimulated by collagen and also concentration-dependently inhibited phospholipase breakdown and intracellular calcium mobilization in human platelets stimulated by thrombin (Sheu et al., 2003). The mechanism involved may be that magnesium sulphate may inhibit the activation of phospholipase breakdown and thromboxane $A_2$ formation, thereby leading to inhibition of intracellular $Ca^{2+}$ mobilisation and $Na^+/H^+$ exchanger (Sheu et al., 2003).

In the work previously reported by Radomski et al., (2005), carbon nanoparticles were studied to see their effects on platelet aggregation *in vitro*. The carbon particles investigated were multiplewall (MWNT), singlewall (SWNT) nanotubes, C60 fullerenes (C60CS) and mixed carbon nanoparticles (MCN) (0.2-300 μg/ml). Incubation of platelets with MCN, MWNT, SWNT, but not C60CS, resulted in a concentration-dependent increase in platelet aggregation. The order of efficacy was: MCN >= SWNT>MWNT>SRM1648 ($p<0.05$, n=6-10). Collagen was used as aggregation agent at concentration of 5 μg /ml. At the sample concentration of 300 μg /ml, MCN presented an aggregation effect similar to collagen (70 ± 3 % versus 76 ± 6 %, n=8). The size of the nanoparticles ranged from 1-100 nm.

## 9.3 Effects of nanoparticles on collagen induced human platelet aggregation

### 9.3.1 PLGA and CS-PLGA nanoparticles

The inhibition study was carried out by measuring the abilities of nanoparticles to inhibit the collagen induced aggregation on human platelets. The collagen concentration used to induce platelet aggregation was 2 μg/ml and the inhibition abilities of PLGA (No.16) and CS-PLGA (No.25) nanoparticles were evaluated under different concentrations from 0.01-100 μg/ml. The light transmittance (%) changes of platelets when incubated with PLGA nanoparticles (1 μg/ml) and collagen (2 μg/ml) are shown in Figure 9.8. Nanoparticles were preincubated with human platelets for 1 min before the addition of collagen.

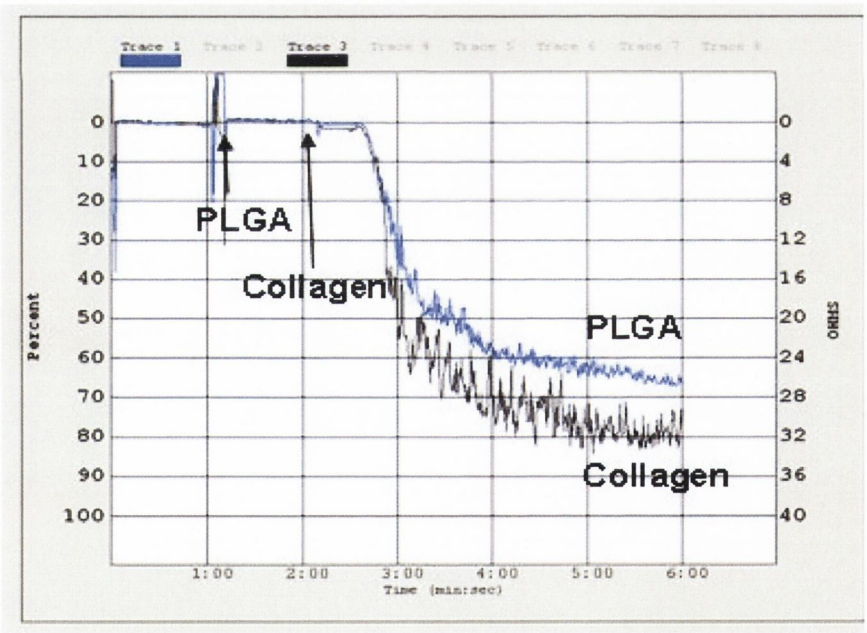


Figure 9.8 The effect of PLGA nanoparticles (No.16) on collagen induced platelet aggregation at the concentration of 1 μg/ml. Collagen concentration was 2 μg/ml.

The arrows (↑) indicate the time at which samples were added. From Figure 9.8 we

can see that at the end of scan (6 minute), the light transmittance (%) of platelets incubated with pure collagen was higher (~32%) than the one incubated with PLGA nanoparticles and collagen (~26%). Since the increase in light transmittance is associated with the formation of platelet aggregations, the presence of PLGA nanoparticles decreased the platelet transmittance (%) and inhibited collagen induced platelet aggregations.

The effect of CS-PLGA nanoparticles (No.25) (1 μg/ml) on collagen (2 μg/ml) induced platelet aggregation is also shown in Figure 9.9.

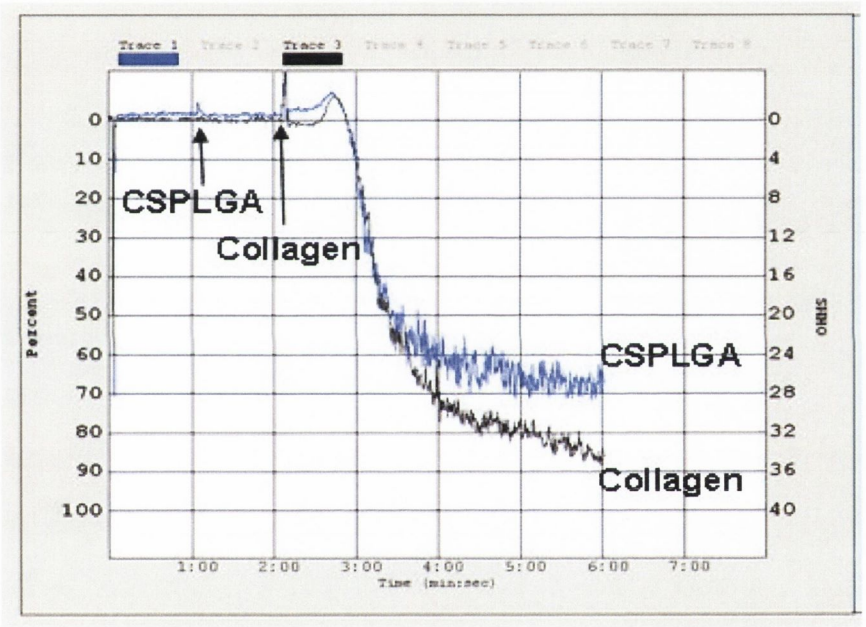


Figure 9.9 The effect of CS-PLGA nanoparticles (No.25) on collagen induced platelet aggregation at the concentration of 1 μg/ml. Collagen was 2 μg /ml.

The presence of CS-PLGA nanoparticles also decreased the platelet transmittance (%) and inhibited collagen (2 μg/ml) induced platelet aggregations. Other sample concentrations, from 0.01 to 100 μg/ml were also tested and the inhibition results are shown in Figure 9.10 (n=3). At a concentration of 100 μg/ml, PLGA and CS-PLGA nanoparticles inhibit collagen (2 μg/ml) induced platelet aggregation of

21.3 ± 3.3 % and 16.7 ± 4.1 % inhibition (mean ± SD, n=3), respectively.

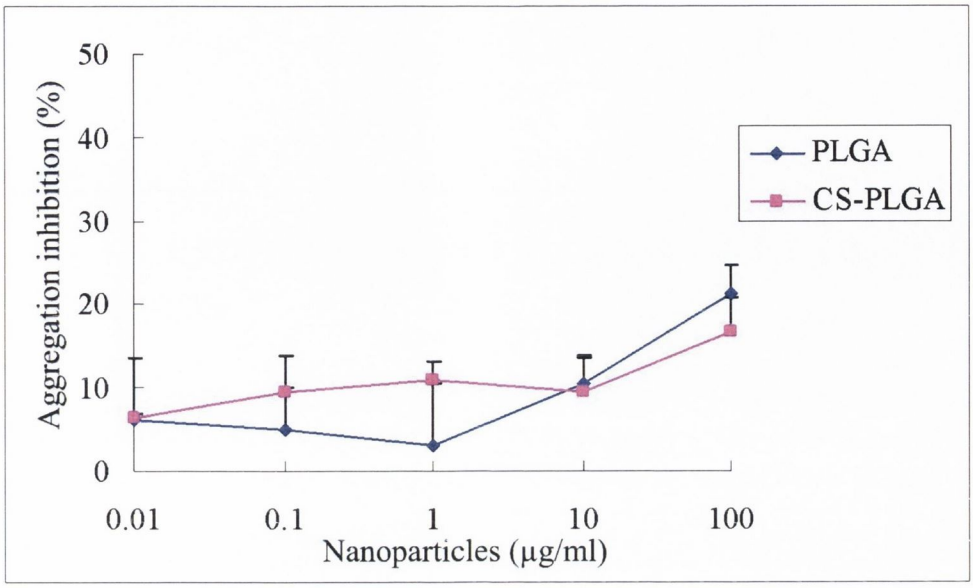


Figure 9.10 Inhibition effects of PLGA (No.16) and CS-PLGA (No.25) nanoparticles on collagen induced platelet aggregation.

Figure 9.10 indicates that when the particle concentration increased, the inhibition effects of both of the nanoparticles increased. There was no significant difference between the inhibition effects of PLGA and CS-PLGA nanoparticles in the concentration range studied (0.01 μg/ml - 100 μg/ml). The mechanism of inhibition of platelet aggregation by PLGA is not entirely known.

In terms of pharmaceutical excipients, other particles could also inhibit platelet aggregation. Cetyl alcohol/polysorbate nanoparticle is one of the few types of nanoparticles which can inhibit platelet aggregation in a dose-dependent manner. As reported by Koziara et al., (2005), cetyl alcohol/polysorbate nanoparticles with a mean size of 67.0±17.5 nm were used to study their compatibility with blood. Human α-thrombin (THR) was used as aggregation agent at concentration of 0.1 U/ml. As a result, at the particle concentration of 5 μg /ml, 10% of the inhibition effect on THR induced platelet aggregation was detected and when the

concentration was increased to 75 μg /ml, the inhibition effect was increased to 40%. The mechanism of the action of the cetyl alcohol/polysorbate nanoparticles is not known (Koziara et al., 2005).

## 9.3.2 Chitosan nanoparticles

Chitosan nanoparticles CS-F NP (No.33), CL113 NP (34), CL213 NP (35) and G213 NP (36) were used to study their effects on collagen (2 μg/ml) induced platelet aggregation. Different concentrations of samples from 0.01-100 μg/ml were measured and the results are shown in Figure 9.11. Nanoparticles were preincubated with human platelet for 1 min before the addition of collagen.

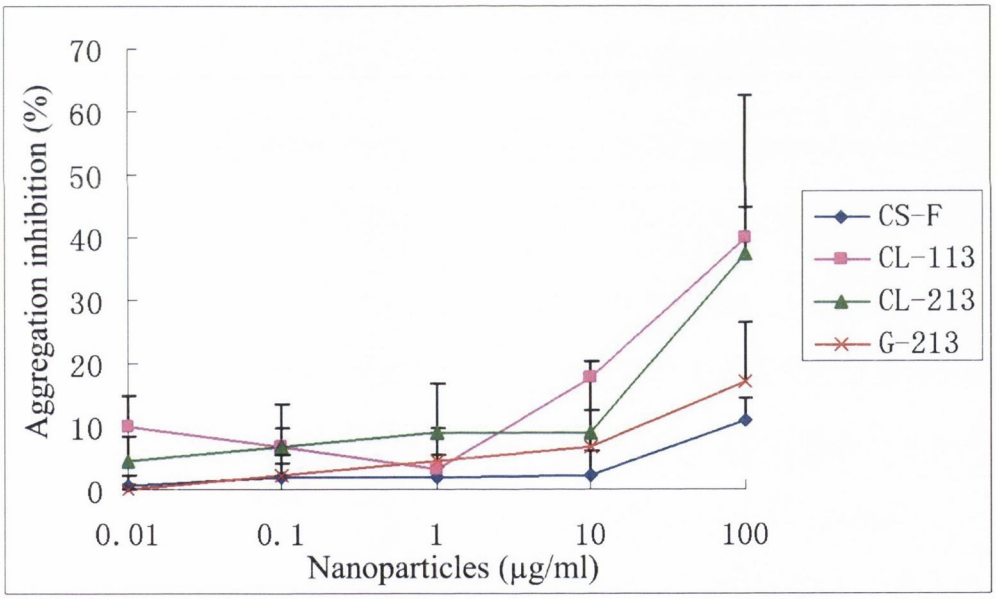


Figure 9.11 Effects of chitosan nanoparticles on collagen (2 μg/ml) induced platelet aggregation (n=4).

Figure 9.11 indicates that when the concentration of the chitosan particles increased, the inhibition effects increased. There were no significant differences between the inhibition effects of chitosan (Fluka), chitosan CL113, CL213 and G213

nanoparticles when the nanoparticle concentrations ranged from 0.01 μg/ml to 100 μg/ml. At the concentration of 100 μg/ml, chitosan nanoparticles inhibit collagen (2 μg/ml) induced platelet aggregation of 10.9 ± 3.6 %, 40.0 ± 5.0 %, 37.4 ± 25.2 % and 17.1 ± 9.4 % inhibition (mean ± SD, n=3), respectively.

### 9.3.3 PLGA nanoparticles loaded with indomethacin and ketoprofen

Petrusewicz and the co-workers (1995) tested the *in vitro* and *in vivo* antiplatelet activity of ketoprofen on human blood platelets. Concentrations of the agents were determined as such that caused 25% and 50% inhibition of aggregation of human blood platelets induced by fixed concentrations of collagen (10 μg /ml). At the dose of 7.20 $\times 10^{-7}$ mol/dm$^3$ (0.18 μg/ml) and 5.30 $\times 10^{-6}$ mol/dm$^3$ (1.35 μg/ml), ketoprofen inhibited collagen (10 μg/ml) induced platelet aggregation by 25% and 50%, respectively. In another work by Leach and Thorburn (1982), indomethacin proved to be a potent inhibitor of human platelet aggregation. Over the range of 0.43 μM to 0.43 mM, indomethacin presented a dose-dependent inhibitory effect on collagen (5 μg/ml) induced human platelet aggregation. This inhibition was 10% at 43 μM (0.154 μg /ml) and reached a complete inhibition at 0.43 mM (154 μg /ml) of indomethacin.

The effects of indomethacin PLGA nanoparticles (indomethacin loading: 6.52%) (No.23) and ketoprofen PLGA nanoparticles (No.24) (ketoprofen loading: 4.02%) on collagen (2 μg/ml) induced platelet aggregation were tested and the concentration (1-50 μg /ml) related inhibition (%) is shown in Figure 9.12.

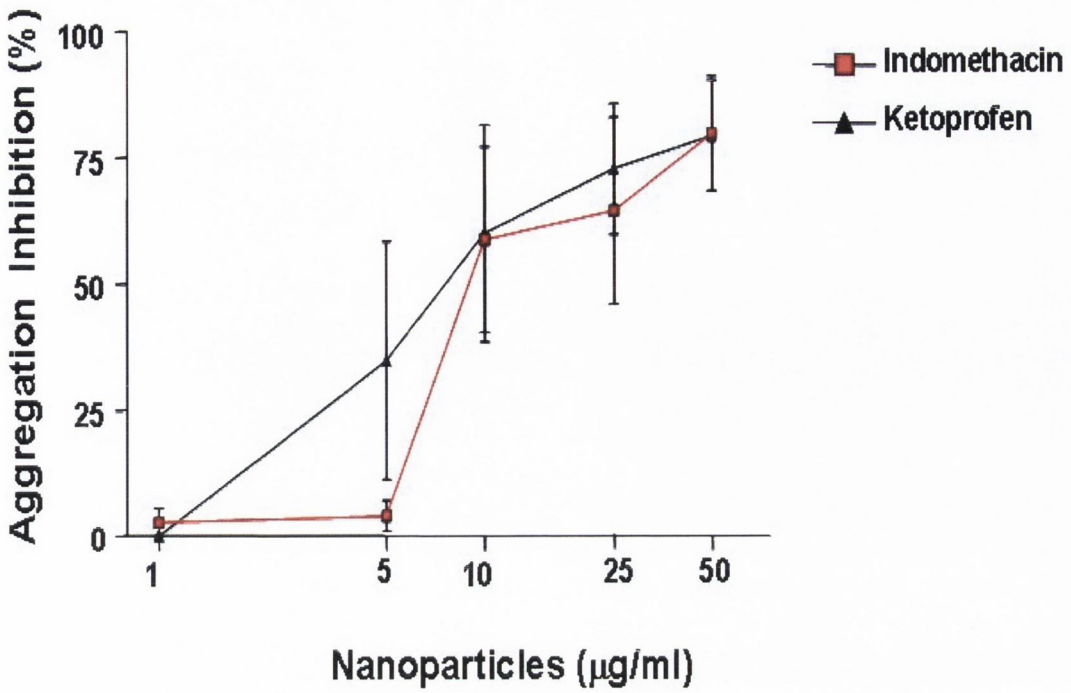


Figure 9.12 Inhibition effects of ketoprofen PLGA nanoparticles (No.23) and indomethacin PLGA nanoparticles (No.24) on collagen (2 μg/ml) induced human platelet aggregations (n=4).

Figure 9.12 indicated that with increasing concentrations, the inhibitory effects of ketoprofen PLGA nanoparticles on collagen induced human platelet aggregations were increased. At the concentration of 50 μg/ml, the inhibitory effect was 77 %. For concentrations of 1 μg/ml to 5 μg/ml, the inhibitory effects of indomethacin PLGA nanoparticles remained relatively constant, and when the concentration was higher than 5 μg/ml, the inhibitory effects were increased with increasing particle concentrations. In this study, there was no significant difference of the inhibitory effect between these two batches of nanoparticles.

In the work reported by Leach and Thorburn (1982), 0.065 μg/ml of pure indomethacin did not present inhibitory effect on collagen induced platelet aggregation, while in the current work, 0.065 μg/ml of encapsulated indomethacin presented an inhibitory effect of 4% and 3.26 μg/ml of pure indomethacin presented

62.5% of inhibitory effect (Leach and Thorburn 1982), while in the current work, 3.26 μg/ml of encapsulated drug presented the inhibitory effect of 77%. Encapsulated indomethacin presented a relatively higher inhibitory effect than pure drug. The inhibitory effects of pure and encapsulated indomethacin are listed in Table 9.1. The inhibition values were estimated from the published figures reported by Leach and Thorburn (1982).

Table 9.1 Inhibitory effects% of pure and encapsulated indomethacin.

| Drug dose (μg/ml) | Effect of pure drug %* | Effect of drug encapsulated % |
|---|---|---|
| 0.0652 | 0 | 4 |
| 3.26 | 62.5 | 77 |

* values were estimated from the work reported by Leach and Thorburn 1982

In the work reported by Petrusewicz et al., (1995), 0.2 μg/ml of pure ketoprofen did not present inhibitory effect on collagen induced platelet aggregation, while in the current work, 0.2 μg/ml of encapsulated ketoprofen presented the effect of 35% and 2 μg/ml of pure ketoprofen presented 30% of the inhibitory effect on collagen induced platelet aggregation, while in the current work, 2 μg/ml of encapsulated ketoprofen presented the effect of 77%. Encapsulated ketoprofen presented higher inhibitory effect in comparison to pure drug. The inhibitory effects of pure and encapsulated ketoprofen are listed in Table 9.2. The inhibition values were estimated from the published figures reported by Petrusewicz et al., (1995).

Table 9.2 Inhibitory effects% of pure and encapsulated ketoprofen.

| Drug dose (μg/ml) | Effect of pure drug%* | Effect of drug encapsulated% |
|---|---|---|
| 0.2 | 0 | 35 |
| 2 | 30 | 77 |

* values were estimated from the work reported by Petrusewicz et al., (1995)

The higher inhibitory effects of encapsulated drugs than pure drugs may be attributed to the presence of PLGA nanoparticles in which drugs were encapsulated. As discussed in section 9.2.1 and 9.3.1, drug free PLGA nanoparticles do not induce platelet aggregation and presented a weak inhibition effects on collagen induced platelet aggregation.

## 9.4 Conclusions

Drug free PLGA nanoparticles (No.16) and CS-PLGA nanoparticles (No.25), together with chitosan nanoparticles of CS-F NP (No.33), CL113 NP (No.34), CL213 NP (No.35) and G213 NP (No.36), did not induce platelet aggregation at the concentrations studied (1 to 500 μg /ml).

The inhibitory effects of the various types of nanoparticles on the collagen induced platelet aggregation were also studied. When the concentrations were increased from 0.01 μg/ml to 100 μg/ml, the inhibitory effects of particles (PLGA, CS-PLGA and chitosan nanoparticles) on collagen (2 μg/ml) induced platelet aggregation tended to increase. At the concentration of 100 μg/ml, PLGA and CS-PLGA nanoparticles inhibit collagen induced aggregation of 21.3 ± 3.3 % and 16.7 ± 4.1 % (mean ± SD, n=3), respectively. Chitosan nanoparticles also inhibit collagen induced platelet aggregation, inhibiting aggregation by around 40%. When the concentration increased from 0.01 μg/ml to 100 μg/ml, the inhibitory effects of both indomethacin and ketoprofen loaded PLGA nanoparticles tended to increase. At a concentration of 50 μg/ml, both particles gave inhibition effects of approximately 77%. Encapsulated drugs resulted in the higher inhibitory effects on platelet aggregation than pure drugs, which may be attributed to the presence of PLGA nanoparticles as a drug carrier.

# RESULTS AND DISCUSSION

## Chapter 10 Effects of chitosan nanoparticles on cells as adjuvant in vaccine study

# 10.1 Introduction

In the work reported by Ozasa and Lavelle, (2007, School of Biochemistry and Immunology, Trinity College), ultrapure chitosan solutions (CL113, CL213, G113, G213) were studied to determine if chitosan has the ability of activating bone marrow derived myeloid dendritic cells (DCs) and to explore the relationship between chitosan composition and efficacy.

## 10.1.1 Chitosan solutions induced DC maturation

In the work reported by Ozasa and Lavelle (2007), all soluble chitosans, CL113, CL213, G113 and G213 induced expression of CD40, CD80 and CD86 but to a lesser extent that of MHC class II on DCs from Balb/c mice. CD 80, 86, 40 are protein cluster of differentiation 80, 86 and 40. MHC class II is the major histocompatibility complex class II molecules. Though inducing of CD40 expression was not significantly different between each soluble form, CD80 expressions were effectively enhanced more by chloride forms (CL113 and CL213) compared with glutamate forms (G113 and G213), implying that CD80 expression is chitosan structure dependent while CD40 expression is not.

The chitosan effect on DC maturation was also studied on DCs from C3H/HeN and C3H/HeJ mice to determine if the effect was induced by LPS (lipopolysaccharide) contamination. LPS is known as an endotoxin. C3/HeN is LPS sensitive strain of mice while C3H/HeJ mice is an LPS resistant mice. The results of surface expression analysis on DCs from Balb/c, C3H/HeJ and C3H/HeN mice suggest that the ability of chitosan to induce DC maturation via upregulating surface markers including MHC class II, CD80 and CD86 was not caused by LPS contamination (Ozasa and Lavelle, 2007).

### 10.1.2 Inducing of IL-6 production by chitosan

The efficacy of chitosan solution on cytokine production by DCs was demonstrated by Ozasa and Lavelle (2007). It was found that all the chitosan solutions induced IL-6 production by DCs at the concentrations from 0.5 μg /ml to 10 μg /ml. The induction effects were not dose-dependent (Ozasa and Lavelle, 2007). IL-6 is a proinflammatory cytokine and plays important roles in innate immune response such as regulation of temperature and gene expression for cytokine generation (Janeway, 2005).

### 10.1.3 Application of toll like receptions (TLRs)

In the work reported by Ozasa and Lavelle (2007), IL-1ß production was significantly enhanced by LPS, Poly I:C or Pam3Csk induced DCs treated with CL213. LPS, Poly I:C and Pam3Csk are three different TLRs. All the soluble chitosan forms at concentrations greater than 2 μg /ml enhanced significantly the level of IL-1B induction by LPS-induced DCs from Balb/c mice. CL213 at concentration of 0.1 μg /ml in the presence of LPS induced a significant level of IL-1B by DCs where those of other soluble forms of chitosan did not. Similar production results of IL-1B, IL-6 and IL-12p40 induced by solution CL213 treated DCs from both C3H/HeJ and C3H/HeN mice in the presence of Pam3Csk, suggested that the effects were free of LPS contamination. No effects on IL-10 and IL-12p70 were detected.

Effects of chitosan solution CL113 on different types of cells such as T-cells by using spleen cells from Balb/c, C3H/HeJ and C3H/HeN mice were investigated. As a result of IL-1ß production, it was found that the higher the soluble CL113

concentration, the greater the enhancement of LPS-induced IL-1B. In contrast, IL-6 and IL-10 production was inhibited by higher concentrations of soluble chitosan. No IFN-γ production was detected by cells treated with chitosan solution CL113.

PMA, a powerful T cell stimulator, was used to detect effect of chitosan (CL213) on spleen cells. IL-4 and IFN-γ productions were significantly enhanced by spleen cells from both C3H/HeJ and C3H/HeN mice treated with chitosan solution CL213.

### 10.1.4 Toxicity to DCs and spleen cells

The cytotoxicity of chitosan solution CL213 on DCs and spleen cells from Balb/c mice was determined (Ozasa and Lavelle, 2007). Cells were removed and stained with Propidium Iodide (PI) to analyse cytotoxicity levels by flow cytometry and, as a result, chitosan can be toxic to both DCs and spleen cells. Cell population shifted as chitosan concentration increased. The cell population on control and DCs treated with chitosan at concentration 1.25 μg /ml appear similarly while shift of cell population presented when chitosan concentration was increased to 2.5 μg/ml, 5 μg/ml and 10 μg/ml respectively, indicating cell death.

### 10.1.5 Chitosan nanoparticles

Although chitosan solutions have been tested on immune cells, there are not many efficacy investigations of chitosan nanoparticles on immune cells, especially DCs. The toxicities of chitosan particles on DCs and spleen cells are also in need of evaluation.

Yuki and Lavelle examined the effect of nanoparticles (CL113 NP, CL213 NP, CL113.2 NP, CL213.2 NP, G213 NP, CL213-CC-NP) prepared in the current work

(No. 34-38, 49). Objectives of these studies were to determine if chitosan nanoparticles have the ability of activating bone marrow derived myeloid dendritic cells (DCs) and the comparative effectiveness of different chitosan nanoparticles. The effects of chitosan nanoparticles on enhancement of cytokine production were measured and compared with and without TLR agonist such as LPS or poly I:C. Endotoxin free chitosan nanoparticles were manufactured and their effect on inducing DCs maturation and cytokine production by DCs and spleen cells were measured and compared with chitosan solutions. Finally, cytotoxicity of chitosan nanoparticles on DCs and spleen cells were investigated and compared to chitosan solution.

## 10.2 Effects of chitosan nanoparticles on DCs

### 10.2.1 Enhancement of IL-1ß production by DCs

To investigate the effect of various chitosan nanoparticles on IL-1ß production by DCs, DCs (6.25 $\times 10^5$ cells/ml) from Balb/c mice were incubated for 24 hours with chitosan samples. Chitosan nanoparticles CL113-NP (No.34), CL113.2-NP (No.37), CL213-NP (No.35), CL213.2-NP (No.38), G213-NP (No.36) at concentrations of 1 or 10 μg/ml, alone or in combination with LPS (5000 pg/ml) or Poly I:C (100 μg/ml) were used as samples and the IL-1ß production was assayed by ELISA. Figure 10.1 compares the results obtained from nanoparticles (CL113 NP, CL213 NP, CL113.2 NP, CL213.2 NP, G213 NP) to those obtained for the corresponding solutions (CL113, CL213, G113 and G213). Control is cells treated with chitosan alone. The results of cytokine assay are the mean cytokine concentration of triplicate assays.

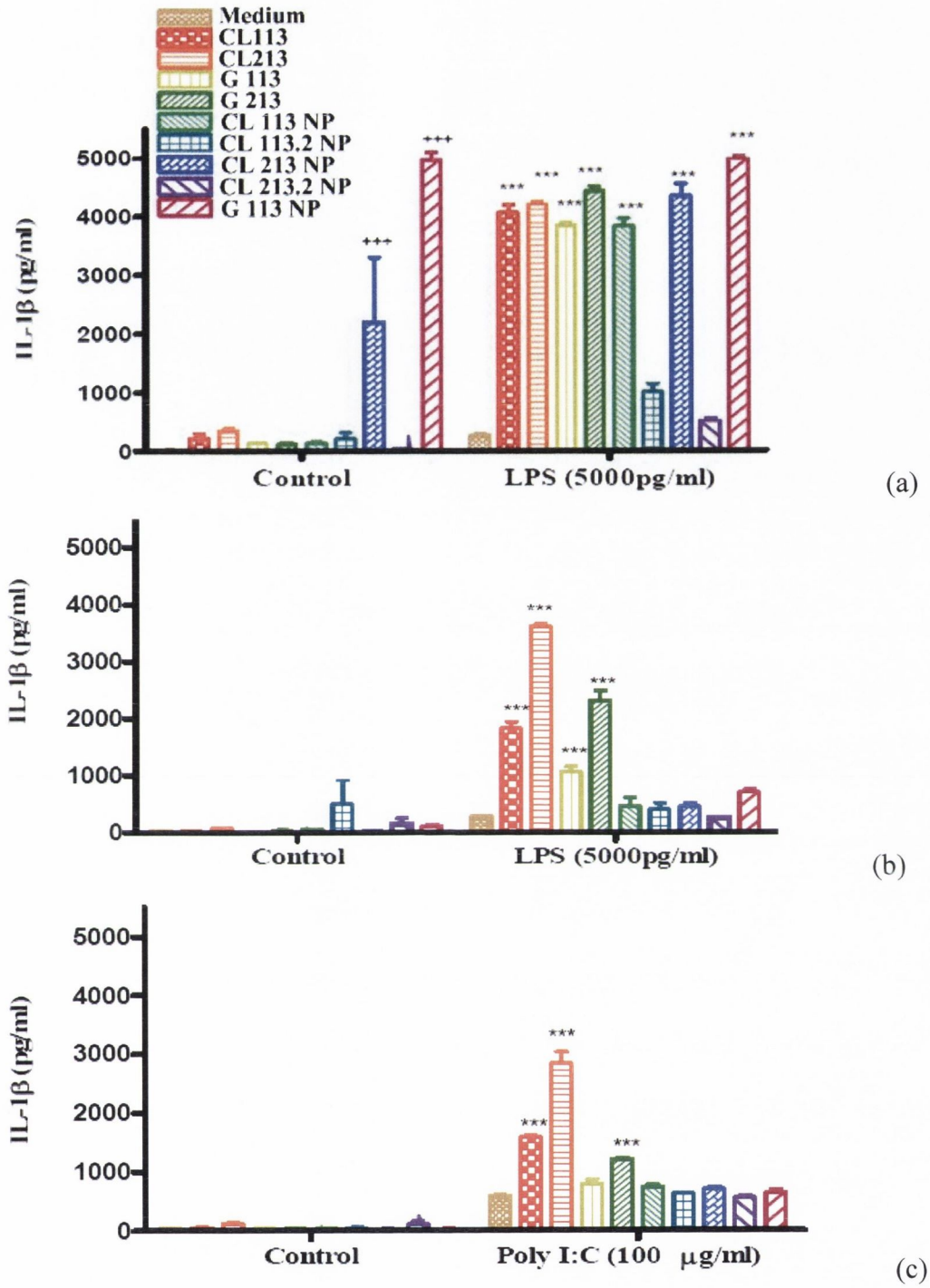


Figure 10.1 Chitosan enhanced IL-1ß production in the presence of LPS or Poly I: C.

a) 10 µg/ml of each chitosan treatment one hour prior to LPS (5000 pg/ml) stimulation,

b) 1 µg/ml of each chitosan treatment one hour prior to LPS (5000 pg/ml) stimulation,

c) 1 μg/ml of each chitosan treatment one hour prior to Poly I:C (100 μg/m) stimulation.

**, $p<0.01$; ***, $p<0.001$ vs. medium of LPS

Most chitosan nanoparticles alone do not induce IL-1ß production except for the CL213-NP and G213-NP particles shown in Figure 10.1a. IL-1ß production was enhanced by DCs treated with chitosan compositions, CL113-NP, CL213-NP and G213-NP nanoparticles at concentration 10 μg /ml in the presence of LPS (Figure 10.1 a). When the particle concentrations decreased to 1 μg /ml, there was no significant difference between IL-1ß levels induced by chitosan nanoparticles in the presence of LPS and Poly I:C, respectively (Figure 10.1b,c).

The solution of chitosan CL213 induced the highest levels of IL-1ß production in the presence of LPS and Poly I:C compared to other chitosan solutions at both concentrations. Also, it can be seen that the higher molecular weight soluble forms of CL213 and G213 enhanced more IL-1ß production than the smaller molecular weight forms CL113 and G113 at both concentrations (Figure 10.1a,b,c). This data shows that there is a relationship between the chitosan composition and IL-1ß production by DCs. The reason is not entirely known yet.

The solutions of chitosan at low concentrations (1 μg /ml) induced relatively higher IL-1ß productions than those induced by nanoparticles in the presence of LPS and Poly I:C (Figure 10.1b,c). At high concentrations (10 μg /ml), the IL-1ß productions induced by solutions and particles were similar in the presence of LPS, except for nanoparticles CL113.2 NP and CL213.2 NP (Figure 10.1a). It was concluded that both of CL113.2 NP and CL213.2 NP nanoparticles contain more residual contents (mostly sulphate anion) than CL113 NP and CL213 NP respectively. The residual content details of chitosan nanoparticles are discussed in Chapter 7.

## 10.2.2 Enhancement of IL-12p40 and IL-12p70 production by DCs

The effects of chitosan nanoparticles on IL-12 productions were examined. DC ($6.25 \times 10^5$ cells/ml) from Balb/c mice were treated with nanoparticles at different chitosan concentrations (1 or 10 μg/ml) alone or in combination with LPS. After 24 hours of incubation, supernatants were removed and assayed by ELISA. Particle examined were chitosan nanoparticles CL113-NP (No. 34), CL113.2-NP (No.37), CL213-NP (No.35), CL213.2-NP (No.38), G213-NP (No.36). The results are shown in Figure 10.2. Control is cells treated with chitosan alone. The results of cytokine assay are the mean cytokine concentrations of triplicate assays.

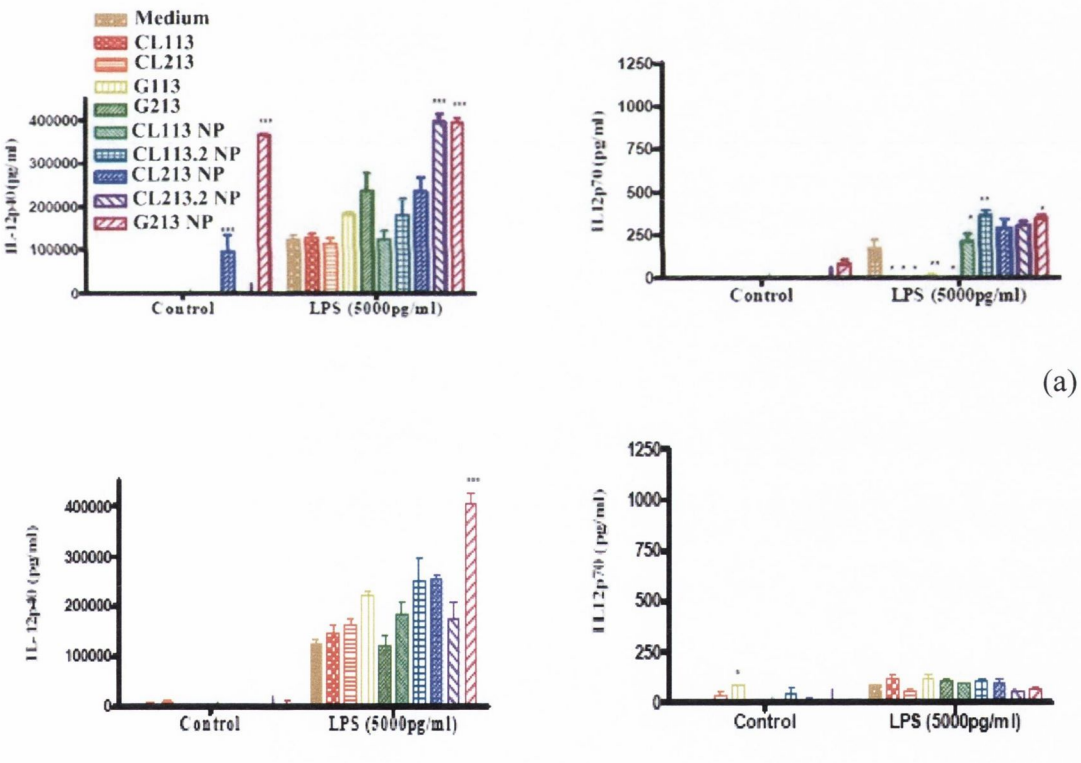


(a)

(b)

Figure 10.2 The enhancement of IL-12p40 and IL-12p70 production by DCs

(a) 10 μg /ml of each chitosan in the presence of LPS (5000 pg/ml),

(b) 1 μg /ml of each chitosan in the presence of LPS (5000 pg/ml).

**, $p<0.01$; ***, $p<0.001$ vs. medium of LPS

Figure 10.2 indicates that chitosan nanoparticles alone didn't induce IL-12p40 productions except for CL213 and G213 nanoparticles at the concentration of 10 μg/ml (Figure 10.2a). In the presence of LPS all chitosan nanoparticles, including CL113-NP (No. 34), CL113.2-NP (No.37), CL213-NP (No.35), CL213.2-NP (No.38) and G213-NP (No.36) induced IL-12p40 productions at both concentrations. Their effects were relatively higher than the effects induced by chitosan solutions (Figure 10.2). Production of IL-12p70 was also induced by chitosan nanoparticles in the presence of LPS. At high concentrations (10 μg /ml), IL-12p70 productions induced by chitosan nanoparticles were higher than the productions induced by chitosan solution. At low concentration (1 μg /ml), the effects were relatively similar.

The effect of particulate chitosan on IL-12p40 and IL-12p70 inductions suggested that these chitosan formulations could be contaminated because it has been reported that endotoxin and other bacterial components are the substances that can trigger IL-12, TNF-α and/or IFN-γ production (Shibata et al., 1997). For this reason, the LPS levels in chitosan nanoparticles were measured and the technique of preparation of nanoparticles was modified to eliminate the likelihood of sample contamination with LPS.

## 10.3 Endotoxin-free chitosan nanoparticles

Endotoxins are found in the outer membrane of Gram-negative bacteria and are members of a class of phospholipids called lipopolysaccharides (LPS). LPS are known to induce a variety of cells to produce cytokines and chemokines, which in turn affect DC movement and maturation. A common pathogenic effect of LPS *in vivo* is fever, but exaggerated responses to LPS may lead to the life-threatening

condition known as endotoxic shock (Luderitz et al., 1982). At present, nanoscience focuses mainly on the research for new materials and techniques, while safety and bimolecular aspects are often postponed to future studies. As a result, contaminants, such as LPS, may lead to erroneous conclusions that cause developers to abandon what might be a promising material.

In order to detect endotoxin containment, PyroGene recombinant factor C assay kit (Cambrex) was employed. The samples were diluted 1:10 and assayed in duplicate. Table 10.1 shows the levels of endotoxin in chitosan particles. LPS concentrations of

1 ng/ml are known to be sufficient to stimulate DCs maturation (Napolitani et al., 2005). The results suggest that the LPS concentrations found in CL113.2-NP, CL213-NP and G213-NP were sufficient to induce maturation of DCs.

Table 10.1 LPS concentrations in chitosan nanoparticles.

| Name of NP | LPS level (pg/ml) (sample diluted to 1:10) |
|---|---|
| CL113-NP | 13.5 ± 4.95 |
| CL113.2-NP | 553 ± 38.2 |
| CL213-NP | 2014 ± 29.0 |
| CL213.2-NP | 10.5 ± 12 |
| G213-NP | 2014 ± 29.0 |

(Samples represent the mean of three determinations ± standard deviation)

Since LPS are naturally present everywhere in our surroundings and can therefore be introduced to the system through the water used as the solvent, chemicals, raw materials or equipment used in the preparation of the nanoparticles (Vallhov et al., 2006), efficient removal of LPS is difficult to achieve. In addition, LPS are thermostable and fairly insensitive to pH changes. Applying high temperatures, such

as 250 °C for 45 min or high concentrations of acids and bases would, according to the Food and Drug Administration (FDA, www.fda.gov), be an efficient method to remove LPS, but such treatment may also affect the properties of nanoparticles, such as aggregation (Vallhov et al., 2006). An alternative way to remove LPS is by running the samples through polymyxin B columns. However, this may lead to the loss of nanoparticles, especially if the LPS bind to the surface of the particles.

Studies were undertaken to optimise the entire production process of nanoparticles to minimise contamination by LPS. In the first place, both the surroundings and the glassware were cleaned with detergent (PyroCLEAN) before being used in the synthesis experiments, and then the synthesis of the nanoparticles was carried out in fume hoods and distilled water was replaced with ultrapure water. The chitosan used was CL213. The resultant chitosan nanoparticles were named with CL213-CC-NP with number of No.49 and used for further bio-interaction study. CC presents Clean Control. The particle size of CL213-CC-NP and morphology were similar to CL213 NPs (No.35). The LPS concentration was smaller than 1 ng/ml.

## 10.4 Effects of endotoxin free chitosan nanoparticles on DCs and spleen cells

### 10.4.1 DC maturation induced by chitosan

To examine the effect of chitosan nanoparticles on surface marker expression on immature DCs, flow cytometry analysis was used to test the effects of CL213-CC-NP particles on DCs from C3H/HeN and LPS-resistant C3H/HeJ mice. DCs ($1\times10^6$ cells/ml) from C3H/HeN mice were incubated over night with CL213 solution (10 μg/ml) or CL213-CC-NP (10 μg/ml). The cells were washed and stained with antibodies specific for CD40, CD80, CD60 and MHC class II.

Comparison of expression of DC surface cell markers between treated (black line) and untreated (grey histograms) DCs are shown in Figure 10.3.

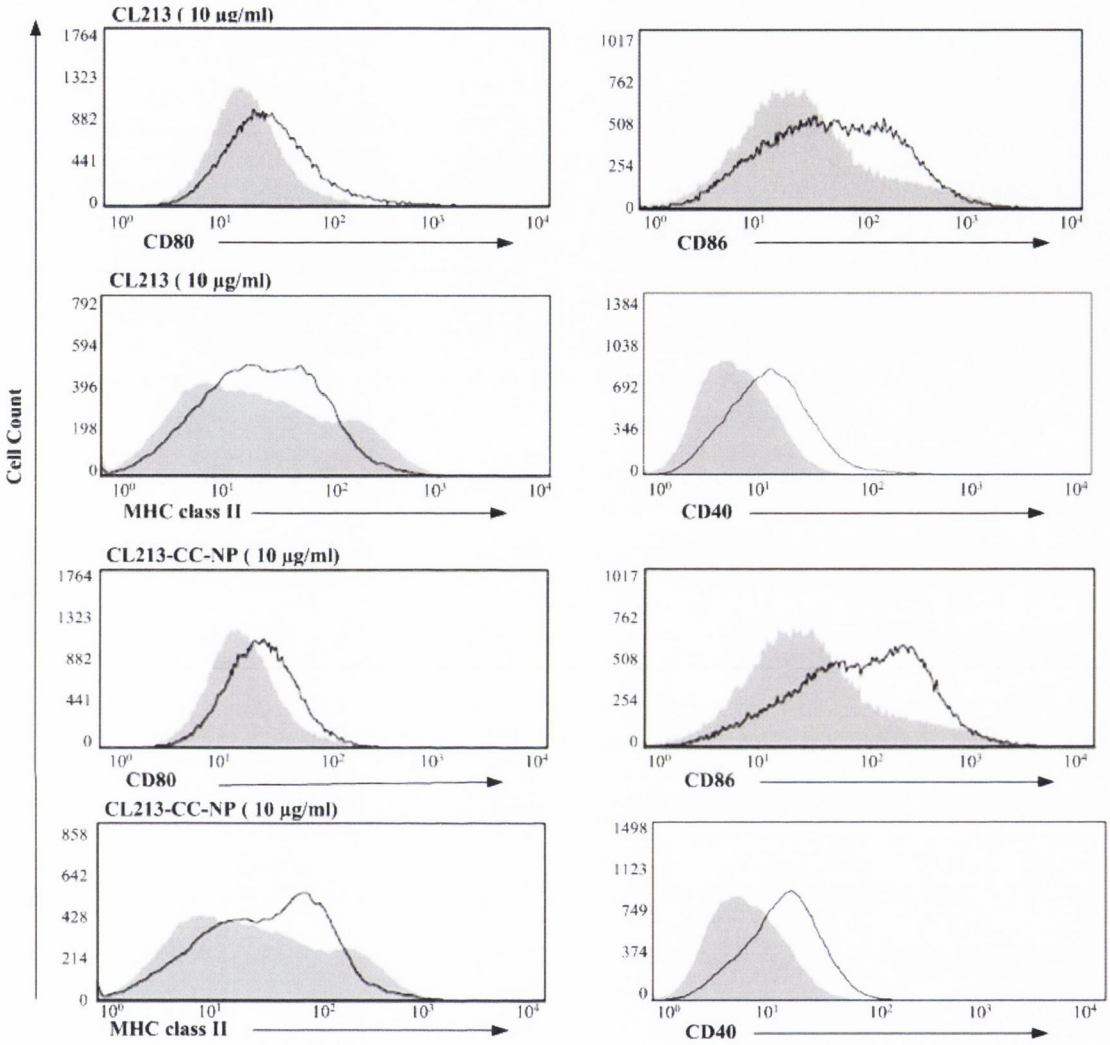


Figure 10.3 Expressions of CD86, CD80, CD40 and MHC class II on DCs ($1 \times 10^6$ cells/ml from C3H/HeN mice) treated with CL213 solution and CL213-CC-NP nanoparticles at concentration of 10 µg/ml.

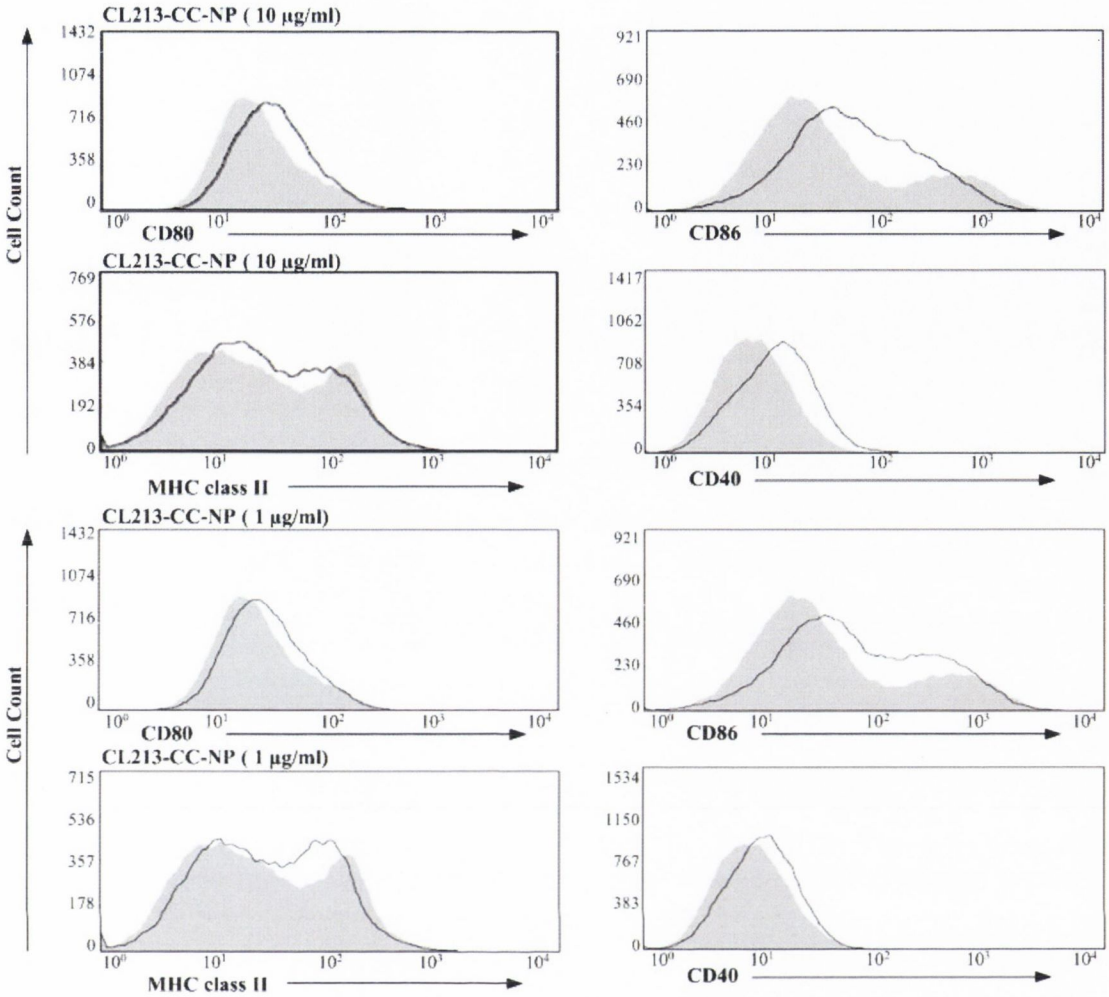


Figure 10.4 Expressions of CD86, CD80, CD40 and MHC class II on DCs ($1 \times 10^6$ cells/ml from C3H/HeJ mice) treated with CL213-CC-NP nanoparticles at concentrations of 1 and 10 μg/ml.

Figure 10.3 indicates that CL213-CC-NP enhanced CD40 and CD86 and to a lesser extent CD 80 and MHC class II when DCs were extracted from C3H/HeN mice. DCs from C3H/HeJ mice were incubated with chitosan particles CL213-CC-NP and the expressions of CD40, CD80, CD86 and MHC class I are shown in Figure 10.4. No obvious differences are observed in cell markers between the nanoparticle-treated (10 μg/ml) DCs from C3H/HeN and C3H/HeJ mice, suggesting that the induction of DC maturation by chitosan particles is not due to the contamination of the samples with LPS (Figure 10.3 and 10.4). Another

concentration of the CL213-CC-NP nanoparticles at 1 μg/ml was used on DCs from C3H/HeJ mice to determine if concentrations have any effect on the expression of cell markers. No significant relationship between the particle concentration and enhancement of surface marker expression was detected (Figure 10.4). Overall, the CL213-CC-NP nanoparticles enhanced the expression of CD40, CD86 on DCs demonstrating that chitosan particles induced maturation of DCs. In the work reported by Ozasa and Lavelle (2007), chitosan solution CL213 also induced DC maturation.

## 10.4.2 Enhancement of IL-1β production by DCs with different TLR agonists

Engagement of TLR agonist facilitates the induction of DC responses and adaptive immunity (Pulendran, 2004; Pulendran and Ahmed, 2006). LPS have been used as TLR agonist to analyse the chitosan effects on IL-1β productions (Figure 10.1). In the current work, other TLR agonists, such as CpG, Poly I:C, Pam3Csk and R879 were used to determine their facilitating effects to chitosan samples on the enhancement of IL-1β production. DCs ($1 \times 10^6$ cells/ml) from Balb/c mice were treated with a solution of CL213 (5 μg/ml) or CL213-CC-NP nanoparticles (5 μg/ml) one hour prior to the addition of Toll agonists: LPS (500 pg/ml), CpG (10 μg/ml), Poly I:C (10 μg/ml), Pam3Csk (10 ng/ml) and R879 (25 μg/ml). After incubation for 24 hours, supernatants were removed and assayed for IL-1β production by ELISA. The results are shown in Figure 10.5. Control is Toll agonist alone. The results are the mean concentration of triplicate assays.

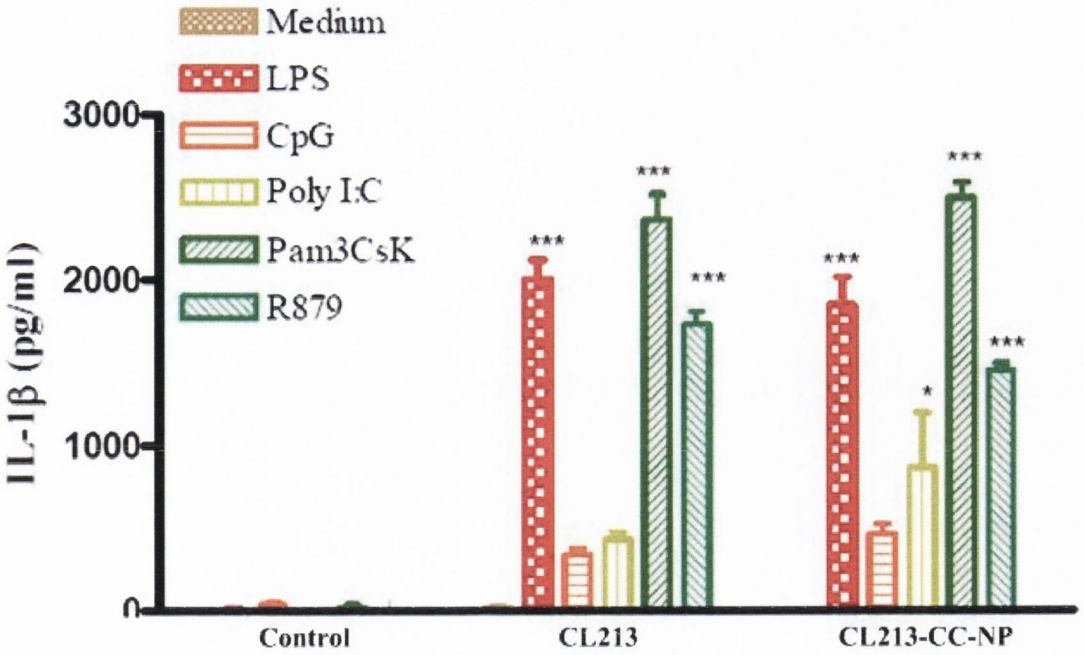


Figure 10.5 Enhancements of IL-1β production in DCs treated with LPS, Pam3Csk, R879, CpG and Poly I:C.

**, $p<0.01$; ***, $p<0.001$ vs. medium of LPS

Significant levels ($p<0.001$) of IL-1β productions were induced by the particle-treated DCs in the presence of LPS, Pam3Csk or R879 in contrast to CpG and Poly I:C (Figure 10.5). Of all the Toll agonists tested, Pam3Csk was shown to be the most effective for synergising with chitosan particles to enhance IL-1β. Since Pam3Csk also facilitated chitosan solution to enhance IL-1β production, Pam3Csk was shown to be the most effective for synergising with both solution and particle forms of chitosan in the enhancement of IL-1β production. IL-1β production is significantly enhanced by DCs treated with CL213-CC-NP in the presence of LPS, Pam3Csk and R879 but not by CpG or Poly I:C.

## 10.4.3 Enhancement of IL-1β production by DCs at different concentrations

As Pam3Csk was shown to be the best for synergising with both chitosan solution and particle to induce IL-1β production (Chapter 10.4.2), it was employed as a Toll agonist in this study. DCs (6.25 $\times 10^5$ cells/ml) from C3H/HeJ mice were incubated with various concentrations of CL213-CC-NP (0.08-10 μg/ml) and stimulated with Pam3Csk (10 ng/ml) for 24 hours. Following incubation supernatants were taken and assayed for IL-1β production by ELISA. The results are shown in Figure 10.6. Control is cells treated with chitosan particles only. The results are the mean concentration of triplicate assays.

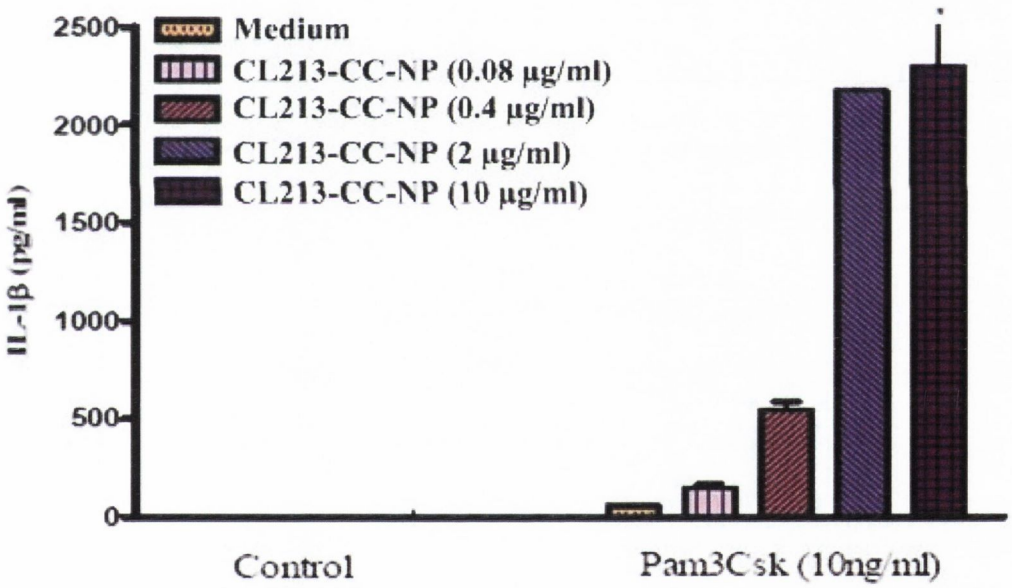


Figure 10.6 Enhancements of IL-1β production in DCs at different concentrations treated with Pam3Csk.

**, $p<0.01$; ***, $p<0.001$ vs. medium of LPS

CL213-CC-NP treated DCs enhanced IL-1β production in the presence of Pam3Csk. Higher levels of IL-1β were induced with higher concentrations of CL213-CC-NP particles (Figure 10.6), indicating a relatively concentration-dependently effects of

chitosan nanoparticles on IL-1β productions in the presence of Pam3Csk. In the work reported by Ozasa and Lavelle (2007), chitosan solution CL213 also induced IL-1β productions in a manner of relatively concentration-dependent.

## 10.4.4 Enhancement of IL-6 and IL-10 production by DCs

The effects of chitosan nanoparticles CL213-CC-NP on other cytokines like IL-6 and IL-10 were assayed. DCs (6.25 $\times 10^6$ cells/ml) from C3H/HeJ were treated with solution of CL213 or CL213-CC-NP and Pam3Csk (1 ng/ml) at different concentrations (0.4 μg/ml, 2 μg/ml and 10 μg/ml). After 24 hours of incubation, supernatants were assayed for production of IL-6 and IL-10 by ELISA. The results are shown in Figure 10.7. Control is cells treated with chitosan particles only. The results are the mean concentration of triplicate assays.

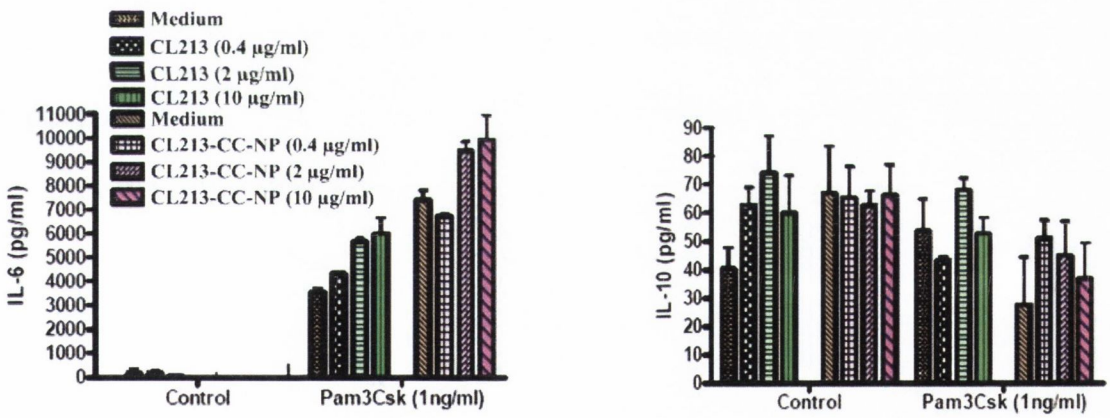


Figure 10.7 Enhancements of IL-6 and IL-10 productions in DCs at different concentrations treated with Pam3Csk.

**, $p<0.01$; ***, $p<0.001$ vs. medium of LPS

Both, the solution CL213 and CL213-CC-NP, enhanced IL-6 productions in a manner of relatively concentration-dependent. Low effects on IL-10 were detected. There were no significant differences in IL-6 productions between solution CL213

and CL213-CC-NP, indicating that both CL213 solution and particle have inducible effects on IL-6 (Figure 10.7).

### 10.4.5 Enhancement of IL-4 and IFN-γ production by spleen cells

The effect of chitosan on spleen cells was investigated by using PMA (phorbol myristate acetate). PMA is a powerful T cell activator and in the current study is used to help the detection of chitosan effects on activated T cells and the possible effects on adaptive immune responses. Spleen cells (6.25 $\times 10^5$ cells/ml) from C3H/HeJ mice were incubated for 1 hour with CL213-CC-NP particles at different concentrations (0.2 μg/ml, 1 μg/ml and 5 μg/ml). After thirty minutes PMA (0.2 ng/ml, 2 ng/ml and 20 ng/ml) was added. After incubation for 24 hours, supernatant were assayed by ELISA. The results are shown in Figure 10.8. Control is cells treated with chitosan particles only. The results are the mean concentration of triplicate assays.

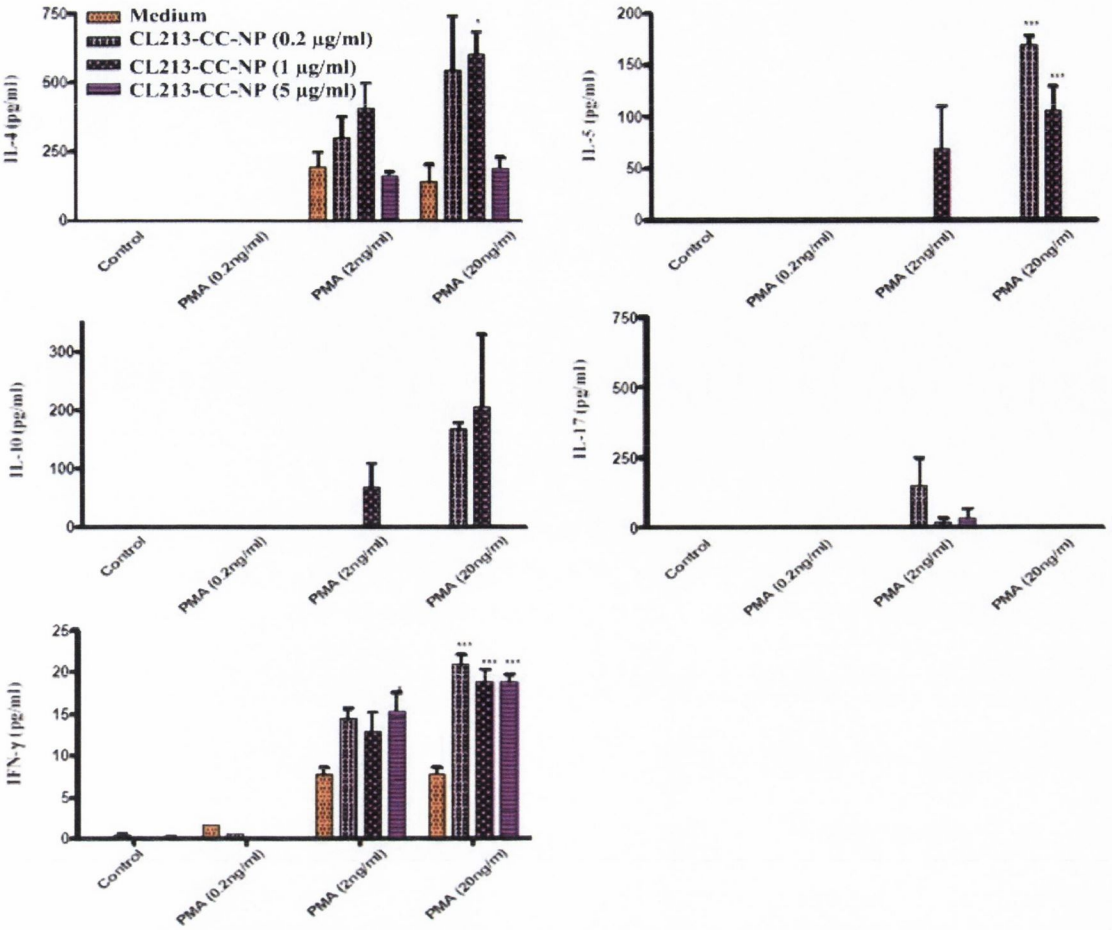


Figure 10.8 Enhancements of IL-4, IL-10, IFN-γ and IL-5 productions in spleen cells at different concentrations.
**, $p<0.01$; ***, $p<0.001$ vs. medium of LPS

Figure 10.8 indicates that the CL2213-CC-NP particles at three concentrations induced IL-4 and IFN-γ productions by spleen cells when PMA was higher than 2 ng/ml. IL-4 production was inhibited at a higher concentration of 5 μg/ml of CL2213-CC-NP indicating that lower concentrations (0.2 μg/ml, 1 μg/ml) of particles are sufficient to induce IL-4 production in the presence of PMA (Figure 10.8). Since solution CL213 can induce IL-4 and IFN-γ production as well (Ozasa and Lavelle, 2007), both solution CL213 and particles have inducible effects on spleen cells to induce IL-4 and IFN-γ production. Although not consistent over the range of concentrations tested, IL-5 and IL-10 productions were induced by chitosan particles CL213-CC-NP at concentrations of 0.2 μg/ml and 1 μg/ml by PMA (2 ng/ml, 20 ng/ml) stimulated spleen cells from C3H/HeJ mice (Figure 10.8).

## 10.4.6 Toxicity of chitosan particles to DCs and spleen cells

In order to determine the cytotoxicity of chitosan particles CL213-CC-NP on DC, DCs (1 $\times 10^6$ cells/ml) from Balb/c mice were incubated with a range of concentrations of solution CL213 and particles of CL213-CC-NP (1.25 μg/ml, 2.5 μg/ml, 5 μg/ml and 10 μg/ml) over night. After washings, cells were stained with PI and assayed by flow cytometry. The Side Scatter (SS) to Forward Scatter (FS) plots are shown in Figure 10.9. In Figure 10.9, the control was unstimulated DCs.

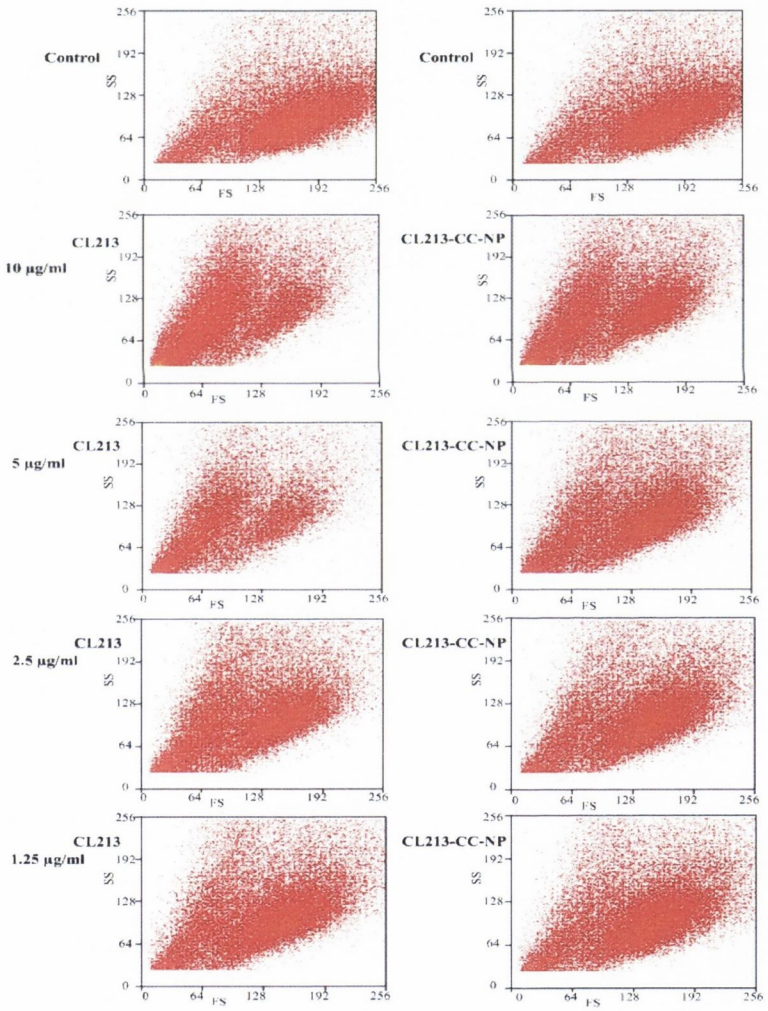


Figure 10.9 Flow cytometry results for CL213 solution and CL213-CC-NP nanoparticle treated DCs at different concentrations.

Figure 10.9 indicates shifts in the cell population as chitosan concentration increases. The cell population in the control is similar to that of the CL213-CC-NP at concentration of 1.25 μg/ml. When the concentration increased to 10 μg/ml, there was a shift of cell population towards to the upper Side Scatter (SS) (Figure 10.9), indicating the death of cells with organelles. Chitosan solution CL213 presented similar results (Figure 10.9). The percentage level of the chitosan toxicity compared to the control is shown in Figure 10.10.

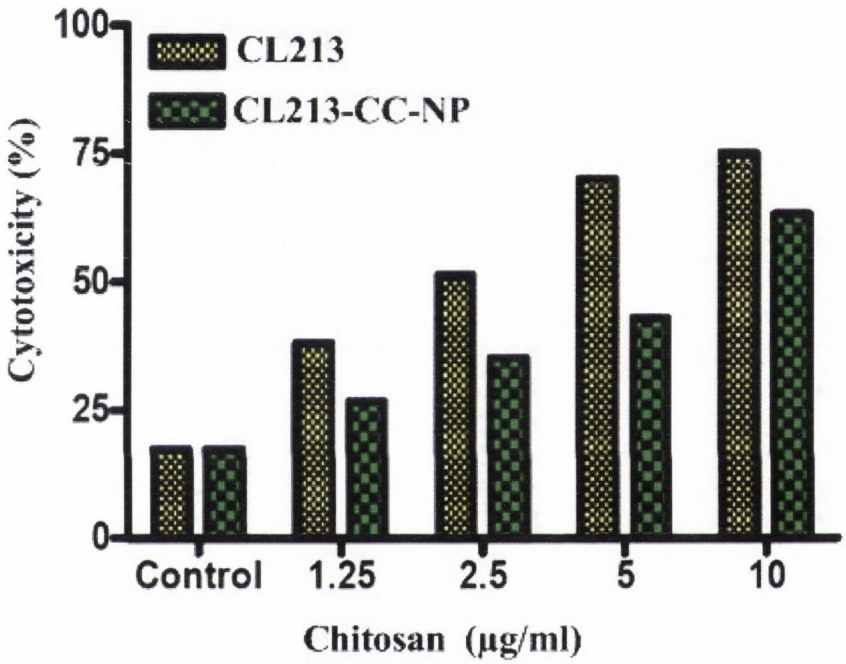


Figure 10.10 Cytotoxicity of chitosan solution CL213 and CL213-CC-NP nanoparticles to DCs from Balb/c mice at different concentrations.

From Figure 10.10 it can be seen that the solution of CL213 is relatively more toxic to DCs than the particulate CL213-CC-NP at the four concentrations. Even at the concentration as low as 1.25 μg/ml, chitosan solution CL213 and particle CL213-CC-NP are toxic to DCs.

Cytotoxicity levels of the CL213 solution and CL213-CC-NP to spleen cells at different concentrations (0.0399-10 μg/ml) are shown in Figure 10.11.

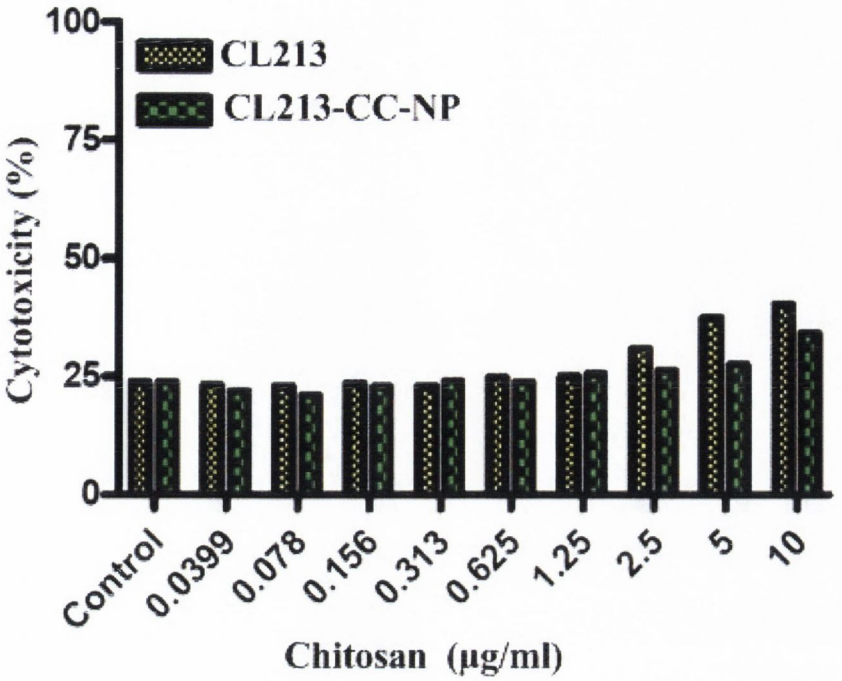


Figure 10.11 Cytotoxicity of chitosan solution CL213 and particulate CL213-CC-NP to spleen cells from Balb/c mice at different concentrations.

At the concentrations lower than 1.25 μg/ml, the nanoparticles presented similar cytotoxicity levels compared to those of chitosan solution CL213. At higher concentrations like 2.5 μg/ml, 5 μg/ml and 10 μg/ml, the cytotoxicity levels of particulate CL213-CC-NP are relatively lower than those of the solution. Compared to the cytotoxicity levels induced to DCs from Balb/c mice, chitosan forms are not as toxic to spleen cells as to DCs. Chitosan solution of CL213 induced relatively more cytotoxicity levels than CL213-CC-NP to both DCs and spleen cells. It may be caused by the fact that chitosan solution (CL213) contains more hydrochloric salt than chitosan nanoparticles (CL213-CC-NP). According to the data supplied by the manufacturer, pure chitosan CL213 used in this study contain 10-20% hydrochloric acid, while the amount of hydrochloric acid in CL213-CC-NP was around 2.0 %, measured by ninhydrin assay.

## 10.5 Conclusions

Preliminary results of the effect of particulate chitosans CL113 NP, CL213 NP and G213 NP on IL-12p40 and IL-12p70 inductions suggested that these chitosan formulations could be contaminated with LPS. LPS levels were measured and production process was successfully optimised to minimise the contamination by LPS.

Chitosan nanoparticles CL213-CC-NP were able to mature DCs by upregulating CD40 and CD60 and to a lesser degree of CD80 and MHC II. IL-1β productions were induced by those nanoparticles in the presence of LPS, Pam3Csk or R879 as Toll agonists. Pam3Csk is the most effective agonist for synergising with chitosan particles to enhance IL-1β production. The inducing effects of IL-1β production by CL213-CC-NP is in a manner of relatively concentration-dependent. CL213-CC-NP can also induce IL-6 and IL-10 productions in DCs at different concentrations when treated with Pam3Csk. When spleen cells were used, particulate CL213-CC-NP can induce IL-4 and IFN-γ productions at different concentrations in the presence of PMA. Chitosan particles are toxic to DCs at a concentration of 1.25 μg/ml and higher concentrations. Compared to the solution of CL213, the solution induced relatively high levels of cytotoxicities to DCs from Balb/c mice. Chitosan forms (solution and nanoparticles) are not as toxic to spleen cells as to DCs. At concentrations higher than 2.5 μg/ml, the solution of chitosan induced relatively more cytotoxicity levels than the nanoparticles to spleen cells from Balb/c mice.

# Chapter 11 General discussion

# 11.1 Introduction

Colloidal drug carriers such as micro and nanoparticles have been studied and used to improve the therapeutic efficacy of drugs, as well as the elimination of the discomfort associated with multiple dosing/injection (Schwarz et al., 1995). Since the performance of particulate drug delivery systems depends on their physical properties such as size, drug loading, and also depends on their nanotoxiology and biointeractions with immune system, micro and nanoparticles (PLGA, CS-PLGA, CS-PVA, CS, HA, HA-CS) formulated in the current study were studied with respect to their physical properties, interactions with platelet aggregations and biointeractions with dendrite cells in the immune system.

# 11.2 Physical properties of micro and nano particles

## 11.2.1 Particle sizes produced using different techniques

The size of particulate drug carriers is always an important property when evaluating cell uptake and phagocytosis in human circulation. In the study reported by Jani et al. (1990), the uptake of polystyrene nanoparticles in organs such as liver, spleen, blood, bone marrow and kidneys were evaluated after oral administration to rats. The size of nanoparticles ranged from 50 nm to 3000 nm and the tissues were assayed by GPC. As a result, 6-7 % of the 50 nm particles accumulated totally in the liver, spleen, blood, bone marrow and kidneys with a blood uptake level of 2.2%. With the increase of particle sizes, the uptake (%) decreased. When particle size was increased to 1000 nm, the cumulative uptake in organs was decreased to 0.8 % and levels in blood were not detectable. When the particle size was increased to 3000 nm, the cumulatively uptake to organs decreased to 0%. Pratten and Lloyd (1986) found that the rate of clearance of 1100 nm particles by cultured rat peritoneal

macrophages to be 10-times greater than for 100 nm particles at similar concentration. The data indicated that there is a size of particle that is too large for uptake by pinocytosis but too small to initiate phagocytosis (Florence, 1997).

PLGA microparticles were prepared by double emulsion technique. When sonication time and power was increased, the median size of PLGA particles loaded with H S A decreased and the size ranges became more uniform. The best PLGA microparticles with high H S A loading and small size span were prepared with ethyl acetate as solvent in contrast to DCM-based particles. The median size of those microparticles was 1.74 μm. H S A loaded PLGA nanoparticles with a median size of 0.52 μm were prepared by double emulsion technique by increasing sonication time and power. Other PLGA nanoparticles loaded with indomethacin and ketoprofen were prepared by single emulsion technique since the drugs are soluble in ethyl acetate. CS-PLGA nanoparticles with chitosan content of 1.77% w/w were prepared by double emulsion technique. The presence of chitosan did not significantly affect the physical properties like size and morphology of the CS-PLGA nanoparticles compared to PLGA nanoparticles. The higher zeta potential of CS-PLGA nanoparticles compared to PLGA nanoparticles indicated the presence of positively charged chitosan. When the content of chitosan increased, the size of the resultant particles increased, which may due to the increasing interactions between chitosan and emulsifying agent PVA. Overall, PLGA micro and nano particles can be prepared by the emulsion technique. The particle size can be controlled by changing the sonication conditions and excipient content.

CS-PVA nanoparticles were initially prepared by the emulsion technique. Chitosan has been shown to be capable of attaching to PVA in solution (Koyano et al., 2000). When ethyl acetate was evaporated, the complex of CS-PVA was formulated and collected by centrifugation.

Chitosan microparticles were prepared by spray drying with and without a crosslinking agent, glutaraldehyde. The median size of the particles ranged from 3 μm to 5 μm. There was no visible change in the morphology of the spray dried chitosan microparticles due to the chemical crosslinking. Chitosan nanoparticles were prepared by precipitation/coacervation method. The median sizes ranged from 0.43 μm to 0.58 μm. There was no visible difference in the morphology of the chitosan nanoparticles made from chitosan chloride and chitosan glutamate. All the particles presented irregular particulate shapes in the nano size range. Overall, spray drying can be used to prepare chitosan microparticles and precipitation/coacervation method can be used to prepared chitosan nanoparticles. Spray drying has been used to produce powders in pharmaceutical and food industry for more than 50 years. It can transfer sample from a solution/slurry to the dried particulate form in a one step process, which makes the industrial manufacturing easier. Precipitation/coacervation is a method that has been used in a lab scale so far. The high sonication power and long sonication time required in this method could make the industial production of particles very expensive and costly.

Hyaluronic acid microparticles were manufactured by spray drying and a median size of the product was 2.69 μm. HA-CS nanoparticles were firstly prepared by precipitation/coacervation with a z-average size of 198 nm. Complex of HA and CS were formed because of their different charges in solutions and sodium sulphate was included as a desolvating reagent to facilitate the phase separation. There was no visible difference in the morphology of HA-CS nanoparticles made from the different salts of chitosan, chloride and glutamate. All the nanoparticles presented similar chitosan content around 45 % (w/w).

Polymer PLGA is polyester which is biocompatible and degradable. It has been widely used in studies as a drug delivery carrier for more than 20 years. Since PLGA is hydrophobic to water, chemical solvents had to be involved in the

preparation of PLGA particles and the elimination of the solvent remains to be a problem. Chitosan is a linear polysaccharide and positively charged at pH of 6.5. It is biocompatible and degradable. Chitosan is soluble in water under the presence of inorganic or organic acids and it is bioadhesive and readily binds to negatively charged surfaces such as mucosal membranes. Hyaluronic acid is a linear polymer of disaccharides and it is a polyanion. It is biocompatible, biodegradable and viscoelastic. It is found in synovial fluid and extracellular matrix in human body, with the highest concentration in soft connective tissues, such as skin and cartilage. Both chitosan and hyaluronic acid are promising polymers used in drug delivery study.

### 11.2.2 Drug releases from different particulate formulations

Drug release is an important property of drug carriers. The controlled release has been considered to increase the immunogenicity of antigens and to reduce the number of immunizations required to induce high titer of immunoglobulin responses (Eldridge et al., 1991).

The releases of H S A from PLGA microparticles prepared with different solvents (ethyl acetate and dichloromethane) were compared. Regardless of the solvent used, *in vitro* release studies showed a burst release, followed by a slower, sustained and degradation controlled release of H S A. Under similar protein loadings and sizes, OVA or OVA-coupled F/G peptide were encapsulated into PLGA microparticles. The release profiles between H S A, OVA and OVA peptide were compared to see the effects of protein molecular weight on release. The resultant releases indicated that the higher the molecular weight of the protein the shorter the time used to reach the highest release rate ($T_{MAX}$). Microspheres encapsulating larger proteins allow initial release of large protein, which would lead to a quicker penetration of the particles by water, causing the formation of interconnecting channels or the release

of protein in pre-existing channels within the particles (Hernadez et al., 1998; Duggirala et al., 1996; Sandor et al., 2001).

The releases of OVA from PLGA nanoparticles with different OVA loadings were compared. All the drug release profiles showed an initial fast release phase followed by a sustained, polymer degradation controlled release phase. When the drug loading increased, the burst release fraction ($F_B$) increased and the time used to reach the highest release rate ($T_{MAX}$) decreased. The increase in $F_B$ indicated an increased initial burst release with increasing loadings. It is attributed to the high concentration of drug dispersed in particles which effectively increased the proportion of drug linked to the particle surface, which is consistent with the model proposed by Gallagher and Corrigan (2000). The reason that particles with higher protein loadings required smaller time to reach the highest release rate ($T_{MAX}$) is ascribed to the accelerated degradation of the polymer and increased polymer permeability in the presence of drug which is also consistent with the model proposed by Gallagher and Corrigan (2000). In the work previously reported by Dunne (2000), weight loss studies were carried out to see the influence of fluphenazine on the weight loss of PLGA microparticles when incubated in PBS buffer. Compared to the drug free PLGA microparticles, the weight loss of PLGA from drug loaded microparticles was considerably faster than the loss from drug free microparticles of similar particle sizes. It indicated that the load of drug fluphenazine on PLGA microparticles accelerated the degradation of the polymer particles (Dunne, 2000).

OVA releases from PLGA particles of different sizes were compared to see the effects of the particle size on the protein release. PLGA nanoparticles with smaller particle size presented a long $T_{MAX}$ time, compared to microparticles with larger sizes. Degradation products formed within small particles can diffuse easily to the surface while degradation products from larger particles have a long path to the

surface of particle. Since this long path could facilitate the autocatalytic degradation of the remaining polymer material, microparticles with large particle sizes demonstrated faster drug release from polymers than small particles (Dunne et al., 2000). In the work previously reported by Dunne (2000), weight loss from drug free PLGA microparticles with different sizes were studied in PBS buffer (pH 7.4) at 37 °C. As a result, some loss in weight ($\leq$ 7%) was observed for all particles during the first 24 hours. This was attributed to the dissolution of low molecular weight oligomers produced during the manufacturing process from the particle surface (Dunne, 2000). This was followed by a period of negligible weight loss after which weight loss increased dramatically (Dunne, 2000). The weight loss showed an induction period because the polymer initially underwent chain scission that did not create low molecular weight polymer chains capable of being solubilised and the polymer must have underwent extensive degradation until that the water soluble monomers and oligomers were produced (Dunne 2000). With increasing particle sizes, the weight loss rate k was increasing with decreased time to reach the maximum weight loss rate ($T_{max}$). The degradation (weight loss) results may help to explain that with increasing particle sizes, the release rate of OVA increased, with a decrease in time to the maximum release rate ($T_{MAX}$).

The release profiles of indomethacin and ketoprofen from PLGA nanoparticles were compared. Ketoprofen indicated a higher burst release compared to indomethacin. The solubility of the drug encapsulated has a positive effect on the burst release constant $K_B$. Since ketoprofen has a higher aqueous solubility (Levis, 2003) than indomethacin, ketoprofen presented a higher burst release. There were no significant differences in OVA releases from CS-PLGA and PLGA nanoparticles with similar particle sizes and loadings. Coumarin-6 release from PLGA nanoparticles encapsulated with H S A was studied. At the first day, coumarin-6 showed a very low burst release, which may be attributed to the low coumarin loading on PLGA nanoparticles.

OVA was adsorbed onto chitosan nanoparticles and presented a quick and complete release within 25 minutes. There were no significant differences between the release profiles from chloride and glutamate chitosan nanoparticles.

Comparing the OVA release from PLGA nanoparticles and chitosan nanoparticles, OVA presented much slower release profiles from the former particles. This may be due to the fact that OVA was encapsulated in PLGA particles and the complete release depended on the degradation of the polymer. Evaluating the OVA release from PLGA nanoparticles with different loadings, the fraction of the initial burst release increased when the drug loading also increased. The time to reach the highest release rate tended to decrease with increasing drug loading, while the rate constant (k) remained relatively constant. The presence of small molecular weight drugs (indomethacin and ketoprofen) and proteins (H S A and OVA) accelerated the degradation of the polymer. Indomethacin and ketoprofen presented much quicker release compared to proteins. This may due to their acidic properties which could accelerate polymer degradation and known to be acid catalysed (Huffman and Casey, 1985; Siepmann et al., 2005). Contrasting the OVA release from PLGA nanoparticles with different particle sizes, the release rate from smaller particles was decreased and the time to maximum release rate was increased.

## 11.3 Effects of nanoparticles on platelet aggregation

The delivery of antigens using nanoparticles results in the possibility of the interaction of nanoparticles with blood and its elements, therefore, the potential of nanoparticles formulated in the current study to induce platelet aggregation and precipitate thrombosis were investigated.

It was found that the drug free PLGA and CS-PLGA nanoparticles, together with chitosan nanoparticles (CS-F NP, CL113 NP, CL213 NP and G213 NP), did not induce platelet aggregations at the concentrations ranging from 1 to 500 μg/ml. Chitosan has haemostatic properties. In the current study, the inhibition effects of chitosan nanoparticles may due to the presence of sulphate anion in the particles. The mechanism of inhibition of platelet aggregation by PLGA nanoparticles is not entirely known.

PLGA and CS-PLGA nanoparticles presented inhibitory effects on collagen (2 μg/ml) induced human platelet aggregation at the concentrations of 0.01-100 μg/ml. When the concentration increased, the inhibitory effects of both of the particles on collagen induced platelet aggregation tended to increase. At a concentration of 100 μg/ml, both PLGA and CS-PLGA nanoparticles inhibited around 20 % of the platelet aggregation induced by collagen. No significant difference was shown between the effects of both PLGA nanoparticles on inhibitory effects. A range of chitosan nanoparticles also inhibited collagen induced platelet aggregation with the percentage inhibition being no more than 40% for concentrations up to 100 μg/ml. There were no significant differences between these chitosan inhibitory effects on platelet aggregation. Overall, PLGA, CS-PLGA and chitosan nanoparticles did not aggregate platelets, but acted as weak inhibitors of collagen induced aggregation *in vitro*. As previously reported (Radomski et al., 2005), some carbon nanoparticles have the ability to activate platelets aggregation and enhance vascular thrombosis. PLGA, CS-PLGA and a range of chitosan nanoparticles may have better safety profile than carbon nanoparticles.

## 11.4 Immune effects of chitosan nanoparticles on dendritic cells (DCs)

The effect of particulate chitosans CL113 NP, CL213 NP and G213 NP on the induction of IL-12p40 and IL-12p70 suggested that these initial chitosan formulations used in the studies could be contaminated. Therefore, LPS levels in the powders were measured and production process was optimised to minimise LPS contamination.

A clean batch of nanoparticulates was prepared - CL213-CC-NP. The particles were able to mature DCs by upregulating CD40 and CD60 and to a lesser degree, MHC II and CD80, suggesting that chitosan provides two signals which are required to stimulate T cells. In addition, it was demonstrated that chitosan synergies with LPS and Pam3Csk in facilitating IL-1β production by DCs. CL213-CC-NP can also induce IL-6 and IL-10 productions in DCs at different concentrations treated with Pam3Csk. Examination of CL213-CC-NP efficacy with spleen cells was investigated. Certainly chitosan efficacy on both IL-4 and IFN-γ production by spleen cells was revealed, indicating chitosan's potent property in cell-mediated immune response. Chitosan (chloride and glutamate) is not as toxic to spleen cells as to DCs. Solution of chitosan chloride CL213 appears to be more toxic than particulate CL213-CC-NP. Compare to chitosan solution, chitosan nanoparticles are neither superior nor inferior to soluble forms in antigen presentation.

In the future work, because of the biodegradability, biocompatibility and viscoelastic properties of hyaluronic acid (Zhong et al., 1994; Prestwitch et al., 1998; Brown and Jones 2004; Hahn et al., 2004), it is of interest to extend investigations on the immune response of HA nanoparticles by DCs and spleen cells to see their potential as drug adjuvant in vaccine study, as well as their effects on human platelet aggregation.

# REFERENCES

Abhay S.P., (1998) 'Hemostatic wound dressing' United States Patent No. 5836970, 1998

Acuto O., and Michel F., (2003) 'CD28-mediated co-stimulation: a quantitative support for TCR signalling' *National Review of Immunology* 3(12): 939-951

Aiba S., (1992) 'Molecular structures and properties of partially N-acetylated chitosans' in: C.J. Brine, P.A. Stanford, J.P. Zikakis (Eds), *Advances in Chitin and Chitosan*, Elsevier, London: 137-144

Anderson, J.M., Shive, M.S., (1997) 'Biodegradation and biocompatibility of PLA and PLGA microspheres' *Advanced Drug Delivery Reviews* 28:5-24

Arshady R., (1991) 'Preparation of biodegradable microspheres and microcapsules: 2. Polylactides and related polyesters' *Journal of Controlled Release* 17:1-22

Audibert F.M., and Lise L.D., (1993) 'Adjuvants: current status, clinical perspectives and future prospects' *Immunology Today* 14(6): 281-284

Baki, Emir 'Human Serum Album (HSA) absorption with Chitosan Microspheres', *Journal of Applied Polymer Science*, Vol.86, 3035-3039 (2002)

Balazs E.A., (1998) In: Laurent TC, editor. 'The chemistry, biology and medical application of hyaluronan and its derivatives' *London: Portland Press*: 185

Balazs E.A., and Leshchiner A., (1986) 'Cross-linked gels of hyaluronic acid and products containing such gels' *U.S. Patent* No. 4582865

Balazs E.A., (1983) 'Sodium hyaluronate and viscosurgery' in D.Miller and R.Stegmann (eds.), Healon (Sodium Hyaluronate). *A guide to its use in ophthalmic surgery*, Wiley, New York, 1983

Balazs E.A., and Leshchiner A., (1987) 'Chemically modified hyaluronic acid preparation and method of recovery thereof from animal tissues' *U.S. Patent* No. 4713448

Balazs E.A., and Denlinger J.L. (1993) 'Viscosupplementation: a new concept in the treatment of osteoarthritis' *Journal of rheumatology* 20: 3-9

Barichell J.M., Morishita M., Takayama K., Nagai T., (1999) 'Encapsulation of hydrophilic and lipophilic drugs in PLGA nanoparticles by the nanoprecipitation method' *Drug Development and Industrial Pharmacy* 25(4): 471-476

Batycky, R., Hanes, J., Langer, L. and Edwards, D.A. (1997) 'A theoretical model of erosion and macromolecular release from biodegrading microspheres' *Journal of Pharmaceutical Sciences* 86: 1464-1477

Benveniste E.N., and Benos D.J., (1995) 'THF-alpha- and IFN-gamma-mediated signal transduction pathways: effects on glial cell gene expression and function' *Faseb Journal* 9(15): 1577-1584

Berthold A., Cremer K., Kreuter J., (1996) 'Preparation and characterization of chitosan microspheres as drug carrier for prednisolone sodium phosphate as model for anti-inflammatory drugs' *Journal of Controlled Release* 39:17-25

Biagini G, Bertani A, Muzzarelli R, Damadei A, DiBenedetto G, Belligolli A, Riccotti G, Zucchini C, Rizzoli C., (1991) 'Wound management with N-carboxybutyl chitosan' *Biomaterials* 12:281-285

Blanco M.D., M.J. Alonso 'Development and characterization of protein-loaded poly(lactide-co-glycolide) nanospheres' *European Journal of Pharmaceutical & Biopharmaceuticals* 43 (1997) 287-294

Bloom G., Gustavson K.H., Swensson A., (1955) 'On the reaction of the thrombocytes to submicroscopic particles in vitro' *Acta Haematologica* 13: 57-63

Bomford R., (1980) 'The comparative selectivity of adjuvants for humoral and cell mediated immunity' *Clinical & Experimental Immunology* 39:435–41

Bos, R.R.M., Rozema, F.R., Boering, G., Nijenhuis, A.J., Pennings, A.J., Verwey, A.B., Boury F., Ivanova T., Panaiotov I. et al. (1995) 'Dynamic properties of poly (D,L-lactide) and polyvinyl alcohol monolayers at the air /water and dichloromethane air /water interfaces' *Journal of Colloid Interface Sciences* 169: 380–392

Bozkir A., Saka Q.M., (2004) 'Chitosan-DNA Nanoparticles: Effect on DNA Integrity, Bacterial Transformation and Transfection Efficiency' *Journal of Drug Targeting* 12, 281-288

Bozkir A., Saka O.M., (2004b) 'Chitosan nanoparticles for plasmid DNA delivery: effect of chitosan molecular structure on formulation and release characteristics' *Drug Delivery* 11: 107-112

Brewer J.M., Alexander J., (1997) 'Cytokines and the mechanisms of action of vaccine adjuvants' *Cytokines, Cellular & Molecular Therapy* 3:233–46

Broadhead J., Rouan E.S.K and Rhodes C.T., (1992) 'The spray drying of pharmaceuticals' *Drug development and industrial pharmacy* 18: 1169-1206

Brown M.B., Jones S.A., (2004) 'Hyaluronic acid: a unique topical vehicle for the localized delivery of drugs in the skin' *Journal of the European Academic Dermatology and Venereology* 19: 308-318

Chandy T., Sharma C.P., (1992) 'Prostaglandin E-immobilized poly(vinyl alcohol) blended chitosan membranes: Blood compatibility and permeability properties' *Journal of Applied Polymer Science* 44: 2145

Chemical and Technical Assessment (2004) 'Polyvinyl alcohol (PVA)' 61st Joint FAO/WHO Expert Committee on Food Addititives (JECFA)

Chen Q., Li X.L., Liu Q., Jiao Q.C., Cao W.G., (2005) 'Investigating the binding interaction of azur A with hyaluronic acid via spectrophotometry and its analytical application' *Analytical and Bioanalytical Chemistry* 382: 1513-1519

Chiou W.L. and Riegelman S. (1971) 'Pharmaceutical applications of solid dispersion systems' *Journal of Pharmaceutical Science* 60: 1281-1301

Chou T.C., Fu E., Wu C.J., Yeh J.H., (2003) 'Chitosan enhances platelet adhesion and aggregation' *Biochemical and Biophysical Research Communications* 302: 480-483

Clint J.H., (1991) 'Surfactant aggregation' published in the USA by Chapman and Hall, New York

Cohen S, Yoshida T, Lucarelli M, Hwang LH, Langer R., (1991) 'Controlled delivery system for proteins based on poly (lactic/glycolic acid) microspheres'. *Pharmaceutical Research* 8:713–720

Cohen H., Levy RJ., Gao J., Fishbein I., Kousaev V., Sosnowski S., Slomkowski S. and Golomb G., (2007) 'Sustained delivery and expression of DNA encapsulated in polymeric nanoparticles' *Gene Therapy* 7: 1896-1905

Coombes, A.G., Yeh, M-K., Lavelle, E.C. and Davis, S.S., (1998) 'The control of protein release from PLGA microparticles by variation of the external aqueous phase surfactant in the water-in oil-in water method', *Journal of Controlled Release* 52: 311-320

Corrigan D.O., PhD theses (2003) 'Preparation and characterisation of spray dried composities of pharmaceutical materials' School of Pharmacy and Pharmaceutical Sciences, Trinity College Dublin

Corrigan D.O., Healy A.M., Corrigan O.I (2005) 'Preparation and release of salbutamol from chitosan and chitosan co-spry dried compacts and multiparticulates' *European Journal of Pharmaceutics and Biopharmaceutics* 62(3): 295-395

Craig, P.H., Williams, J.A., Davis, K.W., Magoun, A.D., Levy, A.J., Bogdansky, S., and Jones, J.P., (1975) 'A biological comparison of polyglactin 910 and polyglycolic acid synthetic absorbable surures' *Surg Gynecol Obstet* 1:141

Crank J., (1975) 'The mathematics of diffusion' Clarendon Press, Oxford

Cui Fude, Cun Dongmei, Tao Anjin, Yang Mingshi, Shi Kai, Zhao Min, Guan Ying, (2005) 'Preparation and characterization of melittin-loaded poly(dl-lactic acid) or poly(dl-lactic-co-glycolic acid) microspheres made by the double emulsion method' *Journal of Controlled Release* 107: 310-319

Cullity B.D., (1978) 'Elements of X-ray diffraction' 2nd Edition, Addison-Wesley, London

Curotto, E., Aros, F., (1993) 'Quantitative determination of chitosan and the percentage of free amino groups' *Anal Biochemistry* 211: 240–241

Cutrigh, D.E., Beasley, J.D., and Perez, B., (1971) 'Histological comparison of polylactic acid and polyglycolic acid sutures' *Oral Surgery* 32:165

Davda, J., Labhasetwar, V. (2002) 'Characterization of nanoparticle uptake by endothelial cells' *International Journal of Pharmaceuticals* 233, 51–59

Desai K.G.H., Park H.J., (2005) 'Preparation of cross-linked chitosan microspheres by spray drying: effect of cross-linking agent on the properties of spray dried microspheres' *Journal of Microencapsulation* 22:377-95

Dinarello C.A., (1997) 'Interleukin-1' *Cytokine Growth Factor Reviews* 8(4) 253-265

Dineen J J., Perlillie P.E., and Finch S.C., (1968) 'Zymosan-induced thrombocytopenia in the rat' *Journal of Reticuloendothelial Society* 5:161-174

Domard A., Varum K.M., Roberts G., (1998) 'Advances in chitin science' vol II France: *Jacques Andre Press*

Donaldson K., Mills N., MacNee W., Robinson S., and Newby D., (2005) 'Role of inflammation in cardiopulmonary health effects of PM' *Toxicology and Applied*

*Pharmacology* 207(2 Suppl): 483-488

Dorati, R., Ida Genta, Luisa Montanari, Francesco Cilurzo, Armando Buttafava, Antonio Faucitano, Bice Conti, (2005) 'The effect of γ-irradiation on PLGA/PEG microspheres containing ovalbumin' *Journal of Controlled Release* 107:78-90

Dornish M., Aarnold M., Skaugrud Q., (1996) 'Alginate and chitosan: biodegradable biopolymers in drug delivery systems' *European Journal of Pharmaceutical Sciences* 4(supplement 1): S153

Duffin R., Clouter A., Brown D., Tran C.L., Stone V. and Donaldson K., (2002) 'The importance of surface area and specific reactivity in the acute pulmonary inflammatory response to particles' *Annals of Occupational Hygiene* 46(Suppl 1): 242-245

Duggirala S.S., Rodgers J.B., DeLuca P.P., (1996) 'The evaluation of lyophilized polymer matrices for administering recombinant human bone morphogenetic protein-2' *Pharmaceutical Development and Technology* 1: 165-174

Dunne M. M., Corrigan O.I. and Ramtoola Z., (2000) 'Influence of particle size and dissolution conditions on the degradation properties of polylactide-co-glycolide particles' *Biomaterials* 21: 1659-1668

Dunne Margaret Mary, PhD thesis, (2000) 'Mechanistic aspects of the degradation and drug release properties of poly-alpha-hydroxyl aliphatic ester nano- and microparticle' School of Pharmacy and Pharmaceutical Sciences, Trinity College Dublin

Earley, B., Kavanagh, O., Adair, B., (2001) 'Biodegradable microparticles as non-live viral vectors for respiratory tract vaccination' Irish agriculture and food development authority, End of project report: http://www.teagasc.ie/research/reports/

Eldridge J.H., Staas J.K., Meulbroek J.A., Tice T.R., Gilley R.M., (1991) 'Biodegradable and biocompatible PLGA microspheres as an adjuvant for staphylococcal enterotoxin B toxoid which enhances the level of toxin-neutralizing antibodies' *Infection and Immunity* 59: 2978

Feinberg R.N., and Beebe D.C., (1983) 'Hyaluronate in vasculogenesis' *Science* 220: 1177-1179

Fitzgerald J.F., PhD thesis (1994) 'Investigation of the mechanisms of drug release from poly-DL-lactide-co-glycolide systems containing basic medicaments and their

hydrochloride salts' in the School of Pharmacy, Trinity College Dublin

Fitzgerald J.F. and Corrigan O.I. (1993) 'Mechanisms governing drug release from poly-alpha-hydroxy aliphatic esters. Diltiazem base release from poly-lactide-co-glycolide delivery systems' *Polymeric Delivery Systems - Properties and Applications, ACS Symposium Series 520, American Chemical Society* 313

Fitzgerald, J.F. and Corrigan, O.I., (1996) 'Investigation of the mechanisms governing the release of levamisole from pol-lactide-co-glycolide delivery systems' *Journal of Controlled Release* 42: 125-132

Florence A.T., (1997) 'The oral absorption of micro and nanoparticles: neither exceptional nor unusual' *Pharmaceutical Research* 14: 259-266

Ford, J.L. (1986), 'The current status of solid dispersions' *Pharmaceutica Acta Helvetiae* 61: 69-88

Fraser J.R.E., Laurent T.C., Laurent U.B.G., (1997) 'Hyaluronan: its nature, distribution, functions and turnover' *Journal of International Medicine* 242:27-33

Freiberg S., Zhu x., (2004) 'Polymer microspheres for controlled drug release' *International Journal of Pharmaceutics* 282: 1-18

Fukuda K., Dan H., Takayama M., Kumano F., Saitoh M., Tanaka S., (1996) 'Hyaluronic acid increases proteoglycan synthesis in bovine articular cartilage in the presence of interleukin-1' *Journal of Pharmacology and experimental therapeutics* 277: 1672-1675

Furness G., (2003) 'Nanotechnology in drug delivery: commercial opportunities for pharma' by PJB publications Ltd, UK

Gabor F., Ertl B., Wirth M., and Mallinger R. (1999) 'Ketoprofen-poly(D,L-lactic-co-glycolic acid) microspheres: influence of manufacturing parameters and type of polymer on the release characteristics' *Journal of Microencapsulation* 16(1): 1-12

Gallagher, K.M., Corrigan, O.I., (2000) 'Mechanistic aspects of the release of levamisole hydrochloride from biodegradable polymers' *Journal of Controlled Release* 69: 261-272

Gang Ruan, Feng Si-Shen and Li Qiu-Tian, (2002) 'Effects of material hydrophobicity on physical properties of polymeric microspheres formed by double emulsion process' *Journal of Controlled Release* 84, Issue 3(5): 151-160

Gilding D.K. and Reed A.M., (1979) 'Biodegradable polymers for use in surgery-poly (glycolic)/poly (lactic acid) homo-and copolymers:1' *Polymer* 20:1459

Glenny A.T., Buttle G.A.H., and Stevens M.F., (1931) 'Rate of disappearance of diphtheria toxoid injected into rabbits and guinea pigs: toxoid precipitated with alum' *Journal of Pathology* 34: 267-275

Glynn M.F., Movat H.A., Murphy E.A., and Mustard J.F., (1965) 'Study of platelet adhesiveness and aggregation with latex particles' *Journal of laboratory and clinical medicine* 65:179-201

Goa K.L., and Benfield P., (1994) 'Hyaluronic acid: a review of its pharmacology and use as a surgical aid in ophthalmology, and its therapeutic potential in joint disease and wound healing' *Drugs* 47: 536-566

Gold E.W., (1981) 'The quantitative spectrophotometric estimation of total sulfated glycosaminoglycan levels Formation of soluble alcian blue complexes' *Biochimica et biophysica acta* 673: 408-415

Gold E.W., (1979) 'A simple spectrophotometric method for estimating glycosaminoglycan concentrations' *Analytical biochemistry* 99: 183-188

Glynn M.F., Movat H.A., Murphy E.A., and Mustard J.F., (1965) 'Study of platelet adhesiveness and aggregation with latex particles' *Journal of laboratory and clinical medicine* 65:179-201

Grette K., (1962) 'Mechanism of thrombin-catalyzed haemostatic reaction in blood' publisher: *Universitetsforlaget Oslo*

Grun J.L., Maurer P.H., (1989) 'Different T helper cell subsets elicited in mice utilising two different adjuvant vehicles: the role of endogenous IL-1 in proliferative responses' *Cell Immunology* 121:134–45

Gupta R.K., Siber G.R., (1995) 'Adjuvants for human vaccines-current status, problems and future prospects' *Vaccine* 13(14) 1263-1276

Gursoy A., Akbuga J., Eroglu L., Ulutin S., (1987) 'The inhibitory effect of liposome-encapsulated indomethacin on inflammation and platelet aggregation' *Journal of Pharmacy and Pharmacology* 40: 53-54

Hahn S.K., Kim S.J., Kim M.J. and Kim D.H., (2004) 'Characterization and in vivo study of sustained-release formulation of human growth hormone using sodium hyaluronate' *Pharmaceutical Research* 21(8): 1374-1381

Hardisty R., M., and Hatton R.A., (1966) 'Platelet aggregation and the availability of platelet factor 3' *British Journal of Haematology*12: 764-776

Hejazi R., Amiji M., (2002) 'Stomach-specific anti-H.pylori therapy. I:preparation and characterization of tetracycline-loaded chitosan microspheres' *International Journal of Pharmaceutics* 235:87-94

Hernadez R.M., Igartua M., Gascon A.R., Calvo M.B., Pedraz J.L., (1998) 'Influence of shaking and surfactants on the release of bsa from plga microspheres' *European Journal of Drug Metabolism and Pharmokinetics* 23: 92-96

Higuchi, T., (1961) 'Rate of release of medicaments from ointment bases containing drugs in suspension' *Journal of Pharmaceutical Sciences* 50:874

Hill G.C., and Holman J.S., (2000) 'Chemistry in context' 5th ed., Walton-on-Thames: Nelson

Hirai A., Odani H., Nakajima A., (1991) 'Determination of degree of deacetylation of chitosan by $^{1}$H NMR spectroscopy' *Polymer Bulletin* 26: 87-94

Hirosue S., Muller B.G., Mulligan R.C., and Langer R. (2001) 'Plasmid DNA encapsulation and release from solvent diffusion nanospheres' *Journal of Controlled Release* 70: 231-242

Hodgson J.T. and Jones R.D., (1985) 'A mortality study of carbon black workers employed at five United Kingdom factories between 1947 and 1980' *Arch Environ Health* 40(5):261–268

Hodgson I., and Wakeman R.J., (2005) 'Removal of metal ions using dead-end filtration' *Short Communication* 31(3): 413-416

Holmgren J., and Czerkinsky C., (2005) 'Mucosal immunity and vaccines' *National Medicine* 11(4 suppl): S45-53

Hohr D., Steinfartz Y., Schins R.P., Knaapen A.M., Martra G., Fubini B. And Borm P.J., (2002) 'The surface area rather than the surface coating determines the acute inflammatory response after instillation of fine and ultrafine $TiO_2$ in the rat' *International Journal of Hygiene and Environmental Health* 205(3):239-244

Horiike S., and Matsuzawa S., (1995) 'Application of syndiotacticity-rich PVA hydrogels to drug delivery system' *Journal of Applied Polymer Science*, Vol.58, 1335-1340

Hardisty R., M., and Hatton R.A., (1966) 'Platelet aggregation and the availability of platelet factor 3' *British Journal of Haematology*12: 764-776

Hejazi R., Amiji M., (2002) 'Stomach-specific anti-H.pylori therapy. I:preparation and characterization of tetracycline-loaded chitosan microspheres' *International Journal of Pharmaceutics* 235:87-94

Hernadez R.M., Igartua M., Gascon A.R., Calvo M.B., Pedraz J.L., (1998) 'Influence of shaking and surfactants on the release of bsa from plga microspheres' *European Journal of Drug Metabolism and Pharmokinetics* 23: 92-96

Higuchi, T., (1961) 'Rate of release of medicaments from ointment bases containing drugs in suspension' *Journal of Pharmaceutical Sciences* 50:874

Hill G.C., and Holman J.S., (2000) 'Chemistry in context' 5th ed., Walton-on-Thames: Nelson

Hirai A., Odani H., Nakajima A., (1991) 'Determination of degree of deacetylation of chitosan by $^{1}$H NMR spectroscopy' *Polymer Bulletin* 26: 87-94

Hirosue S., Muller B.G., Mulligan R.C., and Langer R. (2001) 'Plasmid DNA encapsulation and release from solvent diffusion nanospheres' *Journal of Controlled Release* 70: 231-242

Hodgson J.T. and Jones R.D., (1985) 'A mortality study of carbon black workers employed at five United Kingdom factories between 1947 and 1980' *Arch Environ Health* 40(5):261–268

Hodgson I., and Wakeman R.J., (2005) 'Removal of metal ions using dead-end filtration' *Short Communication* 31(3): 413-416

Holmgren J., and Czerkinsky C., (2005) 'Mucosal immunity and vaccines' *National Medicine* 11(4 suppl): S45-53

Hohr D., Steinfartz Y., Schins R.P., Knaapen A.M., Martra G., Fubini B. And Borm P.J., (2002) 'The surface area rather than the surface coating determines the acute inflammatory response after instillation of fine and ultrafine $TiO_2$ in the rat' *International Journal of Hygiene and Environmental Health* 205(3):239-244

Horiike S., and Matsuzawa S., (1995) 'Application of syndiotacticity-rich PVA hydrogels to drug delivery system' *Journal of Applied Polymer Science*, Vol.58, 1335-1340

Huffman K., Casey D., (1985) 'Effect of carboxyl end groups on hydrolysis of polyglycolic acid' *Journal of Polymer Science: Polymer Chemistry Edition* 23: 1939-1951

Hutchinson F.G., Furr B.J., (1990) 'Biodegradable polymer systems for the sustained release of polypeptides' *Journal of Controlled Release* 13: 279-294

Icrp, (1994) 'Human respiratory tract model for radiological protection' International Commission on Radiological Protection publication 66

Igartua M., Hernandez R.M., Esquisabel A., Gascon A.R., Calvo M.B. and Pedraz J.L. (1998) 'Stability of BSA encapsulated into PLGA microspheres using PAGE and capillary electrophoresis' *International Journal of Pharmaceutics* 169: 45-54

Illum L., Farraj N.F., and Fisher A.N., Gill I., Miglietta M., and Benedetti L.M., (1994) 'Hyaluronic acid ester microspheres as a nasal delivery system' *Journal of Controlled Release* 29: 133-141

Illum L., Farraj N.F., Davis S.S., (1994) 'Chitosan as a novel nasal delivery system for peptide drugs' Pharmaceutical Research 11(8): 1186-1189

Illum L., (1998) 'Chitosan and its use as a pharmaceutical excipient' *Pharmaceutical Research* 15: 1326-1331

Jalil R. and Nixon J.R., (1990) 'Microencapsulation using poly(DL-lactic acid) III: effect of polymer molecular weight on release kinetics' *Journal of microencapsulation* 7(3): 357-374

Janeway C., (1999) 'Immunobiology: the immune system in health and disease in health and disease' 4th edition, *New York Edinburgh*: Garland; Churchill Livingstone

Janeway C., (2005) 'The immune system in health and disease' 6th edition, *New York Edinburgh*: Garland; Churchill Livingstone.823

Jani P.U., Halbert G.W., Langridge J and Florence A.T., (1990) 'Nanoparticle uptake by the gastrointestinal mucosa: quantitation and particle size dependency' *Journal of Pharmacy and Pharmacology* 42:821-826

Jonsson B., Lindman B., Holmberg R. and Kronberg B., (1998) 'Surfactants and polymers in aqueous solution' published in John Wiley & Sons, Chichester, New York, Weinheim, Brisbane, Songapore and Toronto

Johnson D.A., Sowell C.G., Johnson C.L., Livesay M.T., Keegan D.S., Rhodes M.J., Ulrich J.T., Ward J.R., Cantrell J.L., Brookshire V.G., (1999) 'Synthesis and biological evaluation of a new class of vaccine adjuvants: aminoalkyl glucosaminide 4-phosphates (AGPs)' *Bioorganic and Medicinal Chemistry Letters* 9(15): 2273-2278

Jorgensen, L. and Borchgrevink C.F. (1963) 'The platelet plug in normal persons. I. The histological appearance of the plug 15 to 20 minutes and 24 hours after the bleeding and its role in the capillary hemostasis' *Acta Pathol Microbiol Scand* 57: 40-66

Joshi H.N., Stella V.J., and Topp E.M., (1992) 'Drug release from membranes of hyaluronic acid and its esters' *Journal of Controlled Release* 20: 109-122

Joung Y.K., Choi J.H., Park K.M. and Park K.D., (2007) 'PLGA microparticle embedded thermosensitive hydrogels for sustained release of hydrophobic drugs' Biomedical materials 2: 269-273

Kawashima Y., Yamamoto H., Takeuchi H., Kuno Y., (2000) 'Mucoadhesive Lactide/glycolide copolymer nanospheres coated with chitosan to improve oral delivery of elcatonin' *Pharmaceutical Development and Technology* 5(1): 77-85

Kiang T., Wen J., Lim H., Leong K.W. (2002) 'Degree of deacetylation of chitosan effect on gene transfection efficiency in vivo' *Proceed Controlled Release Society* 29: 192

Kibbe A.H., (2000) 'Handbook of Pharmaceutical Excipients' 3rd edition, Washington DC, *American Pharmaceutical Association* 340-344

Kim J.H., Kim J.Y., Lee Y.M. Kim K.Y., (1992) 'Controlled release of riboflavin and insulin through crosslinked poly (vinyl alcohol)/chitosan blend membrane' *Journal of Applied Polymer Science* 44: 1823

Klein J., Hoiejsi V., (1997) 'Immunology' Publisher: Blackwell Publishing Limited

Koyano T., Koshizaki N., Umehara H., Nagura M., Minoura N., (2000) 'Surface states of PVA/chitosan blended hydrogels' *Polymer* 41: 4461-4465

Koziara J.M., Oh J.J., Akers W.S., Ferraris S.P., and Mumper R.J., (2005) 'Blood Compatibility of Cetyl Alcohol/Polysorbate-Based Nanoparticles' *Pharmaceutical Research* 22:1821-1828

Kreuter J., (2004) 'Influence of the surface properties on nanoparticlemediated transport of drugs to the brain' *Journal of Nanoscience and Nanotechnology*

4:484-488

Kulkarni R., Pani K., Neewman C. and Leonard F., (1966) 'Polylactic acid for surgical implants' *Archives of Surgery* 93: 839

Kumbar S.G., Soppimath K.S., Aminabhavi T.M., (2002) 'Synthesis and characterization of polyacrylamide-grafted chitosan hydrogel microspheres for the controlled release of indomethacin' *Journal of Applied Polymer Sciences* 87: 1525-1536

Kuo J.W., Swann D.A., and Preswich G.D., (1991) 'Chemical modification of hyaluronic acid by carbodiimides' *Bioconjugate Chemistry* 2: 232-241
Lafferty K.J., Prowse S.J., Simenovic C.J., Warren H.S., (1983) 'Immunobiology of tissue transplantation: a return to the passenger leukocyte concept' *Annual Review of Immunology* 1: 143-173

Lavelle E.C., (2005) 'Generation of improved mucosal vaccines by induction of innate immunity' Cellular and Molecular Life Sciences 62(23): 2750-2770

Lavelle E.C., and O'Hagan D.T., (2006) 'Delivery systems and adjuvants for oral vaccines' *Expert Opinion on Drug Delivery* 3(6): 747-762

Leach C.M., and Thorburn G.D., (1982) 'a comparative study of collagen induced thromboxane release from platelets of differenct species: implications for human athero sclerosis models' *Prostaglandins* 24(1): 47-59

Leane M.M., Nankervis R., Smith A., Illum L. (2004) 'Use of the ninhydrin assay to measure the release of chitosan from oral solid dosage forms' *International Journal of Pharmaceutics* 271: 241-249

Lee K.Y., Kwon I.C., Kim Y.H., Jo W.H., and Jeong S.Y., (1998) 'Preparation of chitosan self-aggregates as a gene delivery system' *Journal Controlled Release* 51: 213-220

Lee M., Nah J.W., Kwon Y., Koh J.J., Ko K.S., and Kim S.W., (2001) 'Water soluble and low molecular weight chitosan-based plasmid DNA delivery' *Pharmaceutical Research* 18: 427-431

Leenslag J.W., Pennongs A.J., Bos R.R.M., Rozema, FR., and Boering G., (1987) 'Resorable materials of poly(l-lactide).V.I. Plates and screws for internal fracture fixation.' *Biomaterials* 8:70

Lehr, J.A. Bouwstra, E.H. Schacht and H.E. Junginger, (1992) 'In vitro evaluation

of mucoadhesive properties of chitosan and some other natural polymers' *International Journal of Pharmaceutics* 78: 43-48

Levis K., PhD thesis (2003) 'Absorption properties of non-steroidal anti-inflammatory drugs and their amino acid derivatives' School of Pharmacy and Pharmaceutical Sciences, Trinity College Dublin

Lewis DH., (1990) 'Controlled release of bioactive agents from lactide/glycolide polymers' In: Chasin M, Langer R, editors. *Biodegradable polymers as drug delivery systems* New York: Marcel Dekker 1-41

Lide, David R., (1995) 'Handbook of organic solvents' Boca Raton ; London

Linhardt, R.J., (1990) 'Biodegradable polymers for controlled release of drugs' In: *Controlled Release of Drugs*: Polymers and Aggregate systems Edited by M.Rosoff, VCH publishers, New York: 53

Liu Y., Deng X., (2002) 'Influences of preparation conditions on particle size and DNA loading efficiency for poly(DL-lactic acid-polyethylene glycol) microspheres entrapping free DNA' *Journal of Controlled Release* 83: 147-155

Luderitz Q., Galanos C., Rietschel E.T., (1982) 'Endotoxins of gram-negative bacteria' *Pharmacology & Therapeutics* 15: 383-402

Luo Y., Kirker K., and Prestwich G., (2000) 'Cross-linked hyaluronic acid hydrogel films: new biomaterials for drug delivery' *Journal of Controlled Release* 69: 169-184

Majerus, P.W., Smtih, M.B. and clamon G.H.(1969) 'Lipid methabolism in human platelets. I: Evidence for a complete fatty acid synthesizing system.' *Journal of Clinical Investigation* 48: 156-164

Martindale (1999) 'The Complete Drug Reference' 32nd, Parfitt E. (Ed) The Pharmaceutical Press, UK: 1114-1377

Masters, K., (1985) 'Spray drying handbook' 4th edition.

McGee J. P., Stanley S.D. and O'Hagan D.T., (1995) 'Zero order release of protein from poly (D, L-lactide-coglycolide) microparticles prepared using a modified phase separation technique' *Journal of Controlled Release* 34:77-86

Maclauglin F.C., Mumper R.J., Wang J., Tagliaferri J.M., Gill I., Hinchcliffe M., and Rolland A.P., (1998) 'Chitosan and depolymerized chitosan oligomers as

condensing carriers for in vivo plasmid delivery' *Journal Controlled Release* 56: 259-272

Majerus, P.W., Smtih, M.B. and clamon G.H.(1969) 'Lipid methabolism in human platelets. I: Evidence for a complete fatty acid synthesizing system.' *Journal of Clinical Investigation* 48: 156-164

Mao H.Q., Roy K., Troung-Le V.L., Janes K.A., Lin K., Wang Y., August J.T., and Leong K.W., (2001) 'Chitosan-DNA nanoparticles as gene carriers: synthesis, characterization and transfection efficiency' *Journal Controlled Release* 70: 399-421

Mason K.W., Zhu D., Scheuer C.A., McMichael J.C., Zlotnick G.W., Green B.A., (2004) 'Reduction of nasal colonization of nontypeable haemophilus influenzae following intranasal immunization with rLP4/rLP6/UspA2 proteins combined with aqueous formulation of RC529' *Vaccine* 22: 3449-3456

McGehee W. G., Hjort P.F., and Rapaport S.I., (1966) 'Effects of thorium dioxide upon blood clotting and platelets: In vivo studies in rabbits' *Thrombosis Diathermal Haemorrhage* 16: 354-369

Mills S.N. and Davis S.S., (1987) 'Controlled drug delivery, in polymers in controlled drug delivery' *Wright*, Bristol

Miura T, Usami M, Tsuura Y, Ishida H, Seino Y., (1995)'Hypoglycemic and hypolipidemic effect of chitosan in normal neonatal streptozotocin-induced diabetic mice' *Biological and Pharmaceutical Bulletin* 18:1623-5

Miyazaki S., Yamaguchi H., Yokouchi C., Takada M and Hou W.M., (1988) 'Sustained release and intragastric-floating granules of indomethacin using chitosan in rabbits' Chemical and Pharmaceutical Bulletin 36:4033-4038

Mollo A.R., (1999) Ph.D. thesis, School of Pharmacy, Trinity College, Dublin

Mollo A.R., and Corrigan O.I., (2002) 'An investigation of the mechanism of release of the amphoteric drug amoxicillin from poly(D,L-Lactide-co-glycolide) matrics' *Pharmaceutical Development and Technology* 7(3): 333-343

Moller L., Devanier K., Wulff T., Sabra M.C., (2007) 'Haemostatic composition comprising hyaluronic acid' *United States Patent* 20070009578

Morawska L., Moore M.R. and Ristovski Z.D., (2004) 'Health impacts of ultrafine particles-desktop literature review and analyses' Section 5.4, available at

http://www.deh.ov.au/atmosphere/airquality/publications/health-impacts/priorities.htm

Morrow P.E., Haseman J.K., Hobbs C.H., Driscoll K.E., Vu V. and Oberdörster G., (1996) 'The maximum tolerated dose for inhalation bioassays-toxicity vs overload' *Fundamental and Applied Toxicology* 29(2):155-67

Mueller D.L., Jenkins M.K., and Schwartz R.H., (1989) 'Clonal expansion versus functional clonal inactivation: a costimulatory signaling pathway determines the outcome of T cell antigen receptor occupancy' *Annual Review of Immunology* 7: 445-480

Murakami H., Kawashima Y., Niwa T.,, Hino T., Takeuchi H., Kobayashi M., (1997) 'Influence of the degrees of hydrolyzation and polymerization of poly(vinylalcohol) on the preparation and properties of poly(D,L-lactide-co-glycolide) nanoparticles' *International Journal of Pharmaceutics* 149:43-49

Mustard J.F., Glynn M.F., Nishizawa, E. E. and Packham M.A., (1967) 'Platelet-eurfaceinteractions: relationship to thrombosis and hemostasis' *Federal Process* 26: 106-114

Nagamoto T., Hattori Y., Takayama K., and Maitani Y., (2004) 'Novel chitosan particles and chitosan-coated emulsions including immune response via intranasal vaccine delivery' *Pharmaceutical Research* 21:671-674

Naoko S., Atsuya M., Yoshinobu N., Tatsuo A., (2006) 'Synthesis and photochemical properties of a new water-soluble coumarin, designed as a chromophore for highly water-soluble and photolabile protecting group' *Bulletin of the chemical society of Japan* 79: 1753-1757

Napolitani G., Rinaldi A., Bertoni F., Sallusto F., Lanzavecchia A., (2005) 'Selected Toll-like receptor agonist combinations synergistically trigger a T helper type 1-polarizing program in dendritic cells' *National Immunology* 6: 769-776

Newmmar A., Hoet P.H., Dinsdale D., Vermylen J., Hoylaerts M.F. and Nemery B., (2003) 'Diesel exhaust particles in lung acutely enhance experimental peripheral thrombosis' *Circulation* 107(8):1202-1208

Nemmar A., Hoylaerts M.F., Hoet P.H. and Nemery B., (2004) 'Possible mechanisms of the cardiovascular effects of inhaled particles: systemic translocation and prothrombotic effects' *Toxicology Letter* 149(1-3): 243-253

Newmmar A., Vanbilloen H., Hoylaerts M.F. and Nemery B., (2001) 'Passage of intratracheally instilled ultrafine particles from the lung into the systemic circulation

in hamster' *American Journal of Respiratory and Critical Care Medicine* 164(9): 1665-1668

Nemmar A., Hoet P.H.M., Vanquickenborne B., Dinsdale D., Thomeer M., Hoylaerts M.F., Vanbilloen H., Mortelmans L., and Nemery B., (2002) 'Passage of inhaled particles into the blood circulation in humans' *Circulation* 105: 411-414

Nieuwenhuis, P., and Jansen, H.W.B., (1991) 'Degradation of and tissue reaction to biodegradable poly(l-lactide) for use as internal fixation of fractures: a study in rats' *Biomaterials* 12 :32

Oberdörster G., (1995) 'Lung particle overload-implications for occupational exposures to particles' *Regulatory Toxicology and Pharmacology* 21(1):123-35

Oberdörster G., Sharp Z., Atudorei V., Elder A., Gelein R., Kreyling W., and Cox C., (2004) 'Translocation of inhaled ultrafine particles to the brain' *Inhalation Toxicology* 16(6-7): 437-45

Oberdörster G., Oberdörster E. and Oberdörster J., (2005) 'Nanotoxicology: An Emerging Discipline Evolving from Studies of Ultrafine Particles' *Environmental Health Perspectives* V113 (7):823

O'Hagan, D.T., (1998) 'Microparticles and polymers for the mucosal delivery of vaccines', *Advanced Drug Delivery Reviews* 34: 305-320

Oliverira B.F., Santana M.H.A., Re M.I., (2005) 'Spray dried chitosan microspheres cross-linked with L-glyceraldehyde as potential drug delivery systems' *Brazilian Journal of Chemical Engineering* 22(3): 353-360

Ozasa Y., (2007), B.A. (Mod) thesis, School of Biochemistry and Immunology, Trinity College Dublin

Pangburn S.H., Trescony P.V., Heller J., (1982) 'Lysozyme degradation of partially deacetylated chitin, its films and hydrogels' *Biomaterials* 3: 105-108

Panyam, J., Lof, J., O'Leary, E., Labhasetwar, V. (2002) 'Efficiency of Dispatch® and Infiltrator® cardiac infusion catheters in arterial localization of nanoparticles in a porcine coronary model of restenosis' *Journal of Drug Targeting* 10: 515–523

Panyam, J., Dali M.M. , Sahoo, S. K., Ma W., Chakravarthi S.S., Amidon G.L., Levy R.J., Labhasetwar V., (2003) 'Polymer degradation and in vitro release of a model protein from poly(D,L-lactide-co-glycolide) nano- and microparticles' *Journal of Controlled Release* 92 173-187

Paul W.E., (1992) 'Fundamental immunology' 2th edition, *Philadelphia London*: Lippincott Williams & Wilkins p1701

Paul W, Sharma CP (2000) 'Chitosan, a drug carrier for the 21st. century: a review'. *STP Pharmaceutical Science* 10:5–22

Pean J.M., Venier-Julienne M.C., Boury F., Menei P., Denizot B., Benoit J.P., (1998) 'NGF release from poly (DL-lactide-co-glycolide) microspheres: Effect of some formulation parameters on encapsulated NGF stability' *Journal of Controlled Release* 56: 175-187

Peppas, N.A. and Sinclair, G.W., (1984) 'Analysis of non-Fickian transport in polymers using a simplified exponential expression' *Journal of Membrane Science* 17 329

Petrusewicz J., Turowski M., Foks H., Pilarski B., Kaliszan R., (1995) 'Comparative studies of antiplatelet activity of nonsteroidal anti-inflammatory drugs and new pyrazine CH- and NH-acids' *Life Sciences* 56(9): 667-677

Pietzonka P., Rothen-Rutishauser B., Langguth P., Wunderli-Allenspach H., Walter E., Merkle H.P., (2002) 'Transfer of Lipophilic Markers from PLGA and Polystyrene Nanoparticles to Caco-2 Monolayers Mimics Particle Uptake' *Pharmaceutical Research* 19 (5): 595-601

Poltorak A., He X., Smirnova I., Liu M.Y., Huffel C.V., Birdwell D., Alejos E., Silva M., Galanos C., Freudenberg M., Ricciard-Castagnoli P., Beutler B., (1998) 'Defective LPS signalling in C3H/HeJ and C57BL/10ScCr mice: mutations in Tlr4 gene' *Science* 282: 2085-2088

Porporatto C., Bianco I.D., Cabanillas A.M., Correa S.G., (2004) 'Early events associated to the oral co-administration of type II collagen and chitosan: induction of anti-inflammatory cytokines' International Immunology 16: 433-441

Porporatto C., Bianco I.S., Correa S.G., (2005) 'Local and systemic activity of the polysaccharide chitosan at lymphoid tissues after oral administration' *Journal of Leukocyte Biology* 78: 62-69

Pratten M.K., and Lloyd J.B., (1986) 'The effect of size of a particulate substrate on its mode of capture by rat peritoneal macrophages cultured in vitro' *Biochimica et Biophysica Acta* 881: 307-313

Prestwitch G.D., Marecak D.M., Marecek J.F., Vercruysse K.P., Ziebel M.R., (1998)

'Controlled chemical modification of hyaluronic acid: synthesis, applications, and biodegradation of hydrazide derivatives' *Journal of Controlled Release* 53: 93-103

Prout E. G. and Tompkins F. C., (1944) 'The thermal decomposition of potassium permanganate' *Transactions of the Faraday Society* 40: 488

Puebla P., Pastoriza P., Barcia E., and Fernandez-Carballido A., (2005) 'PEG-derivative effectively modifies the characteristics of indomethacin-PLGA microspheres destined to intra-articular administration' *Journal of Microencapsulation* 22(7): 793-808

Pulendran B., (2004) 'Modulating vaccine responses with dendritic cells and Toll-like receptors' *Immunology Review* 199: 227-250

Pulendran B., Ahmed R., (2006) 'Translating innate immunity into immunological memory: implications for vaccine development' *cell* 124(4): 849-863

Qaddoumi M.G., Gukasyan H.J., Davda J., Labhasetwar V., Kim K.J., Lee V.H.L., (2003) 'Clathrin and caveolin-1 expression in primary pigmented rabbit conjunctival epithelial cells: Role in PLGA nanoparticle endocytosis' *Molecular Vision* 9: 559-568

Radomski A., Jurasz P., Alonso-Escolano D., Drews M., Morandi M., Malinski T., Radomski M.W. (2005) 'Nanoparticle-induced platelet aggregation and vascular thrombosis' *British Journal of Pharmacology* 146:882-893

Ramtoola Z., Corrigan O.I. and Barrott C.J., (1992) 'Release kinetics of fluphenazine from biodegradable microspheres' *Journal of Microencapsulation* 9(4): 415-423

Rafi A., Nagarkatti M., Nagarkatti P.S., (1997) 'Hyaluronate-CD44 interactions can induce murine B-cell activation' *Blood* 89: 2901-2908

Ritger P.L., Peppas N.A. (1987) 'A simple equation for description of solute release II Fickian and anomalous release from swellable devices' *Journal of Controlled Release* 5: 7-42

Ritthidej G., Chomto P., Pummangura S., Menasveta P., (1994) 'Chitin and chitosan as disintegrants in paracetamol tablets' *Drug development and industrial pharmacy* 20:2109-34

Robert, P., Mauduit J., Frank R.M. and Vert M., (1993) 'Biocompatibility and resorbability of a polylactic acid membrane for periodontal guided tissue

regeneration' *Biomaterials* 14:5353

Sah, H., Toddywala, R. and Chien, Y.W., (1994) 'The influence of biodegradable formulations on the controlled release of a protein' *Journal of Controlled Release* 30: 201-211

Sah, H., (1997) 'Microencapsulation techniques using ethyl acetate as a dispersed solvent: effects of its extraction rate on the characteristics of PLGA microspheres' *Journal of Controlled Release* 47: 233–245

Sahoo S.K., Panyam J., Prabha S., Labhasetwar V., (2002) 'Residual polyvinyl alcohol associated with poly(D,L-lactide-co-glycolide) nanoparticles affects their physical properties and cellular uptake' *Journal of Controlled Release* 82:105-114

Sandor M., Enscore D., Weston P., Mathiowitz E., (2001) 'Effect of protein molecular weight on release from micro-sized PLGA microspheres' *Journal of Controlled Release* 76: 297-311

Sawayanagi Y, Nambu N, Nagai T. (1982) 'Use of chitosan for sustained release preparations of water soluble drugs' *Chemical and Pharmaceutical Bulletin* 30:4213-4215

Sawayanagi Y., Nambu N., Nagai T., (1983) 'Dissolution properties and bioavailability of phenytoin from ground mixtures with chitin or chitosan' *Chemical and Pharmaceutical Bulletin* (Tokyo) 31 (6):2064-8

Schmidt E.R., and Hankeln T., (1996) 'Transgenic organisms and biosafety: Horizontal gene transfer, stability of DNA and expression of transfers' *Springer* 1st edition

Scholes P.D., Coombes A.G.A., Illum L. et al., (1993) 'The preparation of sub-200 nm poly (lactide-co-glycolide) microspheres for site-specific drug delivery' *Journal of Controlled Release* 25: 145–153

Schwartz J.B., Simonelli A.P., Higuchi W.I. (1968) 'Drug release from wax matrices I analysis of data with first order kinetics and with the diffusion controlled model' *Journal of Pharmaceutical Science* 57: 274-277

Schwarz J.A., Contescu C.I., Putyera K., (1995) 'Encyclopedia of Nanoscience and Nanotechnology' *Marcel Dekker Inc.* 2744

Seferian P.G., and Martinez M.L., (2001) 'Immune stimulating activity of two new chitosan containing adjuvant formulations' *Vaccine* 19:661-668

Shall I., and Ferard G., (2007) 'Comparison of the sensitivity of 11 crosslinked hyaluronic acid gels to bovine testis hyaluronidase' *Polymer Degradation and Stability* 92: 915-919

Shelley T., (2006) 'Nanotechnology: new promise, new dangers' by Fernwood Publishing Ltd, Canada

Sheu J., Shen M.Y., Hsiao G., (2003) 'Inhibitory mechanisms of magnesium sulfate on platelet aggregation in *in vitro* and *in vivo* experiments' *Journal of Thrombosis and Haemostasis* 1 Supplement 1 July, abstract number PO239

Shibata Y., Foster L., Metzger W.J., and Myrvik Q.N., (1997) 'Alveolar macrophage priming by intravenous administration of chitin particles, polymers of N-acetyl-D-glucosamine, in mice' *Infection Immunology* 65(5): 1734-1741

Sidhu, B.K., Washington, C., Davis, S.S., Purewal, T.S., (1993) 'Electrophoretic properties of lactose and salbutamol sulfate suspensions in halogenated solvents' *Langmuir* 9:839–843

Siegel S.J., Kahn J.B., Metzger K., Winey K.I., Werner K. and Dan N. (2006) 'Effect of drug type on the degradation rate of PLGA matrices' *European Journal of Pharmaceutics and Biopharmaceutics* 64: 287-293

Siepmann J., Elkharraz K., Siepmann F., Klose D., (2005) 'How autocatalysis accelerates drug release from PLGA-based imcroparticles: a quantitative treatment' *Bomacromolecules* 6(4): 2312-2319

Sinclair G.W., Peppas N.A. (1984) 'Analysis of non-Fickian transport in polymers using simplified exponential expressions' *Journal of Membrane Science* 17: 329-331

Souillac and Rytting (1999) 'Characterization of delivery systems, Differential Scanning Calorimetry ' *Encyclopedia of Controlled Drug Delivery* 1: 212-227

Steinman L., (2007) 'A brief history of TH17, the first major revision in the TH1/TH2 hypothesis of T cell-mediated tissue damage' *National Medicine* 13(2): 139-145

Stockinger B., (2007) 'Th17 cells: An orphan with influence' *Immunology and Cell Biology* 85(2): 83-84

Su CH, Sun CS, Juan SW, Hu CH, Ke WT, Sheu MT., (1997) 'Fungal mycelia as

the source of chitin and polysaccharides and their applications as skin substitutes' *Biomaterials* 18:1169-1174

Sun H., Pollock K.G.J., and Brewer J.M., (2003) 'Analysis of the role of vaccine adjuvants in modulating dendritic cell activation and antigen presentation in vitro' *Vaccine* 21: 849-855

Sun Q., Wang A., Jin X., Natanzon A., Fayad Z.A., Chen L.C. and Rajagopalan S., (2005) 'Long-term air pollution exposure and acceleration of atherosclerosis and vascular inflammation in an animal model' *Journal of the American Medical Association* 294(23): 3003-3010

Suwa T., Hogg J.C., Quinlan K.B., Ohgami A., Vincent R. and Eeden S.F., (2002) 'Particulate air pollution induces progression of atherosclerosis' *Journal of the American College of Cardiology* 39(6): 935-942

Tajber L., Corrigan O.I., and Healy A.M. (2005) 'Physicochemical evaluation of PVP-thiazide diuretic interactions in co-spray-dried composites-analysis of glass transition composition relationships' *European Journal of Pharmaceutical Sciences* 24: 553-563

Takeda K., Kaisho T., and Akira S., (2003) 'Toll-like receptors' *Annual Review of Immunology* 21: 335-376

Tozaki H, (1997) 'Chitosan capsules for colon-specific drug delivery: improvement of insulin absorption from the rat colon' *Journal of Pharmaceutical Science* 86(9):1016-21

Tinkle S., (2004) 'Nanomaterials: A risk to health at work?' First International Symposium on *Occupational Health Implications of Nanomaterials* 12-14 October, p: 47-52

Tran L., Aitken R., Ayres J., Donaldson K. And Hurley F., (2007) 'Human effects of nanoparticle exposure' *Nanotechnology: consequences for human health and the environment* The Royal Society of Chemistry copyright, p102

Truong-Le V.L., August J.T., Leong K.W., (1998) 'Controlled gene delivery by DNA-gelatin nanospheres' *Human Gene Therapy* 9(12): 1709-1717

Truong-Le V.L., Walsh S.M., Schweibert et al. (1999) 'Gene transfer by DNA-gelatin nanospheres' *Archives of Biochemistry and Biophysics* 361(1): 47-56

Upadrashta SM, Katikaneni PP, Nuessle NO., (1992) 'Chitosan as a Tablet Binder. Drug Development and Industrial Pharmacy Marcel' *Dekker Inc* 18(15): 1701-1708

Vallhov H., Qin J., Johansson S.M., Ahlborg N., Muhammed M.A., Scheynius A., Gabrielsson S., (2006) 'The importance of an endotoxin-free environment during the production of nanoparticles used in medical applications' *Nano Letters* 6(8): 1682-1686

Vila A., Sanchez A., janes K., Behrens I., Kissel T., Jato J.L.V., Alonso M.J., (2004) 'Low molecular weight chitosan nanoparticles as new carriers for nasal vaccine delivery in mice' *European Journal of Pharmaceutics and Biopharmaceutics* 57: 123-131

Viles-Gonzalez J.F., Anand S.X., Valdiviezo C., Zafar M.U., Hutter R., Sanz J. and Badimon J.J., (2004) 'Update in atherothrombotic disease' *Mount Sinai Journal of Medicine* 71(3): 197-208

Visscher, G.E., Robison, R.L., and Argentieri, G.J., (1987) 'Tissue response to biodegradable injectible microcapsules' *Journal of Biomaterial Application* 2:118

Wagner J.G. (1969) 'Interpretation of percent dissolved-time plots derived from in vitro testing of conventional tablets and capsules' *Journal of Pharmaceutical Science* 58(10): 1253-1257

Waalkds T.P., and Coburn H., (1969) 'Comparative effects of glycogen and antigen.sntibody reactions on serotonin and histamine in the rabbit' *Proceedings of The Society for Experimental Biology and Medicine* 101: 122-125

Walter, E., Dreher, D., Kok, M., Thiele, L., Kiama, S.G., Geher, P. and Merkle, H.P. (2001) 'Hydrophilic poly(DL-lactide-co-glycolide) microspheres for the delivery of DNA to human-derived macrophages and dendritic cells', *Journal of Controlled Released* 76: 149-168

Warshaw,A.L, Laster L, and Shulman, N.R (1966) 'The stimulation by thrombin of glucose oxidation in human platelets' *Journal of Clinical Investigation* 45:1923-1934

Washington, C., (1990) 'The stability of intravenous fat emulsions in parenteral nutrition mixtures' *International Journal of Pharmaceutics* 66:1–21

Watt, P.J., Davies, M.C. and Melia, C.D., (1990) 'Microencapsulation using emulsification/solvent evaporation: An overview of techniques and applications' *Critical Reviews in Therapeutic Drug Carrier Systems* 7: 235

Weigel, P.H., Hascall, V.C., and Tammi M., (1997) 'Hyaluronan synthases' *Journal*

*of biological chemistry* 272(22): 13997-14000

Weissmann, B., and Meyer, K. (1954) *Journal of Amemican Chemical Society* 27: 1753–1757

William G.M., Herbert J.Q., (1985) 'Method of achieving hemostasis inhibiting fibroplasia, and promoting tissue regeneration in a tissue wound' United States Patent No. 4532134

Williams III, R.O., Barron, M.K., Jose Alonso, M., Remunan-Lopez, C., (1998) 'Investigation of a pMDI system containing chitosan microspheres and P134a' *International Journal of Pharmaceutics* Vol. 174 (1): 209-222

Wu XS., (1995) 'Preparation, characterization, and drug delivery applications of mucrospheres based on biodegradable lactic/glycolic acid polymers' In: Wise editors. *Encyclopedic handbook of biomaterials and bioengineering* New York: Marcel Dekker, 1151-200

Yang, Y.Y., Chung, T.S., (2001) 'Ng, Morphology, drug distribution, and in vitro release profiles of biodegradable polymeric microspheres containing protein fabricated by double-emulsion solvent extraction/evaporation method' *Biomaterials* 22:231-241

Yang B., Wu Q.Y., Li D.Y., Ruan Y.M., Song M., Xie Y.Q., (2003) 'Effect of the biodegradable chitosan external stent on the early changes in the rabbit vein grafts' *Zhonghua Wai Ke Za Zhi* 41(9): 688-690

Yeh, M.K., Coombes, A.G.A, Jenkins P.G. Davis S.S., (1995) 'A novel emulsification-solvent evaporation extraction technique for production of protein loaded biodegradable microparticles for vaccine and drug delivery', *Journal of Controlled Release* 33:437-445

Yuan X., Li L., Rathinavel A., Hao J., Narasimhan M., He M., Heitlage V., Tam L., Viqar S., Salehi M., (2006) 'siRNA Drug Delivery by Biodegradable Polymeric Nanoparticles' *Journal of Nanoscience and Nanotechnology* 6: 2821–2828

Yuan, Y.R. , Pei, Y., Chen, H.Y., et al. and Patel, D.J. (2006) 'A potential protein-RNA recognition event along the RISC-loading pathway from the structure of *A. aeolicus* Argonaute with externally-bound siRNA' *Structure* 14, 1557-1565.

Zambaux M.F., Bonneaux F., Gref R. et al., (1998) 'Influence of experimental parameters on the characteristics of poly (lactic acid) nanoparticles prepared by a double emulsion method' *Journal of controlled release* 50 (1–3): 31–40

Zhong S.P., Campoccia D., Doherty P.J., Williams R.L., Benedetti L., Williams D.F., (1994) 'Biodegradation of hyaluronic acid derivatives by hyaluronidase' *Biomaterials* 15: 359-365

Zucker, M.B (1947) 'Platelet agglutination and vaoconstriction as factors in spontaneous hemostasis in normal, thrombocytopenic, hepaninized and hypothrombinemic rats' *American Journal of Physiology* 148: 275-288

# APPENDICES

# Appendix I

## List of PLGA micro and nanoparticles

| No. | Name | Drug | Median Size (μm) | Drug Loading (%w/w) | Solvent |
|---|---|---|---|---|---|
| 1 | PLGA MP | H S A | 3.79 | 0.496 | DCM |
| 2 | | | 2.98 | 0.543 | |
| 3 | | | 2.8 | 0.614 | |
| 4 | | | 1.9 | 0.678 | |
| 5 | | | 1.72 | 0.711 | |
| 6 | PLGA MP | H S A | 3.71 | 0.678 | Ethyl acetate |
| 7 | | | 3.43 | 0.452 | |
| 8 | | | 1.77 | 0.805 | |
| 9 | | | 1.82 | 0.672 | |
| 10 | | | 1.74 | 0.842 | |
| 11 | Drug free PLGA MP | --- | 1.69 | 0 | DCM |
| 12 | Drug free PLGA MP | --- | 1.68 | 0 | Ethyl acetate |
| 13 | PLGA MP | OVA-coupled F/G peptide | 2.26 | 0.52 | Ethyl acetate |
| 14 | PLGA MP | OVA | 3.44 | 0.8 | Ethyl acetate |
| 15 | PLGA NP | H S A | 0.56 | 0.521 | Ethyl acetate |
| 16 | Drug free PLGA NP | --- | 0.64 | 0 | |
| 17 | PLGA NP with Coumarin-6 | H S A | 0.741 | 0.515 | |
| 18 | PLGA NP | --- | 3 | 0 | |
| 19 | PLGA NP | --- | Aggregates | 0 | |
| 20 | PLGA NP low loading | OVA | 0.422 | 0.708 | |
| 21 | PLGA NP medium loading | OVA | 0.445 | 2.95 | |
| 22 | PLGA NP high loading | OVA | 0.671 | 5.45 | |
| 23 | PLGA NP | Indomethacin | 0.681 | 6.52 | |
| 24 | PLGA NP | Ketoprofen | 0.542 | 4.02 | |

## List of chitosan-PLGA micro and nanoparticles

| No. | Name | Median size (μm) | Chitosan loading% (w/w) | OVA Loading% (w/w) |
|---|---|---|---|---|
| 25 | Drug Free CS-PLGA NP | 0.581 | 1.77 | ----- |
| 26 | Drug free CS-PLGA MP | 5.15 | 3.15 | ----- |
| 27 | Drug free CS-PLGA MP | 5.56 | 4.20 | ----- |
| 28 | CS-PVA NP (1:2) | 0.478 | 30.2 | ----- |
| 29 | CS-PVA NP (2:2) | 0.516 | 41.3 | ----- |
| 30 | OVA CS-PLGA NP | 0.503 | 1.63 | 5.32 |

All chitosan-PLGA particles were prepared with the use of solvent ethyl acetate

## List of chitosan micro and nanoparticles

| No. | Name | Median Size (μm) | OVA Loading% (w/w) | Preparation Method |
|---|---|---|---|---|
| 31 | CL 213 MP | 3.15 | ----- | Spray drying |
| 32 | CL213/GLU MP | 2.95 | ----- | Spray drying with crosslinking |
| 33 | CS-F NP | 0.431 | ----- | Precipitation/coacervation |
| 34 | CL113 NP | 0.579 | ----- | Precipitation/coacervation |
| 35 | CL213 NP | 0.508 | ----- | Precipitation/coacervation |
| 36 | G213 NP | 0.529 | ----- | Precipitation/coacervation |
| 37 | CL113.2 NP | 0.612 | ----- | Precipitation/coacervation |
| 38 | CL213.2 NP | 0.564 | ----- | Precipitation/coacervation |
| 39 | OVA-CS NP | 0.545 | 30.2 | Precipitation/coacervation |
| 40 | OVA-CL113 NP | 0.468 | 30.8 | Precipitation/coacervation |
| 41 | OVA-CL213 NP | 0.534 | 28.6 | Precipitation/coacervation |
| 42 | OVA-G213 NP | 0.619 | 30.0 | Precipitation/coacervation |

## List of hyaluronic acid micro and nanoparticles

| No. | Name | z-Average Size (μm) | Chitosan Content % (w/w) | Preparation Method |
|---|---|---|---|---|
| 43 | HA MP | 2.69 (median-size) | ------- | Spray drying |
| 44 | HA(F)/CS NP | 0.198 | 42.7 ±9.7 | Precipitation/coacervation |
| 45 | HA(N)/CL113 NP | 0.171 | 43.2 ±5.1 | Precipitation/coacervation |
| 46 | HA(N)/CL213 NP | 0.184 | 45.8 ±6.7 | Precipitation/coacervation |
| 47 | HA(N)/G113 NP | 0.170 | 45.1 ±3.3 | Precipitation/coacervation |
| 48 | HA(N)/G213 NP | 0.177 | 44.8 ±7.9 | Precipitation/coacervation |

## Chitosan nanoparticles prepared by clean control

| No. | Name | z-Average Size (μm) | Preparation Method | Others |
|---|---|---|---|---|
| 49 | CL213-CC-NP | 0.572 | Precipitation/coacervation | Low LPS level |

## Appendix II

## Percentage and amount of protein H S A released from PLGA microparticles made with DCM (No.5) and ethyl acetate (No.10)

| Time (days) | Particle No.5 | | Particle No.10 | |
|---|---|---|---|---|
| | % released | Amount released (μg/mg) | % released | Amount released (μg/mg) |
| 0 | 0 | 0 | 0 | 0 |
| 0.5 | 15.6 | 1.31 | 12.7 | 0.90 |
| 1 | 28.4 | 2.39 | 24.1 | 1.71 |
| 3 | 34.6 | 2.91 | 28.1 | 2.00 |
| 5 | 32.2 | 2.71 | 25.3 | 1.80 |
| 7 | 36.4 | 3.07 | 30.4 | 2.16 |
| 11 | 32.9 | 2.77 | 26.6 | 1.89 |
| 13 | 29.3 | 2.47 | 28.2 | 2.01 |
| 15 | 34.0 | 2.86 | 26.2 | 1.86 |
| 17 | 36.2 | 3.05 | 29.9 | 2.13 |
| 19 | 43.4 | 3.65 | 42.5 | 3.02 |
| 21 | 47.7 | 4.02 | 41.6 | 2.96 |
| 23 | 49.2 | 4.14 | 45.5 | 3.24 |
| 25 | 47.9 | 4.03 | 46.6 | 3.31 |
| 28 | 56.1 | 4.72 | 51.6 | 3.67 |
| 30 | 52.9 | 4.45 | 51.0 | 3.63 |
| 35 | 52.1 | 4.39 | 49.8 | 3.54 |
| 40 | 51.6 | 4.34 | 49.2 | 3.50 |
| 45 | 52.9 | 4.45 | 47.9 | 3.41 |

## Percentage and amount of OVA-coupled F/G peptide (No.13) and OVA (No.14) released from PLGA microparticles

| Time (days) | Particle No.13 | | Time (days) | Particle No.14 | |
|---|---|---|---|---|---|
| | % released | Amount released (μg/mg) | | % released | Amount released (μg/mg) |
| 0 | 0 | 0 | 0 | 0 | 0 |
| 0.5 | 7.7 | 0.39 | 0.5 | 9.88 | 0.79 |
| 1 | 14.7 | 0.73 | 1 | 19.1 | 1.53 |
| 6 | 15 | 0.75 | 5 | 16.3 | 1.3 |
| 11 | 14.8 | 0.74 | 9 | 23.3 | 1.86 |
| 14 | 14 | 0.7 | 14 | 27.6 | 2.21 |
| 19 | 34.5 | 1.73 | 19 | 27.5 | 2.2 |
| 23 | 55.6 | 2.78 | 26 | 47.4 | 3.79 |
| 27 | 68.6 | 3.43 | 33 | 61 | 4.88 |
| 31 | 81.6 | 4.08 | 40 | 63.5 | 5.08 |
| 35 | 89.7 | 4.49 | 45 | 63.6 | 5.09 |
| 40 | 100 | 4.85 | 55 | 63.6 | 5.09 |
| 45 | 100 | 5.03 | 70 | 63.6 | 5.09 |

## Percentage and amount of coumarin-6 and H S A released from PLGA microparticles (No.17)

| | Coumarin-6 | | | Protein H S A | |
|---|---|---|---|---|---|
| Time (days) | % released | Amount released (μg/mg) | Time (days) | % released | Amount released (μg/mg) |
| 0 | 0 | 0 | 0 | 0 | 0 |
| 0.5 | 0.25 | 0.0006 | 1 | 18 | 0.88 |
| 1 | 0.3 | 0.0007 | 5 | 25 | 1.08 |
| 3 | 0.71 | 0.0018 | 10 | 26 | 1.24 |
| 5 | 1 | 0.0025 | 15 | 30 | 1.18 |
| 10 | 3 | 0.0075 | 20 | 44 | 2.06 |
| 15 | 11 | 0.0275 | 25 | 55 | 3.09 |
| 20 | 30 | 0.075 | 30 | 70 | 3.35 |
| 25 | 40 | 0.1 | 35 | 81 | 3.61 |
| 30 | 55 | 0.14 | 40 | 92 | 4.12 |
| 35 | 75 | 0.19 | 45 | 94 | 4.38 |
| 40 | 95 | 0.24 | 50 | 95 | 4.64 |
| 45 | 100 | 0.25 | | | |

## Percentage and amount of OVA protein released from PLGA nanoparticles with different protein loadings (No.20-22)

| Time (days) | Particle No.20 | | Particle No.21 | | Particle No.22 | |
|---|---|---|---|---|---|---|
| | % released | Amount released (μg/mg) | % released | Amount released (μg/mg) | % released | Amount released (μg/mg) |
| 0 | 0 | 0 | 0 | 0 | 0 | 0 |
| 0.5 | 10.1 | 0.718 | 14.4 | 4.26 | 21.3 | 11.6 |
| 1 | 13.3 | 0.943 | 27.7 | 8.17 | 40.7 | 22.2 |
| 4 | 15.9 | 1.12 | 27.8 | 8.21 | 56.1 | 30.6 |
| 7 | 16.5 | 1.17 | 31.5 | 9.3 | 63.4 | 34.6 |
| 12 | 22.2 | 1.57 | 32.9 | 9.7 | 68.5 | 37.3 |
| 17 | 28.5 | 2.02 | 44.4 | 13.1 | 77 | 42.0 |
| 23 | 31.7 | 2.25 | 59.3 | 17.5 | 80.8 | 43.6 |
| 28 | 38.7 | 2.74 | 64.1 | 18.9 | 86.3 | 47.0 |
| 32 | 45.7 | 3.23 | 70.8 | 20.9 | 88.9 | 48.5 |
| 37 | 49.5 | 3.5 | 76.3 | 22.5 | 91.5 | 50.0 |
| 43 | 51.4 | 3.64 | 82 | 24.2 | 93 | 50.7 |
| 47 | 57.1 | 4.04 | 85.4 | 25.2 | 97.7 | 53.2 |
| 51 | 60.9 | 4.31 | 88.8 | 26.2 | 100 | 54.5 |
| 56 | 59 | 4.18 | 90.2 | 26.6 | 100 | 54.5 |
| 60 | 61.5 | 4.36 | 96.6 | 28.5 | 100 | 54.5 |
| 65 | 60.2 | 4.27 | 99 | 29.2 | 100 | 54.5 |
| 70 | 63.4 | 4.49 | 92.9 | 27.4 | 100 | 54.5 |

**Percentage (%) and amount of drug released from PLGA nanoparticles loaded with indomethacin (No.23) and ketoprofen (No.24)**

| | Particle No.23 | | Particle No.24 | |
|---|---|---|---|---|
| Time (days) | % released | Amount released (μg/mg) | % released | Amount released (μg/mg) |
| 0 | 0 | 0 | 0 | 0 |
| 0.5 | 8.67 | 15.2 | 35.4 | 14.2 |
| 1 | 26.3 | 17.1 | 45.2 | 18.1 |
| 4 | 25 | 16.3 | 51.9 | 20.8 |
| 7 | 29.1 | 19 | 61.5 | 24.6 |
| 10 | 41.8 | 27.3 | 76.1 | 30.4 |
| 12 | 58.4 | 38.1 | 82.1 | 32.8 |
| 14 | 72.8 | 47.5 | 96.1 | 38.4 |
| 17 | 100 | 65.2 | 102 | 40.8 |
| 23 | 100 | 65.2 | 101 | 40.5 |

**Percentage and amount of protein OVA released from CS-PLGA nanoparticles (No.30)**

| Time (days) | % released | Amount released (μg/mg) |
|---|---|---|
| 0 | 0 | 0 |
| 0.5 | 33.3 | 17.1 |
| 1 | 50.2 | 26.7 |
| 4 | 50.6 | 26.9 |
| 7 | 53.6 | 28.5 |
| 10 | 60.7 | 32.3 |
| 13 | 66.9 | 35.6 |
| 16 | 67.9 | 36.1 |
| 19 | 77.8 | 41.4 |
| 24 | 79.4 | 42.2 |
| 28 | 81.6 | 43.4 |
| 34 | 94.3 | 50.2 |
| 39 | 95.6 | 50.9 |
| 44 | 104 | 55.4 |
| 51 | 103 | 55 |
| 58 | 108 | 57.5 |
| 65 | 107 | 56.9 |
| 70 | 108 | 56.9 |

**Percentage and amount of OVA released from chitosan nanoparticles (No.39-42)**

| Time (minutes) | CS-F NP, Particle No.39 | | CL113 NP, Particle No.40 | |
|---|---|---|---|---|
| | % released | Amount released (μg/mg) | % released | Amount released (μg/mg) |
| 0 | 0 | 0 | 0 | 0 |
| 3 | 49 | 222 | 54 | 249 |
| 6 | 63 | 285 | 66 | 305 |
| 12 | 87 | 394 | 88 | 407 |
| 18 | 95 | 434 | 94 | 434 |
| 25 | 100 | 453 | 100 | 462 |

| Time (minutes) | CL 213 NP, Particle No.41 | | G213 NP, Particle No.42 | |
|---|---|---|---|---|
| | % released | Amount released (μg/mg) | % released | Amount released (μg/mg) |
| 0 | 0 | 0 | 0 | 0 |
| 3 | 47 | 202 | 52 | 233 |
| 6 | 61 | 262 | 68 | 305 |
| 12 | 85 | 365 | 88 | 395 |
| 18 | 95 | 408 | 96 | 431 |
| 25 | 100 | 429 | 105 | 471 |

# Appendix III

## Calibration curves of protein standards for protein concentration determination

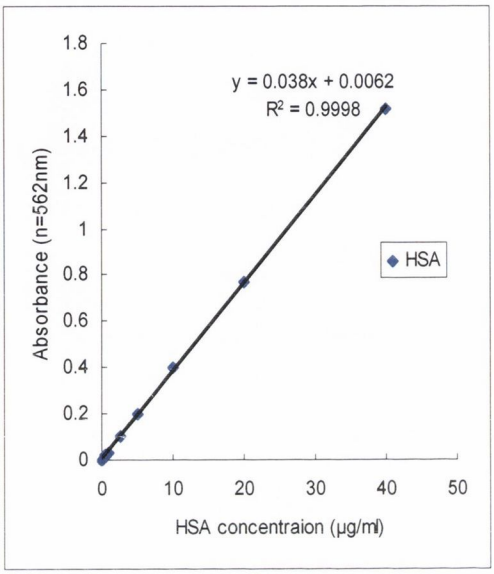


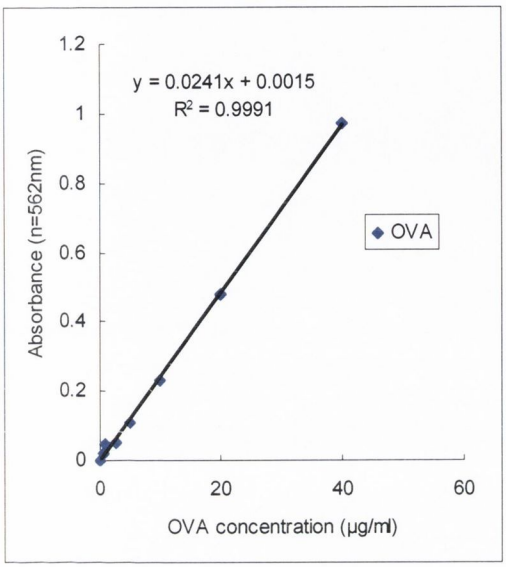


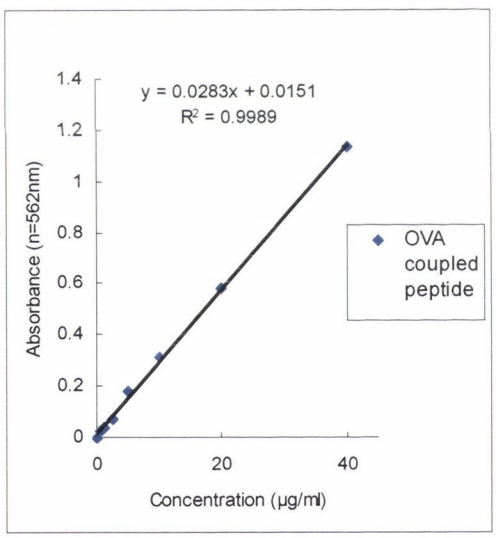

## Calibration curves of NSAID standards for concentration determination

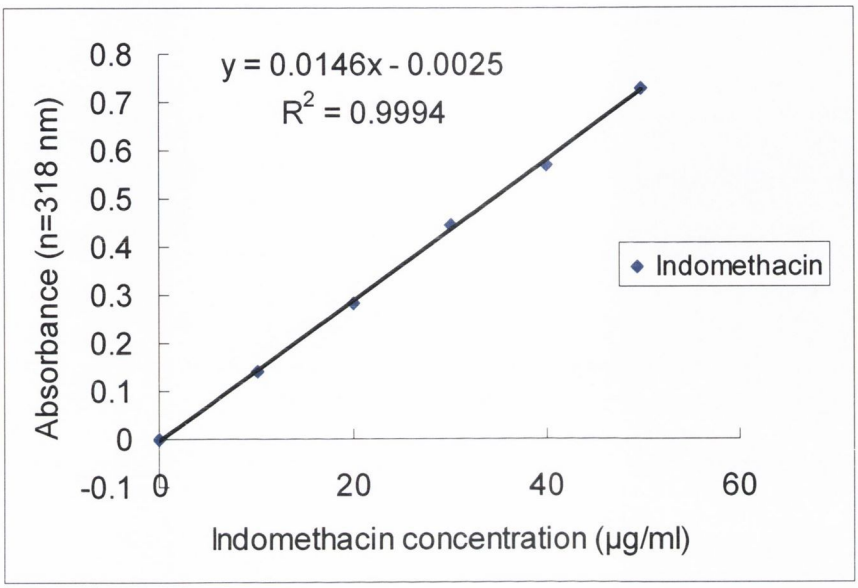


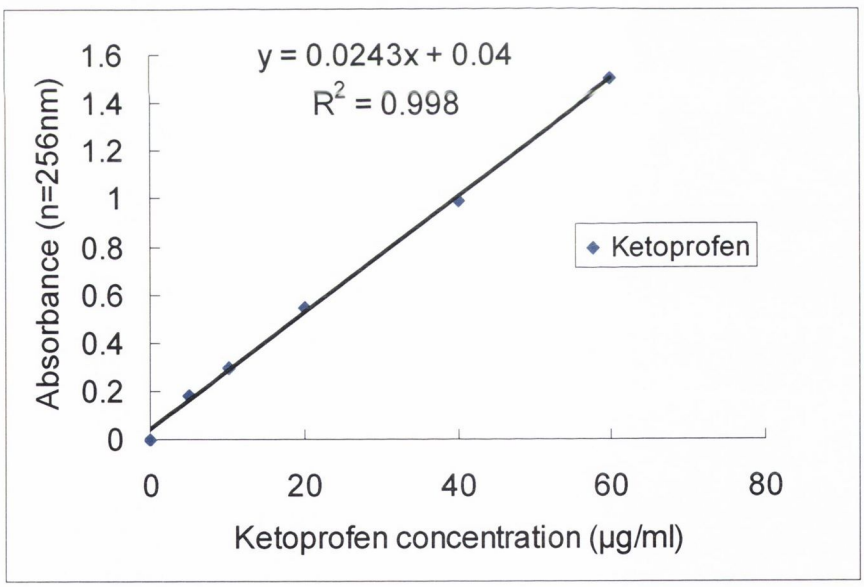

# Calibration curves of chitosan standards for concentration determination

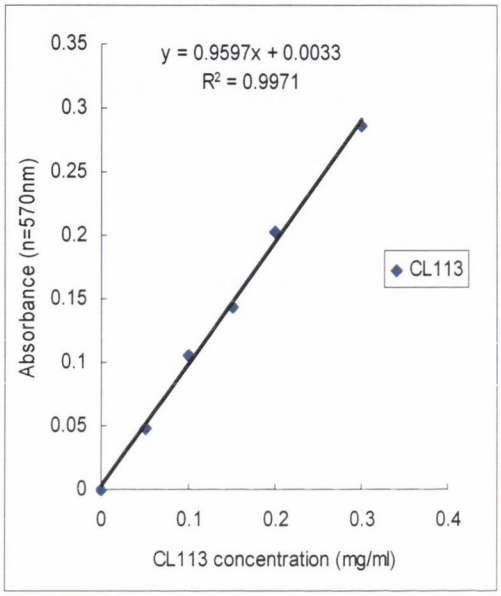


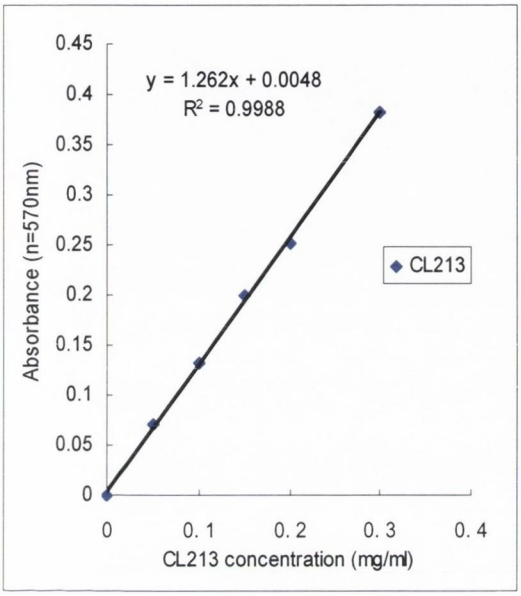


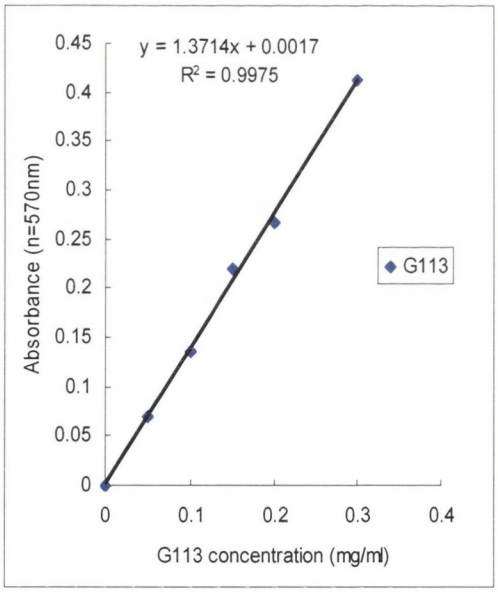


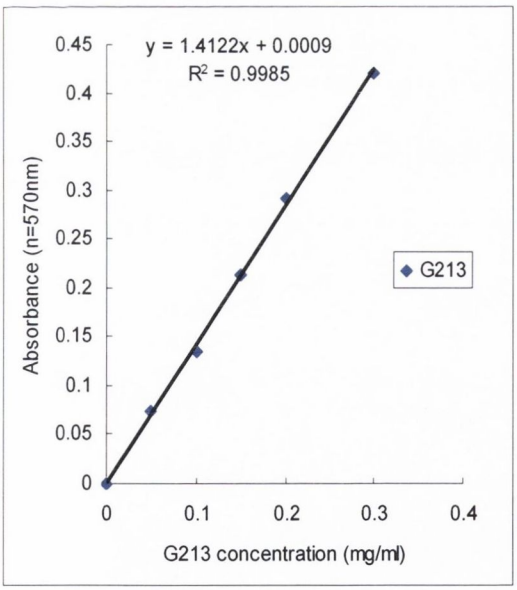

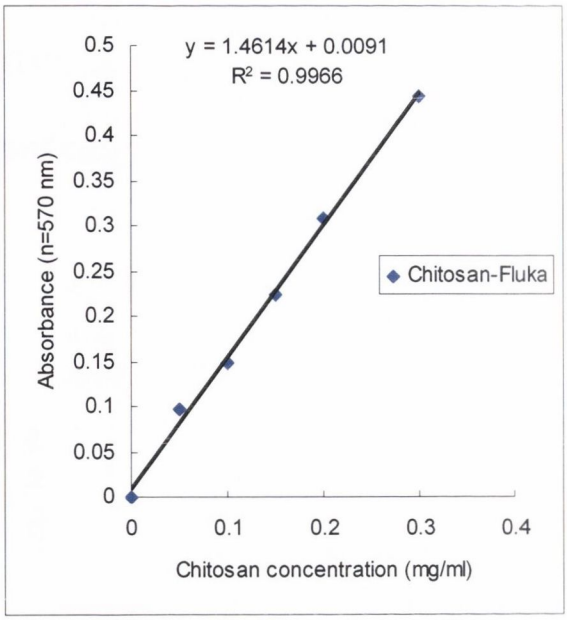


## Calibration curve of PVA standards for concentration determination

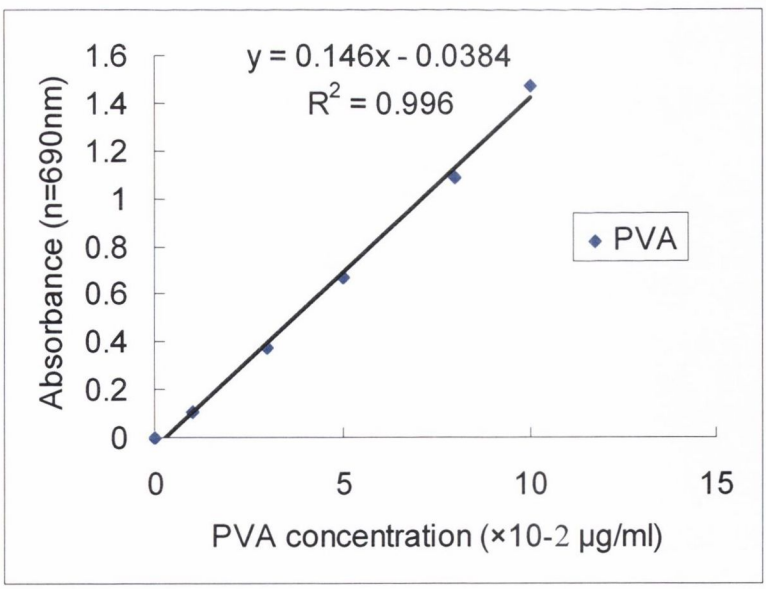

## GPC sample calibration curve of polystyrene standards for PLGA molecular weight determination

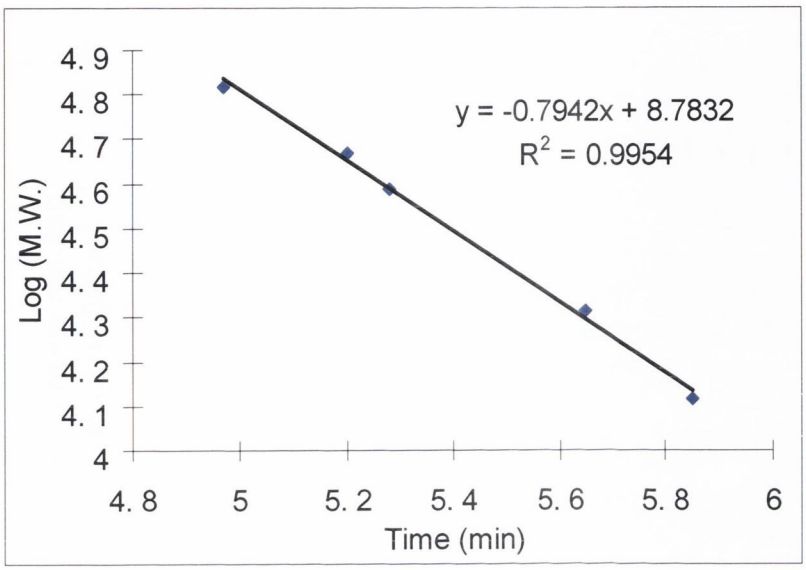


## GPC sample calibration curve of polymer standards for chitosan molecular weight determination

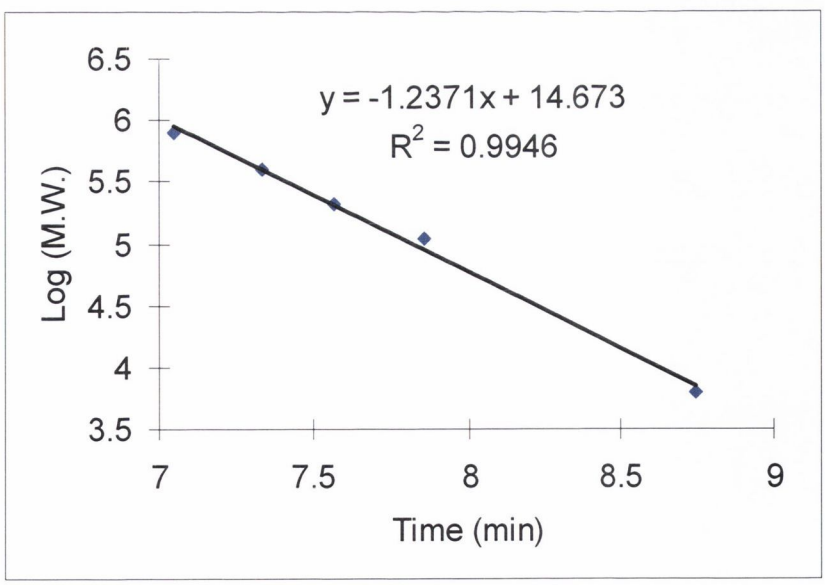

**Calibration curve of coumarin-6 standards for concentration determination**